Genetic biomarkers in uveal melanoma: an exploration using high-resolution array comparative genomic hybridization

By

Nawal Alshammari

A thesis submitted in partial fulfilment of the requirements for the degree of Doctor of Philosophy

Supervisors: Dr. Karen Sisley
Dr. David Hammond

The University of Sheffield
Faculty of Medicine Dentistry & Health
Department of Oncology and Human Metabolism

3rd of January 2017

Acknowledgments;

In the Name of Allah, most gracious, most Merciful.

I am heartily thankful to my supervisors Dr. Karen Sisley and Dr. David Hammond, for their patient guidance, motivation, and continuous support during my PhD study. Their guidance helped me in all the time of research and writing of this thesis. I could not have imagined having a better advisor and mentor for my study.

My sincere thanks also go to all members of the Rare Tumour Research Group who gave me access to research facilities, and were supportive and helpful in more ways than they can imagine. The technical team in histopathology core facility laboratory in particular Mrs. Maggie Glover for her patience and support, and nurse Rhona Jaques Macmillan nurse from the NHS for her great effort in revising all patients clinical note. Without their precious support, it would not be possible to conduct this research.

I am indebted in terms of gratitude towards my family; the best parents in the world (Turkia and Sulaiman) whom words alone cannot express my eternal appreciation. My lovely husband Badr and my daughter Aleen for being patient with me and without their love and endless support, I would not have completed this journey successfully. My sincere thanks also goes to my siblings, in particular my brother Daher, for believing in me and helping me to overcome many difficulties, All My brothers and sisters for their endless emotional and spiritually support throughout writing this thesis and my life in general and their love have been invaluable for me.

Last but not the least; I would like to acknowledge my friends in Sheffield for all the support and the fun we had for the last four years, and help me feel like home.

Finally, I dedicate this work to Allah the Creator who made everything possible.

Abstract

Uveal melanomas (UM) are aggressive ocular tumours of adults that are typically characterized by chromosomal aberrations such as loss of 1p, 3, 6q, and gain 6p, and 8q. Of these monosomy 3 (M3) and 8q+ are powerful predictors of prognosis. The relationship of changes affecting chromosome 6 is however more ambivalent, having been linked to both good and poor prognosis, and yet both regions have not been well defined, which suggest the presence of one or more oncogenes in 6p and tumour suppressor gene in 6q. Therefore, different chromosome 6 alterations may have a variable impact on the prognosis of UM, and ultimately contain genes that contribute to the development and metastasis of this disease. It is likely that these changes can act as moderators to the tumour outcome.

Although UM disseminates haematogenous with high propensity for the liver, and hepatic involvement reported in over 90% of patients, infrequently some patients will however initially present with metastases in sites other than the liver.

The aim of this thesis was to address both central issues. Firstly to better understand how genetic biomarkers identify UM that will metastasize, and whether they can be used to further subtype UM. Secondly to see if potential driver genes could be identified that may lead both to an improved understanding of UM metastasis and how to treat it. The approach taken was to use customised high-resolution aCGH. Which, because it was specifically designed for UM, was hoped to identify recurrent focal SCNA that could have been missed by previous studies using lower resolution and unfocussed approaches, such as chromosomal CGH, classical karyotyping, or even BAC arrays. Altogether 137 primary UM were analysed, and as part of a small pilot study possible drivers were further investigated using IHC

TABLE OF CONTENTS

LIST OF FIGURES

LIST OF TABLES

LIST OF ABBREVIATIONS

ABC	Avidin–biotin complex
Acetylated BSA	Acetylated form bovine serum Albumin
ADM-2	Aberration Detection Method algorithm-2
AE	Elution buffer
Ag	Antigen
AL	Lysis buffer
Alu I	Restriction Endonuclease from Arthrobacter luteus
AMD1	Adenosylmethionine decarboxylase 1
Amp	Amplification
ANCA	Average number of copy alterations
ATL	Tissue lysis buffer
AW1	Wash buffer 1
AW2	Wash buffer 2
BAP1	BRCA1 Associated Protein 1
BGNoise	Background Noise
BRAF	B-Raf Proto-Oncogene, Serine/Threonine Kinase
C	Choroid
CB	Ciliary Body
CDKN2A	p16/cyclin-dependent kinase inhibitor 2 A
CGH	Comparative genomic hybridization
Chr	Chromosome
CM	Cutaneous melanoma
CNVs	Copy number variations
COMS	Collaborative Ocular Melanoma Study group

COXPD14	Combined oxidative phosphorylation deficiency 14
Cy3™	Cyanine 3 fluorophore
Cy5™	Cyanine 5 fluorophore
Cyanine 3-dUTP	Cyanine 3-deoxyuridine triphosphate
Cyanine 5-dUTP	Cyanine 5-deoxyuridine triphosphate
DDEF1	Development and differentiation enhancement factor 1
Del	Deletion
DLRS	Derivative Log2Ratio spread
DLRSD	Derivative Log2 Ratio Standard Deviation
DNA	Deoxyribonucleic acid
E	Epithelioid
E- cadherin	Epithelial cadherin
EIF1AX	Eukaryotic Translation Initiation Factor 1A, X-Linked
EMT	Epithelial–mesenchymal transition
EtOH	Ethanol
Exo-klenow	Exonuclease activity of DNA polymerase I
FARS2	phenylalanyl-tRNA synthetase 2, mitochondrial
FASST2	Fast Adaptive States Segmentation Technique 2
FDR	False detection rate
FE	Feature extraction
FFPE	Formalin Fixed Paraffin Embedded
FISH	Fluorescence in situ hybridization
FOXQ1	Forkhead box Q1
gDNA	Genomic DNA
GI	Genetic instability
GISTIC	Genomic Identification of Significant Targets in Cancer

GNA11	Guanine nucleotide binding protein (G protein), alpha 11 (Gq class)
GNAQ	Guanine nucleotide binding protein (G protein), q polypeptide
HMM	Hidden Markov Model
IHC	Immunohistochemistry
Kb	Kilobase pairs
LOH	Loss of heterogeneity
M	Mixed cell
M3	Monosomy 3
MAPK	Mitogen-activated protein kinase
MCR	Minimal common region
MFI	Metastatic free interval
MHM	Multi hepatic metastasis
Ml	Millilitre
MLPA	Multiplex ligation-dependent probe
mM	millimole
MSA	Microsatellite analysis
NBS1	Nijmegen breakage syndrome 1
ng/µl	nanogram/microliter
NHM	Non hepatic metastasis
nm	Nanometer
NRAS	Neuroblastoma RAS viral oncogene homolog
OaCGH	Oligonucleotide CGH arrays
PCR	Polymerase Chain Reaction
pmol	Picomole
QC	Quality Control
qPCR	quantitative polymerase chain reaction

Rsa I	Restriction Endonuclease from *Rhodopseudomonas sphaeroides*
RGI	Relative genetic imbalance
Rpm	Revolutions per minute
RT	Room temperature
S	Spindle cell
S/N	Signal-to-noise ratio
SCNAs	Somatic copy number aberrations
SD	Standard deviation
SF3B1	Splicing Factor 3b Subunit 1
siRNA	Small interfering Ribonucleic acid
SKY	Spectral karyotyping
SNR	Signal to Noise Ratio
SPG77	Autosomal Recessive Spastic Paraplegia 77
STAC	Significance Testing for Aberrant Copy Number
STOP	Suppressors of tumorigenesis and/or proliferation
UM	Uveal melanoma
UV	Ultraviolet
WT	wiled type
(-)	Loss
(+)	Gain
(i)	Isochromosome
µl	Microliter

1 Chapter one

Introduction

1.1 Cancer as a genetic disease

In the developed world Cancer is the second major cause of death (Stewart and Kleihues, 2003; cancer research UK, 2014). Cancer is a process of uncontrolled cell growth known to arise through the alteration of multiple genes. Over the past hundred years, many theories have been suggested to explain cancer initiation and progression. One of the first studies that identified cancer as a genetic disease was in 1902 by Theodor Boveri, who suggested that unlimited cell growth is a result of chromosomal mutation Boveri, (1929, 1914); as reviewed by (McKusick, 1985, Knudson, 2001, Harris, 2008). Such mutations result in generating abnormal genes, called oncogenes meaning cancer causing genes, or cause some genes to be abundantly over-expressed and behave as oncogenes even if they were not mutated (Haber and Stewart, 1985, Zhou et al., 2007). Other mutations may target genes that in effect suppress cancer development or "tumours suppressor genes" as they are known (Stratton et al., 2009). In 1960, Nowell and Hungerford discovered the first chromosomal abnormality associated with cancer; identifying a translocation between chromosome 9 and 22, which was later called the Philadelphia translocation, and occurs in chronic myeloid leukaemia (Nowell, 1976, Nowell, 2007). Many other cancers however are not found to be a result of a single mutation or translocation. In 1911, Peyton Rous hypothesized that cancer might be caused by viruses as reviewed by (Becsei-Kilborn, 2010) whilst in 1916 Ernest Tyzzer proposed that somatic mutation might be the cause behind cancers (Tyzzer, 1916, Wunderlich, 2007). Moreover, another theory appeared in 1953 claiming that accumulation of mutated genes is the main cause of cancer (Nordling, 1953). Currently, much evidence supports the theory that the initiation of cancer occur after the accumulation of different mutations in genes responsible for cell growth and differentiation (Olopade and Pichert, 2001). Such mutations might be a result of unrepaired DNA damage, which in turn might be caused by occasional mutations or an error in the cell replication process that escaped programmed cell maintenance (Jackson and Loeb, 1998, Cahill et al., 1999)

Several changes of cancer cells have been described within the genome at different levels, ranging from large-scale chromosomal amplification and deletion to small nucleotide base mutations. Thus, these changes lead to alteration to the normal expression of genes that regulate cell differentiation and proliferations causing a malignant cancer cell phenotype. Somatic mutation in cancer cell genome is classified based on the consequence to cancer development such as 'driver' mutations, which

play a role in the initiation of tumorigenesis and evolution of cancer, and others called 'passenger' that acquired during the cancer development and do not certainly contribute to cancer pathogenesis (Stratton et al., 2009). The number of driver mutations in cancer cells is highly likely to vary between cancer types.

Identification of amplified or deleted regions in a set of tumours helps in identifying the genes involved in cancer development, where the oncogenes are thought to be located in amplified regions and tumour suppressor genes in lost genomic regions. The achievement of proper tumour classification requires a methodology to detect the breakpoints defining the altered regions in genomic patterns, by assigning the terms normal, gained or lost to each chromosomal region.

Among cancers in general, deletion of tumour suppressor genes and amplification of oncogenes are common events involved in tumour progression, although certain aberrations have been shown to be recurrent and accumulating, and to lead to the cancer phenotype, resulting in the formation of recurrent somatic copy number aberrations (SCNA), which may give a clue to the pathogenic mechanism (Hanahan and Weinberg 2011). Therefore, analysis of SCNA has led to the identification of genes with roles in tumour progression in various cancer types, and suggested a Therapeutic approach including hepatocellular cancer (Zender, Spector *et al*. 2006), lung cancer (Weir, Woo *et al*. 2007, Chitale, Gong *et al*. 2009), ovarian cancer (Eder, Sui *et al*. 2005) and many others.

Across the entire genome, Beroukhim and colleagues found that in the majority of cancer types, the most frequent SCNA are either very short genomic regions (focal), or the length of chromosome (arm-level) in the form of deletion or amplifications. Around 10% of the cancer genome is affected by focal SCNA, and it is thought that the occurrence of focal SCNA is more likely to coincide with high amplitude (homozygous deletion or many more copies), compared with whole arm level events (Beroukhim, Mermel *et al*. 2010).

1.1.1 Genetic instability in cancer

During the past few decades huge progress has been made in cancer genomics research, strengthened by research on the sequence of the human genome in 2000 that explained the basis of how tumours are driven by various genomic alterations

(Lander et al., 2001). Molecular and cytogenetic studies helped to reveal a wide number of variations in the human genome that could contribute, beginning with single-nucleotide polymorphisms, small deletions or insertion polymorphisms, to large-scale copy number variation in the form of gain and losses to the genomic DNA (Albertson and Pinkel, 2003). Recently, the use of powerful molecular techniques such as next generation sequencing has helped to define the small molecular substitutions in the genomic DNA, which are driven by molecular alterations (Meyerson et al., 2010). Indeed, the analysis of the genomic sequence has helped in understanding cancer biology, and provides an insight into cancer diagnosis and therapy.

Karyotyping analysis for the majority of cancer types shows an abnormal number of chromosomes (aneuploidy), with significant genomic structural rearrangements (Hanahan and Weinberg, 2011). Nevertheless, most of the solid tumors were found chromosomally unstable, as well as knowing the ability to display both intra- and inter tumor heterogeneity.

Chromosomal instability is known by the presence of a high rate of amplification and deletion of whole chromosomes (Lengauer et al., 1997), therefore, the presence of chromosomal instability in most aneuploid solid tumors is an important hallmark of genomic instability related to cancer. Nevertheless, the presences of both chromosomal imbalance and aneuploidy known to be related to disease poor prognosis and development of tumor progression, in addition to increase the resistance to chemotherapy (Carter et al., 2006, Weaver and Cleveland, 2006, Lee et al., 2011, McGranahan et al., 2012). However, an understanding of the mechanisms causing aneuploidy and chromosomal imbalance associated with tumour aggressiveness could lead to advances in cancer therapy.

As mentioned earlier cancer is a progressive disease with a series of accumulating genetic aberrations, therefore, elevated genetic instability is recognised as advanced stage in cancer and enabling the tumour to progress and spread (Nowell, 1976, Stratton et al., 2009). More recently, a new study has identified an extreme version of genetic instability whereby a single mysterious event can devastate chromosomes in cancer cells, leading to massively damaged chromosomes. The study by Stephens *et al.* (2011) introduced the chromothripsis phenomenon as a new mechanism for genetic instability in cancer; it was first discovered in a chronic lymphocytic leukaemia patient who had a massive genetic rearrangement of chromosome 4. Therefore, chromothripsis can be defined as a catastrophic cellular event where one or a few chromosome arms, or chromosomal subregions, are shattered into ten to a hundred pieces and are reassembled incorrectly; with a reported occurrence in 2-3% of general

cancers (Stephens et al., 2011). The cause of this series of different rearrangements in one chromosome is still unclear but it has been suggested that this damage could occur during chromosomal condensation and segregation errors in mitosis (Meyerson et al., 2010, Stephens et al., 2011, Crasta et al., 2012). Although the mechanisms and the cause are ambiguous, it can, however, occur in a wide variety of tumours, and could be a useful prognostic marker for various cancer types. Chromothripsis can thus indicate tumour progression and poor outcome. Similarly so can an increase in genomic imbalances as a measure to determine the relative genetic instability, and can be determined by measuring the number of chromosomal copy alterations per tumour to assess the average number of copy alterations (ANCA) (Ried et al., 1999). Both forms of genetic instability have been reported in malignant melanoma using array-based CGH and are linked to metastases with poor prognosis (Hirsch et al., 2013).

1.1.2 DNA damage

There are many environmental agents, such as chemicals or ultraviolet light (UV), that act as carcinogens and are capable of causing DNA damage (Greenblatt et al., 1994, Multani et al., 2000). Around 70% of cancers in western populations are caused by the exposure to such environmental agents; in addition to an unhealthy lifestyle (Doll and Peto, 1981, Bertram, 2000, Danaei et al., 2005, Bernstein et al., 2009). Tobacco smoke exemplifies chemical carcinogens and is found to contribute to the tumorigenesis of many cancers, such as lung and oral cancers, through affecting the respiratory epithelial cells and changing their behaviour into abnormal cells (Parkin et al., 1994, Fiala et al., 2005, Steiling et al., 2008). Physical carcinogens, such as UV or radiation, can also damage the DNA by breaking the bonds between its double strands leading to cell damage (Hall and Angele, 1999). Approximately 90% of skin cancer cases are caused by sun exposure and the effect of the UV light (Ramos et al., 2004, Boniol et al., 2012). Other risk factors that might cause cancer are microorganisms such as bacteria or viruses (IARC, (1994). For example, *Helicobacter pylori* bacteria are known to play a role in causing gastric cancer (Baik et al., 1996, Farinati et al., 1998, Ding et al., 2007). Moreover, Human Papilloma Virus (HPV) is suggested to be an oncogenic virus correlated with many cancers such as prostate cancer (Dmochowski et al., 1977, Adami et al., 2003)*,* breast cancer (Lawson et al., 2009) but mainly with cervical cancer (Schiller and Lowy, 2001, zur Hausen, 2001). Hepatitis B and C on the other hand, are highly linked to liver cancer (Hussain et al., 2007) and non-Hodgkin lymphoma

(Giordano et al., 2007), while Epstein-Barr virus is believed to contribute to Hodgkin lymphoma (Araujo et al., 2006).

The chance of being affected by cancer dramatically increases with age. This might be because cells lose their capacity to control the cellular abnormalities or environmental carcinogens (Roh and Lyle, 2006, Chung et al., 2011, Meng and Lu, 2012). In general, the main cause of many cancers remains unclear, but with innovation and development of biotechnology including cytogenetic studies, mutational sequencing, genomic arrays, and next generation sequencing including whole genome, exome and transcriptome sequencing the understanding of cancer is increasing.

1.2   Melanoma overview

Melanoma is a malignant tumour that originates from neural crest derived melanocytes, and is responsible for melanin pigment production in the skin, hair, and the uveal tract of the eye (Slominski et al., 2004). During development, melanocytes can give rise to a phenotypically diverse type of melanomas (Bastian, 2014, Mort et al., 2015). The most common type of melanoma found in the Caucasian population is cutaneous melanoma where the western countries have higher incidences, with the highest reported reported for Queensland Australia. Statistically, melanoma is the fifth most common cancer diagnosed in the United States (Jemal et al., 2009, Iannacone et al., 2015). Cutaneous melanomas often have numerous chromosomal aberrations with gains or losses to portions or whole chromosomes (Curtin et al., 2005). The most known oncogene mutations are *KIT*, *BRAF*, and *NRAS*, which are detected in 70% of melanoma cases, though, most of these mutations can be attributed to direct UV exposure (Greene et al., 2009, Dumaz, 2011, Luke and Hodi, 2012, Bastian, 2014). Melanoma is accompanied by some features such as immune system spontaneous regression, which is more common in melanoma compared to other types of cancer (Liszkay et al., 2005, Kaur et al., 2008, Kalialis et al., 2009). The majority of melanomas (90%) are diagnosed as primary tumours without evidence of metastasis, and as such would have up to 10 year survival. Prognosis of melanoma becomes poorer with the progression into stages that include metastasis, where even a small tumour has the ability to metastasise and lead to an unfavourable outcome (Balch et al., 2009, Thompson et al., 2011)

1.3   Uveal melanoma

1.3.1   Brief overview

Although UM is rarer than cutaneous melanoma (CM) and behaves differently (Singh et al., 1988), the incidence of mortality is higher in UM (Jemal et al., 2010).   Uveal melanoma (UM) is the most common aggressive intraocular tumour in adults, with a reported incidence of 1200-1500 cases annually. The highest incidence, as with cutaneous melanoma, is amongst Caucasians (Egan et al., 1988, Hu, 2005, Ramaiya and Harbour, 2007, Singh et al., 2011), where UM roughly accounts for 80% of all non-cutaneous melanomas (Scotto et al., 1976).. UM can originate anywhere in the uveal tract from neural-crest melanocytes, and most of UM arise from choroid tissue, accounting 80-90% of the UM cases, followed by ciliary body with 7%, and the smallest fraction with only 3% arising from the Iris (figure 1.1) (Singh et al., 2004, Damato, 2006)
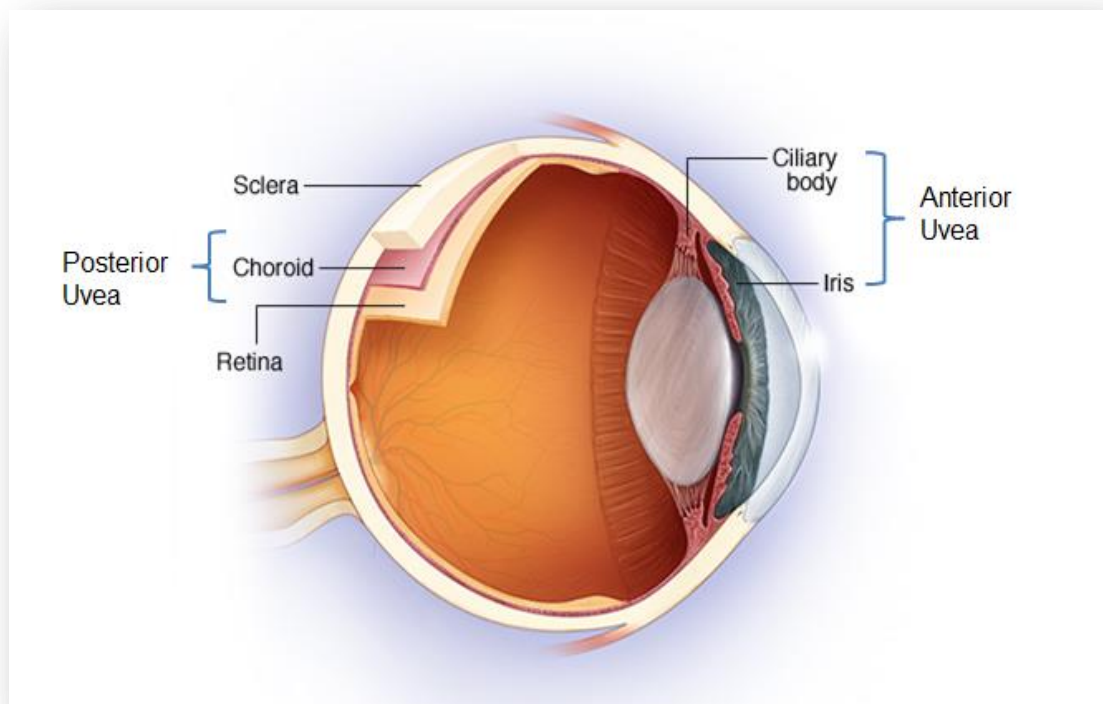
Figure 1.1 Structure of the eye indicating the origins of uveal melanoma

Eye diagram showing the origin of UM that mainly arise in the choroid, the layer between the sclera and the retina, or ciliary body, or iris. Choroid and ciliary body represent the posterior uveal melanomas, and iris represents the anterior melanomas. *Figure Modified from www.uveitis.org.*

1.3.2 Aetiology of UM

UM is not associated with gender and males and females can be affected equally, however, the risk increases spontaneously with age (Egan et al., 1988). UM and CM share the same cell type (melanocyte), and both have higher incidences in the light skin population but they differ in their aetiology and pathogenicity (Singh et al., 2001, Balch et al., 2010). The concentration of melanin in the uveal tissue varies with the eye colour. Patients with bright eye colour such as grey, blue, and green tend to have less melanin concentration compared to individuals with darker eye colour such as brown eye colour (Panda-Jonas et al., 1996). The fair phenotype, including lightly coloured iris, fair skin colour, blond hair, and blue eyes predisposes to UM, in addition the presence of melanocytic lesions, ocular or cutaneous nevi and freckles is also correlated (Gallagher et al., 1985, Tucker et al., 1985, Seddon et al., 1990, van Hees et al., 1994, Schmidt-Pokrzywniak et al., 2009). In regards to environmental factor such as UV exposure, CM is well studied and directly linked to UV exposure, however, evidence linking UM to the solar UV is still inconclusive (Singh et al., 2004, Shah et al., 2005). Although some studies suggest that UV could be a risk factor for UM (Holly et al., 1990), another study did not find any association (Pane and Hirst, 2000). To date no environmental factors or dietary habits have been found to be associated with UM development (Singh et al., 2004). In addition, UM is rare to present in a familial form, while CM have 10% familial genetic predisposition (Canning and Hungerford, 1988, Egan et al., 1988, Singh et al., 1996, Kodjikian et al., 2003).

1.3.3 Metastases and survival

Several histological and genetic factors predict the disease metastasis such as; tumour thickness and diameter, ciliary body involvement, the presence of epithelioid cells with a high mitotic index, lymphocytic infiltration, vascular network abnormalities, gene expression class 2, and chromosomal aberration such as 8q gain, deletion in chromosome 3 and gain or loss in chromosome 6. (Folberg et al., 1993, de la Cruz et al., 1990, Singh et al., 2001, Onken et al., 2004). The majority of these factors will be detailed in subsequent sections.

CM spread through the lymph nodes from skin to brain, liver, lung and other soft tissue (Gragoudas et al., 1991, Hurst et al., 2003, van den Bosch et al., 2010). However, ma-

lignant melanoma of the uvea disseminates heamatogenously with high propensity for liver, due to the absence of lymph node drainage in the uveal tract (Yucel et al., 2009). Tumour cells disseminate directly to the blood circulation, then to the liver ((Diener-West et al., 2005). Although, 50% of the patients eventually developing liver metastasis, around 90% of those patients however, have a 5 years mortality rate irrespective to the type of the treatment (Gragoudas et al., 1991, Diener-West et al., 2005, Singh et al., 2005).

If the melanoma penetrates the sclera and infiltrates the conjunctival lymphatics to regional lymph nodes, and circulate around the body exiting the vascular system it will then metastasize to organs other than the liver. It has been found in different studies that approximately half of the patients with liver metastasis may develop an extra hepatic metastases including to lung (24%), bone (16%) and a minority to the skin and brain, with a 19-28 month survival rate (Collaborative Ocular Melanoma Study, 2001, Kujala et al., 2003, Bedikian, 2006). Despite the fact that patients with liver as the onset of metastases have the worst survival, patients with no liver metastases or the liver is not the first site of metastases however have more favourable prognosis (Kath et al., 1993). Furthermore, patients with iris melanoma tend to have better survival compared to patients with choroidal melanoma, while ciliary body involvement predicts the worst prognosis, based on 5-10 years follow up (Shields et al., 2009, Singh et al., 2011). Metastatic spread of UM was found to occur in 25% of patients within 5 years survival rate and 34% of patients by 10 years survival rate, and once the metastases were detected the majority of the patients die within 1-2 years (Diener-West et al., 2005). Therefore, the mean survival of metastatic disease was only few months and the long-term survivals are rare (Gragoudas et al., 1991, Kath et al., 1993, Collaborative Ocular Melanoma Study, 2001). Therefore, despite the improvement in the diagnosis and of the primary tumour, there have been no corresponding improved survival rates (Singh and Topham, 2003).

1.3.4 Treatment of metastatic UM

UM characterized by having a multidrug resistance phenotype that is highly resistant to chemotherapy and many treatments fail to improve survival rate (Gragoudas et al., 1991, Alexander et al., 2000, Baggetto et al., 2005). Despite the advance treatment of UM, half of newly diagnosed patient are dying once hepatic metastases have been

established, with median survival of 4-6 months (Gragoudas et al., 1991, Kujala et al., 2003, Ramaiya and Harbour, 2007). Treatment of UM mainly depends on the size and location of the tumour, and includes enucleation of large tumours, with resection and radiotherapy for small to medium tumours (Margo, 2004). Different hypotheses have been proposed to explain the rate of metastasis encountered by UM patients, for example, it was believed that the best management of the tumour is enucleation; however, Zimmerman *et al* argued that tumour enucleation for UM patient may accelerate the spread of tumour cells leading to metastases (Zimmerman et al., 1978). An alternative theory is based on a histopathological study, suggests that UM cells are highly resistant to radiotherapy because they were still visible in the irradiated specimens (Manschot and Van Strik, 1987). More recently, the Collaborative Ocular Melanoma Study (COMS) group suggested that regardless of tumour size, or primary treatment there was no improvement in survival rates (1990, Finger, 1997). To date, there is no successful management approach capable of reducing metastatic-caused deaths. Recently, It was hypothesized that this problem might be related to the micro-metastasis, (Eskelin et al., 2000, Borthwick et al., 2011). In general, several factors could improve the survival rate such as adjuvant, preemptive systemic therapy for micro-metastatic patients (Harbour, 2009), but overall, there are no effective therapies for metastatic UM (Augsburger et al., 2009). Although some suggested therapies including the use of mitogen-activated protein kinase (MEK) inhibitors show some remarkable successes (Harbour, 2012, Carvajal et al., 2014), the use of these therapies are promising but not well established.

1.3.5 Prognosis of Uveal Melanoma

The clinical outcome of the patients with UM depends on the development of metastases, and a number of clinical, histopathological and genetic factors help in predicting the disease prognosis. The first histologic differentiation of UM was in 1931 by Callender (Zimmerman et al., 1978) divided UM into 6 groups, Spindle A and B, epithelioid, necrotic, fascicular and mixed cells. The most widely prognostic factor used to assess the severity and prognosis of UM are cell morphology and tumour stage (Hu, 2005)Hu *et al*., 2005), involvement of posterior UM (Ciliary body), as well as location and thickness of the tumour been regarded as the leading prognostic indicator in UM (McLean et al., 1977, Gragoudas et al., 2002, Diener-West et al., 2005). More objective parameters has been emerged as result of extensive cytogenetics and DNA studies, including

cytogenetic markers, as chromosomal abnormalities (Prescher et al., 1990, Sisley et al., 1997, Onken et al., 2010).

Histologic cell typing is, however, subjective to variation in UM survival interpretation, where the presence of the spindle cells with scant cytoplasm/elongated nuclei known to correlate with good prognosis during the low mitotic rate (number of mitosis/mm^2). This is known to be an independent prognostic factor in melanoma sub-classification and other cancer type (Gass, 1985, Vaisanen et al., 1999, Scolyer et al., 2006). Furthermore, the presence of epithelioid cells which characterized by large polymorphic round cells with oval nuclei and well-defined cytoplasmic membrane, associated with poor prognosis, and high metastatic rate as a result of high mitotic indices (Grossniklaus et al., 1995, Toth-Molnar et al., 2000, Gill and Char, 2012). Therefore, the coexistence of both cell types may indicate an intermediate prognosis (Lai et al., 2008). Nevertheless, tumour diameter is another important clinical prognostic factor in UM progression, where the tumour diameter correlated negatively to the prognosis, (the bigger tumour diameter detected the poorest prognosis and less survival). Approximately 53% of cases with large tumours (16 to 18 mm) correlated with high mortality rates (Seddon et al., 1983, Margo, 2004). Tumours that arise in the choroid and ciliary body (Posterior UM) are considered more aggressive and associated with the worst prognosis with 50% death rate within 5-7 years (Prescher et al., 1990, Sisley et al., 1990). However, the use of these parameters alone or combined without knowing the genetic type of the tumour is not conclusive, and cannot provide comprehensive estimation of prognosis. UM can be classified based on the presence of changes affecting chromosomes 1, 3, 6 and 8, and recently, UM was divided into two molecular classes based on metastatic risk and gene expression profile; class I is described by low metastatic risk while class II has high metastases potential (Onken et al., 2004, Finger and th Edition, 2009, Onken et al., 2010). The genetic classification of the tumour will be explained in more detail in the following sections.

1.3.6   Genetic basis of UM

UM is characterised by a low degree of aneuploidy and genomic instability compared to other tumour types (Cross et al., 2003). The most frequently found non-random chromosomal aberrations in UM are loss of one copy of chromosome 3, or monosomy 3 (M3) and losses in 1p, 8p and gains of 6p and 8q (Griffin et al., 1988, Prescher et al., 1990, Sisley et al., 1990, Horsman et al., 1990, Aalto et al., 2001). These common

chromosomal alterations of UM assist in predicting prognosis (Sisley et al., 1990, Sisley et al., 1997, Aalto et al., 2001, Loercher and Harbour, 2003, Kilic et al., 2005). The first study which dealt with UM chromosomal abnormalities was in 1985 (Rey et al., 1985), and the majority of cytogenetic studies were performed in the 1990s (Prescher et al., 1990, Sisley et al., 1990, Horsman and White, 1993, Singh et al., 1994, Prescher et al., 1995, Prescher et al., 1996, Sisley et al., 2000, Naus et al., 2001). Initially cytogenetic analysis was used to detect chromosomal aberrations in UM, but karyotyping only detects simple chromosomal changes such as near diploid and pseudodiplooid karyotypes as well as gross aberrations (Horsman et al., 1990, Prescher et al., 1990). There are also limitations to the technique, as it is challenging to get good quality metaphases from solid tumours due to the need for actively growing tumour cells. Moreover, solid tumours are more complex and heterogeneous, which make it harder for them to be studied by cytogenetics and in particular to identified small frequent aberrations. Improvements were made with the introduction of fluorescence in situ hybridization (FISH), which allowed non-dividing UM cells to be analysed for gross alterations of the most commonly altered chromosomes (Naus et al., 2002). Nowadays, advanced DNA- based techniques including comparative genomic hybridization array (CGH), multiplex ligation-dependent probe (MLPA), and microsatellite analysis (MSA) are used to diagnose UM and monitor its prognosis (Parrella et al., 1999, Tschentscher et al., 2000, Onken et al., 2007, Damato et al., 2009).

1.3.6.1 Chromosome 3

There is a well-established association of M3 (loss of one copy of chromosome 3) with UM, therefore, the involvement of this alteration is considered to be a primary event in UM (Prescher et al., 1994). This abnormality is highly associated with metastases-related death and poor prognosis in UM (Sisley et al., 1990, Prescher et al., 1996, Damato et al., 2007, Shields et al., 2007), and in addition studies related to metastatic death correlated larger tumour diameter, and aggressive cell types with M3 (Prescher et al., 1996, Kilic et al., 2006, Shields et al., 2011, Damato et al., 2009). Conversely the presence of disomy 3 (normal copy of chromosome 3) predicts better prognosis (Trolet et al., 2009), while intermediate prognosis is suggested by partial deletion of chromosome 3 and may increase risk of metastases (Cross et al., 2006). It was proposed that chromosome 3 might contain tumour suppressor genes that could play an important role in tumour progression.

1.3.6.2 Chromosome 8

Gain of long arm of chromosome 8 is often seen as a non-random alteration in UM and linked to the outcome, and many studies indicate that 8q gain is prognostic indicator associated with reduced patient survival (Sisley et al., 1997, White et al., 1998, Cassoux et al., 2014). Furthermore, isochromosome 8q, the formation of an abnormal chromosome from two copies of the long arm of 8 i(8q), is often associated with M3 in ciliary body melanomas and correlates closely with poor prognosis (Sisley et al., 1997, White et al., 1998, Patel et al., 2001). In studies undertaken in Sheffield, roughly, 50% of the cases had M3 and gain of one copy of chromosome 8, and a poor prognosis was associated with these cases (Sisley et al., 1997). The incidence of 8q gain ranges from 55-70% in UM based on the technique used, and techniques such as comparative genomic hybridisation, spectral karyotyping (SKY) and aCGH tend to detect higher frequencies (Speicher et al., 1994, Naus et al., 2001, Sisley et al., 2006, Ehlers et al., 2008, Hammond et al., 2015). In addition the different studies may well have variation in the levels reported because of the cohort of patients studied, since chromosome 8 abnormalities were often found in larger tumours, and it is assumed that 8q may contain certain genes linked to metastatic phenotype (Prescher et al., 1994). More evidence for the association of 8q gain and metastasis comes from studies of the metastatic lesions themselves, in which 8q is the most frequently observed finding, and further evidence suggests that the greater the number of copies of 8q the shorter the disease free interval (Sisley et al., 1997, Hammond et al., 2015). On the other hand, some studies indicate that gain of 8q with or without M3 is not a reliable factor for predicting poor prognosis (Kilic et al., 2005, Ehlers et al., 2008).

1.3.6.3 Chromosome 1

Loss of the short arm of chromosome 1 is frequently observed in many tumours, specifically chromosomal region 1p36, including cutaneous melanoma, neural crest derived neuroblastoma, and the presence of 1p deletion is known to be a predictor of unfavourable prognosis in these cancers (Caron et al., 1996, Knuutila et al., 1999). In UM deletion of 1p has been detected predominantly in metastasizing tumours with M3 (Naus et al., 2001), and Aalto et al reported loss of chromosome 1p as a marker in the tumour progression (Aalto et al., 2001). Furthermore, the concurrent loss of 1p, M3 and

gain of 8q are strongly associated with metastasis related to death in UM patients (Kilic et al., 2005, Kilic et al., 2006), and Sisley *et al*, demonstrate an association between 1p deletion and large ciliary body melanomas (Sisley et al., 2000). These studies suggest that a tumour suppressor gene /genes located in 1p36 could be involved in UM progression. Although loss of 1p seems to occur with other alterations, there are cases of UM without any other chromosomal alteration but at this time, the significance needs to be determined (Caron et al., 1996, Casciano et al., 2002, Poetsch et al., 2003).

1.3.6.4 Other chromosomal changes in UM

One of the most frequently altered chromosomes in UM is chromosome 6 with both the long and short arms affected, and the relevance of these changes will be discussed later. There are other chromosomal aberrations reported in UM, including 9p deletion (Speicher et al., 1994, van der Velden et al., 2001, Abdel-Rahman et al., 2006), rearrangement of chromosome 11 that may associate with spindle cell and choroidal melanomas, which could relate a better prognosis (Dahlenfors et al., 1993, Speicher et al., 1994, Sisley et al., 2000, Sisley et al., 2006). In addition, Trisomy 21 and deletions of 16q are both suggested to have a role in UM progression (Horsman and White, 1993, Sisley et al., 2000, Kilic et al., 2006).

1.3.7 Deregulated genes in UM

Relatively little is known about the molecular pathogenesis underlying UM progression. The first oncogene was reported in late 90s and was suggested to have a role in UM development is p16/cyclin-dependent kinase inhibitor 2 A (*CDKN2A*) (Ohta et al., 1996, Merbs and Sidransky, 1999, van der Velden et al., 2001). In contrast to this finding, germline mutations in *CDKN2A* are very rare in UM tumours (Singh et al., 1996, Soufir et al., 2007). Since, M3 is the most commonly reported alteration, many studies have sort to identify potential tumour suppresser genes located on it, including the suppressor gene fragile histidine triad (*FHIT*), (Zeschnigk et al., 2003). Chromosome 8q implicated in the prognosis of UM, has been a clear focus of research and several genes located on 8q have been associated with UM prognosis, such as *development and differentiation enhancement factor 1 (DDEF1), Nijmegen breakage syndrome 1 (NBS1),* and *c-myc*. Most of these genes lead to DNA damage and cellular invasion, therefore,

all indicated a negative prognosis (Ehlers and Harbour, 2005, Ehlers et al., 2005, Singh et al., 2007). Furthermore, the *C-myc* oncogene on chromosome 8q has been proposed to play a role in UM prognosis based on over-expression of the c-myc protein (White et al., 1998). Parrela *et al* reported that approximately 70% of UM cases have an extra copy of chromosome 8 with amplification of *c-myc* gene (Parrella et al., 2001). The presence or absence of *c-myc* over-expression has been associated with both poor and good UM prognosis (Mooy et al., 1995, Chana et al., 1999, Royds et al., 1992). Other more specific molecular genetic changes associated with UM have been identified recently and linked to prognosis including *GNAQ* and *GNA11*, whereas *BRAF* and *NRAS* known as discriminator between UM and CM (Edmunds et al., 2003, Cruz et al., 2003, Zuidervaart et al., 2005, Landreville et al., 2008). In addition to *BAP1, SF3B1,* and *ELIF1AX* mutations have been recently related to UM prognosis.

1.3.7.1 GNAQ and GNA11

Genetic mutation studies in UM are widely expanded because of the availability of the advanced technology in genetic screening. Recent studies have highlighted the most frequent mutation in UM is a somatic mutation in the guanine nucleotide binding protein (G protein), q polypeptide (GNAQ) which located at chromosome 9q21, in addition to guanine nucleotide binding protein (G protein), alpha 11 (Gq class) (GNA11) at 19p13.3 (Van Raamsdonk et al., 2004, Van Raamsdonk et al., 2010). Approximately, 40-50% of the UM patients are found to have *GNAQ* mutations in their primary tumours and up to 28% in metastatic UM, with 85% of blue nevi also have *GNAQ* mutations. In addition, somatic mutations of *GNA11* are found in 34% of primary UM and up to 63% of metastatic tumour, but it was not detected in extraocular tumours (Van Raamsdonk et al., 2009). The higher frequency of *GNA11* in metastatic UM suggests there is an association with poor prognosis, however not all studies agree (Van Raamsdonk et al., 2009, Harbour et al., 2010). Therefore, activating mutations in both genes was found in approximately 80% of all UMs, regardless of tumour class (Van Raamsdonk et al., 2009, Van Raamsdonk et al., 2010). The majority of the mutations are located at codon Q209 of exon 5 of the gene, in a region of the catalytic domain (GTPase) of *GNAQ*, where the minority of the mutations located in exon 4 affecting codon 183 (Glatz-Krieger et al., 2006, Onken et al., 2008, Van Raamsdonk et al., 2009, Lamba et al., 2009, Van Raamsdonk et al., 2010). Mutation at codon 209 usually occur as a result of glutamine (Q) amino acid substitution to leucine (L) in both *GNA11/GNAQ*, or glutamine (Q) amino acid substitute to proline (P) in *GNAQ*, furthermore, mutation in codon

183 caused by arginine (R) substitute to a cysteine (C) (Kalinec et al., 1992, Landis et al., 1989).

GNAQ and *GNA11* both encode for heterotrimeric G-protein subunits (Gαq, Gα11 respectively), which regulate signals between the downstream signalling pathway and G-protein coupled receptors (Neves et al., 2002). *GNAQ*, located on chromosome 9q21, and coding for the GTP-binding protein activates the MAPK pathway by stimulating the G-protein coupled receptors and regulate the cell cycle cascade (Weber et al., 2003, Dunn et al., 2005).The *GNAQ* mutation is found to occur early in UM tumorigenesis, and is observed in all stages of tumour progression, suggesting it is a potential initiator of the tumour transformation (Onken et al., 2008, Harbour et al., 2010). In addition, as previously mentioned, the *GNAQ* mutation has a weak correlation with metastatic rate, and is insufficient for tumour transformation with no association with uncontrolled proliferation, therefore, mutations in *GNAQ* and *GNA11* do not predict the disease prognosis (Bauer et al., 2009, Van Raamsdonk et al., 2009, Populo et al., 2011). However, Van Raamsdonk et al suggested that *GNAQ* mutation produces spontaneously metastasising tumour in mice, where the expression of both genes (*GNAQ* and *GNA11*) in mice lead to melanocyte transformation and increased signals through the MAPK pathway ((Van Raamsdonk et al., 2010). Therefore, the upregulation of pathways through mutations of *GNAQ* and *GNA11* represent interesting targets for therapeutic approaches, either by targeting the mutation in G-protein alpha subunit itself or its downstream signalling pathway through treatment with MEK inhibitors that can counteract the upregulation of the MAPK pathway caused by both mutations (Besaratinia and Pfeifer, 2011, Harbour, 2012).

1.3.7.2 BAP1 mutation

Recently, familial inheritance of autosomal somatic germ line mutation of BRCA1-associated protein-1 (*BAP1*) was identified by the next-generation sequencing technique, and identified as a tumour suppressor gene in UM and located at chromosome 3p21.1 (Harbour et al., 2010, Abdel-Rahman et al., 2011, Bronkhorst et al., 2011, Goldstein, 2011). Mutations in the *BAP1* gene are found in 84% of patients with metastatic UM and it has the tendency to occur later in UM progression (Harbour et al., 2010). Moreover, *BAP1* mutations have the ability to transfer the gene expression profile from class 1 to class 2 in UM (Harbour et al., 2010). Despite the genetic dissimilari-

ties between *BAP1* and *GNAQ*, targeting both genetic defects might have a great therapeutic advantage (Harbour et al., 2010).

1.3.7.3 BRAF and NRAS mutations

BRAF (B-Raf Proto-Oncogene, Serine/Threonine Kinase) and *NRAS* (neuroblastoma RAS viral oncogene homolog) mutations (present in high percentage in CM) both have a well-known role in CM, with each oncogene activating the Mitogen-activated protein kinases (MAPK) pathway by stimulating the mitogen-activated protein kinase 1 (MEK1) (Davies et al., 2002, Akslen et al., 2005). Despite the deregulation of the MEK pathway, *BRAF* and *NRAS* mutations are rarely presented in UM (Edmunds et al., 2003, Cruz et al., 2003, Zuidervaart et al., 2005, Landreville et al., 2008). However, in contrast a few studies have identified *BRAF* mutation in UM such as the study conducted by Malaponte *et al* who presented a UM case with a *BRAF* mutation (Malaponte et al., 2006). In contrast, approximately 50% of conjunctival nevi are found to carry a BRAF mutation, while other studies found a *BRAF* mutation in conjunctival and iris melanomas but not uveal (Cohen et al., 2003, Spendlove et al., 2004, Thomas, 2006, Henriquez et al., 2007). In general, the relationship between *BRAF* mutations and UM is still unclear and needs more investigation.

1.3.7.4 Recent driver mutations in UM

The most recent driver mutations in UM are *SF3B1* (Splicing Factor 3b Subunit 1) and *EIF1AX* (Eukaryotic Translation Initiation Factor 1A, X-Linked), both thought to occur during tumour progression, *SF3B1* mutation have been identified in low grade UM with better prognosis as well as *EIF1AX* (Harbour et al., 2013, Martin et al., 2013). Furthermore, they found both genes mutated mostly in the presence of disomy 3, and less was found in UM harbouring partial deletion of M3, again suggestive of a good prognosis.

So to summarise, five common mutations in UM have been identified to date, *GNAQ*, *GNA11* were classified as an early events in tumour formation, and not associated with prognosis (Onken et al., 2008, Van Raamsdonk et al., 2009), while the other 3 genes (*BAP1*, *SF3B1*, and *EIF1AX*) were found to occur later in tumour progression, in a mutually exclusive manner and prognostically significant. *BAP1* was demonstrated as possible predictor of bad prognosis, and *SF3B1*, *EIF1AX* as being better prognosis in-

dicator (Harbour et al., 2013, Martin et al., 2013, Decatur et al., 2016). Although, these 5 genes have been found to be commonly mutated in UM they are not really sufficient to predict the outcome, which is still strongly based on relative genetic imbalance

1.4 Ambiguity of chromosome 6 changes in UM

The role of other genetic alterations and chromosomal changes is to some extent fairly defined. However, changes of chromosome 6 are frequently observed, but less is known about the genes involved and the implications of the changes. Whole or partial gain of 6p is more common than loss, though molecular cytogenetic analysis has described the gain of 6p by different mechanisms, including centromeric misdivision, which has led to triplication of 6p and formation of an isochromosome (Squire et al., 1984). Other changes include partial or complete gain of 6p resulting in unbalanced chromosome translocations, in addition to focal amplification in distinct region of 6p. Abnormalities of chromosome 6 have been also described in other tumours, where gain of 6p was found as a frequent occurring event in cutaneous melanoma, retinoblastoma, osteosarcomas and lymphoid tumours (Chen et al., 2000, Ozaki et al., 2002, Bastian et al., 2003, Lau et al., 2004, Zielinski et al., 2005). Furthermore, the correlation of 6p gain with a decrease in the patient survival was reported in cutaneous melanoma and some type of sarcomas (Ozaki et al., 2002, Namiki et al., 2005). Whereas, deletion of 6q was reported in many cancer types including cutaneous melanoma, acute lymphoblastic leukaemia and was found to correlate with poor clinical outcome, which may suggest a presence of tumour suppressor genes at 6q (Healy et al., 1998, Mancini et al., 2002). In UM alteration of chromosome 6 is frequently observed in both gain of the short arm and loss of the long arm, with formation of isochromosome 6p and the correlation with survival has been described in many studies, Aalto et al, illustrate that 6q loss associated with poor outcome and decrease survival (Aalto et al., 2001). In contrast to this White et al, showed that 6p gain was associated with increased survival even if it is correlated with M3 and a gain of 8q (White et al., 1998). Sisley et al. reported that the rearrangement of chromosome 6 with translocation events has been found in 70% of UM cases and this alteration may have a strong association with outcome in UM (Sisley et al., 2006). However, using more advance molecular cytogenetic techniques like microarray 6p was still found to correlate more with better prognosis (Onken et al., 2004).

Partial or whole gain of 6p is much more common than 6q loss in UM, although the majority of molecular and cytogenetic analysis has reported 6p amplification, and been linked to more favourable prognosis. 6q has attracted less attention and is associated more with tumour metastases and was found to be a late event resulting from tumour progression. (Prescher et al., 1990, Gordon et al., 1994, Singh et al., 1994, Speicher et al., 1994, Prescher et al., 1995, White et al., 1998, Sisley et al., 2000, Naus et al., 2001, Kilic et al., 2006, Damato et al., 2009). Many more studies showed that gain of 6p is associated relatively to good prognosis, and less likely to correlate with M3 (Prescher et al., 1995, Ehlers et al., 2008, Landreville et al., 2008). Accordingly, Parrella et al. (1999) proposed a bifurcated pathway for tumour progression explaining the mutually exclusive changes of M3 and chromosome 6p gain in both groups, followed by 8q loss among choroid tumours (Parrella et al., 1999) (Figure 1.2).
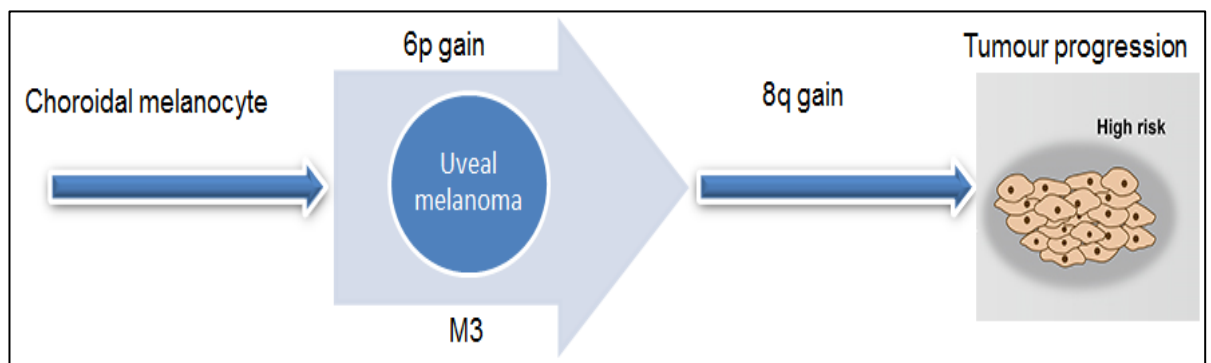
Figure 1.2 Bifurcated pathway in the tumour progression proposed by Parrella et al (1999)

A proposed model illustrating genetic tumour progression of posterior UM, where most tumours undergo either alteration in 6p or M3, with both groups subsequently followed by 8q alterations (Figure modified from Parrella et al., 1999)

In complete opposition, many cytogenetic studies show M3 with 6p gain occurring in the same tumour (Prescher et al., 1990, Sisley et al., 2000, Tschentscher et al., 2000, Aalto et al., 2001, Hughes et al., 2005). In addition, it has been suggested that the formation of isochromosome 6 is highly likely to be associated with M3 (Aalto et al., 2001). Therefore, it is possible that two genetic pathways do exist and both pathways are correct based on the alterations of chromosomes 3 and 6 that correlate with the tissue origins of the tumour (Sisley, 2015), as shown in (Figure 1.3).
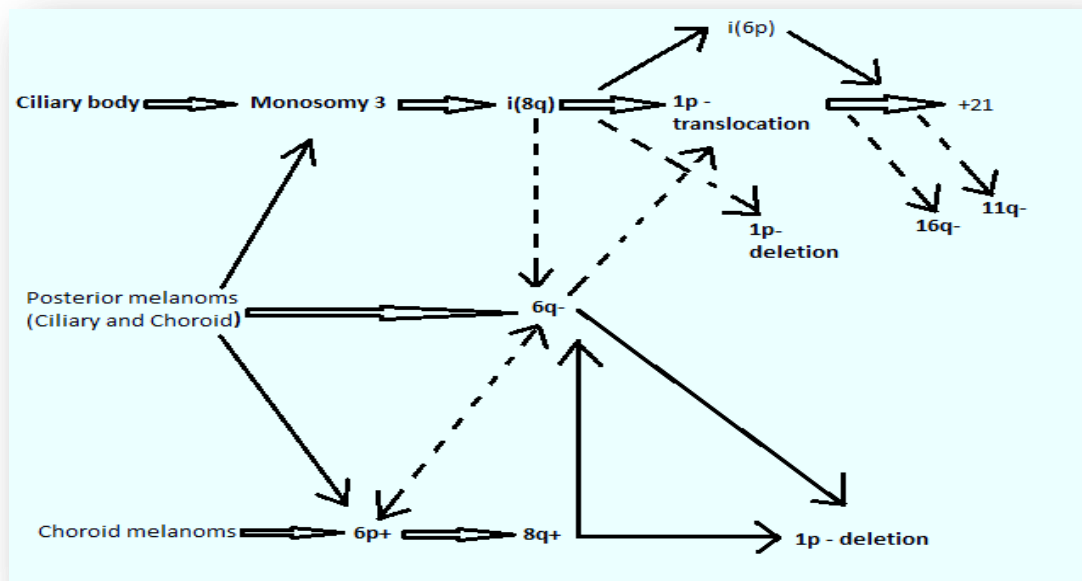
Figure 1.3 Two genetic pathways in uveal melanoma that correlate with the tissue origins of the tumour

The two pathways explain the chromosomal involvement of the most shared regions in ciliary body and choroid melanoma, despite the mechanistic differences between them; therefore, the presence of mixed ciliary and choroid melanomas as a group shows an involvement in both pathways. The dashed lines explain the possibility of these chromosomal changes contributing to and interacting between the pathways, but this is not well established (Figure adapted from Sisley, 2009; 2015)

Using a wide range of techniques such as FISH and array CGH, the breakpoints of 6p gain and 6q loss have been mapped. The most common region of 6p gain was around the centromere, and 6q deletion was narrowed to 6q16.1-6q22 (Horsman and White, 1993, Gordon et al., 1994, Speicher et al., 1994, Sisley et al., 2000, Kilic et al., 2006). Although these findings are conflicting and the relationship between chromosome 6 and prognosis is still difficult to define, this suggests the presence of one or more oncogenes on 6p and a tumour suppressor gene in 6q that may be involved in UM progression. In general, nothing is yet known with certainty, and the meaning of the genetic changes of chromosome 6 remains ambiguous; determining the relevance of chromosome 6 is therefore complicated and requires further study.

1.5   Hypothesis and Aims of the study

Chromosome 6 changes are known to be associated with both CM and UM. In UM, these changes have been suggested to be indicative of a good prognosis, but our studies suggest that in some instances certain alterations are associated with poor outcome. Therefore, we hypothesized that:

Chromosome 6 changes are relevant to the prognosis of uveal melanoma and contain genes that contribute to the development and metastasis of uveal melanoma.

As alterations of chromosome 6 in UM can result in both the loss and gain of different regions of the chromosome, determining the relevance of chromosome 6 is therefore complicated. This study sets out to provide a comprehensive overview of all the changes that affect chromosome 6 in UM in order to identify the candidate genes involved. So far, no study has undertaken a comprehensive investigation of chromosome 6, and to achieve a complete picture a series of UM patients was studied using a high-resolution custom array CGH. This methodology will investigate how specific regional involvement of chromosome 6 is associated with the clinical behaviour of the patients. This broad ranging study is expected to produce clinically relevant information that can be used in the assessment of patients, identifying high-risk uveal melanoma patients that will benefit from further intervention. The identification of the genes involved will assist the development of a more targeted treatment approach and work towards individualised care for uveal melanoma patients.

The aim of this study is mainly to analyse genomic profiles in a large series of ocular tumours, elucidate the genetic prognostic factors of UM, and identify new markers that correlate with disease outcome, and create a model based on genomic classifier for metastatic risk assessment.

2 Chapter two

Materials and Methods

2.1 PATIENTS AND TUMOUR SAMPLES

2.1.1 Ethics Statement

Ethical approval (15/NW/0230) was obtained from the National Research Ethics Committee for the collection and use of fresh and archival tissue sample. Written informed consent was taken from patients prior to the collection of fresh tissue and peripheral blood, all data from archival tissue were analysed anonymously. Tumour and matched blood was collected and stored according to the principles of the Declaration of Helsinki and the use of tissue was in compliance with the Human Tissue Act, 2004.

2.1.2 Tumour samples

Tumour samples were collected as fresh specimens and/or archival Formalin Fixed Paraffin Embedded (FFPE) blocks from UM cases collected between 1994 and 2015 at the Histopathology Department of the Royal Hallamshire Hospital, Sheffield, UK.

2.1.3 Fresh Tumour Samples

Fresh tumour sample were obtained from 137 patients diagnosed with primary UM who underwent enucleation between July 1994 and March 2015 at Sheffield Teaching hospital. Tumours were macroscopically examined by an experienced pathologist and were immediately snap frozen and stored at –80°C until DNA preparation (the Ocular oncology unit at the Royal Hallamshire Hospital, Sheffield, UK). All tumours with matched normal blood were extracted using standard methods, which was available for the archive samples as well.

2.1.4 Formalin Fixed Paraffin Embedded (FFPE) Samples

Tumour pieces were dissected in theatre and formalin fixed, the post-fixation process was completed in the Histopathology laboratory. FFPE sections were chosen based on the availability of FFPE blocks of UM primary tumour, and the outlined tumour area were then scraped off subsequent 5µm sections for immunohistochemistry.

2.2 Material

2.2.1 General Laboratory Reagents

General lab reagent were purchased from a number of suppliers

Latex examination gloves, Schottlander® UK

Plastic universal tubes (25ml), Centrifuge tubes (15ml, 25ml, 50ml), Eppendorf Microfuge tubes (0.2, 0.5, 1.5 and 2ml), Sarstedt®, UK

Plastic disposable pipettes Scientific Laboratory Supplies®, UK

10, 20, 200 and 1000µl pipette tips, and filter pipette tips StarLab®, UK

0.22um sterile filters Millipore®, UK

Sterile scalpels Swann Morton®, UK

Sterile needles Becton Dickinson®, UK

Ethanol

Molecular Grade H_2O

Method-specific reagents are described in subsequent sections.

2.2.2 DNA Extraction for Array CGH and sequencing

DNA Extraction Kit: DNeasy® Blood and Tissue Kit was purchased from (Qiagen) comprising; DNeasy® mini spin columns, Collection tubes, Proteinase K, Tissue Lysis Buffer (Buffer ATL), Lysis Buffer (Buffer AL), Wash Buffers (Buffers AW1 and AW2)- 33ml of 100 ethanol added, and Elution Buffer (Buffer AE).

2.2.3 Array Comparative Genomic Hybridisation

Restriction digestion enzymes and Random Priming with Exo-Klenow Labelling Kit:
Genomic Sure Tag DNA Labelling Kit PLUS (purchased from Agilent P/N 5190-3399, USA), comprising

Restriction digest enzyme Alu I, 25 µL

Restriction digest enzyme Rsa I, 25 µL

10X Buffer C, 130 µL

Acetylated Bovine Serum Albumin (10µg/ml)

Random Primers, 265 µL

5X Reaction Buffer, 525 µL

10X dNTP Mix, 265 µL

Labelling fluorophore Cyanine 3-dUTP (1.0 mM), 75 µL

Labelling fluorophore Cyanine 5-dUTP (1.0mM), 75 µL

Exo-Klenow fragment, 55 µL

Nuclease-free water, 1.5 mL

All stored at -20ºC.

Labelled DNA Purification:

Amicon® Ultra 0.5ml 30kDA filters and 1.5ml microfuge collection tubes (Millipore)

Cot-1 DNA: 1mg/ml Cot-1 DNA (Invitrogen) stored at -20ºC

Hybridisation Kit: Oligo aCGH Hybridisation Kit (Agilent) comprising

> ➢   2X Oligo aCGH Hybridisation solution
> ➢   10X Blocking Agent

Stored at room temperature.

 Blocking Solution:

CGH*block*® (Agilent) stored at -20ºC

Hybridisation Assembly: Microarray hybridisation assembly comprising

> ➢   SurePrint® G3 Human CGH Microarray Slide - 4 × 180K pre-set random genomic probes (Agilent)
> ➢   Hybridisation Gasket Slide
> ➢   Hybridisation Chamber Kit - SureHyb® enabled, Stainless Steel

All obtained from Agilent, Stockport, UK.

Hybridisation Oven: Microarray Hybridisation Oven (Agilent) equipped with removable rotator rack

Wash Buffer Kit: Oligo aCGH/ChIP-on chip Wash Buffer Kit comprising

> ➢   Oligo aCGH Wash Buffer 1
> ➢   Oligo aCGH Wash Buffer 2

Scanner: SureScan High-Resolution Microarray Scanner all provided by (Agilent Technologies, Santa Clara, CA, USA).

2.2.3.1   aCGH microarray slides

Glass slides containing 4 microarrays each utilising over 180,000 probe sequences were chosen to cover regions of the genome known to be commonly aberrant in UM with greater density. These regions included chromosomes 1, 3, 6, 8 and 11.

2.2.4 Genetic sequencing by polymerase chain reaction (PCR)

Thermocycler

All PCR reagents was provided by (Bioline UK) comprisng:

- IMMOLASE DNA Polymerase
- 10x Immobuffer
- 50mM MgCl2 solution (working concentration of 0.5mM to 1.5mM depending on primer set.
- DNTPs with a concentration of 100mM (dATP, dCTP, dGTP, dTTP), and a concentration of 25mM dNTPs, prepared by adding 25µL of 100mM dNTP to 100µL of molecular grade water.

All components should be stored at -20°C

Primers (lyophilised) with concentration of 10pmol/µL (GNAQ exon 5, GNAQ exon 4 GNA11 exon 5, GNA11 exon 4, and BRAF), all primers were optimised previously by Dr. Rachel Doherty, and were synthesised by Eurofins MWG operon.

Primer design

Forward and reverse primers for BRAF, GNAQ, and GNA11 were manually designed previously for gene targets using the sequences available on the NCBI database. Primer sequences were then produced by Eurofins MWG operon (Mudher and Doherty et al., 2013)

All primer sequences used in this thesis are summarised in a table2.1 below

Oligonucleotide primers	Sequence (5'->3')
GNAQ exon 5 Forward	AGA AGT AAG TTC ACT CCA TTC CC
GNAQ exon 5 Reverse	TTC CCT AAG TTT GTA AGT AGT GC
GNAQ exon 4 Forward	TCTTTTTCTCCCACCCCTTGC
GNAQ exon 4 Reverse	TTGTTTTGAAGCCTACACATGATTCC
GNA11 exon 5 Forward	CGC TGT GTC CTT TCA GGA TG
GNA11 exon 5 Reverse	CCT CGT TGT CCG ACT
GNA11 exon 4 Forward	GTGCTGTGTCCCTGTCCTG
GNA11 exon 4 Reverse	GGCAAATGAGCCTCTCAGTG
BRAF Forward	TCA TAA TGC TTG CTC TGA TAG GA
BRAF Reverse	GGC CAA AAA TTT AAT CAG

Table 2.1 A summary of Oligonucleotide primers used in this study

2.2.5 Agarose Gel Electrophoresis

Agarose powder (Bioline Ltd., London, UK) was stored at room temperature and gels
were prepared just before use.

Running Buffer: 10X TAE (Tris-Acetate-EDTA) was diluted from 50X stock solution
prior to use.

Stock solution prepared by dissolving 48.4g TRIS-base with 11.4mL Glacial Acetic Acid
and 3.7g EDTA together and making up to 1L with deionised water, and stored at room
temperature.

Electrophoresis Unit: Multi sub choice horizontal electrophoresis unit (Geneflow),
comprises

- ➢ Samples comb
- ➢ Gel casting tray
- ➢ Electrophoresis tank

Power Source: basic power supply for electrophoresis Power-Pac 3000 (Bio-Rad
Laboratories Ltd., UK).

Ethidium bromide: 1g ethidium bromide (10mg/ml) dissolved in 100ml dH2O and stored
at 4ºC

DNA Ladder: 1kB DNA ladder (1mg/ml) (Promega) stored at 4°C

Loading Buffer: Thermo Scientific 6X DNA Loading Dye, prepared by adding 25mg bromophenol blue to 3ml glycerol and making up to 10ml with dH2O then stored at 4°

2.2.6 Immunohistochemistry

Peroxidase quenching Solution: 0.3% H_2O_2 in methanol, freshly prepared by adding 30 ml Hydrogen peroxide (H_2O_2) (Sigma) to 270ml Methanol

Target Retrieval Solution (10x): 1:10 working solution prepared by adding 10ml DAKO to 90ml deionized water adjusted to pH 6.0.

Blocking Serum: Normal goat serum (Vector Laboratories) was stored at 4°C diluted in PBS with Casein to give a 10% working concentration.

Primary Antibodies: All primary antibodies were provided by Abcam UK, stored at 4°C and diluted in 2% normal goat serum (diluted in PBS).

All antibodies used in this study and their conditions are summarised in Table 2.2 below.

Antibodies	Type	Source	Class	Control tissue	Dilution and conditions
Anti-FOXQ1	polyclonal	Rabbit	IgG	human kidney tissue	1:400 overnight at 4°C
Anti-AMD1	polyclonal	Rabbit	IgG	Human mammary tissue	1:200 overnight at 4°C
Anti-FARS2	polyclonal	Rabbit	IgG	Human colon tissue	1:200 overnight at 4°C

Table 2.2: A summary of primary antibodies used in this study and their conditions

Secondary Antibodies: Secondary antibodies (goat anti-Rabbit, Biotinylated IgG from Vector) were stored at 4°C and diluted 1:200 in 2% blocking serum (diluted in PBS) to give working solution.

Biotin/Avidin Peroxidase Kit: VECTASTAIN® ABC kit (Vector) stored at 4ºC and used according to manufacturer's instructions

Peroxidase Substrate Kit: DAB Peroxidase (HRP) Substrate Kit (with Nickel), 3,3'-diaminobenzidine (Vector) stored at 4ºC and used according to manufacturers' instructions

Mounting media: DPX mountant (Sigma) preserves the stain stored at room temperature and used in a fume hood.

2.3   Methods

2.3.1   Isolation and Purification of DNA

2.3.1.1   DNA Isolation

Genomic DNA from tissue and whole blood was extracted using Qiagen DNeasy® Blood and Tissue Kit. Briefly, the kit works on the principle of protease lysis and digests the protein to release the DNA, then binding the genomic DNA to the silica-based membrane; which have a feature of selective DNA absorbance in the presence of high concentration of chaotropic salts. Followed by two washing steps to ensure the removal of the biomolecules contentment, and pure DNA is then eluted.

2.3.1.2   Fresh Frozen Tissue preparation and lysis

Frozen Tissue (25mg) was placed in 1.5ml nuclease-free microfuge tube with (180µl) tissue lysis Buffer ATL, and Proteinase K (20µl) was added and mixed by vortexing, tubes then was transferred on a heat block at 56°C and incubated for up to 24 hours, with periodic vortexing until the tissue was completely lysed. . Then a mixture of 200µl of AL buffer and absolute ethanol (200µl) was added to each lysed samples and immediately mixed by vortexing. The samples was then transferred to a single labelled

DNeasy® mini spin column placed in a 2 ml collection tube and centrifuged at 8000 rpm for 1 minute

2.3.1.3 Washing

Wash Buffer AW1 (500µl) was added to the each mini spin column and centrifuged at 6,000 × g for 1 min. the spin column was then transferred to a new collection tube, and The collection tubes with the flow-through were discarded. Then followed by second wash step where buffer AW2 (500µl) was added, and samples were then centrifuged at 16,000 × g for 3 min.

2.3.1.4 DNA Elution

DNA from fresh frozen tissue was eluted in AE buffer, and the volume of the eluent used depending on the desired DNA concentration and yield, less eluent volume used for more DNA concentration and lower overall yield, and *vice versa*.

Following the second wash, the DNeasy mini spin column was placed in a new 2 mL microfuge tube and (200µl) of elution buffer (AE) were added directly to the spin column and incubated at room temperature for 1 minute to bind any remaining DNA, and then were centrifuged at 6,000 × g for 1 minute; this step was repeated for a maximum yield of DNA. The DNeasy mini spin column was discarded and Eluted DNA were then stored at 4°C

2.3.2 Peripheral blood samples (reference DNA)

Normal DNA was purified from peripheral blood samples using the Qiagen's DNA extraction kit (QIAamp Blood Midi kit). 2mL of peripheral blood was added to 200µl of proteinase K and 2.4 ml AL lysis buffer in a 15mL centrifuge tube, with a proper vigorous shaking for 1 minute, and then was incubated at 70°C for 10 minutes. Followed by 2ml of absolute ethanol was then added in order to ensure the efficient binding to each reaction tube and mixed to yield a homogeneous solution. All the contents were then transferred to a QIAamp Midi column and placed in a fresh 15ml centrifuge tube provided by the kit, and was centrifuged at 1850$_x$$g$ for 3 minutes.

43

followed by two washing steps (2mL AW1 centrifuge at 4500$_x$$g$ for 1 minute and AW2 for 15 minutes), and after each wash the flow through was discarded and a the midi spin column was transferred to fresh 15mL tube.

DNA from peripheral blood was eluted by adding 300µl elution buffer (AE) to the midi spin column, and then centrifuged at 4500$_x$$g$ for 2 minutes for maximum concentration of the DNA, and the elution step was repeated to increase the DNA yield. The midi spin column was discarded and Eluted DNA were then stored at 4°C.

2.3.3   Genomic DNA quantification and purity assessment

The concentration and purity of the DNAs after isolation from tumour tissue and reference blood was assessed and quantified using a UV/VIS spectrophotometery as NanoDrop™ ND-1000 (Thermo Fisher Scientific, Wilmington, USA). The instrument used to measure the double stranded DNA, by calculating the DNA concentration using modified Beer-Lambert equation to correlate the calculated absorbance with nucleic acid concentration as following; **c = (A * e)/b,** where *c* is DNA concentration in ng/µl; **A** is the absorbance at 260nm, **e** is the wavelength dependent absorbance coefficient (50ng·cm/µl for double-stranded DNA), **b** is the path length in cm.

The concentration of the gDNA was quantified in ng/µl, the Absorbance measurements used to measure different molecules at specific wavelengths and the nucleic acids found to have absorbance at 260nm. Therefore, the purity of DNA was assessed by the ratio of absorbance at A260/A280, which indicates the absence of protein contamination. while a second parameter used to measure DNA purity is the ratio of A260/A230 in order to assess the contamination with salt and some solvents including EDTA carbohydrates and phenol, which all absorbed at 230nm (Wilfinger et al. 1997).

All of the samples were measured to document the original concentration of the DNA, and then diluted to achieve the required dilution for aCGH labelling reaction. The quality of the DNA, however, is a crucial factor in array CGH for obtaining superior data

The following protocol was used to quantify the DNA: the surface of the optical lens was wiped with lint-free wipes and the instrument initialized with 2µl of nuclease-free water, a similar amount of the eluent was loaded to serve as a blank solution. Then the DNA samples were loaded to be measured with proper cleaning of the optical surface between samples. The values for A260/280 and A260/230 were suitable for the analysis within the acceptable ratio (greater than 1.8 and 2 respectively) to assess DNA purity.

2.3.4 Agarose Gel Electrophoresis

Agarose gel was prepared in 2% concentration by dissolving (1g) Agarose powder in 50 ml of 1xTEA buffer in a conical flask, mixed properly and heated for 2 minutes (until all the powder dissolve) in a microwave oven. The Agarose solution was allowed to cool for two minutes and then (5μl) of Ethidium bromide was added with a gentle mix. A gel-casting tray was prepared with a rubber seal around the tray edges, and the Comb was inserted in position, the size of the comb used depended on the required width of the wells. The gel was then poured into the casting tray and left for 30 min to cool and harden. The comb was subsequently removed, and the gel then placed in a sub cell electrophoresis gel tank, submerged in 1XTAE as a running buffer. To determine the size of the PCR products, 1KB standard size marker used according to the expected size of the DNA fragments as a control. To load the gel, add 6x loading buffer (1μl) loading buffer to 5μl of each sample alongside the hyperladder, was mixed by pipetting and then loaded to the wells. Electrophoresis was carried out at 100V for 55 minutes, and a Digital imaging system with UV light (UV trans-illuminator gel document system) was used to visualised the size of the PCR products and photographed.

2.3.5 Standard Polymerase Chain reaction (PCR) for BRAF, GNAQ, GNA11 genes

2.3.5.1 Standard PCR

Standard PCR was used to amplify the section of the gene containing the mutation for BRAF, GNAQ, and GNA11 by using DNA polymerase and design specific primers (detailed in section 2.2.4)

2.3.5.2 2PCR amplification of BRAF gene product with template size (224bp)

- Master mix for standard PCR was prepared at separate room than the amplification room, using filter tips (Eppendorf® Pipette Tips) with a clean set of pipettes. And the Mastermix of PCR reaction was mad up in a sterile PCR hood.

- PCR kit with extracted DNA was transferred to the working area, where the following reagent kept at RT to thaw down including immunobuffer, MgCl2,

Primers (Forward and reverse), dNTPs, with the nuclease free water. The entire reagents were having a proper centrifugation before being opened.

- Immolase enzyme was placed in a pocket of ice.

- Forward and Reverse BRAF Primers was diluted into 1:10 (1 µl of the primers into 9 µl of nuclease free water)

- In a separate 1.5 Eppendorf tube, the following reagents were added for each sample in addition to a Negative control.

    1. Water   16.75 µl

    2. Immunobuffer   2.5 µl

    3. 1.5mM MgCl2   0.75 µl

    4. dNTPs   0.5 µl

    5. BRAF Forward primer 1 µl

    6. BRAF Reverse primer 1 µl

    7. immolase   0.5 µl

- In a fresh 0.5 microfuge tube 23 µl of the MMX was added with 2 µl of 100ng of DNA sample, the solution was mixed with a gently pipetting, and quick spin before being transferred to the amplification area. Microtube were then inserted in automated PCR machine (Thermocycler) programmed for BRAF as a Touchdown PCR with the following PCR conditions

95°C for 10 Minutes

95°C 30 seconds
60°C 30 seconds   3 Cycles
72°C 60 seconds

95°C 30 seconds
58°C 30 seconds   3 Cycles
72°C 60 seconds
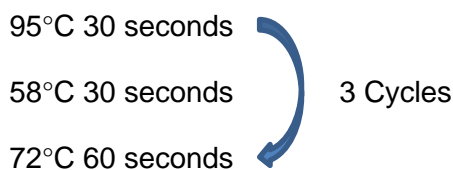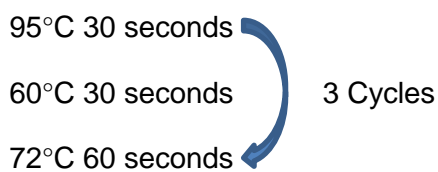
95°C 30 seconds
56°C 30 seconds   3 Cycles
72°C 60 seconds

95°C 30 seconds
54°C 30 seconds   30 Cycles
72°C 60 seconds

Hold on 4°C

2.3.5.3 PCR amplification of GNAQ gene product with template size (317bp)

A mastermix of PCR solution was prepared for GNAQ as following:

1. Water   16.75 µl
2. Immunobuffer   2.5 µl
3. 1.5mM MgCl2   0.75 µl
4. dNTPs   0.5 µl
5. GNAQ Forward primer   1 µl
6. GNAQ Reverse primer   1 µl
7. immolase   0.5 µl

In a fresh 0.5 microfuge tube 23 µl of the prepared MMX was added with 2 µl of 100ng of DNA sample, the solution was mixed with a gently pipetting, and quick spin before being transferred to the amplification area. Microtube were then inserted in automated PCR machine (Thermocycler) programmed for GNAQ standard PCR with the following PCR conditions

95°C for 10 minutes

95°C for 30 seconds (Denaturation)
60°C for 30 seconds (Annealing)   35 cycles
72°C for 90 seconds (Elongation)

2.3.5.4 PCR amplification of GNA11 gene product with template size (147bp)

A mastermix of PCR solution was prepared for GNA11 as following:

1. Water   17.25 μl
2. Immunobuffer   2.5 μl
3. 0.5mM MgCl2   0.25 μl
4. dNTPs   0.5 μl
5. GNA11 Forward primer   1 μl
6. GNA11 Reverse primer   1 μl
7. immolase   0.5 μl

- In a fresh 0.2 microfuge tube 23 μl of the MMX was added with 2 μl of 100ng of DNA sample, the solution was mixed with a gently pipetting, and quick spin before being transferred to the amplification area. Microtube were then inserted in automated PCR machine (Thermocycler) programmed for GNA11 as a Touchdown PCR with the following PCR conditions

95°C for 10 Minutes

95°C 30 seconds
62°C 30 seconds   3 Cycles
72°C 60 seconds

95°C 30 seconds
59°C 30 seconds   3 Cycles
72°C 60 seconds

95°C 30 seconds
56°C 30 seconds   3 Cycles
72°C 60 seconds

95°C 30 seconds

53°C 30 seconds   30 Cycles

72°C 60 seconds

Hold on 4°C
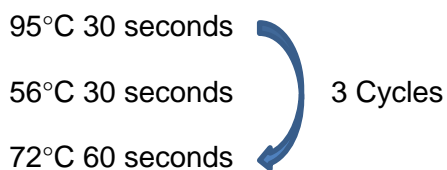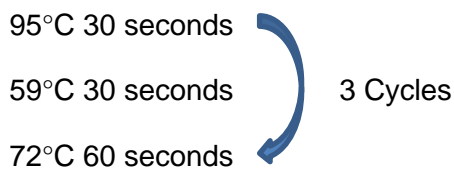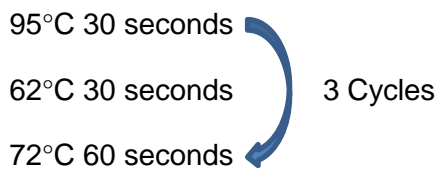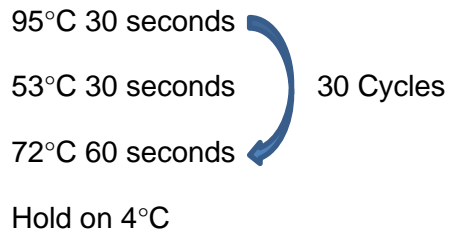
- To test the PCR products, 5µl of DNA product was loaded in the designated wells in the agarose gel (prepared in section), with 1kb marker loaded in the first well. The gel was run toward the anode at 100V for 55 minutes, and to visualise the size of the PCR products the gel was then exposed to a Digital imaging system with UV light and photographed.
- Amplified DNA template was stored at 4°C.

2.3.5.5 DNA purification and Sequencing

The core sequencing facility at Sheffield Medical School (University of Sheffield, UK) carried out the DNA purification and sequencing of all samples. 10µl of each DNA template with a target sequence was send to genomic core facilities with with1:100 diluted primers as following; (BRAF Forward primer, GNAQ and GNA11 Reverse primer)

Sequencing file then translated using Finch TV (V.1.4.0) software, to analysed the chromatogram files, and display the DNA sequence in a graphs.

2.3.6 Genome-wide analysis using array-based comparative genomic hybridisation (aCGH)

2.3.6.1 Array-based Comparative Genomic Hybridisation

Oligonucleotide Array-based Comparative Genomic Hybridisation is a relatively recent molecular technique used to analyse the whole genome to detect copy number aberrations in tumour DNA. Briefly, two gDNAs isolated from tumour sample and matched reference DNA was obtained from peripheral blood samples for each patient, were labelled with two different fluorophores, Cyanine 5 and Cyanine 3 (Cy5™, Cy3™) respectively. The samples were then co-hybridised to a custom microarray slide, with over 180,000 oligonucleotide probes specifically developed for uveal melanoma and used to target regions of interest including known oncogenes. The array slide was then washed and scanned.

The ratio of the fluorescence intensity of the labelled DNA probes between the tumour sample and the reference DNA that has been hybridised to each target was then quantified by a digital analysis system. The result were shown as an ideograms where the differential intensity of the fluorescent dyes at each probe serving as substitute for the ratio of copy numbers of probe sequence in the tumour vs. reference genome. The main array steps are shown schematically in Figure 2.1

2.3.6.1.1 Customised array VS other type of array

Array CGH involves co-hybridising of two differentially fluorescent-labelled fragments of test and reference DNA to a set of annotated DNA sequence (probes) on microarray slides. The copy number differences between the tumour and the normal DNA detected by measuring the ratio of fluorescence at each probe, against their mapped genomic location. Target probe could be Bacterial Artificial Chromosomes (BACs), oligonucleotides, or cDNA sequences, and detection of somatic copy number aberrations (SCNAs) at level of single gene or specific exon depended on the probe number, type and size on the array (Barrett et al., 2004).

The Agilent oligonucleotide array CGH (OaCGH) was thus customised to focus on specific areas of the genome. The highest OaCGH resolution methods available is (60-mer oligonucleotide probes) which contain up to a million probe on a single array slid, and the detection of SCNAs can be as high as1-2 Kilobase pairs (kb) (Barrett et al., 2004, Tan et al., 2007). Probes for chromosome 6 had a mean spacing of 14.5kb

compare to the off shelf array with approximate probe mean spacing of 36.6Kb. The slide was designed for UM clinical applications and was provided in a 4 x 180k format (Hammond et al., 2015). In order to obtain a superior aCGH results, pure high molecular weight DNA from UM fresh frozen tissue and patient's own circulating lymphocytes was essential. Therefore, array CGH was used to further investigate the genetic aberration that motivate the development of UM and uncover area of chromosomal gain and loss that contains oncogenes and tumour suppressor genes.
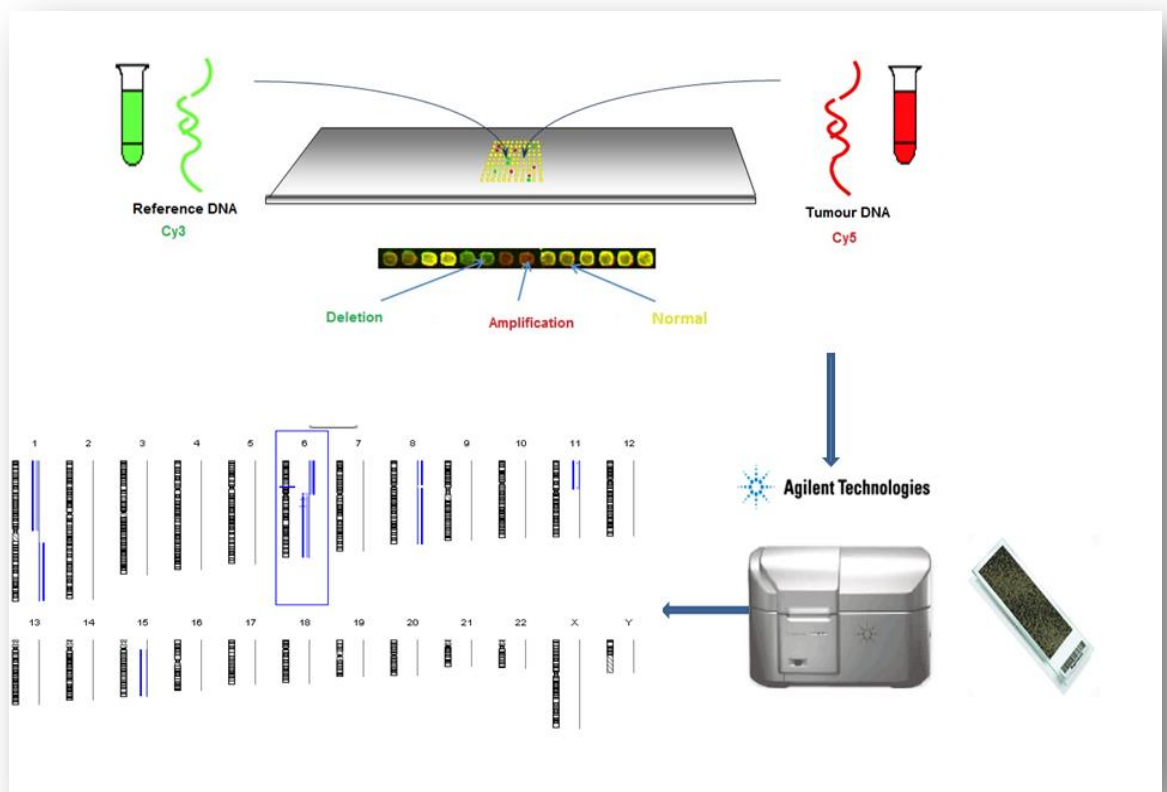
Figure 2.1 Schematic diagram Oligonucleotide Microarray-based Genomic Hybridisation

The figure illustrates hybridization of two labelled gDNAs, the tumor with Cy5 and the reference with Cy3 fluorophore to a microarray slide with complementary sequence binding probes. The ratio of the fluorescence intensity is then calculated and the reference compared to the tumor DNA; if there is, an increase in the sample signal compared to the reference signal then that indicates there has been a gain or duplicate of that genomic region (amplification) and represented by red. Conversely, if there is a decrease in the sample signals relative to the reference then there is likely to be a loss of that genomic region (deletion) and represented by green. The yellow spots (equal

amount of green and red) indicate normal binding of the different probes of the reference genome to the patient's DNA.

2.3.6.2 DNA Labelling (Random Priming with Exo-Klenow)

The Agilent aCGH labelling system uses random priming with Exo-klenow (enzymatic methods) of the DNA polymerase enzyme to label the gDNA samples with different fluorescently labelled nucleotides for aCGH analysis, and uses Cot-1 DNA to block the binding of the repetitive elements prior to hybridising the gDNA to the genomic array. The fluorescence ratio signals of the reference and the test are determined, and providing relative information about copy number changes of the sequence of the test genome compared to the sequence of the normal genome with chromosomal deletion or duplication (Pollack et al., 1999, Barrett et al., 2004, Shaffer et al., 2007, Hayashi et al., 2011).

Briefly, whole genomic DNA obtained from fresh frozen melanoma tissue with reference DNA was digested at specific restriction sites, then denatured and labelled using random primers with Exo-Klenow fragment DNA polymerase, together used to amplify the target DNA while fluorophore-labelled dUTP nucleotides combined at the 3' ends of newly-synthesized DNA fragments. Any uncombined fluorescent nucleotides were then cleaned up from the system to reduce the background fluorescent signals in the experiment.

For a typical array experiment, tumour DNA was matched with comparable amount of reference DNA (either extracted from normal blood from the same patient or commercial DNA), and 0.5 - 1µg of gDNA of tumour and reference was labelled consecutively in separate reactions, prior to labelling the purity and concentration of the DNA samples was determined as described in section 2.

2.3.6.3 *DNA Restriction Digestion*

For each 4 × 180K microarray slide an equivalent volume of 1 µg DNA for 8 samples (4 tumours and 4-matched reference DNA) were placed in placed in clean 0.2ml PCR tubes, and made up 20.2µl with nuclease free water, where necessary.

The protocol started with DNA digestion for both test sample and the control by adding two restriction enzymes Alu I and Rsa I to digest the DNA into smaller strands with random distance. a digestion master mix was prepared, containing 2µl nuclease-free water, 2.6µl 10x buffer C as a restriction buffer, 0.2µl Acetylated BSA (10µg/µl) to stabilize the reaction with 0.5µl of Alu I and Rsa I enzymes, for each reaction. A total of (5.8µl) of the digestion master mix was added to each reaction tube containing 20.2µl gDNA to make a total volume of 26µl. The reaction tubes were then transferred to a thermal cycler with heating block (Eppendorf* Mastercycler* Thermal Cyclers, USA) incubated at 37°C for two hours, then turned at 65°C for 20 minutes and samples were held at 4°C until ready for labelling. The digested DNA were kept overnight in –20°C.

2.3.6.3 Enzymatic Labelling Reaction

Agilent's labelling kit was used to label the digested DNA with dUTP fluorophore; 5µl of random primers were added to each reaction tube (containing restriction digested DNA), making up the volume to 31µl and then incubated 95°C for 3 minutes, then held at 4ºC for 5 minutes.

During the incubation, labelling master mix was prepared with Cy5-dNTP for tumour DNA and Cy3-dNTP for reference DNA in separate tubes, on ice and in dim conditions, as outlined on Table 2.3 below

Component	(µL)per reaction	(µL) per 5 reaction
5x Buffer	10	50
10x dNTP	5.0	25
Cyanine 5-dNTP or Cyanine 3-dNTP	3.0	15
Exo-Klenow fragment	1.0	5
Final volume of Labelling	19.0	95

Table 2.3: Labelling Master Mix Components

A total 19µl of labelling master mix was added to each reaction tubes to make 50µl total volume, mixed by pipetting up and down. The tubes were then transferred to the thermal cycler (Eppendrof) and incubated at 37°C for 2 hours, then at 65°C for 10 minutes, and samples were held at 4°C until clean up.

2.3.6.4 Clean-up of Exo-Klenow Labelled DNA

Labelled gDNAs were purified by removing any unincorporated fluorophore-labelled nucleotides using Amicon® 30kDa filters (Sure Tag DNA labelling kit purification columns, Agilent, USA), the filters trap the labelled gDNA fragments based on their larger size. In prior to wash, labelled gDNA was centrifuged for 1 minutes at 6,000 x g to drive the contents off the tubes walls and lids. Each labelling reaction was mixed with 1X TAE (430µl) and transferred to a labelled Amicon® filter placed in 1.5 mL collection tube and centrifuged at 14,000 x g for 10 minutes at room temperature. The flow-through was removed and discarded and further 1X TAE (480µl) was added to each filter followed by a second centrifugation at 14,000 x g for 10 minutes. The flow-through and collection tube were discarded and the filters inverted into fresh collection tubes.

The inverted filters were centrifuged at 1, 000 *x g* for 1 minute at room temperature to yield a flow through volume of approximately 21µl clean labelled DNA.

Measurement of DNA Labelling Efficiency

NanoDrop® ND-1000 UV-VIS Spectrophotometer was used to determine of labelled gDNA, using the same procedure that was described for DNA quantification (in section 2.3). The instrument measures the absorbance of the DNA concentration at wavelength (260 nm), Cy3- and Cy5-dyes concentrations at (550, 650 nm respectively). The absorbance coefficient was set for double-stranded DNA at 50ng·cm/µl, and (1X TE) blank solution was used. From each labelled samples 2.0µl was taken for NanoDrop to calculate the parameters for evaluating the efficiency of labelling to determine the yield of gDNA, and the amount of dye per microgram of DNA were used to calculate Specific Activity. The calculation for these parameters is shown below with expected optimal values summarised in table2.4.

DNA Yield (µg) = $\frac{\text{DNA concentration (ng/µl) x sample volume (µl)}}{\text{1000 ng/µl}}$

Dye Specific Activity = $\frac{\text{dye concentration (pmol/µl) x1000}}{\text{gDNA concentration (µg/µl)}}$

.
Table 2.4: Expected yield and specific activity Values for DNA labelling efficiency

	Cyanine-3 (pmol/µg)	Cyanine-5 (pmol/µg)
Input gDNA (µg)	0.5-1.0	0.5-1.0
DNA yield (µg)	5.0 to 10.0	5.0 to 10.0
Dye Specific Activity (pmol/µg)	25 to 55	20 to 40

If labelling was optimal, 19.5µl of the tumour and matched normal DNA sample were then combined in a fresh 0.2 microfuge PCR tube prepared for hybridisation, or stored in the dark at -20ºC until ready for hybridisation.

2.3.6.6 Pre-hybridisation Blocking

Prior to hybridisation 10x Blocking Agent was prepared by adding 1350µl of nuclease free water to a vial containing lyophilized 10x blocking agent and left 60 minutes at room temperature with a proper vortex mixing before used, using the Agilent Oligo aCGH/ChIp-on-ChIp Hybridisation Kit, according to manufacturers' instructions. Repetitive DNA sequences in the labelled DNA samples were blocked with COT-1 DNA.

Combined tumour with matched blood were transferred to a fresh 0.2ml PCR tube, and a hybridisation master mix was prepared as summarised in table 2.5. Then 71µl master mix was added to each reaction tube with a proper mixing by pipetting up and down with a total volume of 110µl. Tubes were then pulse centrifuged and transferred to a thermocycler for 3 minutes at 95°C and then at 37°C for 30 minutes, held at 37ºC until ready for hybridisation assembly.

Table 2.5: Hybridisation Master Mix Components for Labelled Samples

Component	Volume per tube (µl)	Per 5 tubes (µl)
Human Cot-1 DNA	5	25
10X Blocking Agent	11	55
2x Hybridization buffer	55	275
Total volume	71	355

2.3.6.7 Microarray Hybridisation and Assembly

2.3.6.7.1 Hybridisation Assembly

One clean 4X microarray gasket slide was loaded into the SureHyb® chamber base with the gasket label facing up and aligned with the rectangular section of the chamber base. Then 100µl of each labelled sample was slowly dispensed into a gasket in a 'drag and dispense' manner. A custom microarray slide was then carefully placed,

active "Agilent- labelled" side down, onto the gasket slide, the sandwich-pair were assessed for a proper alignment, and the SureHyb® chamber cover put in place over the sandwiched slides. The clamp was then slid gently onto both pieces and tightened to complete the assembly. The assembly was rotated vertically to wet the microarray slide and ensure that air bubbles are freely mobile. The chamber assembly was then placed in the rotator rack of the microarray hybridisation oven set to 65ºC and set to rotate at 20 rpm and hybridized 24 hours

2.3.6.7.2 Post-Hybridisation Washing and Scanning

Two wash conditions were set up before the hybridisation assembly was removed from the Incubator. The first wash setup consisted of a sterile storage bottle filled with Agilent Oligo aCGH/ChIP-on-Chip Wash Buffer 2 and warmed overnight at 37°C incubator for optimal performance, with a glass dish 3. Second, wash setup started by using high quality Milli-Q ultrapure water to rinse the glass dishes, slide racks and the stir bars. Then glass dish 1 and dish 2 were filled with aCGH wash 1 buffer at Room temperature, a slide rack was placed in dish 2 with a magnetic stirrer with a rotating stir bar in place. While glass dish 3 was filled with a pre-warmed aCGH Wash Buffer 2 and maintained on a heated magnetic stirrer with a rotating stir bar in place.

At the end of 24 hours of hybridisation, the SureHyb® chamber assembly was taken out of the Hybridisation Oven and then assessed to ensure that all bubbles were still mobile. It was then laid on a horizontal surface and the clamp unscrewed and gently slid off. The chamber cover was then carefully lifted off the slide sandwich, which is removed and transferred to glass dish 1, to detach the array-gasket sandwich using plastic forceps and the gasket slide allowed to drop to the bottom of the glass dish. The microarray slide was then immediately transferred to the slide rack in dish 2 and washed for 5 minutes at room temperature. Quickly, so that the slide is not allowed to dry, the slide rack was then transferred to dish 3 and the slide washed for exactly 1 minute at 37ºC. The slide rack was then removed slowly to minimize the formation of droplets on the slide, which is then placed in a slide holder for immediate scanning.

The microarray Slides were then scanned using the Agilent Surescan® high-resolution technology microarray scanner with control software (version 8.5.1), (Agilent) configured as recommended by manufacturers. The scanned images were saved in Labelled Image File Format (.TIFF), which was examined for microarray damage or hybridisation artefacts.

2.3.6.8 Microarray Data Processing

2.3.6.8.1 Array Quality Assessment and Feature Extraction

Scanned images at 3μm resolution were analysed using Feature Extraction software v11.0.1.1(Agilent). The software normalises the fluorescent intensity and calculates the ratio of the red and green dyes at each probe, and expressed them on a logarithmic scale (probe $\log_2$-ratio). $\log_2$-ratios for all probes were then exported as Text (.txt) format, and the FE software produces a Quality Control (QC) report to evaluate the reproducibility and reliability of the microarray experiments, including statistical metric and the threshold values used for acceptance of array CGH data as valid based on these metrics are summarised in table 2.6 below.

One of the important parameter to determine the reliability of the microarray result is a Derivative Log Ratio Spread (DLRS), and it was calculated by measuring standard deviation of the $\log_2$ ratio difference between consecutive oligonucleotide probes, where a smaller SD indicates less background noise. The other parameters including average background noise and signal-to-noise (S/N) ratio were determined by calculating the mean signal intensities of the red and green dyes, at all genomic probes and then compared to nonhybridising control probes.

Table 2.6: QC Metric thresholds for Array CGH Experiments

Derivative $\log_2$ Ratio Standard Deviation (DLRSD)	This metric calculates the standard deviation of the log ratio differences between consecutive probes, to smooth the data and estimate the measure of the noise of an array.	Excellent: <0.2 Good: 0.2–0.3 Evaluate: >0.3
Background Noise (BGNoise)	This metric is calculated as the standard deviation of the signals on the negative control probes after rejecting the outliers features.	Excellent: <5 Good: 5–10 Evaluate: >10
Signal to Noise Ratio (SNR)	This metric calculates the ratio signal to noise by dividing the signal intensity by BGNoise. To distinguish the real signal from the signals obtained due to the experimental variation.	Excellent: >100 Good: 30–100 Evaluate: <30

2.3.6.9 Microarray analysis

Agilent Genomic Workbench (version 7.0.4.0) analytics software with aCGH licence obtained from http://www.genomics.agilent.com was used to analyse, visualise and detect any chromosomal aberration from microarray profiles. The Agilent Genomic software required a design file match to the feature extraction files; therefore, Agilent GEML-based (*.xml) array design files were imported prior to any FE data, with a genome built specifically for the design file. In each experiment, Agilent Feature Extraction (*.Txt) data files were imported to the software and a new experiment was created for the FE files. The data were first processed by applying preselected filters. A centralization algorithm was applied to centre the log ratio. The QC metric in the original data (see table 2.2) were assessed. Afterwards, the data were analysed by applying the Aberration Detection Method (ADM-2) algorithms with the threshold adjusted to 6, and the Genomic viewer was used to display this data alongside the chromosome ideograms.

2.3.6.9.1 Aberration Detection using Nexus software

Genomic copy number aberration were identified for each individual array using the FASST2 (Fast Adaptive States Segmentation Technique 2) algorithm in Nexus Copy Number Software v7.5 (Biodiscovery). The algorithm uses a Hidden Markov Model (HMM) – based approach which uses many states instead of estimating the copy number state at each probe, to cover further possibilities, such as mosaic events (including cancer data which can often encloses significant mosaicism and normal cell contamination). These state values are then used to make calls based on a specified log_2 ratio threshold.The significant p-value threshold was set at 5.0×10^{-8} and requiring 3 contiguous probes to identify an aberration. Log ratio threshold value of +0.20 and 1.14 were used to identified a single and two or more copy number gain respectively, while the losses were determined by using log ratio threshold between -0.23 and -1.1. All threshold values were based on analysis software manufacturers' recommendations. Aberrations were presented as ideograms (graphical genomic plots) and can be viewed at whole genome level, chromosomes or single gene, for easy visual analysis (Figure 2.1).

2.3.7 Immunohistochemistry (IHC) for formalin fixed, paraffin-embedded tissue (FFPE)

5µm sections from FFPE were collected onto positively charged slides and dried overnight in an oven at 37ºC, IHC was performed using a modified modified Avidin-Biotin-Peroxidase Complex (ABC) method (Vector Laboratories, Peterborough, UK) and as described by Hsu et al (Hsu et al., 1981), at the histopathology core facility laboratory with the help of (Mrs. Maggie Glover). Briefly, tissue sections were treated to expose the relevant antigen and block non-specific antibody binding, which was minimised by incubating sections in 10% species-specific relevant normal serum for 30min at RT. They were then incubated with the desired specific primary antibody at its optimum dilution (Table 2.2). Sections were then washed and a relevant biotinylated secondary antibody, which binds to the FC portion of any bound primary antibody, was added. To detect the presence of the target antigen in the tissue, a colorimetric reaction was used in forms of complexes of avidin molecule linked to an enzyme reporter system and bound to the secondary antibody.

Tissue were incubated in the absence of the primary antibody, as a negative control, however the positive controls and test sample were incubated with primary antibody diluted in blocking serum, and these control were included in every run.

2.3.7.1 Antibody optimization

All antibodies used in this study were optimised prior to staining, based on manufacturer recommended conditions were used as a guide, with a range of antibody concentration. In this study, three independent observers (Nawal Alshammari (NA), David W. Hammond (DWH) and Karen Sisley (KS)) assessed the specific antibody staining with minimal non-specific background staining, and identified the optimal antibody conditions as summarised in table 2.2.

2.3.7.2 Tissue Preparation and Antigen Retrieval for Immunohistochemistry

Prior to staining , Tissue sections were dewaxed by placing them in two consecutive xylene for 10 min each, the tissue were then dehydrated through immersion in a graded series of Ethanol (100% EtOH for 5min, 100% EtOH for 3min, 95% EtOH for 3min). Endogenous peroxidase activity was blocked by placing the section in 3% H_2O_2/methanol for 30 min at room temperature (RT), then subsequently washed for 5 minutes in PBS.

Antigen retrieval treatment was an essential step for the preparation of FFPE tissue for staining, and it was carried out by immersing the tissue section in Target Retrieval Solution, to detach the protein cross- links clusters formed from formalin particles on the tissue's antigen binding sites. The complexity of this cluster increased in the tissue with longer formalin embedding time, therefore the inadequate Antigen retrieval treatment will remain some clusters will shield the Ag binding site from Antibody (Ab) attachment. Many Ag retrieval methods were available in the lab, and the method that been applied in this study started by Immersing the tissue sections in in pressure cooker in 0.01M Tri-sodium citrate (pH6) for 2 minutes incubation, then the tissues were allowed to cool down in the same buffer for approximately an hour after. Followed by two subsequent PBS washing for 5 minutes, before the rest of staining steps are completed.

2.3.7.3 Blocking and Primary Antibody Incubation

A wax pen was used to outline the relevant area of tissue sections, and then a 10% appropriate blocking serum (goat serum and casein) was applied and incubated at room temperature for 30 minutes, to block the non-specific background staining. The blocking serum was then removed by tapping the slides, and then primary antibody was diluted in 2% blocking serum and added to the positive control and the test slides. For the negative control 2% blocking serum (without antibody) was applied. Slides were then incubated overnight at 4°C.

2.3.7.4 Secondary Antibody Incubation and Immunoreactivity

Slides were washed twice in PBS for 5 minutes each, and appropriate Secondary antibodies (goat anti-Rabbit, Biotinylated IgG from Vector) was diluted in 2% blocking serum was applied on all slides and incubated at RT for 1 hour. During the second Ab incubation, ABC reagent was prepared and allowed to stand for 30 minutes. The slides were then washed in two baths of PBS 5 minutes each, and ABC reagent was applied and incubated at room temperature for 30 minutes. Followed by two PBS washes 5 minutes each, then prepared peroxidase enzyme substrate 3–3 diaminobenzidine solution (DAB) was prepared freshly and applied on the slide, incubated at room temperature and allow the stain to develop until the desired brown stain intensity reached (up to 10 minutes), and the reaction was stopped by washing the sections with deionized water.

2.3.7.5 Counterstaining and Mounting

The slides were rinsed in tap water for 3-5 minutes, and then the sections were counterstained for 60 seconds in Gill's haematoxylin, and then washed with running tap water for 5-10 minutes until the water ran clear. The sections were then dehydrated with graded series of EtOH with 3 minutes incubation each (70%, 95%, 100%), under a fume hood the slides were cleared two consecutive incubations in xylene for 3 minutes each. While still wet with xylene, the sections were then mounted with DPX, covered with 22 × 40mm coverslips, and allowed to dry overnight. Slides were then examined using a light microscope at the appropriate magnification.

3 Chapter Three

Implication of 6p changes and potential for identifying subsets of Uveal Melanoma

3.1   Introduction

Until recently, little was known about the genetic changes of this aggressive tumour, and compared with many cancers, the majority of UM display a relatively low degree of aneuploidy and genomic instability. Certain genomic alterations are commonly reported as associated with UM, mainly chromosome 1, 3, 6 and 8 have been identified using different methodologies including (FISH, CGH, MSA, MLPA and aCGH) (Horsman and White, 1993, Gordon et al., 1994, Speicher et al., 1994, Sisley et al., 2000, Kilic et al., 2006, Aronow et al., 2012, Cassoux et al., 2014). All of these alterations are considered to have a prognostic relevance, but the prognosis of uveal melanoma is most closely linked to those changes of 3 and 8, and while 1p is considered as an indicator of poor prognosis, the role of 6p is less clear cut (Prescher et al., 1996, Sisley et al., 1997, White et al., 1998, Sisley et al., 2000, Aalto et al., 2001, Damato et al., 2010).

Changes of chromosome 6 are frequently observed in the form of both a gain of the short arm and loss of the long arm, with formation of isochromosome 6p (Aalto et al., 2001), and this alteration is often seen with M3 and gain of 8q and loss of 1p. Overall partial or whole gain of 6p is more common than 6q loss in UM, and the majority of molecular and cytogenetic analysis has reported 6p amplification, as linked to a more favourable prognosis. Paradoxically, 6q, although the focus of fewer studies, appears to be associated more with tumour metastases. (Prescher et al., 1990, Gordon et al., 1994, Speicher et al., 1994, Singh et al., 1994, Prescher et al., 1995, White et al., 1998, Sisley et al., 2000, Naus et al., 2001, Kilic et al., 2006, Damato et al., 2007). This suggests the presence of one or more oncogenes on 6p and a tumour suppressor gene in 6q that may be involved in UM progression. Initially in 1998 White et al, reported 6p amplification in a large series of posterior UM, and found it was predictive of better prognosis even with correlation with the poor indicators of M3 and 8q gain (White et al., 1998). Tumours with 6p gain have been suggested to represent a separate group of UM with an alternative genetic pathway, in the absence of M3 (Prescher et al., 1995, Sisley et al., 1997, Ehlers et al., 2008, Landreville et al., 2008), leading to the assumption of the bifurcated pathway that was proposed by Parrella 1999, with mutually exclusiveness of 6p and M3 based on microsatellite analysis (Parrella et al., 1999). There is however conflicting information on the role of chromosome 6 and survival, and this may in part reflect the technologies used to study these changes, as a study using MFISH demonstrated that approximately 70% of UM had involvement of chromosome 6, a much higher rate than had been reported previously (Sisley et al., 2006). Studies using conventional karyotyping and global analysis such as MLPA, and BAC arrays without

extensive genome coverage may underestimate the involvement of chromosome 6. For example, an MLPA study with 452 patients found that M3 with 8q in the absence of 6p associated with worst prognosis, confirming the bifurcated pathway and associated 6p gain with a good outcome. The weakness of this study was the short follow up, on average of less than two years (Damato et al., 2010). Therefore, the role of chromosome 6 in determining prognosis in UM remains confused. Past studies have either used simplistic approaches that may have underestimated its presence, have too few samples, or have insufficient follow up to confirm the association, where the average survival was 18-24 months, with a 5 year maximum follow up. Array CGH provides a comprehensive assessment of the genome, but has issues when dealing with heterogeneity. For UM there have been few studies that have taken this approach, but recently a big aCGH study was presented with a median of 28 months follow up (Ranging from 1-147 months) and confirmed that M3 with 8q gain is the highest risk group with 2 years metastatic free interval (MFI) (Cassoux et al., 2014), but made no clear recommendation on the role of chromosome 6. Other array studies have also similarly confirmed or not interrogated the data for chromosome 6 involvement (Damato et al., 2007, Damato et al., 2010, Cassoux et al., 2014). The most recent study to use array CGH attempted to improve the application of the technology to UM by the use of a specifically designed customised array (Hammond et al., 2015).

For UM the mutational studies look promising, but there is no conclusive evidence and insufficient survival data to strongly demonstrate a relationship to prognosis with mutations (Harbour, 2012). The specific focus of this investigation was therefore to delineate the role of chromosome 6 and to clarify some of the confusion over the prognostic implications of chromosome 6 in UM. Whilst relating them to 3 and 8 changes. Array CGH was used to make this assessment as the development of high-resolution microarray CGH over the past several years has proven its value for analysing copy number variation using oligonucleotide probes, facilitating detailed analysis of a cancer genome in a single experiment. For this investigation CGH array used had been specifically designed to reflect our knowledge of the most highly implicated chromosome alterations in UM, and contained a higher density of probes representing unique genomic sequences for 1, 3, 6 8 and 11 (Hammond et al., 2015). The analysis was designed to investigate all reported changes of chromosome 6 in comparison with cases of UM for which no changes were found. On this basis, UM with only 6p could be compared with those having 6p and 6q alterations simultaneously with UM with other chromosome 6 alterations, or with those with no 6 alterations at all.

3.2 Results

3.2.1 UM samples

This study included 53 cases where the analysis was performed by Dr. David Hammond, Ocular oncology unit, and a further 84 primary UM were extracted during this investigation including the 21 cases that were reported in the study by Hammond et al., 2015. The UM samples selected for analysis were from patients treated between July 1994 and March 2013. They included a mixture of prospective cases and also cases for which long term follow up was available. The majority of the cases for the series were selected blind with no prior knowledge of the genetic changes or outcome. As a secondary investigation a consideration of genetic alterations in relations to site specific metastasis was undertaken (chapter 5). For the UM in this part of the study there was some selection based on prior cytogenetic evidence, and clinical information on metastasis, amounting to the selection in total of less than 40 cases. Combined together the total number of UM for which aCGH was performed was 137 cases. The selection criterion was therefore entirely based on the availability of frozen tumour material that produced sufficient good quality DNA for array.

3.2.2 Clinical Data

Clinical data was collected after the analyses were completed for all cases. The clinical supportive data was variable for the series as a whole, as many patients had been referred from a long distance and subsequently lost to follow up. For some patients follow up was very short, whilst for others incomplete information was available on the clinical-pathological characteristics. Indeed, it subsequently became apparent that some cases included were not posterior UM, but were other ocular tumours, including iris, conjunctival and in one instance a leiomyoma. Of the 137 cases included in the study 72 (55.3 %) were male and 57 (43.8%) were female, which is comparable to previous studies, however, the sex of 8 patients were not confirmed (Kujala et al., 2003, Mooy and De Jong, 1996). Similar patterns to previously reported studies were also observed for the age range of the patients which was from 11 to 89 years. The mean diameter of the UM ranged from 6.26 to 22.25 mm, and in the series 46 cases were classified as having spindle cells, 60 with mixed cells and 12 with epithelioid cells, again comparable with previous studies where the presence of epithelioid cells

indicates worst prognosis as shown in figure (Figure 3.1A). Tumour locations were also reported in this study and 60% of UM patients presented with tumours arising from the choroid, 19% were ciliary body and 21% a combination between choroid and ciliary body. Our survival data was comparable to previous studies, and showed that patients with tumours involving the choroid alongside the ciliary body were considered to be more aggressive and associated with the worst prognosis; with 50% death rate within 5-7 years as shown in figure (3.1B) (Prescher et al., 1990, Sisley et al., 1990, Diener-West et al., 2005, Shields et al., 2011). Although the tumours located in the iris (I) along with CB tend to have the worst prognosis, the number of tumours involving only the Iris melanomas in this series was low (5%) and was not enough to be significant. In this study, the total follow up ranged from 2 - 200 months with average of (51.6 month), and only 15 patients out of 137 were completely lost to follow up. Initial analysis of clinic-pathological parameters for the series therefore suggest that this current investigation is representative of the UM distribution reported previously, and that there has been no selection bias in this study. Therefore, after consideration of the clinical-pathological parameters for the series, the analysis then considered the stratification of cases into each chromosome 6 sub- group.
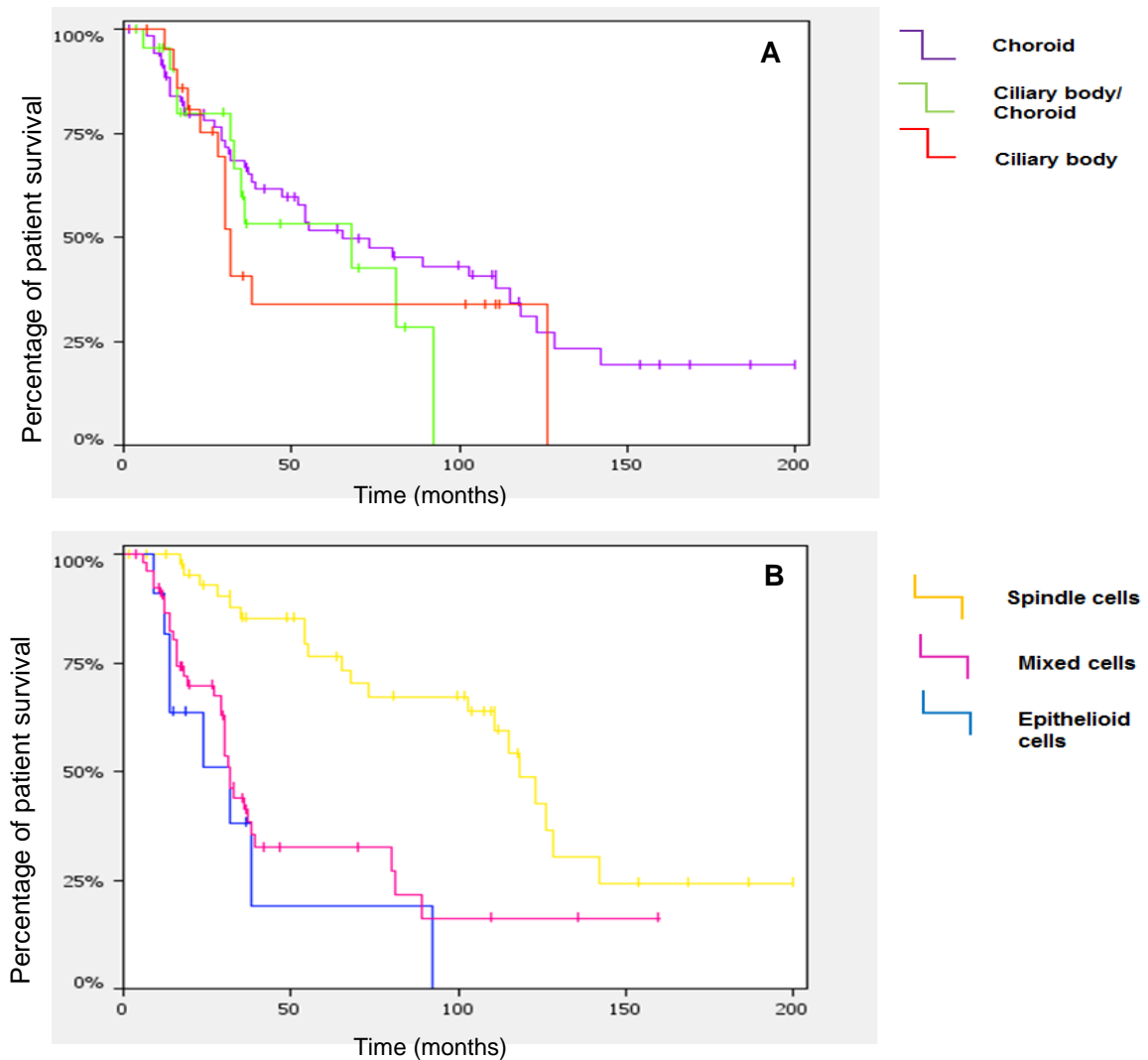
Figure 3.1 Kaplan-Meier curve indicate the disease specific mortality according to cell morphology and tumour location

The Y-axis represents the percentage of patient survival; X-axis is representing survival time by months. **A**. survival in relation to tumour location illustrating that tumours with ciliary body involvement (CB) have a worse prognosis than those of the choroid (C). **B** Survival in relation to cell type, epithelioid tumours (E) have the worse prognosis and then tumours with spindle cells (S) the best. (No follow up data for 15 patients)

Images output from Biodiscovery's Nexus v8.

3.2.3 Validation of Microarray results

In aCGH the ideal genetic platform is characterised by having a high resolution, high hybridization intensity and low level of experimental variation or noise. The majority of the aCGH experiments in this study represent such an ideal genetic platform, after

hybridisation on a designed oligonucleotide array comprising 180,000 probes concentrated on known UM chromosomal alterations (1, 3, 6, 8, and 11). The series comprised 137 UM with DNA from each patients normal blood used as a reference in most cases, in order to compensate for copy number variation across the genome, and ensure that copy number alteration calls were more likely to be accurate and associated with the disease. Based on the normalized Log_2 ratios, a quantitative analysis with copy number changes was derived for each tumour.

Aberration detection module (ADM-2) algorithm (2.0) with a threshold of 6.0 was used based on the distribution of the probes. The feature extraction software calculates the log_2 ratio to identify the copy number differences between the reference and the test sample; the gains and losses in the genomic region are calculated as a ratio that is plotted against the genomic position. The first step in data processing compares and normalises the data, by using a normalisation algorithm. For each array the fluorescence ratio is normalised around zero by finding a constant value to add to or subtract from all values on the array; the algorithm then adjusts the ratio values (log_2). The result was then validated as follows, log_2 ratio >0.6 is considered amplification and shown in red, log_2 ration ≤−1.0 is considered deletion and shown in green, and the black dots represent the normalized value around zero which is between 0.6 and -1.0. The data were analysed and the results were used to classify UM into subgroups based on the type of abnormality affecting chromosomes 6. This classification is explained more in depth in section (3.2.4).

3.2.3.1 Array Quality

In the current study, the signal intensities of both green and red dyes for all DNA samples were of much higher than the threshold recommended by the manufacturer. The quality of the microarray experiment was assessed by Derivative Log Ratio Spread (DLRS), which measures the probe-to-probe consistency and represents the noisiness of the array data. A low DLRS value means that the data has better ability to identify small aberrations due to small probe-to-probe variability, whilst high values tend to have a poor detection of CNA. The manufacturer's recommended value for DLRS when using DNA from freshly frozen tissue is ≤0.3. All DLRS values for the array experiments fell into the recommended range.

3.2.4 Group classification of UM

Based on past genetic investigations of UM (karyotypes, array, MLPA etc) alterations of chromosome 6 are considered to affect between 30-50% of cases, and the changes mainly involve an amplification of 6p, as discussed earlier (Prescher et al., 1996, Sisley et al., 1997, White et al., 1998, Sisley et al., 2000, Aalto et al., 2001, Damato et al., 2010). The involvement of chromosome 6 in UM can therefore be categorised into 4 groups, as represented in figure 3.2.
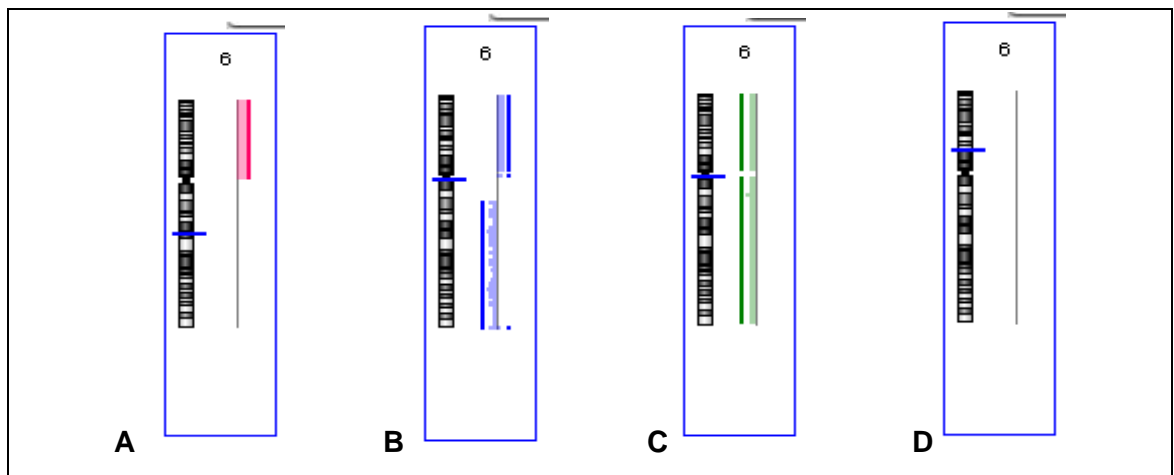
Figure 3.2 The range of Chromosome 6 abnormalities found in Uveal melanoma, as established from analysis of previous cytogenetic, molecular, and molecular cytogenetic published studies. The results are presented as those that would be obtained from aCGH analysis.

A) Amplification (red bar) to the right side of the vertical zero line and represents group 6p gain. **B)** A 6p amplification (blue bar to the right of the zero line) in association with 6q deletion (blue bar to the left of the zero line) with possibly the formation of isochromosome 6p i(6p). **C)** Alterations of chromosome 6 that do not confirm those previously detailed, and where no gain for 6p occurs, for instance a deletion of the entire chromosome (presented by green bar to the left of the zero line) **D)** the last group where no significant changes in chromosome 6 are identifiable.

Using the results of the array-CGH the 137 UM's were sub-divided depending on whether they had alterations of chromosome 6 or not, and if they did whether they affected one or both chromosomes arms. All abnormalities of chromosome 6 were confirmed by two software analysis packages (Agilent workbench, and Nexus) as described in chapter 2 section (2.3.6.10). The groups are thus as follows:

3.2.4.1 Chromosome 6p gain only (GROUP 1)

This group is represented by a gain only of 6p where the alteration spans from 6pter-6p12.1 as depicted in Figure 3.2 A. This type of rearrangement produces a trisomy for 6p. The majority of the tumours in this group have a whole arm gain (6pter-6p12.1) as illustrated in figure (3.3a), partial gains were detected with the smallest regional gain as 6pter-6p21 previously reported by (White et al; 1998). The results are detailed later in the chapter.
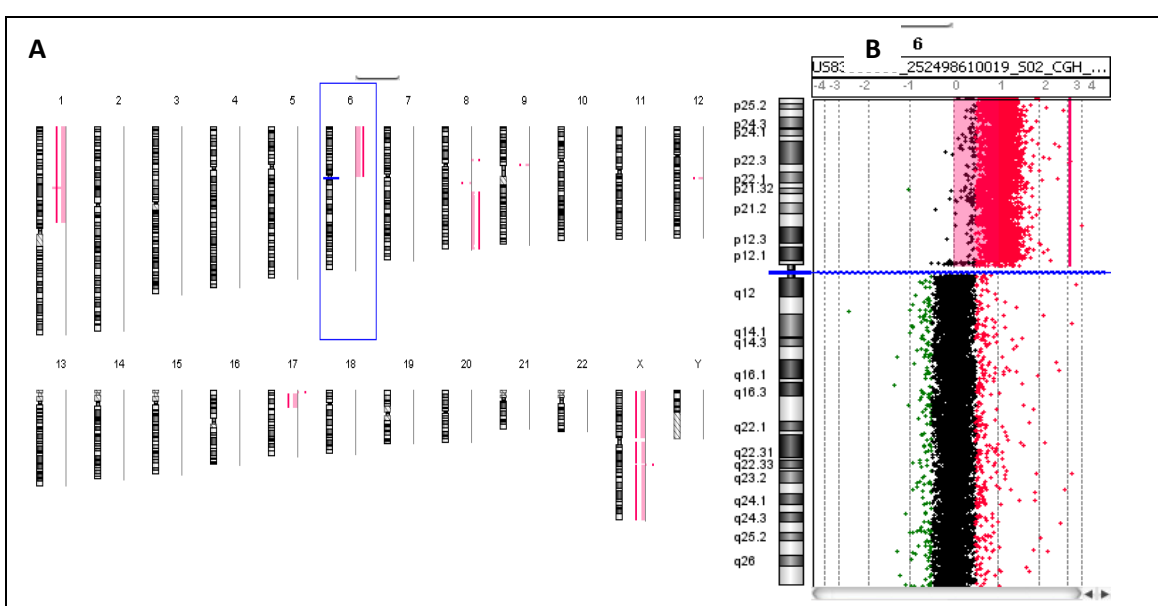
Figure 3.3 Array-based CGH ideograms of chromosomal aberration in primary UM

A: Genomic view illustrating abnormalities of all chromosomes affecting UM case with alterations involving chromosomes 1, 6, 8 (all classically associated with UM) and chromosome 17. In this UM the chromosomal aberration detected on chromosome 6 is a gain affecting the short arm, 6p and places this tumour into the category of group 1. **B**: A high resolution image of chromosome 6 with identified areas of amplification (red bar) in the p arm (6pter-6p12.1), the amplified area is presented by the number of the sequential probes above the zero greater than the threshold with $\log_2$ ratio (>0.6)

Images output from Agilent Genomic workbench v7.0.4. The ADM2 algorithm was used to detect all the CNAs

3.2.4.2 Chromosome 6p gain/q loss i(6p) (GROUP 2)

In this group the frequently occurring events is the gain of 6p with loss of 6q, with possible formation of isochromosome i(6p), the majority of the tumours in this group was detected as a form of i(6p) as shown in figure (3.4, 3.10), and the rest presented in form of whole or partial 6p gain with 6q loss. The breakpoint toward the centromere for 6p with regional gain of 6pter-6p12.2 and loss of chromosomal region 6qter-6q12 was detected. The results are detailed later in the chapter
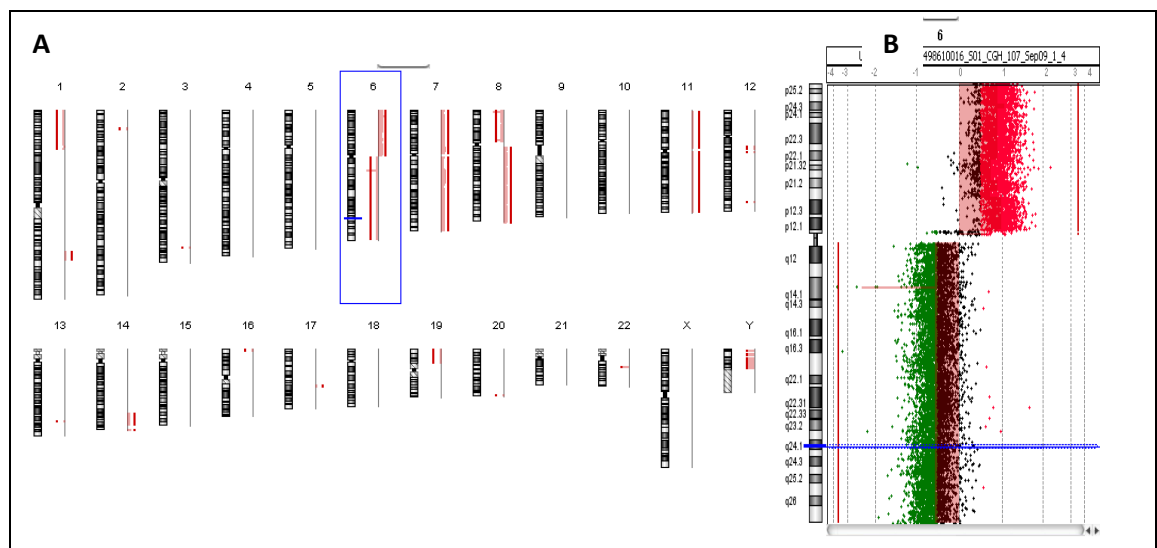
Figure 3.4 Array-based CGH ideograms of chromosomal aberration in primary UM

A: Genomic view illustrating abnormalities of all chromosomes affecting UM case with alterations involving chromosomes 1, 6, 8, 11 (all classically associated with UM) and chromosome 7. In this UM the chromosomal aberration detected on chromosome 6 is a gain affecting the short arm, 6p with loss of 6q and places this tumour into the category of group 2. **B:** High resolution chromosome 6 graphical views identified areas of areas of amplification in the p arm showing the value with log$_2$ ratio (>0.6), and the area of deletion, where the number of the sequential probe below the zero with log$_2$ ratio (–1.0). The black dots represent the normalised value around the zero.

Images output from Agilent Genomic workbench v7.0.4. The ADM2 algorithm was used to detect all the CNAs

3.2.4.3 Other chromosome 6 changes (GROUP 3)

The current group were classified based on other chromosome 6 changes including, entire chromosomal deletions or amplification, as shown in figure (3.5A), or partial deletion and amplification in different regions of chromosome 6 as shown in figure (3.5C). The majority were presented as 6q loss only, and it was found that this group were highly associated with genetic instability and aneuploidy in the current tumours as shown in Figure (3.11).
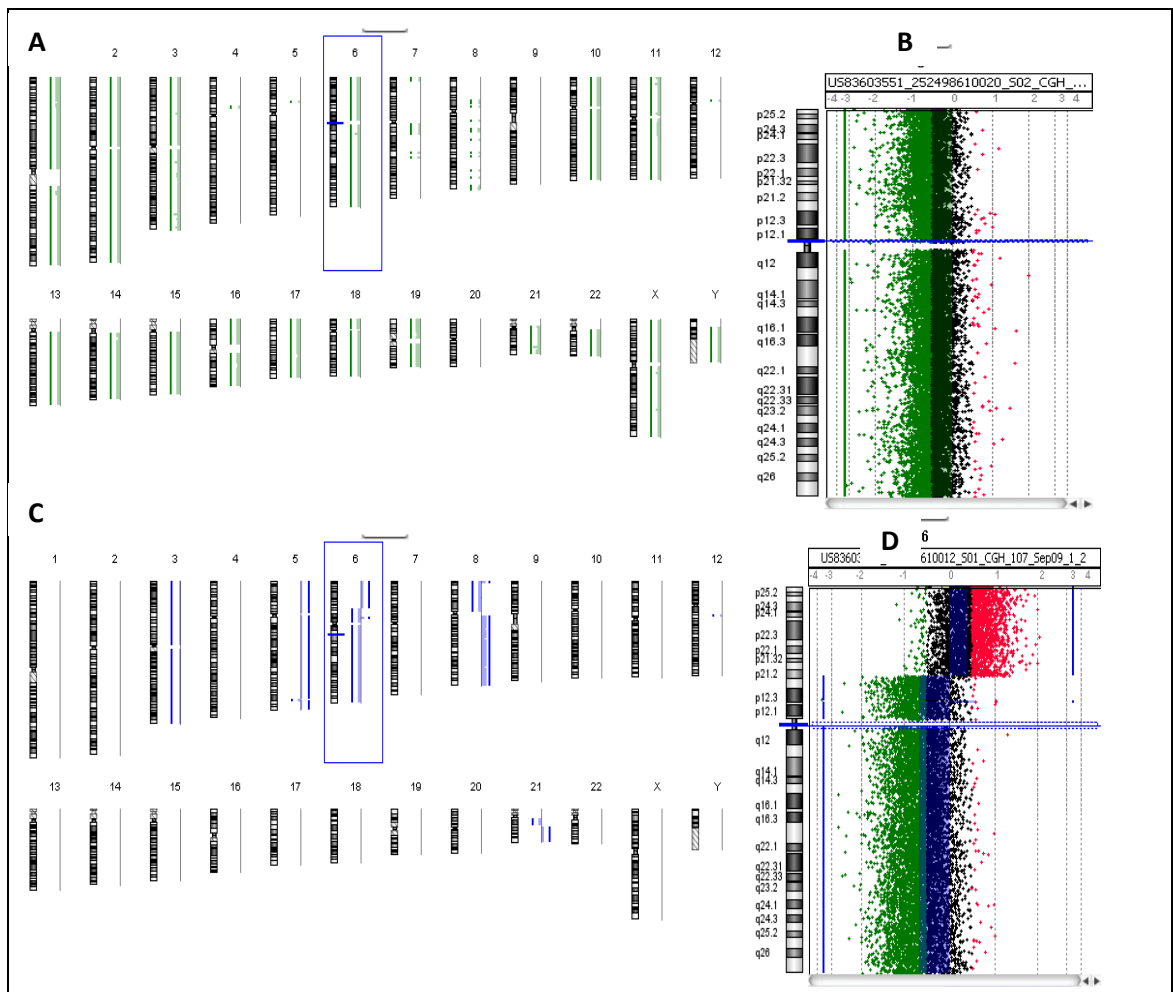
Figure 3.5 Array-based CGH ideograms of chromosomal aberration in primary UM

A: Genomic view illustrating the chromosomal aberration detected on chromosome 6 showing monosomy 6 as an example of group 3 with M3.deletion of the majority of the chromosomes demonstrating a high level of genomic instability. **B:** Chromosomal view showing 6p25.5-q26 deletion represented by green dots with $\log_2$ ratio (<–1.0). **C:** Genomic view in illustrating the chromosomal aberration detected on chromosome 6 showing gain and loss in the p arm with q arm deletion as another example of group 3,

where a part of 6p was deleted rather than amplified, in association with 3 and 8 changes. **D**: Chromosome 6 view showing gain in the region p21.2–p25.2 (red dots), and loss in the region p21.2-q27 (green dots)

Images output from Agilent Genomic workbench v7.0.4, and ADM2 algorithm was used to detect all the CNAs

3.2.4.4 No significant changes in chromosome 6 (group 4)

This group is classified based on the absence of 6 alterations as shown in figure (3.6), although this group has no 6 changes it represents M3 with highest frequency followed by 8q gain and i(8q) with 1p changes. This group represents genetically stable tumours, as shown in Figure (3.12).
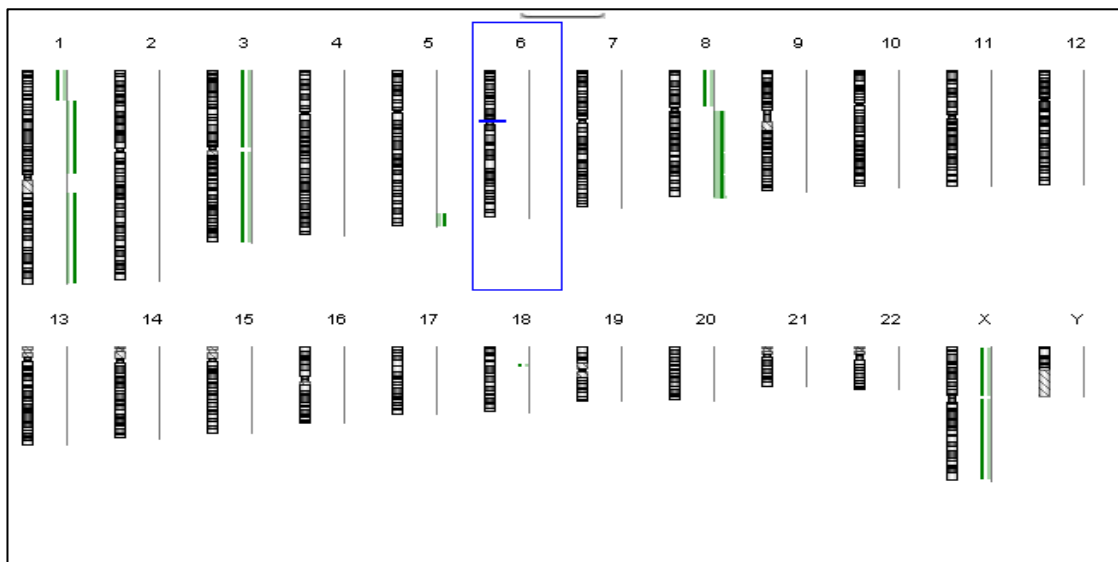
Figure 3.6 Array-based CGH ideograms of chromosomal aberration in primary UM

Genomic view illustrating abnormalities of all chromosomes with alterations involving chromosomes 1, 3, 8 (all classically associated with UM) in the presence of normal copy of chromosome 6 and places this tumour into the category of group 4. The bar to the left of the zero line represents deletion and the bar to the right of the zero line represents chromosomal gain.

Images output from Agilent Genomic workbench v7.0.4, and ADM2 algorithm was used to detect all the CNAs

3.2.5 Overview of the findings of aCGH analysis for the 137 UM series

By subdividing the results of the aCGH for the 137 UM in this series into groups based on the category of chromosome 6 change they had (or did not have), it was found that approximately 60% of all UM cases had some abnormality of chromosome 6, a figure higher than reported in most studies (Prescher et al., 1990; Gordon et al., 1994; Speicher et al., 1994; Becher et al., 1997; Sisley et al., 2000; Naus et al., 2001; Kilic et al., 2006, Singh et al., 1994; Prescher et al., 1995; White et al., 1998; Damato et al., 2009). It was observed that amongst UM with abnormalities of chromosome 6, the various groups representing the types of changes were equally represented affecting approximately 20% of the cases (figure 3.7).

Percentage of chromosome 6 changes

■ Group1   ■ group2   ■ group3   ■ group4

Group1 (28/137) — 20%
Group2 (29/137) — 21%
Group3 (28/137) — 20%
Group4 (52/137) — 39%
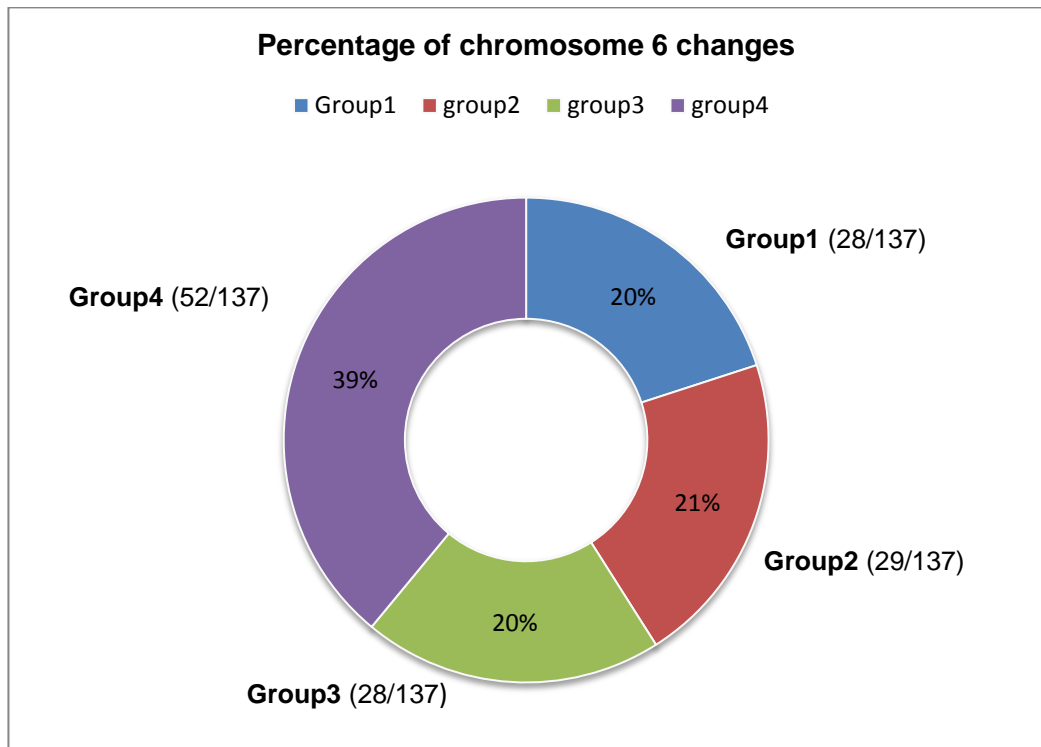
Figure 3. 7 Classification of the types of chromosome 6 abnormalities in a series of 137 UM.

The series was subdivided, without prior knowledge of the tumour location, on the basis of the type of abnormality if present for chromosome 6. The 3 groupings for chromosome 6 were roughly equally represented amongst the series.

3.2.6   Association of chromosome 6 with 1, 3 and 8 changes

The evidence for the non-random involvement of chromosome 1, 3 and 8 is well documented, all have been implicated as indicators of poor prognosis, and M3 and 8q+ are often reported as occurring together in association in up to 50% of UM (Sisley et al., 1997). In this current series of 137 UM, the frequency was as follows: 1p-/q+ (40%), M3 (66%), 6p+/q- (60%), 8q+(75%), 8p- (30%) figure 3.8.
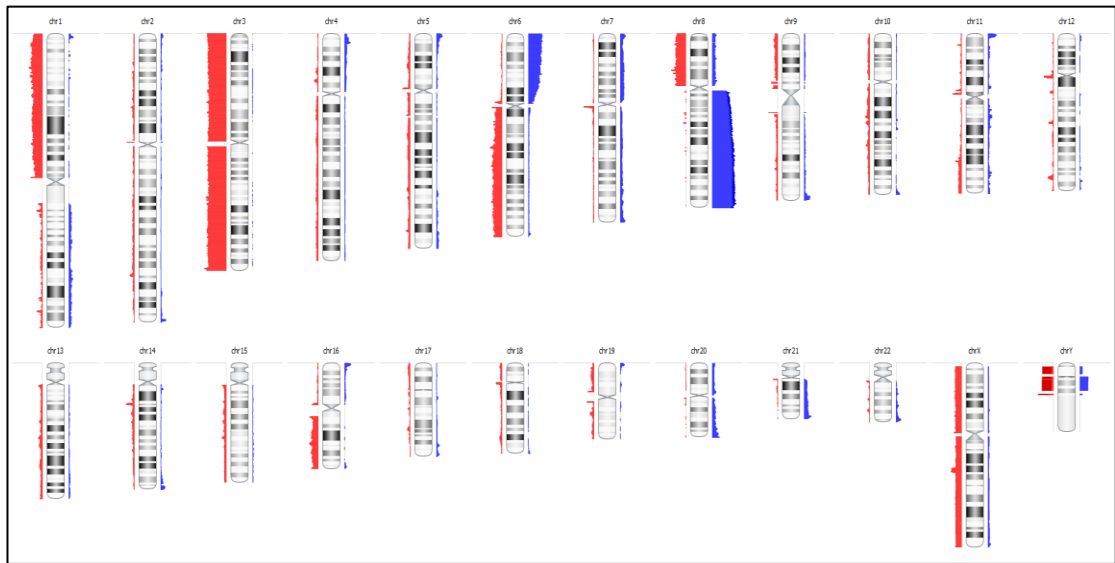
Figure 3.8 genomic view ideogram for common copy number aberration among 137 primary UM tumours

The figure demonstrates the frequency of commonly aberrant regions plotted as a function of their chromosomal positions. Blue bars to the right of the chromosome represent amplifications, and red bars to the lefts represents deletions. The heights of the bars demonstrate the frequency of alterations among the cases. This mainly encountered losses of 1p, M3, 6q, 8p, and gains of 6p, and 8q.

All CNAs are detected using the FASST2 algorithm

The observed incidence of involvement for chromosomes 1, 3, 6 and 8 in this series of 137 UM is comparable to the frequency reported in a previous study using the same customised aCGH (Hammond, et al; 2015), and is not altogether surprising, as this current study represents an extension of the original investigation, now including almost twice the number of UM allowing for a more comprehensive interpretation of the data.

Analysis of the series to compare the association between chromosome 6 changes and those of chromosomes 1, 3 and 8, found that gain of 6p was not mutually exclusive to M3, as had been reported previously, UM with M3 were however more likely to fall into the groups where there was no gain of 6p (groups 3 and 4). It was also apparent that 8q+ with or without M3 was found in the majority of cases in group 2 (Table 3.1). Detailed breakdowns of the relationship for all chromosomes within each group are presented in figures 3.9 -3.12.

	Chromosome 1 Changes	Monosomy 3 (M3) and partial losses	Changes of chromosome 8
Group 1 (6p+) **Total cases= 28**	**1p-** : 8 cases (28%)	**M3**: 5 cases (17%) **Partial del**: 4 cases (14%)	**8q+**: 12 cases (43%) **8p-** :4 cases (14%) and 3 of these cases i(8q) associated with M3
Group 2 **6p+/6q-** **Total cases= 29**	**1p-** : 16 cases (55%) **1q+**: 7 cases (24%)	**M3**:7 cases (24%) **Partial del**: 6 cases (20%)	**8q+**: 27 cases (93%) **8p-**: 10 cases (34%)
Group 3 other 6 **Total cases= 28**	**1p-** :16 cases (57%) **1q+**:9 cases (32%)	**M3**: 24 cases (86%)	**8q+**: 21 cases (75%) **8p+/-** 19 cases (68%)
Group 4 no 6 changes **Total cases= 52**	**1p-**: 21 cases (40%) **1q+**: 2 cases (3.8%)	**M3**: 46 cases (88.5%) **Partial del**: 1 case only	**8q+**: 13 cases (25%) **i(8q)**: 28 cases (54%)

Table 3 1: demonstrating the relationship between different changes of chromosome 6 and abnormalities of chromosomes 1, 3 and 8 in a series of 137 UM analysed by aCGH.

Note: *percentage was calculated based on alterations of chromosomes 1, 3, 8 out of total number of cases in each group*
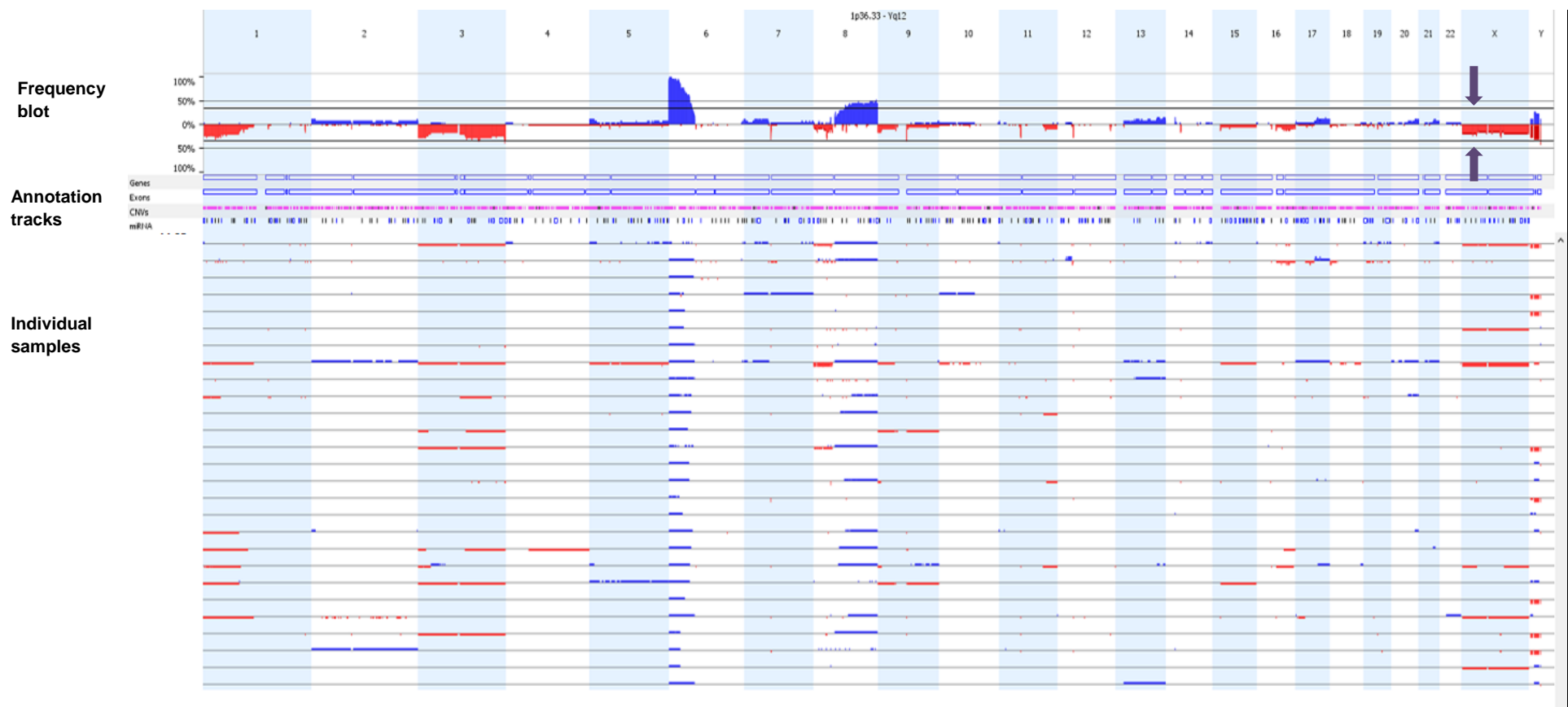
Figure 3.9 Genome and chromosome view demonstrate the association of group 1 (6p+) with chromosomes 1, 3 and 8 changes.

Genomic view displays the information on all of the chromosomes for different samples at once. The y-axis designates the percentage of the alteration in the selected samples at specific point along the genome. Horizontally along the top blue lines plotted above the 0% indicates copy number gain, and red indicate copy number loss events and plotted below 0% baseline. The black horizontal line marked with purple arrows in the figure above indicates the **Aggregate percentage cut-off** value. The figure delineates the frequency of 6p+, 1p-, M3, and 8q+ and it shows that 6p+ is highly associated with 8q+, with low percentage of chromosome 3 changes.

Images output from Biodiscovery's Nexus v7.5, and FASST2 algorithm was used to detect all the CNAs
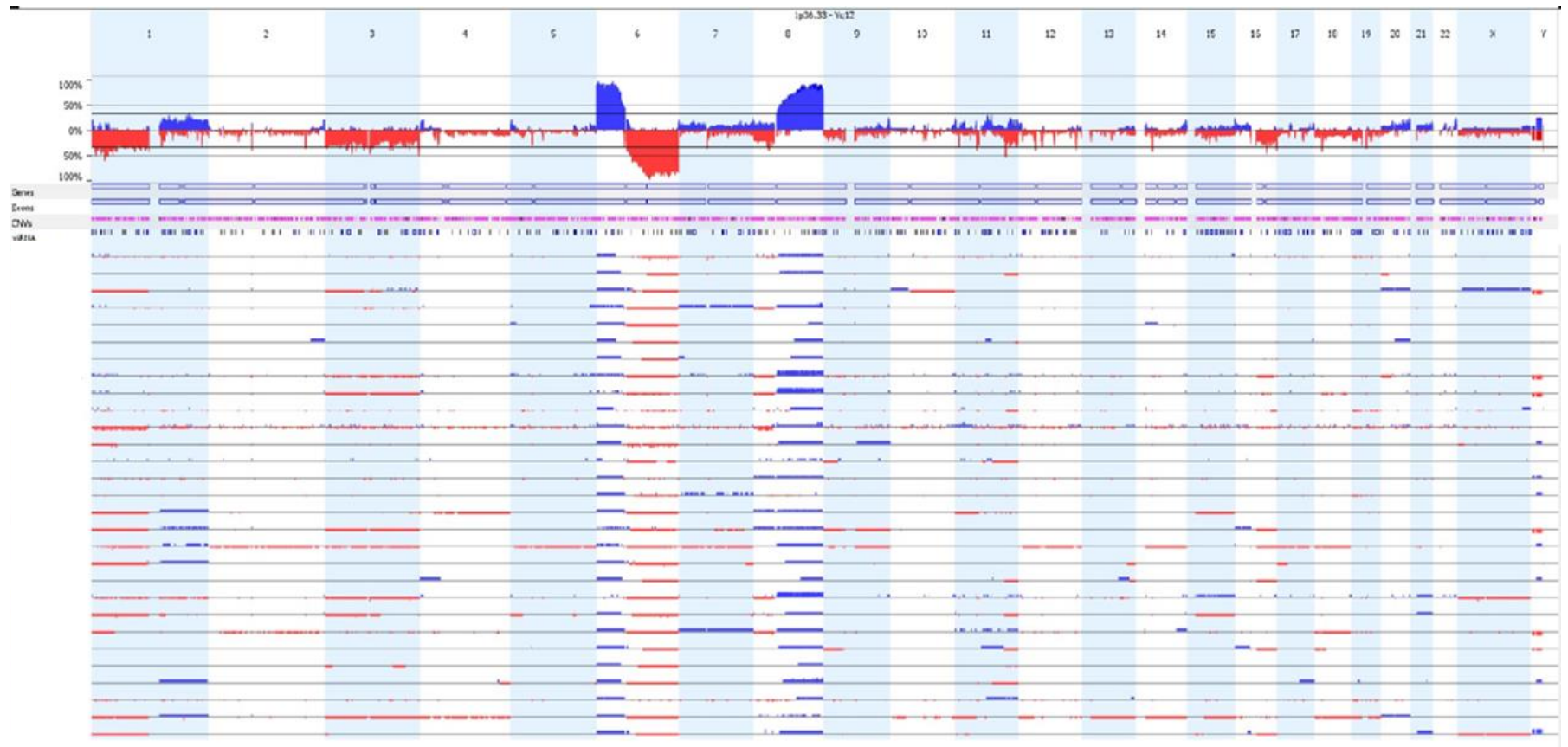
Figure 3.10 Genome and chromosome view demonstrate the association of group 2 (6p+/6q-) with chromosomes 1, 3 and 8 changes.

Genomic view displays the information on all of the chromosomes for different samples at once, horizontally along the top blue lines indicates copy number gain and red indicate copy number loss events. The figure above illustrates the frequency of 6p gain/q loss with chromosomes 1, 3 and 8 changes.

Images output from Biodiscovery's Nexus v7.5, and FASST2 algorithm was used to detect all the CNAs
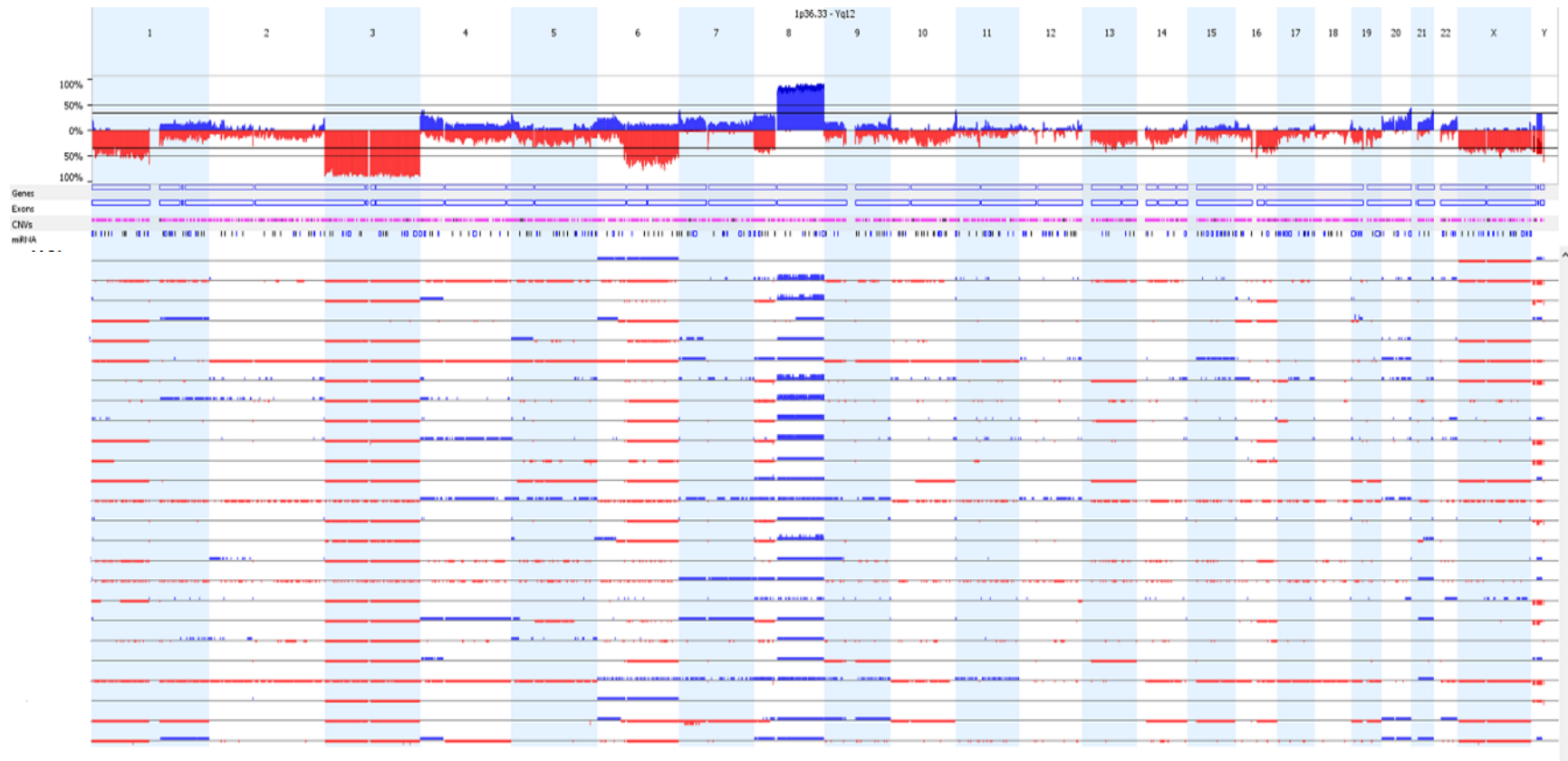
Figure 3.11 Genome and chromosome view demonstrate the association of group 3 with chromosomes 1, 3 and 8 changes.

Genomic view displays the information on all of the chromosomes for different samples at once, horizontally along the top blue lines indicates copy number gain and red indicate copy number loss events. The figure above illustrates the frequency of chromosome 6 abnormalities with chromosomes 1, 3 and 8 changes.

Images output from Biodiscovery's Nexus v7.5, and FASST2 algorithm was used to detect all the CNAs
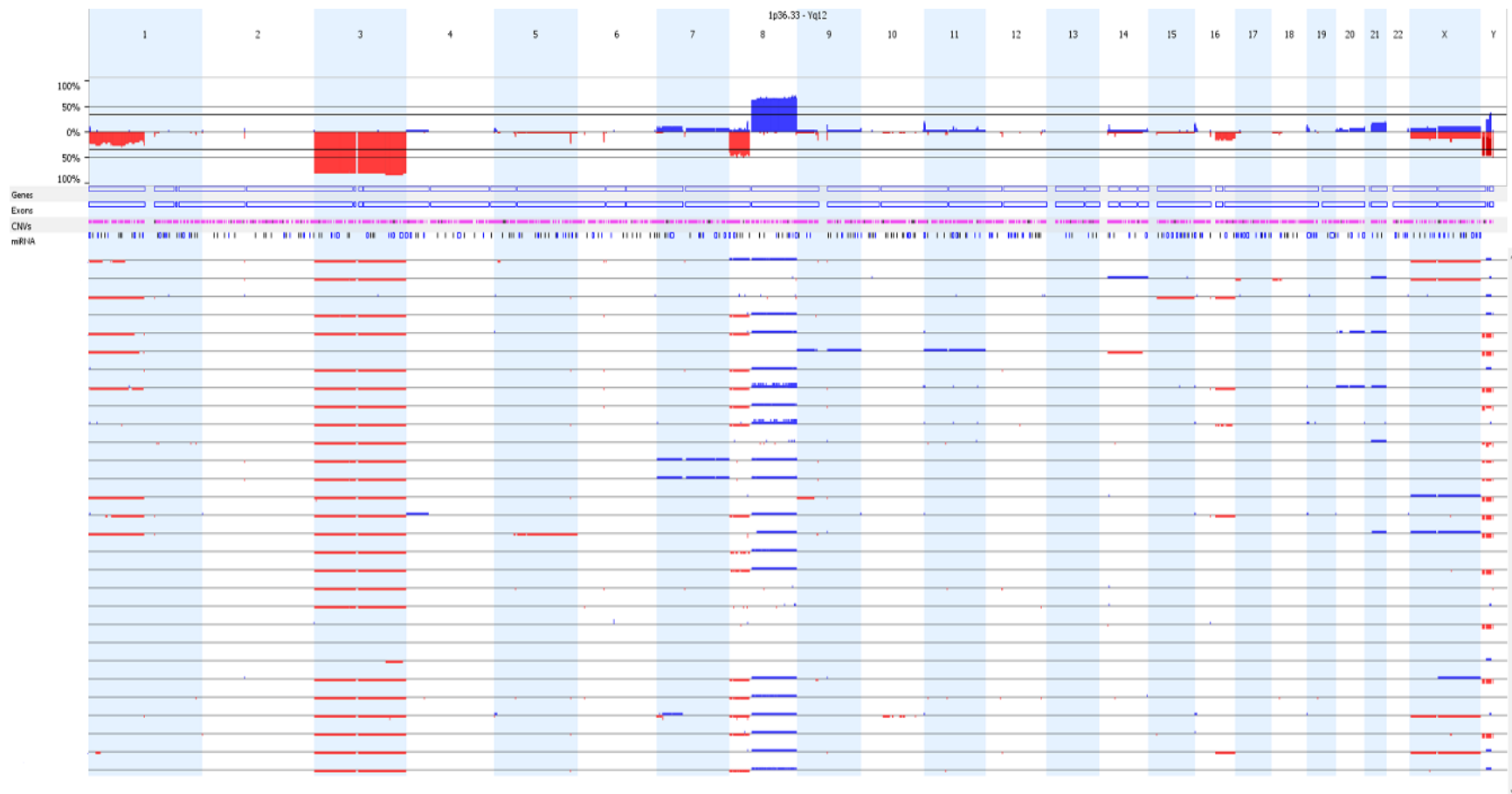
Figure 3.12 Genome and chromosome view demonstrate the association of group 4 with chromosomes 1, 3 and 8 changes.

Genomic view displays the information on all of the chromosomes for different samples at once, horizontally along the top blue lines indicates copy number gain and red indicate copy number loss events. The figure above illustrates an example of the frequency of chromosomes 1, 3 and 8 abnormalities in the absence of chromosome 6 changes.

Images output from Biodiscovery's Nexus v7.5, and FASST2 algorithm was used to detect all the CNAs

3.3 Genetic biomarkers as predictors of survival; using Kaplan-Meier analysis amongst the classified groups

Survival analysis was performed to confirm that this current series of UM (137 cases) had similar survival based on the use of genetic biomarkers to determine prognosis. Survival analysis in this study was generated using the Kaplan –Meier feature within the Nexus v8.0 and assessed patient survival based on their involvement of chromosome 6 changes. Analysis measures survival function from diagnosis to patient death for every patient in the selected groups. The follow up range for group1 was (4-169 months) average 69.8 months with 69.2% survival average, group 2 with average 62.53 months ranged (2-200 months) follow up, and 44.4% survival average, group 3 follow up range (11-187 months) average 41.36 months with 26.08% survival average, in addition to group 4 with (2-123 months) average of 37.6 months and 32.75% survival. The survival data showed that group 3 with mainly 6q loss, M3 and 8q gain have the worst prognosis, followed by group 4 with M3 and 8q gain, while group 1 with 6p gain showed better prognosis and group 2 with i6p presented an intermediate survival as illustrated in figure 3.13A. When survival analysis was reworked to include only patients known to have died from metastasis or those still alive (ie exclusion of patients with deaths unrelated to UM or where the cause of death was unknown), figure (3.13B) the survival was clearly increased for group 1 and for group 2 it became clear the prognosis was more intermediate. There was little change for groups 3 and 4 confirming the patients in these groups mainly dies because of metastasis and that these associations predict a poor outcome.
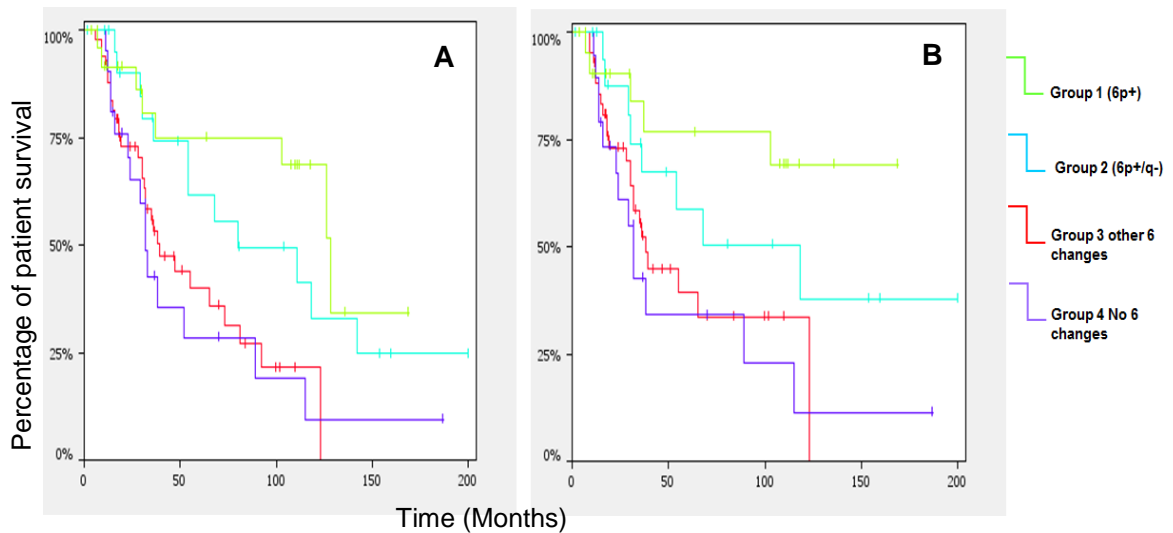
Figure 3.13 Kaplan-Meier curve display of the pattern of survival rates over time, and indicate the disease specific mortality among the groups.

Survival analysis considered all deaths for each group, and calculates the chance of patients dying from UM or the chance of surviving at particular time. **A**. Analysis measures survival function from diagnosis to patient death. Group 1 with 6p gain only shows a better survival rate compared to the other groups, while group 2 with i6p tend to have an intermediate survival, group 3 with mainly 6q loss, M3 and 8q gain presents the worst survival followed by group 4 in the absences of chromosome 6 changes. **B**. Analysis measures survival function from diagnosis to patient death from UM metastasis only, showing groups 1 and 2 presenting a better survival compare to group 3 and 4.

3.4   Clustering of the UM primary tumours using Nexus software

In the previous sections the UM in the series have been grouped on the basis of abnormalities of chromosome 6 which was determined by assessment of individual array profiles. Within each of the 4 groups there was a random distribution for the involvement of chromosome 1, 3 and 8. To look in more detail at the pattern of chromosome 6 changes in relation to those of the other chromosomes, the UM in the series were clustered by similar aberration profiles using a complete linkage hierarchical clustering algorithm. The analysis has as its basis changes of chromosome 6 for each cluster and then determines the most represented alterations associated with each cluster. Each cluster indicates the similarity in aberrations for chromosomes 1, 3 6 and 8, and helps understand the pattern in the data set.

The software deals with variations in the quality of each array (in terms of hybridization efficiency and specificity) and terms it mosaic data, by using a structure with multiple scales to build a hierarchy of data points with a specified threshold. The largest cluster within the series, representing 68% of UMs, was where all of the UM had M3, 6p+/q-, and 8q+ with 1p deletions. Despite the fact that clustering took an unsupervised approach (i.e. no chromosome abnormality selected), the analysis identified a small cluster (2 UM) where the only change was 6p gain, and therefore confirmed that changes of 6p could be considered as a differential factor among the tumour series. In total 8 clusters were identified and the details are presented in Figure 3.14 and confirm that the relationship between chromosomes 1, 3, 6 and 8 is a complex association.
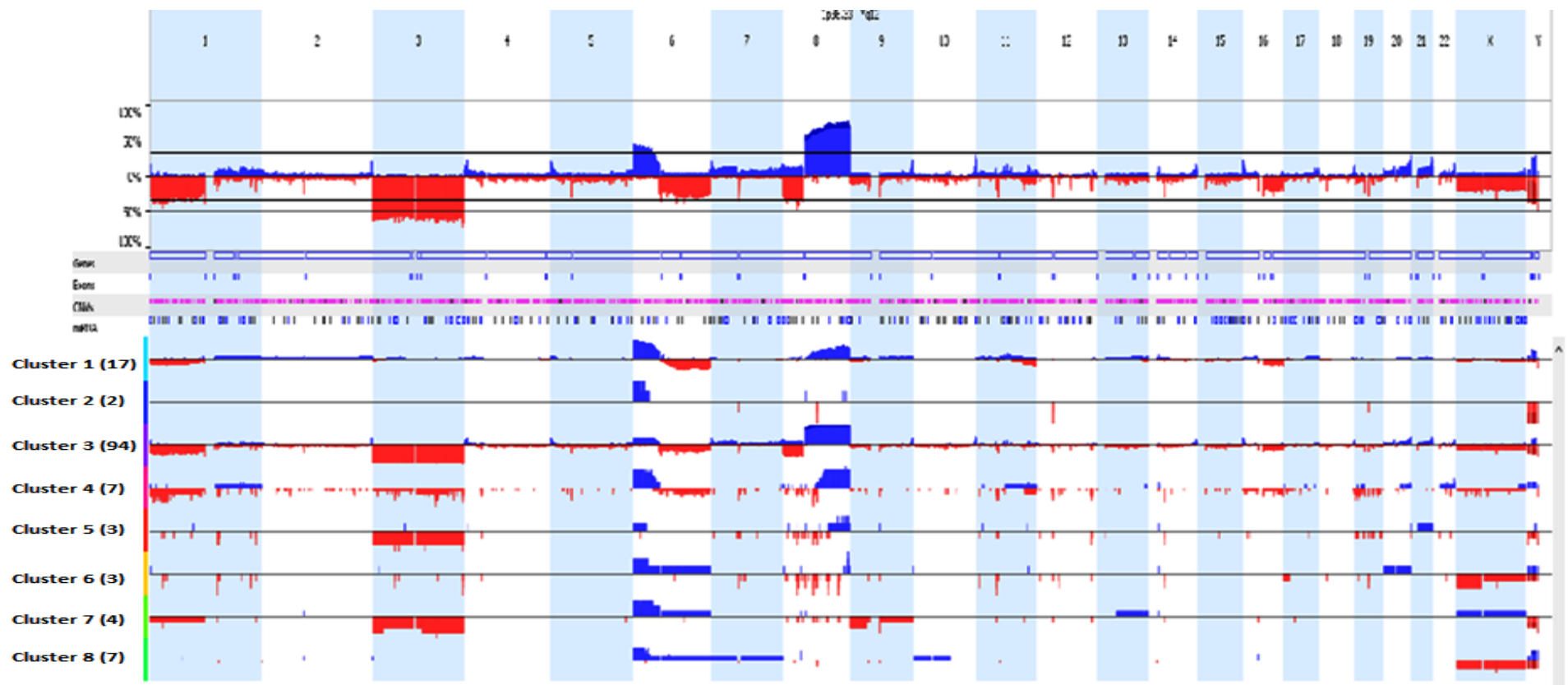
Figure 3.14 Genomic view and complete hierarchical clustering, demonstrate the clustering groups of the entire UM cases.

Panel A, genomic view represent samples were clustered into groups with different aberration profiles using complete linkage hierarchical clustering algorithm. The copy number ratio was selected when clustering was performed to displays the copy number frequency plot for each cluster group. The first cluster (cluster1) presented the involvement of 6p gain, q loss in the absence of 3 abnormalities. Cluster 2, were the smallest and contain two tumours with only 6p gain, with no other changes. The largest was cluster 3, where it shows M3 with 8q+/p- and 1p deletion in the presence of 6 alterations. The rest of the clusters demonstrate the involvement of 6p either with 3 and 8 changes or without. The most unstable with SCNA affecting most chromosomes was cluster 4, and clusters 4, 5 and 6 all seemed to have high but focal abnormalities of chromosome 8, in particular the short arm.

3.5   Genetic instability in UM

Unlike most solid tumours, UM do not usually demonstrate high levels of Genetic Instability (GI) (Cross *et al.*, 2003). In the current series it was thought aneuploidy also considered as GI, could be useful in tumour characterisation. Of the UM in this series approximately 17.5% (24/137) had a range of 60-90% of gain and loss of arm-level and focal somatic copy number alterations (SCNAs). Increased GI were assessed by looking at percentage of the average number of copy number alterations (ANCA) by measuring the number of chromosomal copy alterations per tumour (Ried *et al.*, 1999)**.** ANCA value for this group was 9 it was measured by dividing the total number of copy alterations (gains and losses) in this group of GI tumours (24) by the total number of tumour analysed (137). Previous studies have suggested that the presence of M3 associates with a tendency for increased aneuploidy and GI in UM (Ehlers et al; 2008). In this study, most of the highly GI tumours presented with equal percentage of 3, 6, and 8 abnormalities (Figure 3.15).
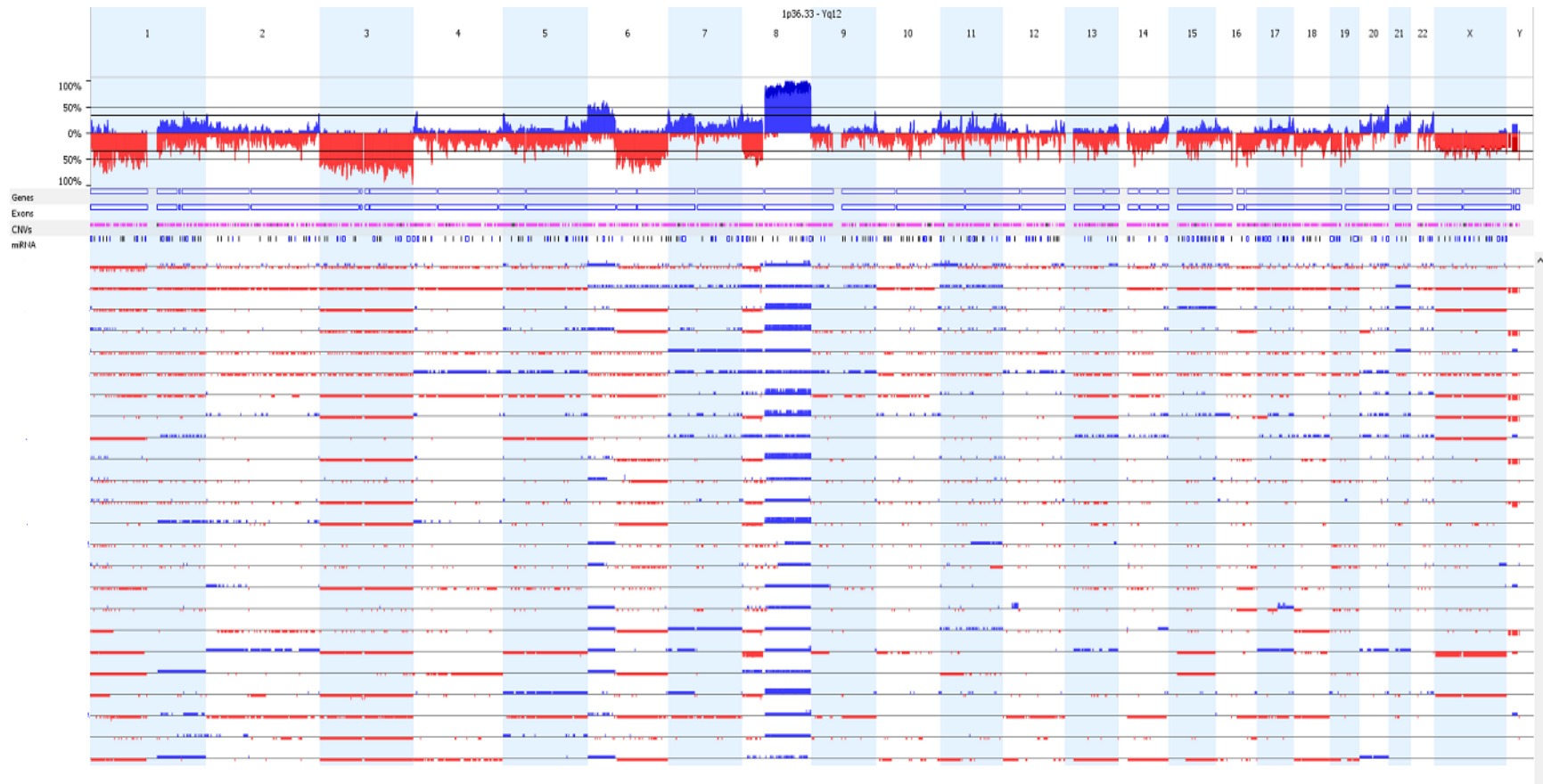
Figure 3.15 Genome and chromosome view demonstrate genetically instable tumours

Genomic view displays the information on all of the chromosomes for different samples at once. The y-axis designates the percentage of the alteration in the selected samples at specific point along the genome. Horizontally along the top blue lines plotted above the 0% indicates copy number gain, and red indicate copy number loss events and plotted below 0% baseline. The figure illustrates the presence of chromosomes 3, 6 and 8 alterations with highly genomic instable tumours.

3.5.1 Chromothripsis as a genetic marker

Chromothripsis is a catastrophic process leading to the generation of complex genomic rearrangements, with multiple genomic alterations effecting one or few chromosomes, and is strongly linked to poor prognosis (Hirsch et al., 2013). As part of the criteria suggested by Rausch and colleagues, at least 10 copy number changes need to affect a single chromosome (Rausch et al., 2012). Notably, two tumours in this series (Mel 57, Mel 38) were found to have a possible chromothripsis-like aberration patterns, where chromosome 5 had shattered into a massive number of pieces and reassembled into complex genomic rearrangements that differ from other chromosomal aberrations (Figures 3.16, 3.17, 3.18). For Mel38 the chromothripsis event resulted in an overlapping rearrangement of chromosome 5 that was randomly distributed across the genome rather than clustered at focal regions. Overall, the tumour (Mel38) presented with a high level of deletions and amplifications across the genome, and clinically represents very poor prognosis. These complex genomic rearrangements have not been previously reported in UM.
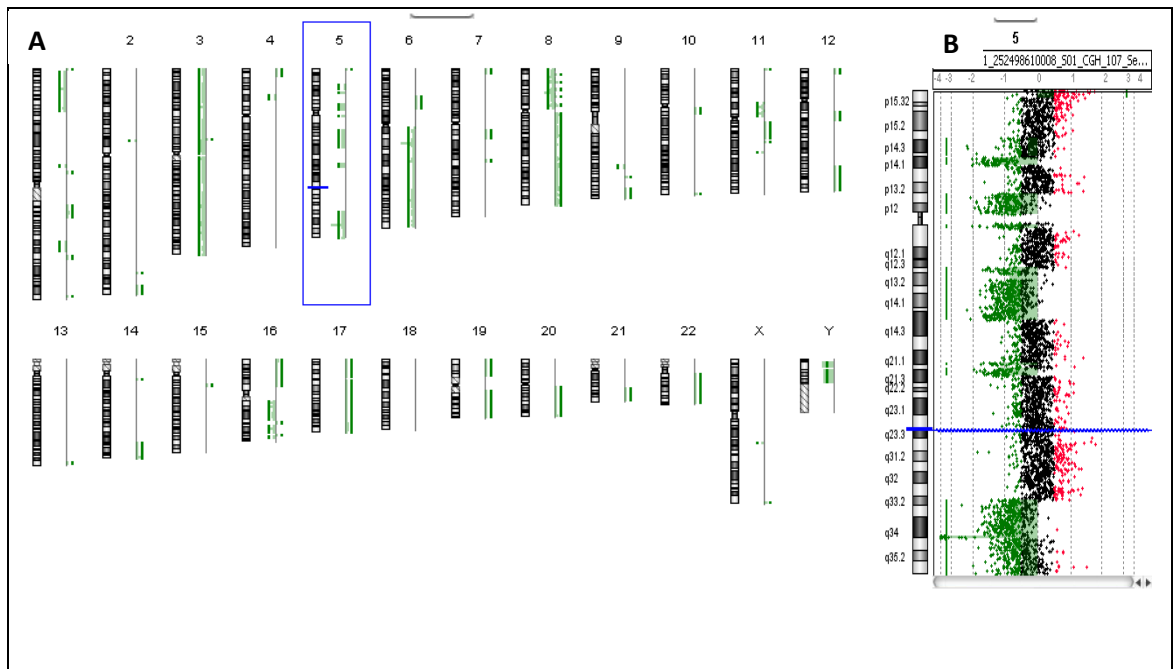
Figure 3.16 Array-based CGH ideograms of chromosomal aberration in primary UM.

The figure illustrates the chromosomal gains and losses in UM case**. (A)** genomic view of aCGH profile, showing the presence of genome-wide distributed chromosomal alterations. **(B)** Illustrates a chromosome 5 view with the possible presence of chromothripsis-like aberration patterns that are confined to segmental regions (*Images output from Agilent Genomic workbench v7.0.4, and ADM2 algorithm was used to detect all the CNAs)*

Note; The chromothripsis-like aberration patterns for chromosome 5 were detected with both Agilent and Nexus software.
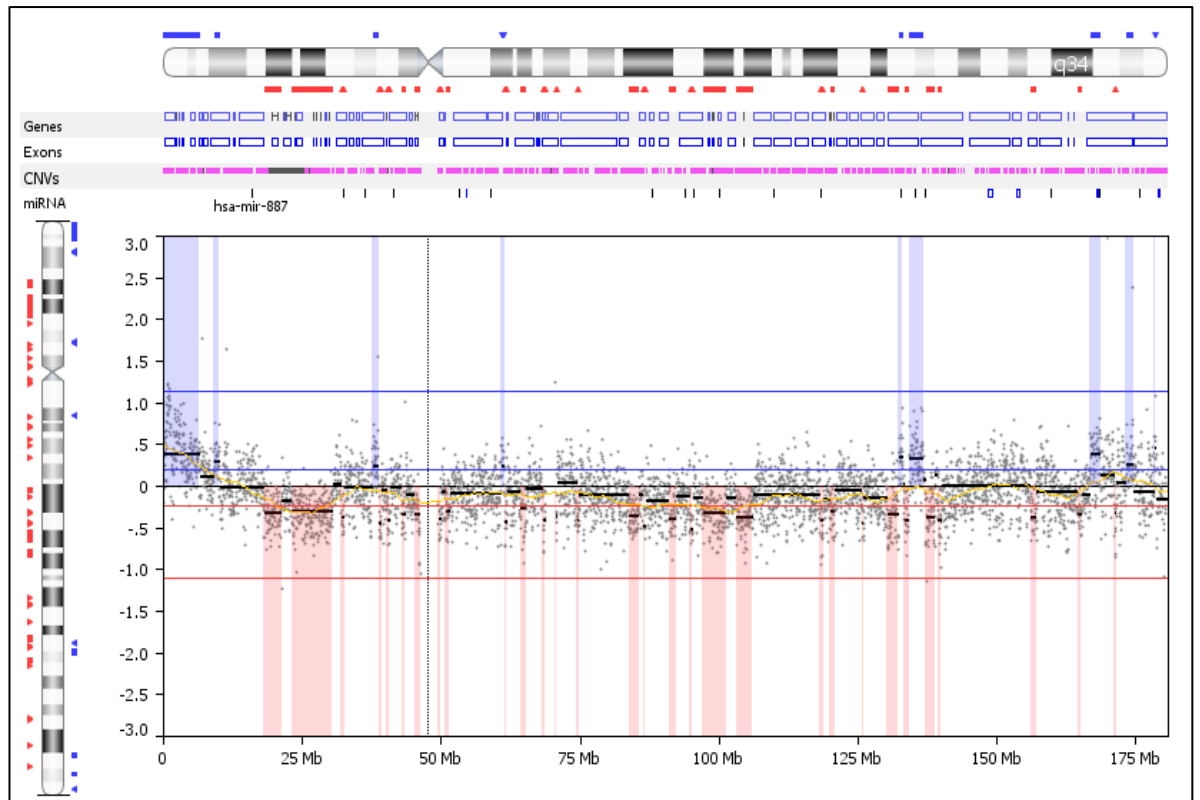
Figure 3.17 High-resolution graphical view representative chromothriptic-like events detected in Mel38.

Higher resolution graphical views of Chromosome 5 showing the altered regions of copy number gains and losses defining a chromothriptic-like event using the FASST2 algorithm, represented by red triangle to the left (loss) and blue triangle to the right (gain) of the chromosome. The x-axis represents full length of chromosome 5, and y-axis represents the $\log_2$ ratio of tumour/reference. The dots represents individual probes, where the horizontal blue line above zero represents the detection of copy number amplification with corresponding blue shaded area above, and the red line below the zero line represent the detection of single copy deletions with corresponding red shading below the zero line.
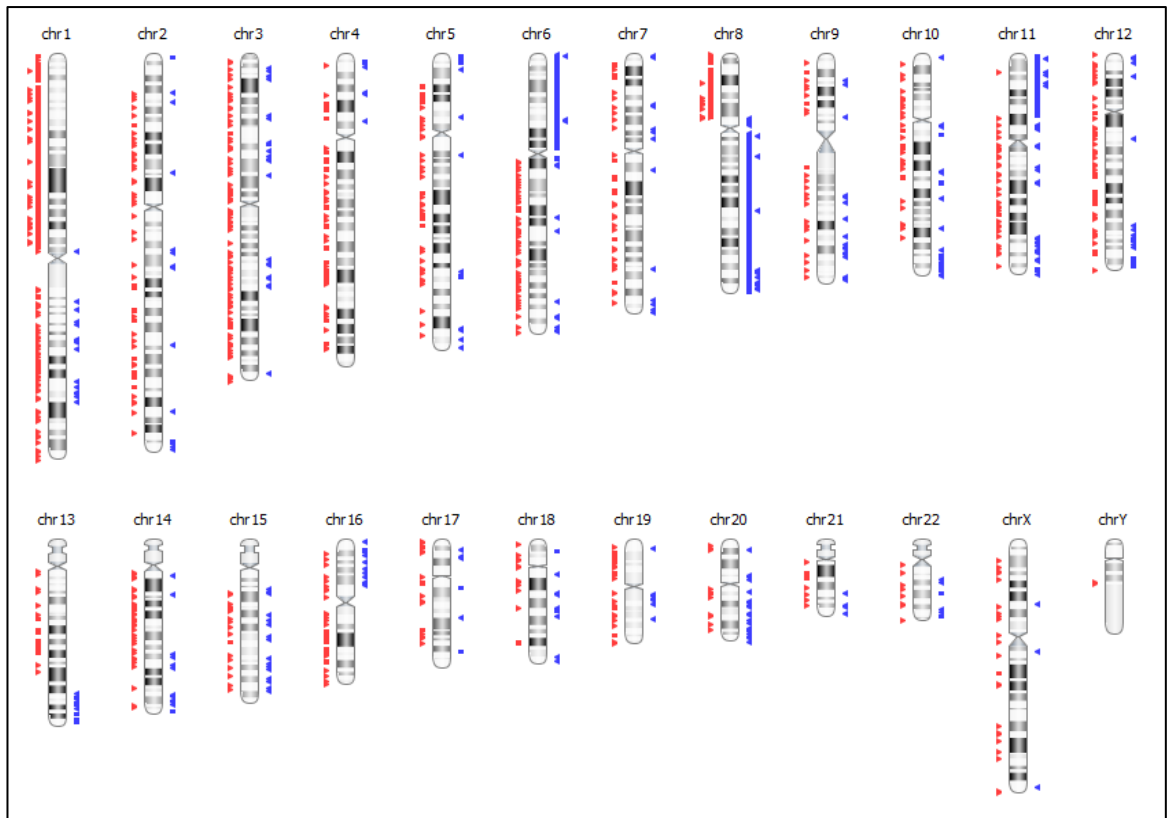
Figure 3.18 Graphical whole-genome views of copy number aberrations in Mel 38.

Whole genomic view represents highly aberrant regions called by FASST2 algorithm, are presented by blue tringles or lines to the right of each corresponding chromosome (amplification), and the red lines or triangle to the left of each chromosome (deletion). High level of amplification and deletions represented by double blue and red line or tringles respectively, possibly indicating multiple chromothriptic-like events affecting the majority of the chromosomes.

3.6 Discussion

The use of archival fresh frozen tissue is generally considered to be the best for a wide range of chromosomal analyses as the DNA extracted is of a much better quality than that obtained from FFPE. In this study, a specifically designed aCGH was used to detect the chromosomal abnormalities in a large series of primary UM that included tumours known to have metastasised. The series of patients had comparable incidences reported amongst UM for involvement of clinical features, confirming that there was no bias in our selection of UM to study (Toth-Molnar et al., 2000, Gill and Char, 2012). Furthermore the incidence for chromosomal involvement was comparable to past reports (figure 3.8) (Sisley et al., 1990, Sisley et al., 1997, Aalto et al., 2001, Loercher and Harbour, 2003, Kilic et al., 2005, Damato et al., 2010, Cassoux et al., 2014, Hammond et al., 2015). Regardless of the methodology used M3 with 8q is consistently associated with a worst prognosis. Most of these earlier studies however have not used a technique that has been designed to specifically consider the known genetic alterations of UM. In this investigation a customised design aCGH was used that had been developed by Dr Hammond to focus on known chromosomal regions implicated in UM (Hammond et al., 2015). Therefore, the data form this study could provide a better insight into our understanding of the implications of these alterations. Alterations of chromosome 6 in UM can result in a gain of 6p and a loss of 6q (Aalto et al., 2001) and in this series 61% of UM had an abnormality of chromosome 6 which is more frequent that reported in previous studies (Prescher et al., 1995; White et al., 1998; Onken et al., 2004; Ehlers et al., 2008; Landreville et al., 2008). The higher frequency in this series maybe because some other methodologies used underrepresented chromosome 6 changes e.g. MLPA, since a study using MFISH found that approximately 70% of UM have alteration in chromosome 6 as the most widespread alteration in UM, ((Sisley et al., 2006). It was found in this series that there was a roughly equally split for abnormalities affecting just the p or q arm or both arms (groups 1-3).

Past studies have suggested structural abnormalities of chromosome 6 occur without changes of chromosomes 1p, 3 and 8, so much so that 6p gain and M3 were proposed to be mutually exclusive events, and a bifurcated pathway for tumour progression of UM was suggested by Parrella in 1999 (Kath et al., 1993, Prescher et al., 1995, White et al., 1998, Parrella et al., 1999, Cross et al., 2005, Hughes et al., 2005, Landreville et

al., 2008, van Gils et al., 2008). As an extension of this observation, most previous studies link 6p gain to a more favourable prognosis associating 6p gain with non-metastasizing tumours, while M3 occurs mainly in metastasizing tumours. Alternatively 6p gain may present an earlier stage of a pathogenic sequence with an alternative genetic pathway (Sisley et al., 1997, Hoglund et al., 2004, Ehlers et al., 2008, Landreville et al., 2008). In this current investigation only 29/137 UM did not have M3, and all of these cases had 6p gain in some form (cluster 1, 2, 6 and 8) figure 3.17, which is suggestive of a bifurcated pathway. However for all the other cases in the series there was involvement of M3, and indeed amongst those UM without M3, but with 6p gain there were changes of chromosomes 1 and 8, and only 1 cluster (cluster 2) representing just 2 UM presented with just 6p gain. Furthermore, the sequence of association in the current study delineates that 6p gain followed by 8q gain and M3 can occur in the same tumour, which has been suggested by Sisley (2000). Therefore, the current analysis disagrees with a bifurcated pathway model, corresponding to the previously observed close association between M3 and 6p gain occurring in the same tumour (Prescher et al., 1990; Sisley et al., 2000; Tschentscher et al., 2000; Aalto et al., 2001; Hughes et al., 2005). However, the suggested results in the current study do not necessarily reflect the sequence of events within the tumour. Although a clear association between isochromosome 6 formation (group 2) with M3 and i(8q), was found as previously suggested by Prescher et al., proposing that the formation of isochromosomes in UM is more associated with the loss of a DNA copy of chromosome 3 (M3) (Prescher et al., 1995) and the disease prognosis. At the same time, this study delineates that the coincidence of the isochromosome formation of 6p and 8q could occur at any level of interaction between the groups and not necessarily with M3. Chromosome 6 rearrangement in group 3 was strongly associated with i(8q), M3 and 1p deletions, this group was genetically unstable. Such abnormalities could indicate that alternative pathways may be available in the tumour progression of the classified groups, and shows an involvement in the two genetic pathways that have been proposed by Sisley (2009). In the absence of chromosome 6 abnormalities, the changes to chromosomes 3 and 8 showed approximately the same percentage of abnormalities, although most previous studies indicate that M3 is the primary event in the origin of subgroups in UM (Sisley et al., 1990; Prescher et al., 1995; Damato et al., 2007; Shield et al., 2007., Sisley et al., 2009). Since chromosome 6 was detected in high frequency in our series of primary UM, it would be reasonable to suppose that chromosome 6 alterations might occur prior to 3, and this suggests that chromosome 6 may represent a future subgroup of UM with specific prognostic implications. Even

when the data was unsupervised, clustered findings demonstrate that the biggest group was alteration M3 and 8q gain in addition to 6 involvement.

These findings suggest that there is considerably cross over in the genetic alterations and that chromosome 6 alterations are not independent of the other changes and the relationship is complex.

In term of prognosis although abnormalities of chromosome 6 have not been independently associated with survival previously, this study demonstrates the association of 6p gain with patient survival. Overall, the patients in this study have a long follow up (21 years approximate average). It was found that progression-free survival was longer for group 1, and shorter for group 3 with worst prognosis for patients when liver metastasis was the end point. Therefore, the data suggested clear differences in the association with other changes including 1, 3 and 8, and potentially differences in the regions of 6p gained in subgroups of UM. Nevertheless, the data suggested that 6p gain has a role in UM prognosis as well as that of chromosomes 3 and 8, certainly in groups 2 and 3. Although the association of 6p with a better prognosis was confirmed in this study, some of the tumours has a very poor outcome when harbouring only 6p gain with M3 and i(8q), and one case presented with 6p gain and 8q gain only, where the patients developed a multi-hepatic metastasis with very poor prognosis. Therefore, care should be taken when interpreting the relationship between 6p+ and other changes related to tumour progression. In UM, 6q deletion was considered to be a late event in tumour progression (Prescher et al., 1990), and associated more with poor prognosis and tumour metastasis (Aalto et al., 2001). In this study, a total of 36% of the cases showed an involvement of 6q, although the presence of 6q in group 3 associated more with ploidy and 8q associated with more unstable in clustering analyses, and patients belong to this group showed decreased disease free interval presented with metastatic UM. These finding are in total agreement with previous investigations suggesting the association of 6q with tumour metastasis (Singh et al., 1994, White et al., 1998, Damato et al., 2009)

3.6.1 Genetic instability in the UM primary tumours

Although UM is characterised by a low degree of aneuploidy and the karyotype changes are less complex compared to other solid tumours (Papadopoulos et al., 2002, Cross et al., 2003) , this study supports the fact that most of UMs are quite

stable; even when using a powerful technique like aCGH. Most of the UMs in this series had a high level of stability, with a low incidence of chromosomal alteration. Despite the relatively low number of cases, there have always been some UMs with a higher level of instability. Array CGH indicates a variable level of genomic instability in primary UM, with recurrent chromosomal rearrangements. The accumulation of multiple genetic alterations as genomic instability on more than 18% of the genome was reported in this study, with varying levels of occurrence. Previously it has been assumed that tumours with M3 contain more aneuploidy than disomy 3, or 6 and 8 changes, suggesting that presence of M3 leads to accumulation of aneuploidy and increase genomic instability in UM (Ehlers et al., 2008). In this study however, most of the highly genomic instable tumours presented with equal percentage of 3, 6, and 8 abnormalities. The majority of the small subset of tumours with higher levels of genomic instability was correlated more with group 3 and some with group 2; thus, the presence of tumour instability and chromosomal aneuploidy was found to be associated more with 6q aberrations, and this suggests the possible contribution of multiple genes in tumour progression. Indeed a potential new subtype was identified whereby random changes of chromosome 6 appeared to associate with unusually highly unstable UM (Figure 3.15).

The ANCA index, however, could present a valid parameter for the assessment of tumour progression, where the correlation of genomic instability and the tumour aggressiveness was clearly demonstrated previously (Carter et al., 2006, Weaver and Cleveland, 2006, Lee et al., 2011, McGranahan et al., 2012).

Moreover, complex genomic arrangements with a number of chromosomal alterations were noticed in a few cases. Including two cases presenting chromosome 5 with a massive genomic rearrangements and belonging to groups 2 and 3, this could be examples of a new phenomenon called chromothripsis, recently reported in 2011 by Stephens et al. The defining hallmarks of chromothripsis explain catastrophic cellular events where one or a few chromosomal regions are shattered into more than ten pieces and are reassembled incorrectly, with a reported occurrence in 2-3% of general cancers (Stephens et al., 2011). One tumour (Mel38) was found to have chromosomal overlapping rearrangements and randomly distributed across the genome rather than clustered in focal regions, which presented a different pattern from chromosomal aberrations previously described in primary UM. Although, this tumour was presented with very poor prognosis surviving 12 days only after liver metastasis was detected, Therefore, the presence of these complex genomic rearrangements in this study could suggest a new genetic marker in UM associated with rapid prognosis and metastasis.

In summary, this investigation suggests that there is not a clear bifurcated pathway in UM that depends on 6p gain with an alternative being driving by M3, the relationships between the interplay of changes of chromosomes 1, 3, 6 and 8 is complex. However, 6p does identify patients with better prognosis and 6q associated with worse prognosis. It is also apparent from this study that group 3 which had more 6q involvement, and also clustering where 6q involved had more unstable tumours, greater ploidy, and indeed the crises event of chromothripsis occurred to UM in this groups. Therefore it could be agreed that 6p does distinguish more on the basis of instability, and that increased genetic instability associates with later stages of tumour progression (Hanahan and Weinberg, 2011). More advanced metastatic tumours have more instability. This could drive genetic variation, creating genetically distinct subgroups of UM.

On this basis, it would be good to look in more depth at the genes affected and to consider the interplay between 6p and 6q rearrangements. Therefore, the structural rearrangement of chromosome 6 appears to be associated with the malignant progression of the tumour and identifying the breakpoints involved in these alterations may lead to identifying the genes responsible for such behaviour, which will be dealt with in more depth in chapter 4.

4 Chapter Four

Identification of candidate genes on chromosome 6, associated with primary uveal melanoma, by aCGH

4.1 Introduction

Gaining an improved understanding of the molecular genetics of UM and its potential to characterise subtypes, has an important role in the current understanding of the pathology of UM. Defining regions of amplified or deleted copy numbers in a DNA sequence can identify genes involved in tumour progression, and aCGH makes the assessment of these changes possible. Across the entire genome, Beroukhim and colleagues found that in the majority of cancers the most frequent SCNA (deletions or amplifications) are either very short genomic regions (focal), or the length of the chromosome (arm-level). Around 10% of the cancer genome was observed to be affected by focal SCNA, and it was thought that the occurrence of focal SCNA was more likely to coincide with high amplitude (homozygous deletion or many more copies), compared with whole arm events (Beroukhim et al., 2010). Focal SCNA would hence be statistically more likely to target particular genes, and from a research perspective the smaller and more defined the region, the easier it is to achieve the identification of target genes (Beroukhim et al., 2010).

Unlike many solid tumours UM is remarkably consistent for its pattern of chromosome changes affecting 1, 3, 6 and 8, however the actually driver genes involved are poorly understood, in part due to the fact that these changes involve whole arm events. Chromosome 6 although consistently implicated in UM has changes that are unlike those of M3 and 8q gain. since different changes can affect both arms, that can occur together, or in isolation, and importantly unlike M3 and 8q gain (which are whole arm events) there is more evidence for smaller regional changes affecting chromosome 6 (van Gils et al., 2008). In the previous chapter, a specifically designed high-resolution aCGH had been used to analyse how the different types of alterations of chromosome 6 affected patient outcome. The study confirmed that real differences could be attributed to the various changes of chromosome 6 in UM. These abnormalities of chromosome 6 are ideally suited to an aCGH approach, and by using a bespoke high resolution array it was hoped to identify recurrent focal SCNA, especially the small size aberrations that they might have been missed by previous investigations using lower resolution techniques, such as chromosomal CGH or even BAC arrays, and spectral karyotyping (Speicher et al., 1994, Naus et al., 2001, Sisley et al., 2006, Ehlers et al., 2008). In this chapter, the focus is on identifying candidate genes individual to the different alterations of chromosome 6 that could act as drivers and influence patient outcome. In the previous chapter, aCGH was able to establish the smallest area affecting 6p and 6q. The regions therefore of interest are possible oncogenes in the 6p12–6pter region,

and tumour suppressor genes on chromosome 6 long arm, particularly the region 6q 21–6q26. These regions highlighted in this current study, compare with previous regional identifications suggested in UM (van Gils et al., 2008), and in this section of the study identification of potential target "drivers" was undertaken.

4.2 Array CGH data analysis work-flow chart

In this study the amplification of 6p produced as a result of structural abnormalities extended for approximately 35Mb (6p12–6pter region), and in the main the whole arm of chromosome 6 was affected but a region of 45Mb (6q 21–6q26) was implicated. Despite aCGH refining the regional involvement, both of these regions are too large to immediately pinpoint the candidate oncogenes. Analysing aCGH data in combination with the Nexus software tool provides a validated shortlist of candidate genes on chromosome 6, through a combination of approaches to survey the measurable probability that SCNA were non-random events. Therefore, genes influenced eventually by these non-random SCNA represented a shortlist of candidate 'driver' genes, that can be examined further for potential relevance on the basis of their biological significance. The overview for the identification of candidate genes is summarised in figure 4.1, and in the subsequent sections the methodology is explained in more depth. The basis of aCGH aberration calling algorithms has been previously discussed in chapter 2 (section 2.3.6.9)
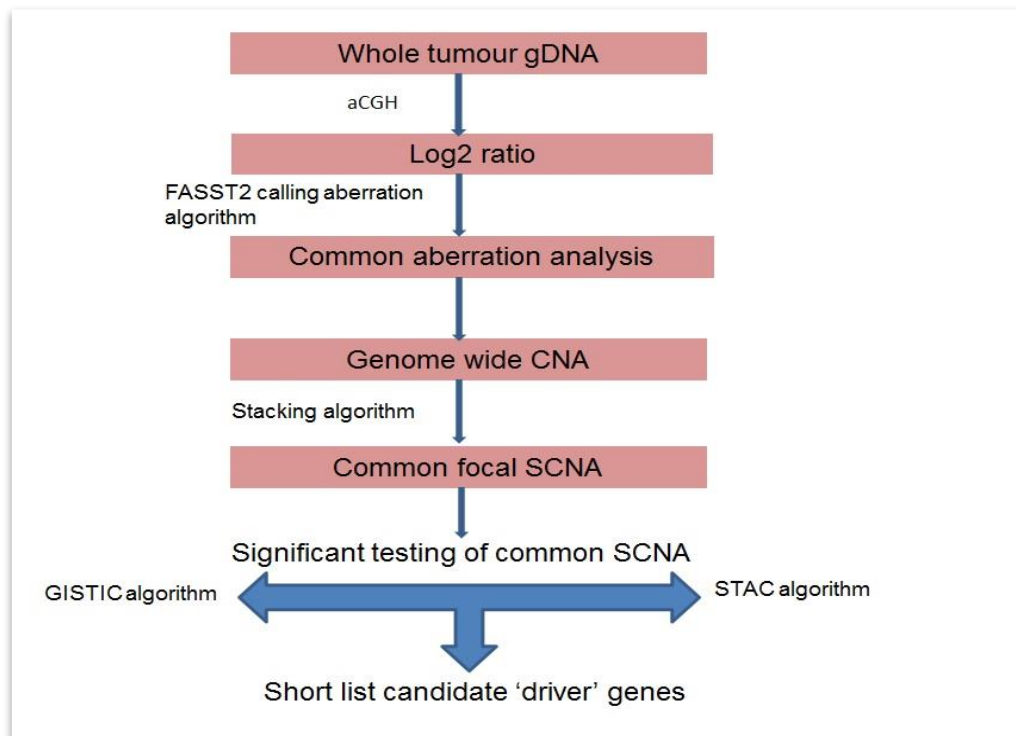
Figure 4.1 Overview of Array CGH work-flow a methodology utilized to identify the candidate genes in this study.

4.2.1 Identification of common focal SCNA

For simplicity sake, the strategy of Beroukhim and colleagues was adopted, whereby larger size SCNA of 5Mb or more (including whole arm events) were considered generally as gains or losses. Consequently, these larger SCNA events were differentiated from focal SCNA with a median length (1.8 Mb) which were introduced as amplifications and deletions (Beroukhim et al., 2010). Utilizing a stacking algorithm, all SCNA distinguished within particular genomic regions in a set of UM cases from each group were 'stacked' over each other to generate a frequency plot as represented in figure 4.3. Therefore, the highly altered segments or the common focal SCNAs can be "stacked ", which allows the minimal common region (MCR) of overlap to be identified amongst the SCNA covering that locus (figure 4.5). The MCR region is statistically highly likely to contain targeted genes (Beroukhim et al., 2010). Where the threshold frequency of focal SCNA was reduced to (20-30%) to increase the sensitivity of the data analysis (Figure 4.6)

4.2.2 Exclusion Criteria for Focal SCNA including *Germ-line Copy Number Variations*

Copy number variations (CNV) refers to a sequence of DNA found in germ-line DNA for which copy number differences can be distinguished between individuals that is "polymorphic". They are defined in the human genome as structural variations with a size > 0.5 to 1 kilobase (Valsesia et al., 2013). In spite of the fact that CNV are not confirmed to bring any direct pathological consequences , there are phenotypic variations reported where associations between CNVs and complex genetic traits (multifactorial disorders) and with disease susceptibility and development with phenotypic variation has been reported (McCarroll and Altshuler, 2007, Conrad et al., 2010). In this study to differentiate CNV from the focal SCNAs a comparison was made to differentiate CNV from the common focal SCNAs, comparison was made between the SCNAs identified in the study with known CNVs using the Database of genomic Variants, and all common focal SCNAs were found to be completely overlapped by CNVs. These were further examined for SCNA breakpoints and the frequency of aberrations using a high resolution methodology (http://dgv.tcag.ca/dgv/app/home; (Iafrate et al., 2004). To exclude SCNA from a subsequent analysis, they have to be identified as likely CNVs, which occurs only if they contain any of the following criteria: 1) they hold no known genes which are highly likely to have functional consequences; 2) they show deletion in some samples and amplification in others with the same identical pair of breakpoints as normal population variations; and 3) the aberration breakpoints for both 5' and 3' match precisely with known CNVs. An example of a CNV is demonstrated below in Figure 4.2 and findings related to a CNV in UM are discussed later in chapter 5.
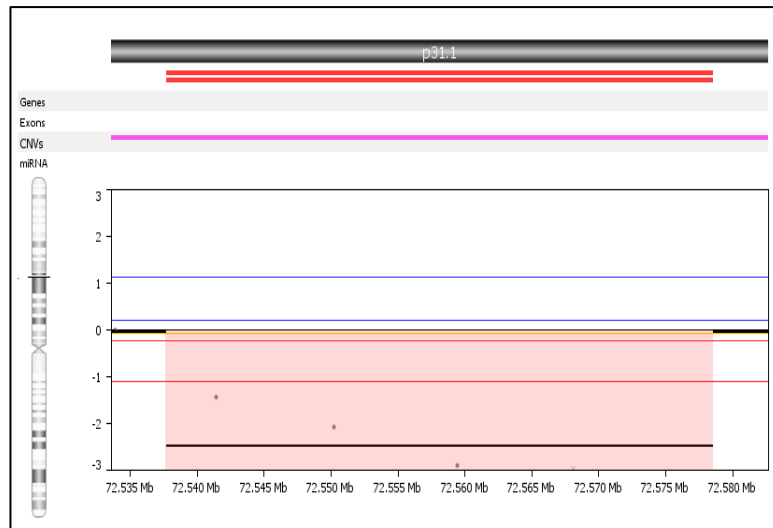
Figure 4.2 Regional deletion represented by Frequency plot showing an example of aberrant region that represents a copy number variations CNVs

Chromosomal ideograms represent UM case with focal deletion, the region below the vertical line represented by double red strips (pink shading below zero line) shows a regional deletion with 40Mb approximate size, lies completely within known CNV area (represented by the purple line) and contains no gene loci, it was therefore excluded from the analysis to be likely CNV.

Images output from Biodiscovery's Nexus v7.5, and FASST2 algorithm was used to detect all the CNAs and the known CNVs.

4.2.3 Significance testing of common recurrent copy number alteration regions

4.2.3.1 Common Aberration Analyses

To evaluate the common focal copy number aberrations across a set of UM in each of the classified groups, the high frequency of aberrant regions in the genome was determined to be statistically significant by two validated statistical methods, STAC and GISTIC (see below). Both tools are adopted in Nexus Software (Biodiscovery®) to identify the potential driver aberrations based on their frequency of occurrence, using the SCNA that have already been identified using the FASST2 calling algorithm. Although, both methods apply different statistical approaches (summarised in table 4.1), they overall provide a significant testing to make the data more robust (Rueda et al., 2013).

4.2.3.1.1 Genomic Identification of Significant Targets in Cancer (GISTIC)

The GISTIC algorithm was introduced by Beroukhim et al. in 2007, and is used to identify significant regions of the genome that are amplified or deleted across a set of tumours. The method incorporates both the frequency of occurrence and the amplitude of aberrations, using a G score for each region (a combination score of frequency and amplitude). GISTIC then assesses the statistical significance of each aberration by defining the probability of a score occurring by chance, comparing it against random genomic wide disruption aberrations by applying false detection rate (FDR) corrected for multiple tumours, and assigns a q-value for that region (set of values that will lie between 0 and 1). For each significant region, the method identifies 'peak regions' which have the greatest frequency and amplitude for alteration, which, as statistically indicated, comprises the affected genes with maximal G-score and minimal q-value. GISTIC results are more sensitive at catching lower frequency significant regions (Beroukhim et al., 2007).

4.2.3.1.2 Significance Testing for Aberrant Copy Number (STAC)

The STAC algorithm was introduced by Diskin *et al.* in 2006, to identify the statistical significance of DNA copy number aberrations which are stacked on top of each other such that they would not occur randomly, across multiple array experiments. This global frequency statistical approach uses the permutations of SCNA in each chromosomal arm to determine how likely this SCNA is to occur at any location with a certain frequency, using a p-value cut-off of 0.05 to highlight the common aberrant regions, which have higher frequency than randomly occurring aberration by chance (Diskin et al., 2006).

Overall, using combined approaches will often yield similar or overlapping results and provide a comprehensive analysis.

Table 4.1 the differences between the STAC and GISTIC algorithm

	STAC	GISTIC
Region Selection	Identify the frequency of aberrations	Identify both frequency and amplitude of aberration
Null Model (statistical significance)	Permutation of regions within a chromosome arm	Permutation of probes over the entire genome
Correction for Multiple Sample Testing	Does not require correction	Requires false discovery rate correction
Peak Region identification	NO	YES
Output (significance)	Confidence for regions	p-values

4.2.4 Assessment of Shortlisted Candidate Genes

The GISTIC and STAC statistical approaches generated a validated shortlist of candidate genes, and these genes were then examined individually for biological function and their involvement in cancer, using the Atlas of Genetics and Cytogenetics in Oncology and Haematology (http://AtlasGeneticsOncology.org). The database contains detailed information on each gene, focused on the gene implications in cancer, including cytogenetics and clinical entities in cancer and cancer-prone hereditary diseases. The atlas is linked to PubMed to provide peer-reviewed articles (Huret et al., 2013). The final list of candidate genes was then assembled for each of the UM groups (as discussed previously in chapter 3). The functional assessment of the identified genes was based on the potential functional implication in various cancer types and their known role in acquisition of cancer hallmarks. For each of the UM groups different candidate genes were identified as most significant. Consideration was not made of group 4 as this aspect of the study was investigating the impact of changes of chromosome 6 and group 4 had no changes of 6.

The list of candidate genes identified in each subgroup of UM with a chromosome 6 change are detailed in table 4.2. For group 1, where there was 6p gain only, the most statistically significant candidate gene was *FARS2,* while the second group was repre-

sented by 6p gain and 6q loss (*FOXQ1* and *AMD1*) respectively. For group 3 where other changes of chromosome 6 were present the *AMD1* was also statistically significant. There was some cross over of genes between the comparable regional involvement for example *FARS2* was significant in group 1 but identified in group 2 although not reaching significance. The final shortlist of candidate genes is shown in table 4.2 and more detail is presented in table 4.3

Table 4.2 Summary of candidate genes identified in chromosome 6 short and long arm

Amplified genes in 6p gain (group 1)	Genes in 6p gain (group 2)	Genes in 6q loss (group 2) Deleted genes	Group 3, 6q loss
LOC101927972	LOC101927691	**AMD1**	MANEA-AS1
FARS2	LOC285768	GTF3C6	MANEA
LOC101927950	**FOXQ1**	RPF2	PRIM2
NRN1		GSTM2P1	AMD1
MIR7853		SLC16A10	
MIR5683			
F13A1			
LY86-AS1			
LY86			

Genes were validated by the GISTIC and STAC statistical approaches in chromosome 6p gain and 6q loss.

Table 4.3 Summary of the most statistically significant candidate genes in chromosome 6, with their percentage of loss and gain.

Candidate genes	Copy Number Gain %	Copy Number Loss %
FOXQ1 (chr6:1,257,674-1,259,993)	44.53	0.73
FARS2 (chr6:5,206,582-5,716,815)	44.53	1.46
AMD1 (chr6:111,242,516-111,323,608)	1.46	39.42

STAC / GISTIC analysis was carried out using Nexus® Copy Number Software and the information for each gene function was obtained from the Atlas of Genetics and Oncology and PubMed literature reviews.

4.3 Group 1 (6p only) identification of *FARS2* (phenylalanyl-tRNA synthetase 2, mitochondrial)

The commonly amplified region of 6p for this group extended from 6p12–6pter, but the most relevant focal SCNA was found at 6p25.1 and in this region *FARS2* gene was located (chr6: 5,206,582-5,716,815). *FARS2* encodes a protein that transfers phenylalanine to its cognate tRNA (mitochondrial phenylalanyl transfer ribonucleic acid [RNA] synthetase). It is required for the charging of the congregate cognate mitochondrial tRNA with phenylalanine, and this protein plays a role in mitochondrial protein translation (Bullard et al., 1999). *FARS2* was the most statically significant driver gene in the specified peak region among the UM group1 (6p gain only) with 28 cases. Using the GISTIC algorithm *FARS2* had a higher frequency and amplitude (indicated by high copy gains), a G-score of 12.56 and a q-value of 2.34e-14 were calculated and the threshold was reduced to achieve the best results (0.25), as shown in Figure 4.3. The stacking analysis results for *FARS2* in group 1 are presented in figure 4.3.
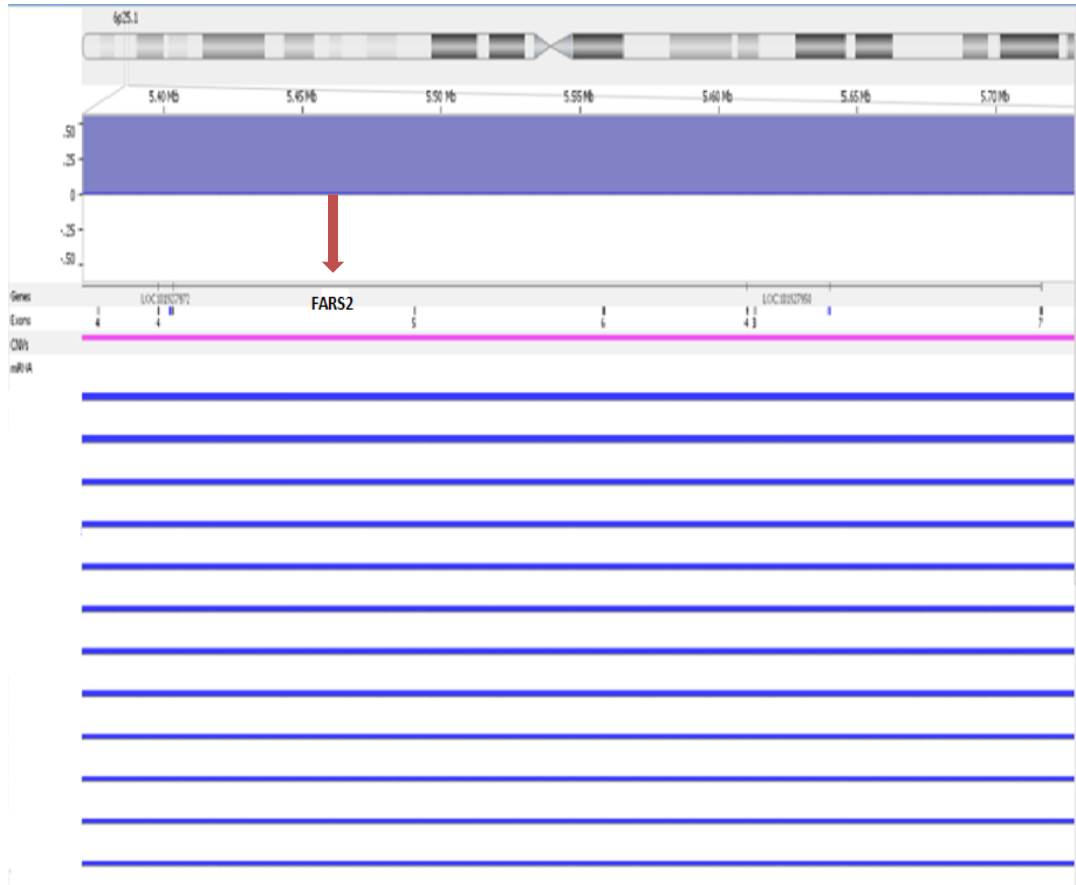
Figure 4.3 Frequency plot of SCNA affecting the FARS2 gene locus

Statistically significant common genomic copy number aberrations among UM cases. GISTIC algorithm was applied to array CGH data for group 1 based on 6p amplification only, in order to identify regions of copy number gain that could be candidate drivers of tumor development. The common aberrant regions are plotted along the x-axis against their chromosomal positions, and the q values are plotted on the y-axis, where the most significant commonly amplified genomic regions are presented by the highest blue bars. Statistically significant genomic regions with maximal G-score and minimal q-value (10 and 0.05 respectively) are highlighted in grey and contain the most important genes in this region, where the red arrow represents the FARS2 gene, located 6p25.1.

All aberrations in each sample were called using the FASST2 Algorithm.

4.4   Group 2 most significant candidate *FOXQ1* (forkhead box Q1)

The commonly amplified region of 6p for this group extended from 6p12–6pter, but the most relevant focal SCNA was located at 6p23-25, and in this region *FOXQ1* gene was located.   The *FOXQ1* candidate gene belongs to the Forkhead transcription factor family, and encodes a protein of 403 amino acids (Bieller et al., 2001), located on chromosome 6p25.3. Abundant studies suggest that *FOXQ1* is an oncogene for many cancer types and is involved in several biological processes (Zhang *et al.*, 2011; Candelario *et al.*, 2012). In this study *FOXQ1* was identified among the UM cases which were grouped based on chromosome 6p gain and 6q loss i(6p) as group 2 with 29 case. By using both the GISTIC and STAC algorithms, 86% (25/29) of *FOXQ1* copy number gains were identified as the most significant focal amplification in group 2, located at 6p25.3, as shown in Figure 4.4. Based on biological functions and their implications in cancer, *FOXQ1* was chosen in this group.
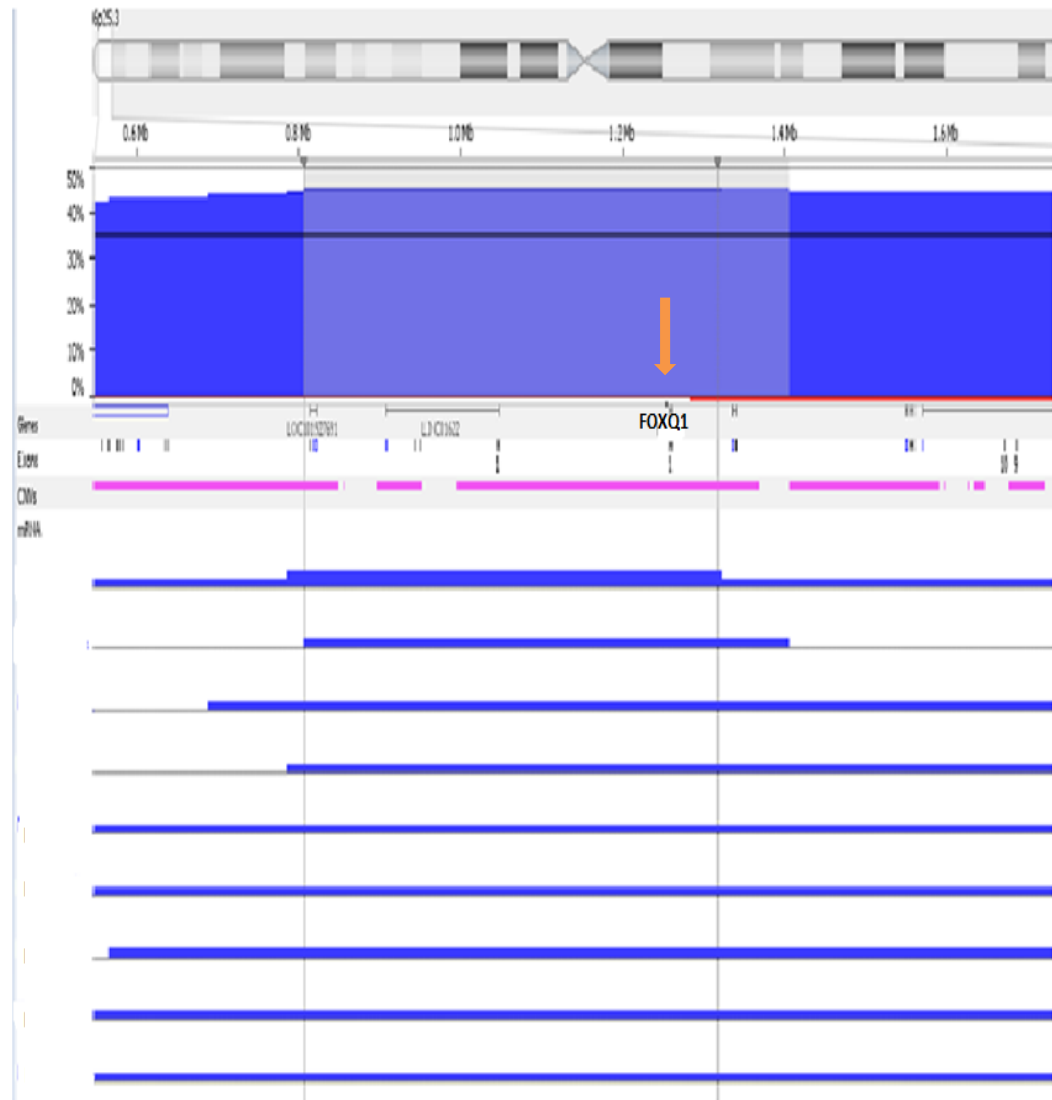
Figure 4.4 Frequency plot of SCNA affecting the FOXQ1 gene locus among UM cases

Stacked SCNA from individual UM cases in group 2 (6p+6q-) showing the most significant candidate genes in this genomic region. The upper panel shows the chromosomal region 6p23-25 and its approximate size, and the middle panel shows the frequency plot of alteration along the y-axis of the corresponding UM cases, while the blue lines represent amplification frequency. The left horizontal line represents individual UM samples. The common aberrant regions are plotted along the x-axis against their chromosomal positions, and the q value are plotted on the y-axis, where the most significant commonly amplified genomic regions are presented by the highest blue bars. Statistically significant genomic regions with maximal G-score and minimal q-value (10 and 0.05 respectively) are highlighted in grey and contain the most important genes in this region, where the orange arrow represents the FOXQ1 gene.

All aberrations in each sample were called using the FASST2 Algorithm

4.5 *AMD1* (adenosylmethionine decarboxylase 1)

The commonly deleted region of 6q for group 2 and 3 extended from 6q21-q26, but the most relevant focal SCNA was found in 53 cases at 6q21-22.1 in this region *AMD1* gene was located in chromosome 6q21. The gene loss was identified among UM cases which were grouped based on chromosome 6p gain and 6q loss i(6p) as well as group 3 (with total number of 57 cases). Using a STAC approach 93% of copy number loss in 6q in group 2 and 3 (111,242,516-111,323,608) were found to be statistically significant (frequency ≥ 30%, $p < 0.05$), as shown in Figure 4.5. Based on biological functions and their implications in cancer, *AMD1* was chosen in this study to be the most significant possible driver gene in 6q loss related to tumour progression.
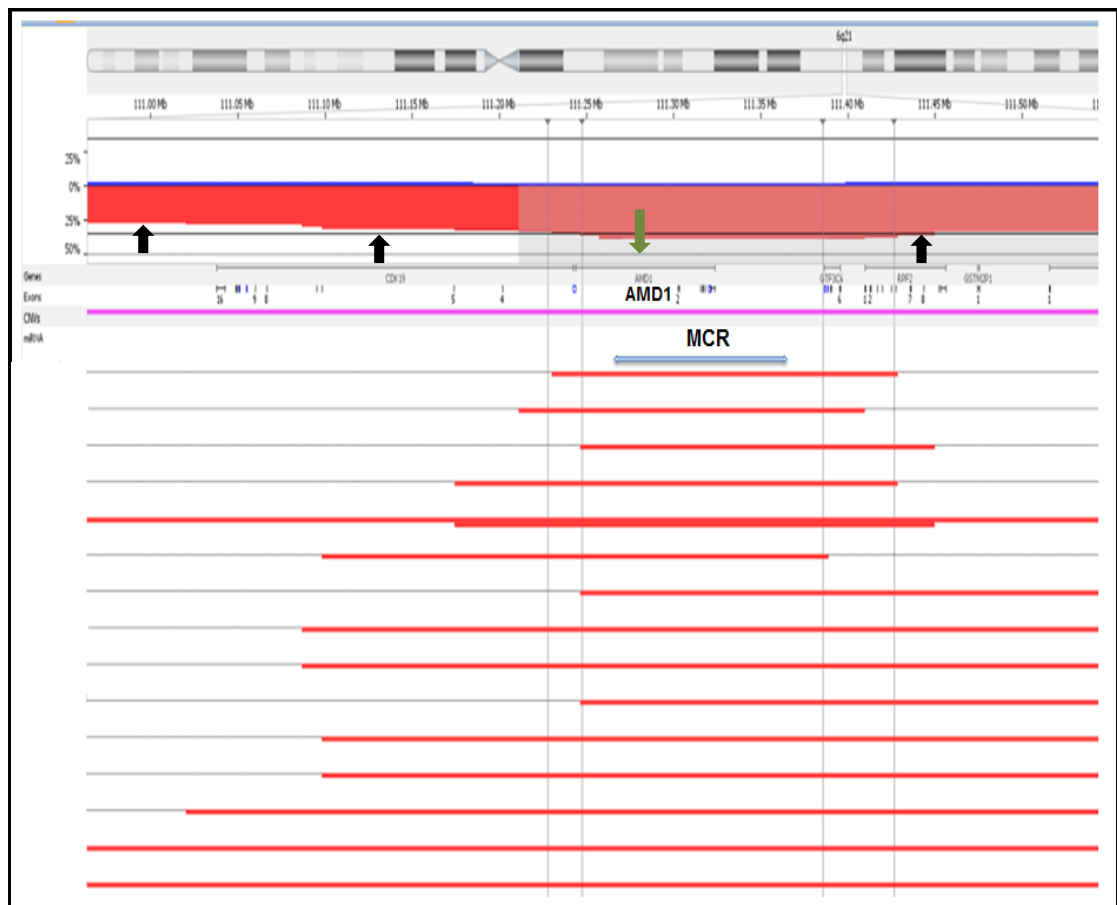
Figure 4.5 Stacked SCNA from individual UM cases among group 2 (6q-)

Showing the most significant candidate genes in this genomic region, in addition to showing an example of a Minimal Common Region (MCR). The upper panel shows chromosomal region 6q21 and its approximate size, and the middle panel shows the frequency plot of alteration along the y-axis of the corresponding UM cases, while the red line represents deletion frequency. The left horizontal line represents individual UM

samples, and the blue bar highlights the MCR region as the smallest aberrant region in all affected UM samples. Statistically significant genomic aberrant regions are highlighted in grey, with a frequency higher than the threshold of 20% (indicated by the black arrows), and represent the most important candidate genes in this region, such as the AMD1 gene (green arrow) located at 6q21.

All aberrations in each sample were called using the FASST2 Algorithm.

4.6   Comparisons of *AMD1* with *FOXQ1* and *FARS2*

For group 2 where there was both gain of 6p and loss of 6q, the two genes that were consistently affected together were *FOXQ1 and AMD1,* and were the most statistically significant in 6p gain and 6q loss i(6q). Among all UM in this study, it was found that *AMD1* loss with a normal copy of *FOXQ1* was presented in 23 tumours as shown in Figure 4.6A, a gain in one copy of *FOXQ1* happened alongside *AMD1* loss in 30 tumours as shown in Figure 4.6B, whereas *FOXQ1* gain only was detected in 32 tumours shown in Figure 4.6C. In the other hand, *AMD1* loss with *FARS2* gain represents a mutually exclusive alteration as shown in Figure 4.6D. Furthermore, 52 tumours shows normal copy numbers from both genes represents group 4 (no 6 changes) as shown in Figure 4.6E.
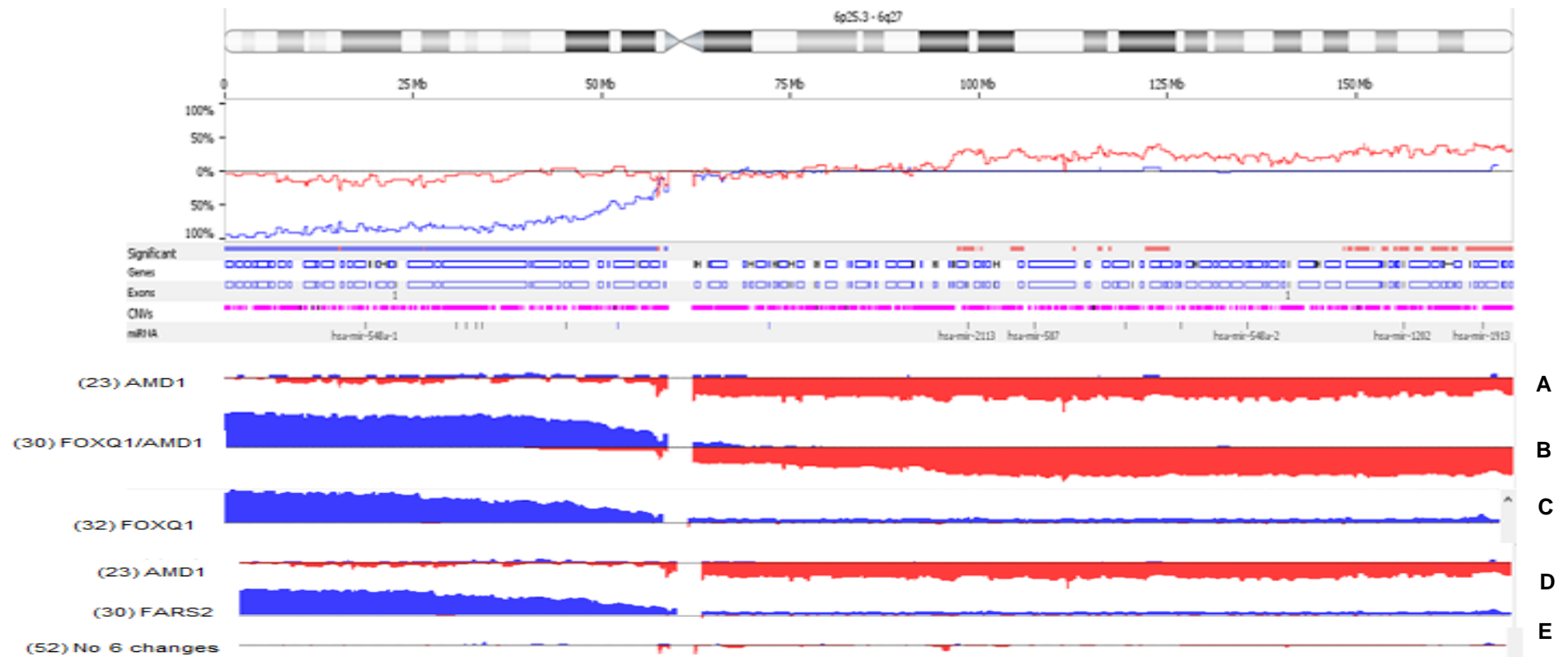
Figure 4.6 Frequency plot of chromosomal view demonstrates the comparisons between FOXQ1 gain and AMD1 loss.

This view of chromosome 6 displays information on *AMD1* loss and *FOXQ1* gain for different samples at one time that represents group 2. The y-axis designates the percentage of alteration in the selected samples at specific points along the genome and presents the $\log_2$ tumour/reference ratio, and the genome coordinates of the ~180,000 probes on the UM custom array positioned by chromosome location on the x-axis. Horizontally along the top, the blue lines plotted above 0% indicate copy number gain, and red indicates copy number loss events plotted below the 0% baseline. **A.** shows *AMD1* loss only with a normal copy number of *FOXQ1* in 23 tumours. **B.** shows that 30 tumours were harbouring *FOXQ1* gain in 6p along with *AMD1* loss in 6q. **C.** 32 tumours showing only *FOXQ1* gain with a normal copy of *AMD1*. **D.** Represents 23 tumours with *AMD1* loss with a normal copy of *FARS2*, conversely 32 tumours with *FARS2* gain and normal copy of *AMD1*. **E.** shows tumours with a normal copy number for both genes represents group 4.

All aberrations in each sample were called using the FASST2 Algorithm

4.7   Association of candidate genes *FARS2*, *FOXQ1* and *AMD1* with chromosomes 1, 3 and 8 abnormalities

To assess the implications of each of the candidate genes on chromosome 6 with UM progression, the relationship with 1, 3 and 8 chromosomal alterations was compared, as described in the sections that follow.

4.7.1   **Association of *FARS2* with chromosome 1, 3, and 8**

Using the unique comparison feature in Nexus it is possible to compare the selected gene (*FARS2*) and the other SCNA across the genome for all UM series. Although *FARS2* is the most significant gene in group 1 (6p only), it was also amplified in group 2 (6p+,q-), and overall it was presented in 61 tumour (45%) as shown in Figure (4.7). In regards to the association of *FARS2* amplification with 1p deletions, M3 and 8q gain, the comparisons showed that amplification of *FARS2* associated more with 8q gain, 1p loss, and less with M3.
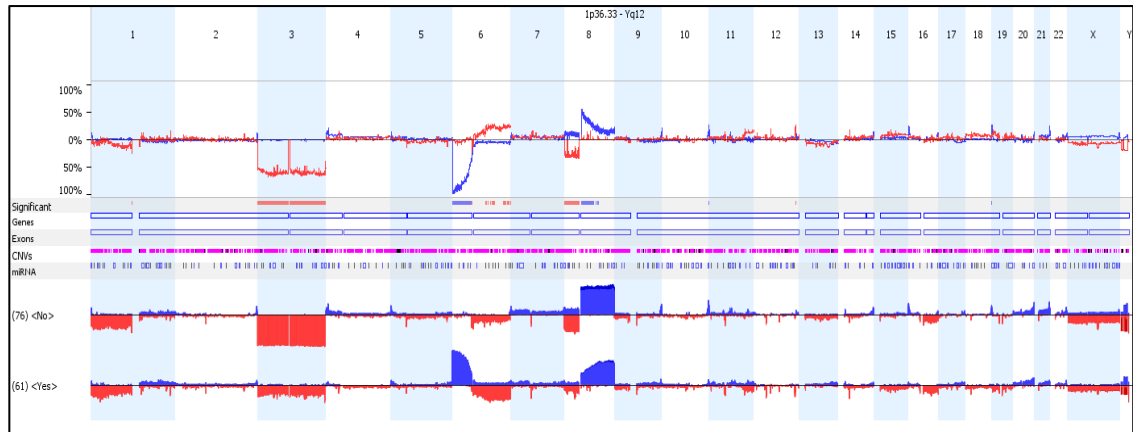
Figure 4.7 Frequency plot of genomic view demonstrates the comparisons of FARS2 amplification with 1p-, M3 and 8q+.

For copy number events, the magnitude of gain or loss is presented as long or short bars, where the gain is plotted above the zero baseline and presented in blue, and the loss is plotted below the zero baseline and presented in red. The long bars illustrate greater magnitude, and the converse for the small bars. *FARS2,* located at 6p25.1, was amplified in 61 tumours, and showed more association with 1p loss and 8q gain compared to the normal copy number of FARS2, which shows a higher association with M3 and 8q gain.
All aberrations in each sample were called using the FASST2 Algorithm

Association of _FOXQ1_ with chromosome 1, 3, and 8

Using the comparison feature in Nexus allows a comparison between the selected gene, FOXQ1, and the other SCNA across the genome for all UM series. Although _FOXQ1_ is the most significant in group 2 (6p+, q-), it was also amplified in group 1 (6p gain only), and overall it was presented in 62 tumours (45%), as shown in Figure 4.8. Although _FARS2_ and _FOXQ1_ together were found to be affected consistently and were the most statistically significant in 6p gain, they have different molecular functions and are expressed in different tissue types. Among all UM in this study, it was found that a gain in one copy of _FOXQ1_ is highly likely to happen alongside _FARS2_ gain, and this could be explained by the close genetic location of the two genes. With regard to the association of _FOXQ1_ amplification with 1p loss, M3 and 8q gain, the comparisons showed that amplification of _FOXQ1_ was associated more with 8q gain and 1p loss, and less with M3.
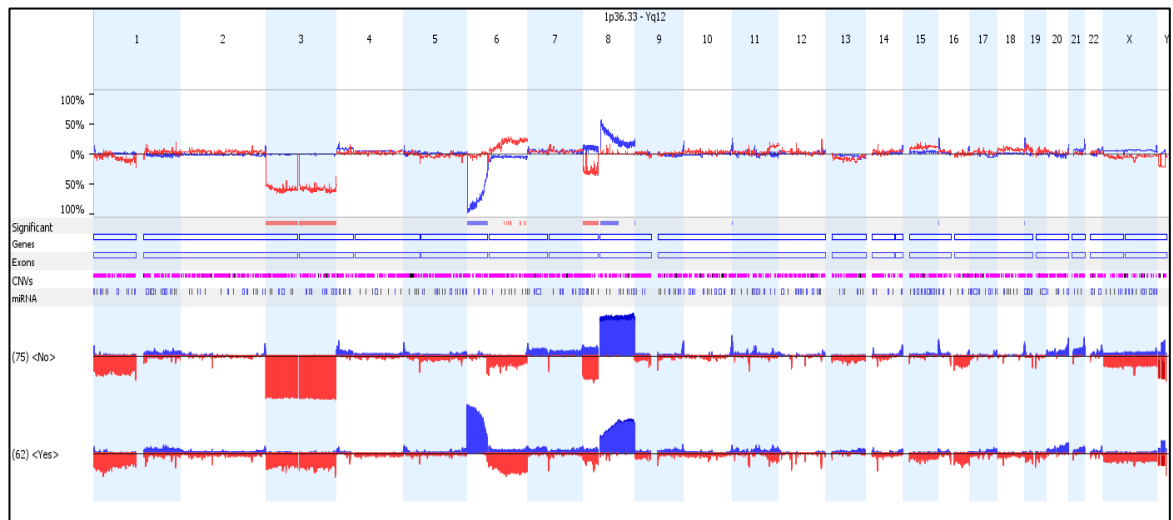
Figure 4.8 Frequency plot of the genomic view demonstrates the comparison of FOXQ1 amplification with 1p-, M3 and 8q+.

For copy number events, the magnitude of gain or loss is presented as long or short bars, where the gain is plotted above the zero baseline and presented in blue, and the loss is plotted below the zero baseline and presented in red. The long bars illustrate greater magnitudes, and the converse for the small bars. _FOXQ1_ located at 6p23-25 was amplified in 62 tumours, and shows more association with 1p loss and 8q gain, compared to the normal copy number of FOXQ1, showing higher association with M3 and 8q gain.
All aberrations in each sample were called using the FASST2 Algorith

Using the comparison feature in Nexus allowed a comparison between the selected gene, *AMD1*, which was the most statistically significant among group 2 (6p+, q-), and the other SCNA across the genome for all UM series. The AMD1 gene was deleted in 53 tumours (42%), as shown in Figure 4.9, and with regard to the association with 1p loss, M3 and 8q gain, the comparisons showed that *AMD1* loss was associated more with M3 and 8q gain, and 1p loss.
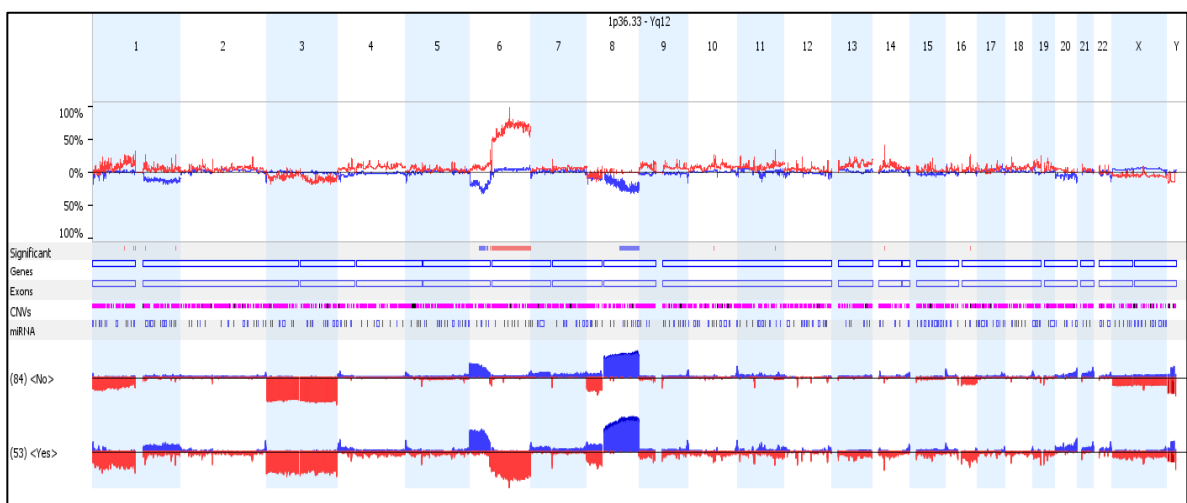
Figure 4.2 Frequency plot of genomic view demonstrates the comparison of ADM1 deletion with 1p-, M3 and 8q+.

For copy number events, the magnitude of gain or loss is presented as long or short bars, where the gain is plotted above the zero baseline and presented in blue, and the loss is plotted below the zero baseline and presented in red. The long bars illustrate the greater magnitude and the converse for the small bars. *AMD1* was located at 6q21 and was deleted in 53 tumours, showing almost equal association with 1p loss, M3 and 8q gain, compared to the normal copy number of *AMD1.*
All aberrations in each sample were called using the FASST2 Algorithm

As a result of the selective analysis of each groups FARS was identified as only involved in group 1, *FOXQ1*, and to lesser extent *FARS* and *AMD1* were found in group 2, *AMD1* was also common to group3 but not group 1. As there was some degree of cross over and also mutual exclusivity another approach was taken to investigate the involvement of these potential drivers in UM. For all of the candidate genes commercial antibodies were available, and their expression was explored in the various subgroups of UM.

4.8   IHC results

4.8.1   Evaluation of protein expression

Immunohistochemical IHC analysis was performed to assess the expression of *FOXQ1*, *FARS2* and *AMD1* on chromosome 6 in UM. IHC was carried out on 5µm-thick tissue sections that were pre-treated to quench endogenous peroxidase activity and expose the epitopes in 1% H_2O_2, as described in Methods in Section 3.2.7. Rabbit polyclonal antibody was generated against specific 36-85 amino acid fragments for FOXQ1, 385-415 fragments for FARS2 and from 1-334 amino acid fragments for AMD1. The antibody was directed against the recombinant protein epitope, then the experiment was visualised using the DAB colorimetric system to detect the protein expression (brown staining), with a counter stain (haematoxylin, blue staining). Cases for immunohistochemical analysis in this study were chosen based on the availability of UM cases immediately available for IHC due the timeframe left for the study. Amongst the UM selected for the IHC study, some UM were known to have amplification in *FOXQ1, FARS2* and deletion in *AMD1* by array CGH. A total of 21 cases comprising 2 representing group1 (6p gain only), 3 representing group 2 i(6p), 7 representing group 3 (6p loss), and 9 from group 4 (no 6 changes). The results of the IHC for all UM are summarised in Table 4.5. All immuno-stained sections were evaluated at 200X magnification, and results were classified as positive and negative based on amount of staining of the UM section (cytoplasmic or nuclear). UM sections were all scored as coded samples so there was no knowledge of the genetic changes for each section. The positives were then sub-classified as weak, moderate or strong based on the stain intensity detected on the tumour cells (Fisher et al., 1994, Adams et al., 1999). The results were assessed by 3 independent observers (NA, DWH and KS).

The main problem with this aspect of the study was the lack of time left so only initial exploratory investigations were undertaken, in which the respective antibodies were optimised, however melanin bleaching was not undertaken (as an effective protocol was not in house at this point). As a result, there was an excessive amount of melanin in some of the tissue sections (Figure 4.10), which could obscure the cellular morphology and make interpretation of expression not feasible. Therefore, a melanin bleaching technique would improve our result, but due to limited time, it was unable to treat the FFPE section with potassium permanganate/oxalic acid melanin bleaching, in order to eliminate the melanin before incubate them with primary antibody. In general, the IHC experiment in this study was to assess the preliminary protein expression of (FARS2,

FOXQ1, and AMD1) in UM tissue, detailed in subsequent sections, and thereby act as a pilot study for later more detailed explorations.
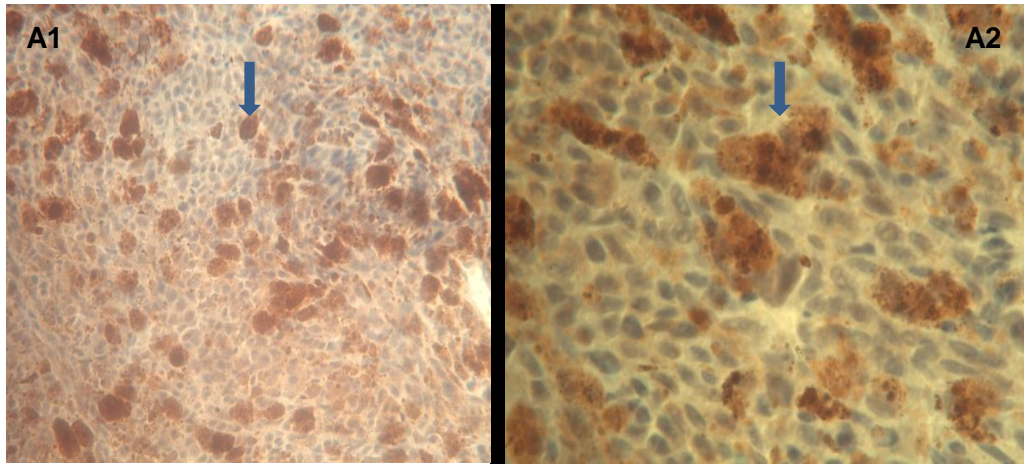
Figure 4.3 Micrographs of UM FFPE stained with AMD1 and FARS2 antibodies respectively.

A1 and **A2** show the accumulation of excessive amounts of melanin in some of the tissue sections. The large brown stain highlighted by the blue arrow represents the melanin, which obscures the cellular morphology.
Images for **A1** were captured at 200x and **A2** at 400x magnification of the original.

4.8.2 FARS2 protein expression

Normal colon tissue was used as a positive control with physiologic FARS2 expression, and the cell showed intermediate to strong positive cytoplasmic staining (Figure 4.11). In some positive cases, the stain was detected in cytoplasmic and nuclear areas, which stained uniformly for group 1 (Figure 4.11F). Negative controls with omitted antibody were set up with every stained section, as shown in Figure 4.11B. The section only showed blue haematoxylin counter-stain, in addition to a positive cytoplasmic stain as a positive control, as shown in Figure 4.11C. While group 2 showed a weak to moderate cytoplasmic stain, group 3 showed strong to moderate cytoplasmic and nuclear stains (Figure 4.11D). Unexpectedly, group 4 (with no amplification of the 6p region containing FARS2), FARS2 protein was still expressed in the tissue with a weak to moderate cytoplasmic and nuclear stain (Table 4.4). The IHC finding showed the FARS2 was overexpressed in UM group 1 tumour cells.
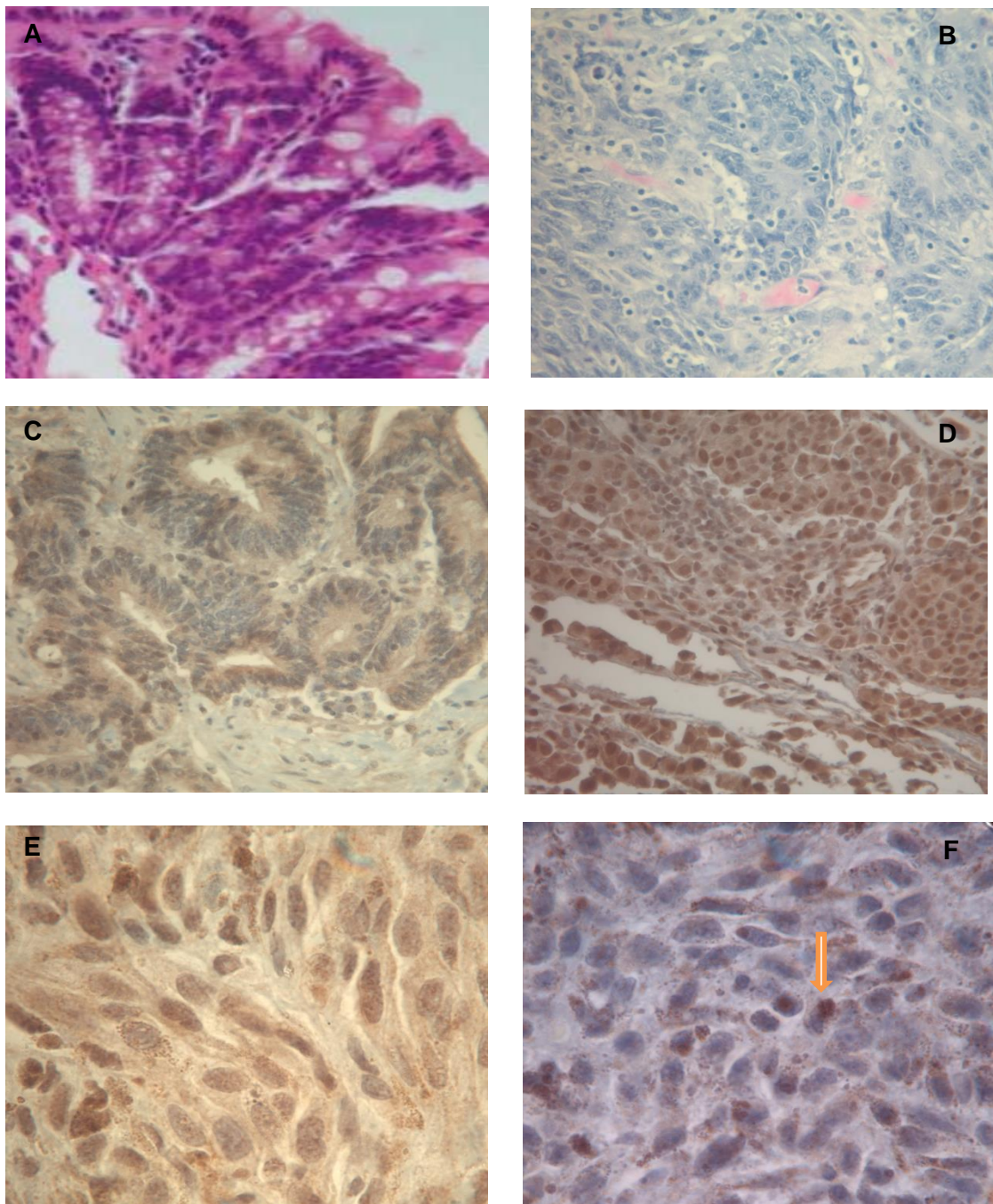
Figure 4.11 Semi-quantitative analysis of FARS2 protein expression in UM samples using Immunohistochemistry

A) Colon FFPE section stained with H&E (obtained from Histopathology laboratory). **B)** Negative control of same normal colon tissue with omitted antibody showing only haematoxylin counter stain. **C**) Represents micrographs of normal colon tissue as a positive control, immune-stained with FARS2 antibody, showing a strong positive cytoplasmic stain (brown) for the cells but not the cellular area with haematoxylin counter stain (blue). **D**) Representative FFPE section of UM cases stained with FARS2 antibody (brown) and classified as a strong cytoplasmic stain with haematoxylin counter stain (blue). **E**) Moderate positive staining captured at 1000x to illustrate the cytoplas-

mic stain. **F)** moderate intensity positive nuclear staining highlighted by the orange ar-
row.

Images for A, B, C, D were captured at 400x magnification of original.

4.8.3 FOXQ1 protein expression

Normal kidney tissue was used as a positive control with physiologic FOXQ1 expres-
sion, and the cell showed intermediate to strong positive cytoplasmic staining (Figure
4.12).

IHC analysis for the FOXQ1 protein was performed to assess its expression in UM tis-
sues. The observed IHC staining patterns are shown in Figure 4.12, and the results
revealed that FOXQ1 was mainly localised on the cytoplasm of positive UM cases. It
was challenging to evaluate the expression of FOXQ1 protein due to the unexpected
expression of a weak stain on the negative control during the optimisation and the test.
If time had permitted the run would have been repeated. A possible explanation could
be cross-contamination due to the high concentration of FOXQ1 antibodies (Figure
4.12). Although a specific stain was detected in the cytoplasm of the epithelial cells of
renal tubules in the normal kidney tissues (4.12C), the UM tissue expressed a weak to
moderate cytoplasmic stain for groups 1 and 4, and a moderate to strong stain for
groups 2 and 3. In support of the current findings two UM cases showed a completely
negative stain, which can be considered as an internal negative control, and used to
validate other UM cases (Figure 4.12F). The IHC finding showed that FOXQ1 was
overexpressed in UM tumour cells categorised as group 2.
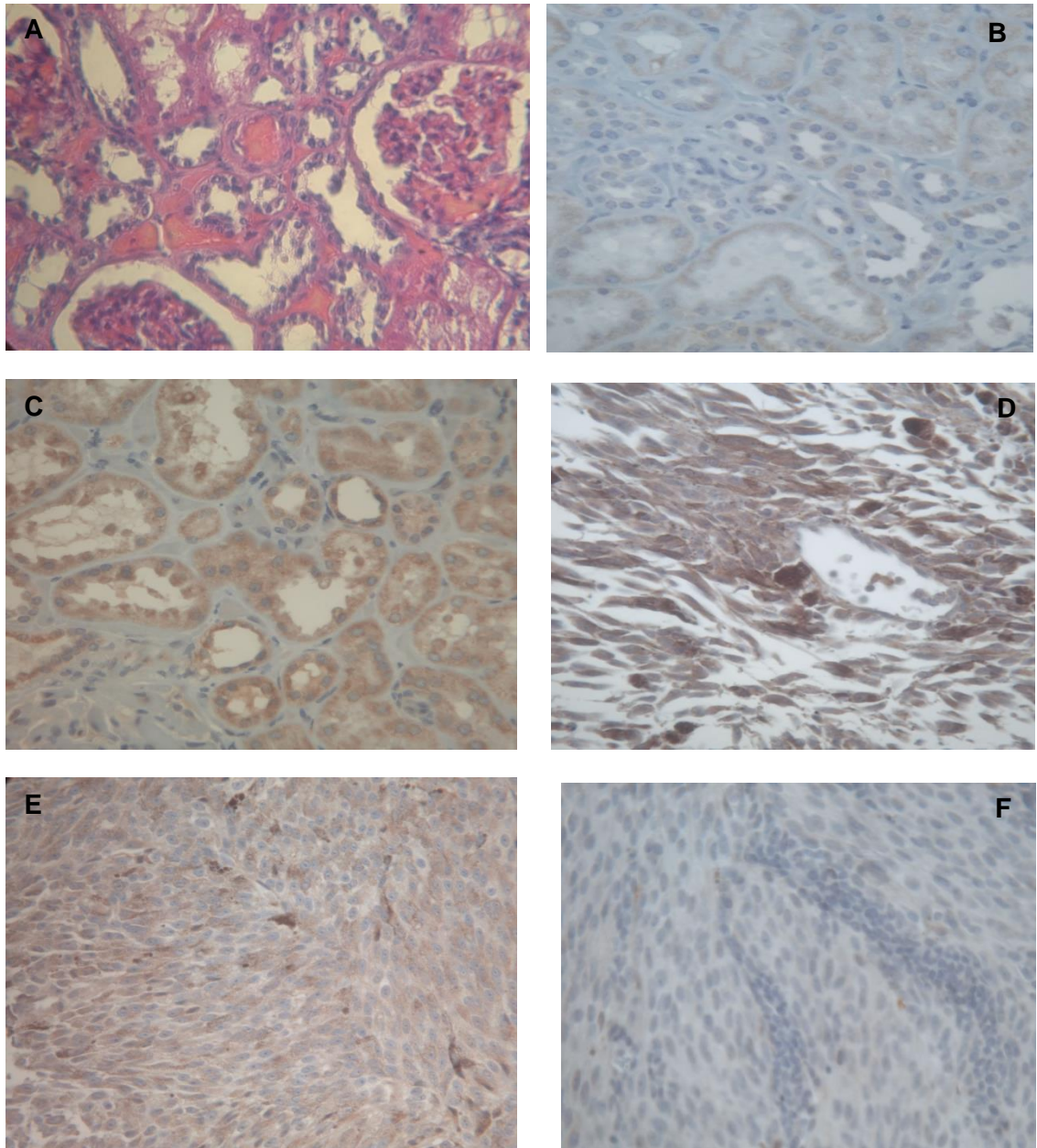
Figure 4.12 Semi quantitative analysis of FOXQ1 protein expression in UM samples using Immunohistochemistry.

A) Kidney FFPE section stained with H&E (obtained from Histopathology laboratory). **B)** Negative control of same normal kidney tissue with omitted antibody showing low cytoplasmic staining with haematoxylin counter stain. **C**) Represents micrographs of normal kidney tissue as a positive control, immune-stained with FOXQ1 antibody showing epithelial cells of renal tubules with strong positive cytoplasmic staining (brown) for cells but not the cellular area, with haematoxylin counter stain (blue). **D**) Representative FFPE section of UM cases stained with FOXQ1 antibody (brown) and classified as a strong cytoplasmic stain with haematoxylin counter stain (blue). **E**) Moderate intensity positive cytoplasmic stain in poorly differentiated UM tissue. **F)** Low expression of FOXQ1 in UM tissue represented a negative IHC reaction as an internal control.

Images were captured at 400x magnification of original.

4.8.4 AMD1 protein expression

Normal breast tissue was used as a positive control with physiologic AMD1 expression, and the cell showed intermediate to strong positive cytoplasmic staining. The observed IHC staining patterns are shown in Figure 4.13. Although the positive staining was localised on the cytoplasm of the UM cells, a combination of cytoplasmic and nuclear positive staining was observed in some of the UM tissues (Figure 4.13F). High to intermediate AMD1 expression was detected in approximately 80% of 21 corresponding adjacent UM tissues, (Table 4.5). However, the *AMD1* gene shows highly significant differential expression between tumors with and without M3, where the protein was highly expressed in-group 3 with association of M3 and 8q+, cases stained with AMD1 detailed in table 4.5, the chromosomal changes for individual cases are explained in Figure 3.11, and the association of M3 and 8q are explained in Figure 4.10
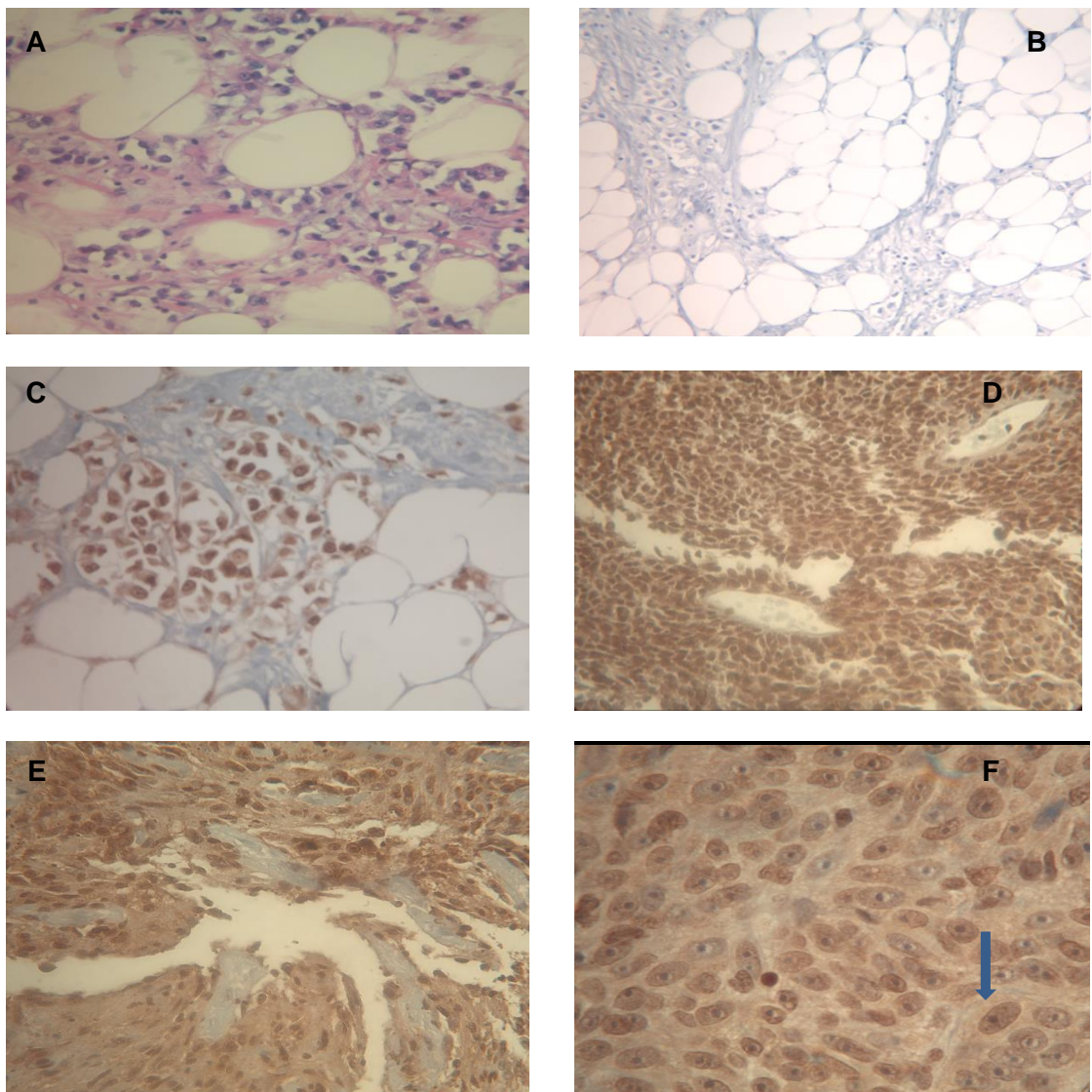
Figure 4.4 Semi quantitative analysis of AMD1 protein expression in UM samples using immunohistochemistry

A) Breast FFPE section stained with H&E (obtained from Histopathology laboratory). **B)** Negative control of same normal breast tissue with omitted antibody, showing only haematoxylin counter stain. **C**) Represents micrographs of normal breast tissue as a positive control, immune-stained with AMD1 antibody showing strong positive cyto-plasmic staining (brown) for the cells, not the cellular area, with haematoxylin counter stain (blue). **D**) Representative FFPE section of UM cases stained with AMD1 antibody (brown) and classified as strong cytoplasmic stain. **E**) Moderate positive staining with haematoxylin counter stain (blue). **F)** Moderate intensity positive cytoplasmic mixed with nuclear staining, highlighted by the blue arrow.
Images for A, B, C, D, E were captured at 400x magnification of original.

Table 4.4: Semi-quantitative scoring system for FARS2, FOXQ1, and AMD1 antibodies

		Anti-FARS2		Anti-FOXQ1	Anti-AMD1	
Mel	**Groups**	**Cyto Stain**	**N stain**		**Cyto stain**	**N stain**
110	1	3\2	3\2	1\2	3\2	0/0
93	1	2\1	2\1	2\2	1\1	2/2
73	2	1\1	0\0	2\3	3\2	0/0
91	2	1\1	2\1	3\3	1\1	2/3
106	2	2\2	0\0	3\2	3\2	0/0
100	3	1\2	2\2	1\2	3\3	0/0
104	3	3\2	2\3	3\2	3\3	0/0
97	3	2\2	2\2	3\2	2\2	0/0
98	3	1\1	2\1	2\2	3\3	0/0
94	3	1\1	0\0	2\2	3\3	0/0
95	3	2\2	0\0	2\2	3\2	0/0
112	3	1\1	0\0	2\3	1\1	3/2
92	4	2\2	2\2	2\2	2\2	0/0
106	4	3\2	3\2	2\2	1\2	0/0
90	4	2\2	2\2	1\2	3\2	0/0
96	4	2\3	2\3	2\1	2\2	0/0
88	4	2\1	0\0	1\1	3\2	0/0
102	4	2\2	0\0	1\1	3\2	0/0
101	4	2\2	0\0	1\2	2\3	0/0
99	4	3\1	0\0	0\0	2\2	0/0
89	4	3\2	0\0	2\2	2\2	0/0

0= Negative stain 1= Weak stain   2= Moderate stain   3= Strong stain

Cyto= Cytoplasmic stain   N= Nucleus stain

Where the left-hand number represents the percentage of stained cells and the right-hand number represents the intensity of the stained cells.
The results were assessed by 3 independent observers (NA, DWH and KS).

Table 4.5: A Summary of IHC protein expression among the classified groups

groups	FARS2 expression	FOXQ1 expression	AMD1 expression
GP1	High to moderate expression (C/N)	Moderate to weak (C only)	Moderate (C/N)
GP2	Weak expression (C> N)	High to moderate	High to moderate (C>N)
GP3	Moderate to weak(C>N)	Moderate	High to moderate (C>N)
GP4	Moderate expression (C>N)	Moderate to low	Moderate (C only)

C= Cytoplasmic stain   N= Nucleus stain   GP= Group

4.9   Associations of the potential driver genes and patient survival

Although the expression of (*FOXQ1*, *FARS2*, and *AMD1*) was confirmed by IHC as a proof of concept study, it was not possible within the timeframe to increase the sample size and include melanin bleaching in order to undertake meaningful analysis. In particular, there were only 2 cases from group 1 so care must be taken not to place too much weight on the findings, but in general terms there were differences observed which suggest further exploration will be of value. Therefore, Nexus 7.5 was used to calculate the survival analysis based on the patients outcome for the whole series (137). The results show that patients with gain in either *FOXQ1* or *FARS2* genes (located on 6p) tend to have better prognosis and increased disease free survival, compared to patients with normal copy of each gene, as shown in Figure 4.14 A, B. On the other hand, *AMD1* deletion (located on 6q) correlates with a poor patients prognosis and a significant decrease in disease-free survival, as shown in Figure 4.14 C.   These findings are in broad agreement with the survival analysis undertaken in relation to chromosome 6 changes in chapter 3 section 3.3
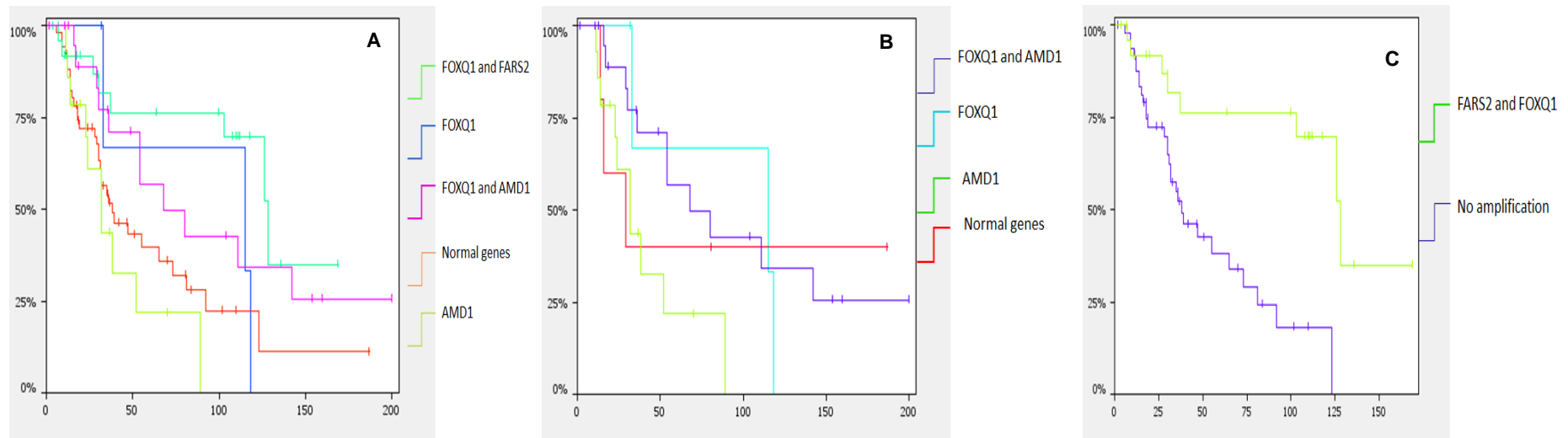
Figure 4.5 Kaplan-Meier survival curves for *FARS2, FOXQ1*, and *AMD1*

The Y-axis represents the percentage of patient survival; the X-axis represents survival time in months. **A**. demonstrates a survival curve for all the amplified and deleted genes (*FOXQ1, FARS2*, and *AMD1* respectively) in addition to the combination of *FOXQ1* and *FARS2/ FOXQ1* and *AMD1*. Overall, A, B, C diagrams demonstrate that deletion of *AMD1* gene associated with reduced disease-free survival compared to the other two genes *FOXQ1* and *FARS2* where the presence of either genes predict better prognosis.

4.10 Discussion

This study was a pilot study designed to see if it was feasible and to verify the findings of aCGH, therefore array CGH analysis was used in this study to identify the possible defective genes that could be responsible for poor prognosis in UM. Within the time limitations of this PhD study, few tumours were available for IHC to study the expression of the selected genes. Further techniques such as melanin bleaching could be optimised to improve our preliminary results, and obtaining the relevant clinical data took more time than expected, and was needed to support the current data. Although to date, more tumour sections have become available to carry on with this study and complete the investigation of the defective genes in 6p gain and q loss, there was insufficient time to stay longer and carry on with this study, to analyse the selected cases in more detail and link them to disease prognosis.

This study indicates that one or more tumour suppressor genes located in the region 6q21, and driver candidate oncogenes located in the region 6p23-25.1, may contribute to tumour progression. Although the structural abnormality of chromosome 6 is too large to point directly to the candidate oncogenes, the fact that small regions of SCNAs of both the p and q arm are involved offers the chance to delineate the specific regions of amplifications and deletions on chromosome 6 which could be involved with UM progression. Using aCGH with the Nexus tool provides a validated shortlist of candidate genes in chromosome 6 using STAC and GISTIC from all UM cases, and defining those most relevant biologically to cancer.

Three novel genes were highlighted in this study, and the functional analysis shows that *FARS2 and FOXQ1* amplification *and AMD1* deletion could possibly be implicated in the tumour progression. To detect the expression of these genes, IHC was used as an effective way to examine UM tissue, and it is an excellent technique to show the exact protein location within the tissue examined. The aim was to compare the expression of FARS2, FOXQ1 and AMD1 among each classified group, as detailed in Chapter 3. The study was limited in number but as a proof on concept study showed that results were broadly in agreement with the expected expression as predicted by amplification of the relevant genes. As such there may be an advantage in the future for a more detailed study and relation to outcome *FOXQ1* was first isolated in 2001 by Bieller *et al*. The gene is a member of the forkhead transcription factor family (Bieller et al., 2001, Jonsson and Peng, 2005), which are involved in many biological processes, in-

cluding cell cycle dysfunction (Candelario et al., 2012), epithelial differentiation, embryonic stem cell differentiation (Zhang et al., 2011, Feuerborn et al., 2011, Ogaki et al., 2011), and neurocognitive functions (LeBlanc et al., 2012). The FOX genes family have been regarded as either oncogenes or tumour suppressor genes, and are closely correlated to tumour progression and prognosis by promoting apoptosis and cell proliferation of cancer cells (Sunters et al., 2003, Fosbrink et al., 2006, Candelario et al., 2012). Previous research has shown the contribution of *FOXQ1* in multiple cancer types, including bladder cancer (Zhu et al., 2013), breast cancer and gastric cancer. In each, it was associated with poor prognosis and tumour metastases (Qiao et al., 2011, Liang et al., 2013). *FOXQ1* was found to be overexpressed in colorectal tumours and to promote tumour growth and angiogenesis, thus playing an important role in enhancing tumorigenicity, and it has been suggested that *FOXQ1* may have a potential therapeutic targets in colorectal cancer (Kaneda et al., 2010, Christensen et al., 2013, Jonsson and Peng, 2005). Overall, over expression of *FOXQ1* in a variety of cancers has been universally related to a poor prognosis including Hepatocarcinoma (Wang et al., 2013, Xia et al., 2014), and non-small cell lung cancer (Feng et al., 2012) . Furthermore, it is suggested that *FOXQ1* overexpression could promote tumour invasion and metastasis in breast cancer, by affecting the E-cadherin (epithelial) level in Epithelial-mesenchymal transition (EMT), where the loss of E-cadherin can promote EMT and act as a tumour suppressor in breast cancer. In addition, *FOXQ1* overexpression is associated with poor prognosis in non-small cell lung cancer, by regulating EMT (Polyak and Weinberg, 2009, Zhang and He, 2013). Overexpression of *FOXQ1* was reported to be associated with the development of laryngeal carcinoma, by enhancing tumorigenesis through its effect on cell cycle progression, cell proliferation, and cell migration (Zhang et al., 2015). In contrast, dysregulated *FOXQ1* leads to inactivation of E-cadherin and promotes EMT. Therefore, loss of E-cadherin function has been implicated in tumour progression and metastasis in various cancer types by reducing cellular adhesion with the tissue, and this leads to increased cellular mobility, in order to allow the cancer cell to invade the surrounding tissue and metastasise (Beavon, 2000, Polyak and Weinberg, 2009). Therefore, the overexpression of the *FOXQ1* oncogene could have a role in UM tumour progression, which could help in patient care in regard to tumour prognosis.

The IHC findings in the present study showed that *FOXQ1* was mainly expressed in the cytoplasm, and FOXQ1 protein level was significantly higher in group 2 tumour cells, compared to groups 1, 3 and 4, which showed lower expression. Thus, the overexpression of *FOXQ1* could be associated positively with the degree of tumour differentiation, and may have the potential to serve as a good therapeutic target in UM, as well

as many cancer types. Although the sample numbers were limited and not distributed equally between the classified groups (Table 4.4), the big challenge was to interpret the expression of *FOXQ1* and link it to a certain group. Therefore, the discussion of these results is based on preliminary data. Although the IHC results were compatible with common aberration analysis by Nexus, where the most statistically significant candidate driver gene in group 2 was *FOXQ1*, more investigation is needed to reveal the role of *FOXQ1* in UM prognosis and metastasis.

The second statistically significant gene on 6p gain is *FARS2*. Defects in nuclear genes encoding mitochondrial aminoacyl-tRNA synthetases have been linked to many paediatric and adult disorders (Konovalova and Tyynismaa, 2013). A few studies have reported that mutation in this gene can cause combined oxidative phosphorylation deficiency 14 (COXPD14) (Elo et al., 2012, Shamseldin et al., 2012, Almalki et al., 2014), and autosomal recessive spastic paraplegia 77 (SPG77) (Yang et al., 2016). Yet no previous study has linked mutation in this gene to cancer development.

The IHC results show that *FARS2* was mainly expressed in the cytoplasm and to a lesser extent in the nucleus of UM cells. Compared to the positive control of the normal colon tissue where the expression was detected only on the cytoplasm. The overexpression of *FARS2* in the cytoplasm and nucleus of the tumour cells was reported in this study to be associated more with group 1 and with the cytoplasm and nucleus, while the other groups showed *FARS2* expression in the cytoplasm more than in the nucleus. The IHC results (Table 4.5) with overexpression of *FARS2* in group 1 being highly compatible with SCNA analysis by Nexus software.

Although up until now there has been no study of linked dysregulation in *FARS2* to any cancer type, where it has always been associated with neurological disorders, our observation suggests that the presence of *FARS2* oncogenes may contribute to the tumour phenotype, and could represent a new pathway in UM based on 6p gain with or without M3.

Somatic deletion in different cancer types often determine the tumour suppressor gene that acts as a driver of tumour development. In this study, *AMD1* was detected as the most significant candidate gene at 6q. *AMD1* encodes S-adenosylmethionine decarboxylase proenzyme (AdoMet), which is a key enzyme in polyamine biosynthesis, and the production of the catalytic reaction (Maric et al., 1995). An elevation in polyamine biosynthesis was found in colorectal cancer, and the concentration was reduced in the tumour using chemotherapy to impair tumorigenicity, blocking the polyamine synthesis

pathway, which has proved their antitumor activity as a potential treatment in colorectal cancer (Zhang et al., 2006). Furthermore, *AMD1* was introduced as a new tumour suppressor gene in lymphoma, and targeting suppressor genes can have therapeutic impact by disabling different genes acting in the same pathway (Scuoppo et al., 2012). In prostate cancer, research shows inhibition of the polyamine pathway associated with a reduction in the expression level of *AMD1*, and this would decrease prostate cancer growth (Gerner et al., 2005, Kaul et al., 2010). Based on these studies, *AMD1* could be a tumour suppressor gene in UM, and it may play a role in tumour prognosis. Furthermore, the current investigations support the concept that large chromosomal deletions can target many tumour suppressor genes, which could contribute to tumorigenesis (Xue et al., 2012). The identified genes in the current study appear to contribute to tumour progression and could be targetable with therapeutics.

The IHC results reveal that *AMD1* was expressed in the cytoplasm, and to some extent in the nucleus of UM cells. Although, the expression of *AMD1* was uniformly across all the groups, it was however, overexpressed in groups 2 and 3, (which mainly showed 6q deletions), and is associated with M3 and 8q gain where they were strongly associated with poor prognosis for UM.

The current investigations support the concept that large chromosomal deletions can targets many tumour suppressor genes that could contribute to tumorigenesis (Xue et al., 2012). In the current study, the identified genes were the most significant within the minimally affected regions, and although the initial observations are interesting there is some confusing on how they may regulate UM growth and progression. It is pertinent that the expression of AMD1, *FOXQ1* and *FARS2* shows significant differences between tumours with and without M3, and overall, in the data using Nexus 7.5, tumours harbouring *FOXQ1* and *FARS2* oncogenes show better survival, whilst the presence of *AMD1* suppressor gene reduced disease-free survival. Some of these findings will hopefully impact on UM patients' care in the future. The observations of this array CGH with IHC need further investigation, since the copy number, alterations are often but not always correlated with gene expression. In addition, more tumour sections should be investigated for gene expression and functional approaches in a model system. In spite of these limitations, the results for this study confirm a wide range of studies, though adding validity to novel observations, and they serve as a starting point for areas of focus in further studies to elucidate pathogenesis in UM.

Overall, this aspect of the study is a pilot study to see if the amplification and deletion of the target genes has any consequences to the expression of the target genes, and

as such may provide an explanation on why these melanomas behave differently. Furthermore, IHC is a relatively cheap and easy to perform technique, which could be adaptable to the classification of UM, in the same measure had *BAP1* assessment is mad {Koopmans, 2014 #474;van de Nes, 2016 #472}, and thus IHC of the target genes would act to validate this findings.

5 Chapter Five

Genetic Alterations in metastasizing Uveal melanoma and relationship to site of presentation.

5.1 Introduction

The use of genetic biomarkers to determine the prognosis of UM patients is now wide spread, and in the previous chapters the relationship of chromosome 6 alterations to outcome was explored in more depth. There is however little understanding of the reasons why genetic biomarkers especially M3 and 8q+ predict poor prognosis. Although the genetic information on primary UM is now substantial, less information is available about the genetic changes found in the hepatic metastases themselves, and reports of metastatic lesions to other sites are almost non-existent (Rey et al., 1985, Aalto et al., 2001, Singh et al., 2009, Trolet et al., 2009). Not surprisingly hepatic metastases also show non-random alterations of chromosomes 1, 3, 6, and 8, but it is of interest that the frequency does not reflect that observed in the primary UM. By far the most frequent alteration in hepatic metastases is 8q gain, ranging from 60 -100% of cases reported, followed by M3 and 6q deletions (Singh et al., 1994, Prescher et al., 1995, White et al., 1998, Damato et al., 2009). Paradoxically although trisomy of 6p is thought to be an indicator of good prognosis, approximately 20% of hepatic metastases will have 6p gain. Equally, loss of 8p has been related to poor prognosis yet is only found in 30% of hepatic metastases. It is clear that although the non-random chromosome alterations are valuable in predicting outcome, the exact relationship to the development of metastatic disease is poorly understood.

Malignant melanoma of the uvea disseminates hematogenously, due to absence of the lymphatic structure of the eye that prohibit passage of the melanotic cells, so the regional lymphatic spread is rare, unless it perforate the sclera and penetrates the conjunctival lymphatics (Yucel et al., 2009). Classically UM metastasize to the liver, and once detected hepatic metastases confer a very poor outcome with patients dying within 6 -12 months of their metastases (Kujala et al., 2003, Bedikian, 2006). The development of hepatic metastases represents the main factor in the failure to improve survival rates over the last 25 years for patients with UM; because the liver metastases are resistant to chemotherapy and tend to be numerous, so are not therefore usually amenable to resection (Bergman et al., 2003). Although the liver is the site of metastases in over 90% of UM patients, metastases also occur at other locations, including bone, lung, brain and skin. Where metastases are widespread the hepatic metastases are invariably the lesions that are detected first (Kath et al., 1993, Kujala et al., 2003, Diener-West et al., 2005, Bedikian, 2006). There are however rare reports (Rietschel et al., 2005) of UM patients that present with non-hepatic metastases, who never develop lesions in the liver, and who survive after metastatic presentation for

longer than those with hepatic lesions. As so little is known about the relationship between genetic biomarkers and metastasis, a better insight may be gained by studying the relationship of genetic changes to the presentation of metastases.

To investigate, UM patients treated in Sheffield where non hepatic lesions were known to have developed were identified. Where aCGH had not already been performed UM samples were identified and analysed (with appropriate ethical approval 15/NW/0230). The investigation into genetic changes and metastatic spread was undertaken in parallel to the aCGH analysis examining the relationship of chromosome 6 changes to prognosis.

Initially 7 UM patients were identified as presenting with non-hepatic metastases. All of these patients shared a genetic abnormality of 1p, which is found in approximately 30 - 40% of UM (Sisley et al., 2000, Aalto et al., 2001, Naus et al., 2002, Kilic et al., 2005, Kilic et al., 2006). To undertake a more robust investigation, it was decided to review the clinical and genetic information available for any UM patient so far recruited in Sheffield for research, including those for which no genetic information was available.

Array CGH analysis already undertaken at this point, had identified other cases with 1p involvement, but where clinical information was unknown (see section 5.2.1 for breakdown). It was also known that earlier karyotypic information (performed by K Sisley) had identified Sheffield UM with 1p deletions, and finally there were other UM cases recruited for other studies, where there was evidence of metastases in addition to hepatic. In effect there were now 4 sub categories of UM cases to explore the potential relationship with genetic biomarkers and metastases, 2 based on clinical associations and 2 on previous genetic findings. For all UM identified in these categories aCGH was undertaken if not already performed. Once all aCGH had been completed a total of 137 UM cases were available, and clinical notes for all patients in the series were re-examined (Rhona Jaques, Macmillan nurse) for the site and sequence of metastatic presentation. In addition to exclude the inclusion of metastatic cutaneous melanoma in the study, where possibly sequencing was performed for *GNAQ, GNA11* and *BRAF*

5.2   Results

5.2.1   Sites of Metastases and genetic background

Originally, only 7 cases were identified, all had the first reported metastases at a site other than the liver (category 1 Non Hepatic metastases NHM). Reviewing the clinical information on research patients identified a further 12 cases with clinical evidence of spread in addition to hepatic metastases (Category 2 Multiple and Hepatic Metastases MHM). Previous cytogenetic evidence for 9 UM confirmed by karyotyping the presence of 1p deletions (category 3) and in addition there were 46 UM for which aCGH data was already available where deletions of 1p were known to be present.

Determining the site of the first detected metastasis was the key discriminator for this study. In addition information was also collected regarding the presentation of metastases in other organs and the sequence for the dissemination of metastases. To ensure there was no bias by selective interrogation of case histories, assessment of clinical notes and follow up for all 137 UM cases analysed by aCGH was undertaken. However due to the time constraints it was not possible to obtain complete updated clinical information for all patients, so analysis was undertaken with the information currently available. Of the series of 137 primary UMs, 54 patients were confirmed to have developed metastases at the point of data analysis.

All samples (74) were successfully analysed, and approximately 70 % of the primary UM had M3 and gain 8q+, of the other most frequently associated alterations chromosome 6 (equal p/q) in 50% of cases. The only abnormality that was common to all cases in the first three categories was partial or complete deletion of 1p. Mutational screening for *GNAQ*, *GNA11* and *BRAF* was performed to exclude cutaneous melanoma, and the majority of the samples were positive for either *GNAQ* or *GNA11* and /or were wildtype for *BRAF*. (data of the 74 patients in this chapter are shown in table 5.1A,B).

The breakdown for all the categories for all changes are presented in figure 5.6

Category 1 Non-hepatic metastases

This group of seven UM patients were the first to be identified, and all presented with non-liver site as the first metastasis, and then for some the liver was involved at a later stage. The most common site of metastasis was the lung with 57% (4/7) of the tumours followed by bone spread with 57% (4/7), and a small percentage of patients developed metastases to brain skin, adrenal, and ovarian. The average survival in this selected group was 77.8 months, which is, approximately (6.5 years). Array data shows that 70 % of these tumours presented with M3 and gain 8q+, and approximately 50% with 6p gain and q loss (Figure 5.6 A). The only abnormality that was common to all cases in the first three groups was partial or complete deletion of 1p as explained in figure 5.1.
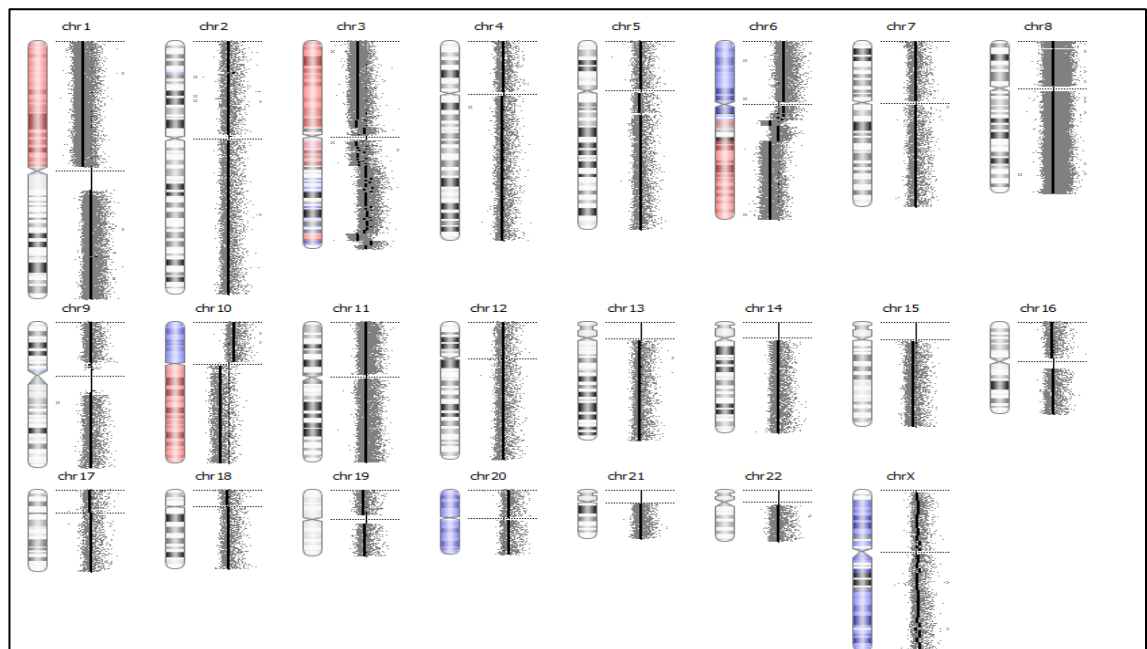
Figure 5.1: aCGH profile of a representative case as an example of Category 1 non-hepatic metastases.

Genome View Ideograms illustrating the aberrant regions on the chromosome are shown as coloured shading (red represent deletion and blue represent amplification), while the black dots represent individual probes. Black vertical line represents magnitude of aberration log$_2$ tumour/reference ratio for the corresponding region on the chromosome. Horizontal distance to the right of the Log ratio represents (Amplification) and the left (Deletion). The current case illustrates the range of CNAs represented by whole chromosome or segmental aneuploidy, where a significant aberration was found (whole arm loss of 1p, partial deletion of 3, gain of 6p and loss of q arm).
Images output from Biodiscovery's Nexus v7.5, and FASST2 algorithm was used to detect all the CNAs.

5.2.1.2 Category 2: Multi-hepatic Metastases MHM

For category 2, 12 UM patients were identified as having liver metastases in addition to multiple organs affected. The most common site of metastases after the liver was the bone with 50%, followed by lung spread with 38.8%, and a small percentage of patients developed metastases to skin, subcutaneous, pancreatic and brain, while two patients classified as having carcinomatosis had a very poor prognosis with 13 months average survival. In total, the average survival in this selected group was 39.8 months, which is, approximately (3.3 years). Data from the aCGH showed that around 90% of the cases had M3 and 60-70 % 8p+/q- with 40-50% equal alteration of 6 (p/q) as shown in Figure (5.6 B). For chromosome 1p an alteration was detected as either a focal, partial or whole arm deletion in the majority of the cases (61%), and the most common focal deletion extended from 1p31.1-p21.3 as shown in figure 5.2.

Figure 5.2 aCGH profile of a representative case as an example of category 2 Multi-hepatic metastases

Genome View Ideograms illustrating the aberrant regions on the chromosome are shown as coloured shading (red represent deletion and blue represent amplification), while the black dots represent individual probes. Black vertical line represents magnitude of aberration log2 tumour/reference ratio for the corresponding region on the chromosome. Horizontal distance to the right of the Log ratio represents (Amplification) and the left (Deletion). The current case illustrates partial deletion of 1p arm (del 1p31.1-p21.3) with M3 and i8q.

Images output from Biodiscovery's Nexus v7.5, and FASST2 algorithm was used to detect al the CNAs

As previously mentioned throughout all of the study, all UM's were paired where possible with their matched normal blood as a reference, to remove germline copy number variation CNVs, to ensure that any somatic copy number variations SCNAs is a genuine change and associated with the disease. In category 1 and 2 some of UMs were analysed against commercial DNA and these had a focal deletion (1p31.1), possibly representing a germline polymorphism. Interestingly this allelic loss on the short arm of chromosome 1 was reported previously in primary UM (Aalto et al., 2001) (figure 5.3)
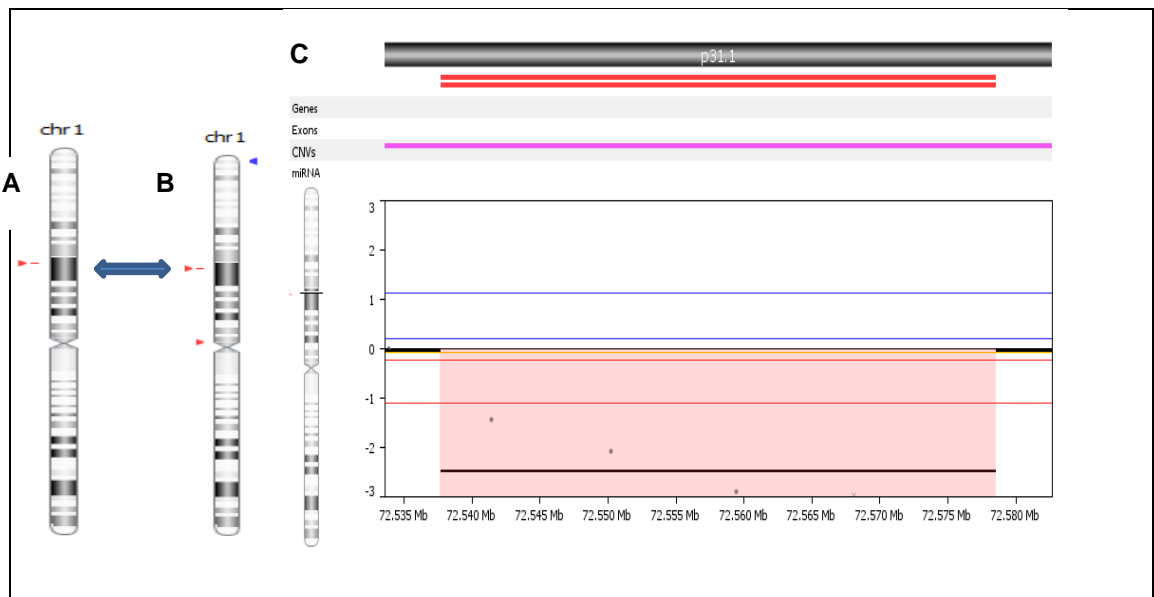
Figure 5.3: Regional deletion represented by Frequency plot showing an example of aberrant region that represents a copy number variations CNVs

A. Chromosome 1 ideograms with representative case of the Non-hepatic metastases (Mel 58), and **B**. Multi-hepatic metastases case (Mel 67). In both cases the aberrant regions are shown as coloured shading on the chromosome (blue represents amplification and red represents deletion), chromosome 1 focal deletion (1p31.1) was detected, although this genetic variant could represent germline CNV. **C.** The region below the vertical line represented by double red straps (pink shading below zero line) shows a regional deletion with 40Mb approximate size, lies completely within known CNV area (represented by the purple line) and contains no gene loci, it was therefore excluded from the analysis to be likely CNV.
Images output from Biodiscovery's Nexus v7.5, and FASST2 algorithm was used to detect all the CNAs and the known CNVs.

Category 3: Previous cytogenetic analysis with deletions of 1p

In this category, 11 cases were identified from previous cytogenetic analysis where there was evidence for deletions of 1p, some of these cases have been previously reported (Sisley et al., 1990, Sisley et al., 1992, Sisley et al., 1997, Sisley et al., 2000). For those where there was no aCGH the analysis was performed and confirmed in 80% an alteration in chromosome 1p as focal, partial or whole arm deletion example shown in figure 5.4. In addition, approximately 60% of the tumours harbouring M3 with 8q gain with 40% had 6p and 50% 6q as shown in Figures 5.6 C. For this category, the most common site of metastases was the liver with 88.8% followed by lung, bone, brain and subcutaneous. In total, the average survival in this selected group was 50.5 months, which is, approximately (4.2 years). Although the follow up for 1 case was lost and cause of death was not confirmed for another patient, overall the prognosis for this group was poor due the liver metastasis.
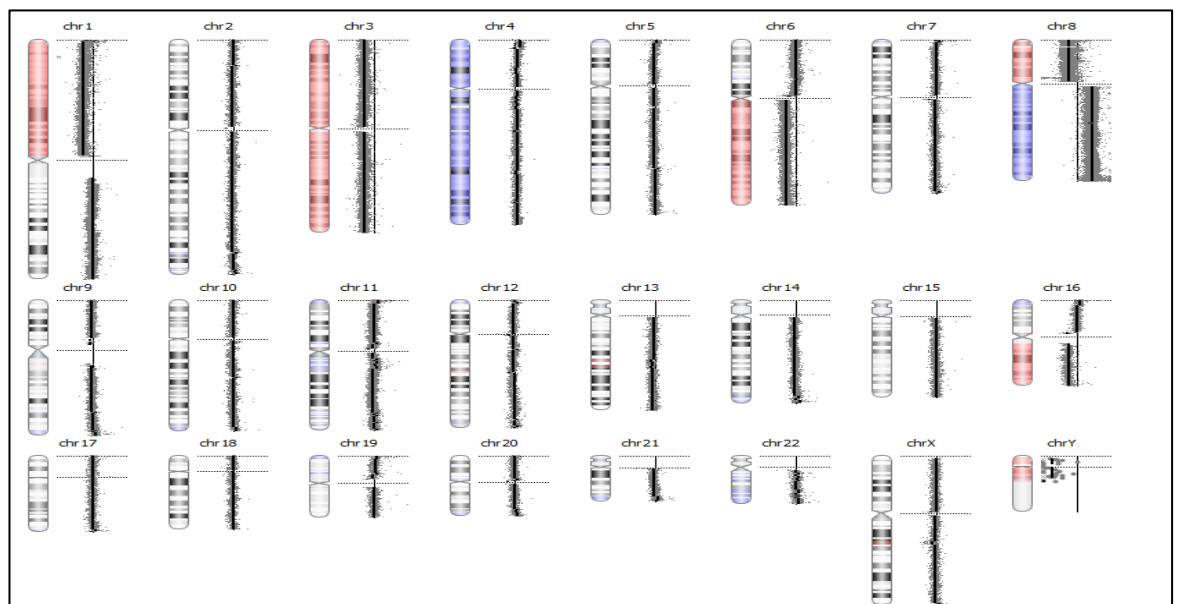
Figure 5.4: Whole Genome ideograms with representative case of 1p del, initially identified by cytogenetics as an example of category 3.

Genome View illustrating the aberrant regions on the chromosome are shown as coloured shading (red represent deletion and blue represent amplification), while the black dots represent individual probes. Black vertical line represents magnitude of aberration $\log_2$ tumour/reference ratio for the corresponding region on the chromosome. Horizontal distance to the right of the Log ratio represents (Amplification) and the left (Deletion). The current case illustrates whole arm loss of 1p, M3, 6q loss and i8q.

Images output from Biodiscovery's Nexus v7.5, and FASST2 algorithm was used to detect all the CNAs

5.2.1.4 Category 4: Chromosome 1p deletion detected by aCGH

This group comprised 46 cases with1p alterations in the form of focal, partial or whole arm deletions, example shown in figure 5.5. These UM were cases from the series of aCGH that had already been performed without prior knowledge of any genetic or clinical associations. Unfortunately for this category more patients were lost to follow up and many cases were analysed prospectively so the associations for this category would consequently be less robust. Nevertheless, 34% of the patients had liver metastasis, with a small percentage of patients developing lung and spinal metastases, while 15% died from unrelated causes. In total, the average survival in this selected group was 40.32 months, which is, approximately (3.36 years). The aCGH data showed M3, with around 60% of the tumours with 8q gain, and approximately 75 % equal alteration of 6 (p/q) as shown in Figures (5.6 C).
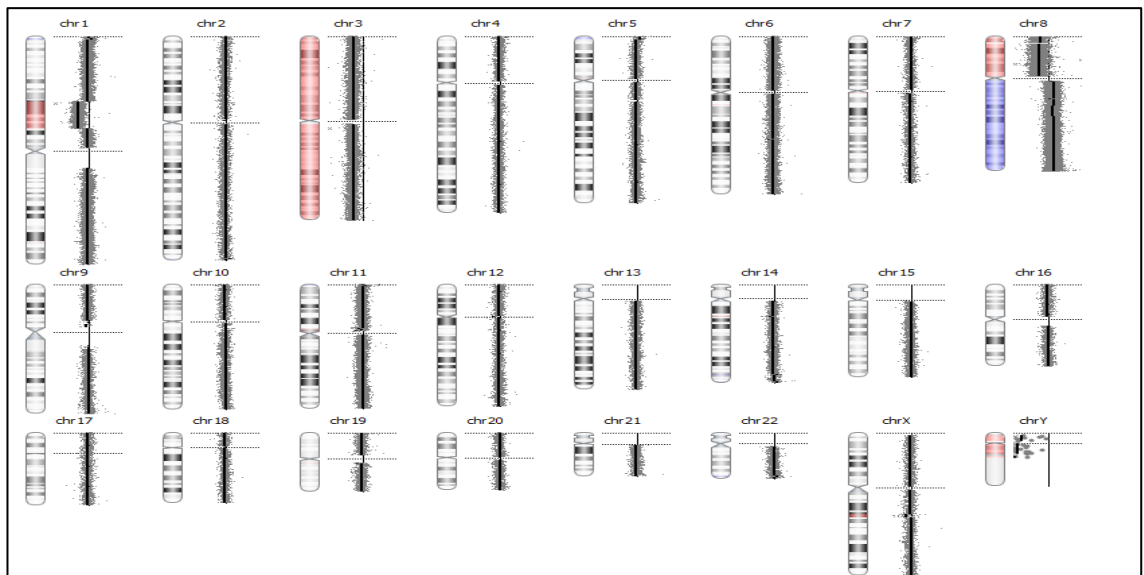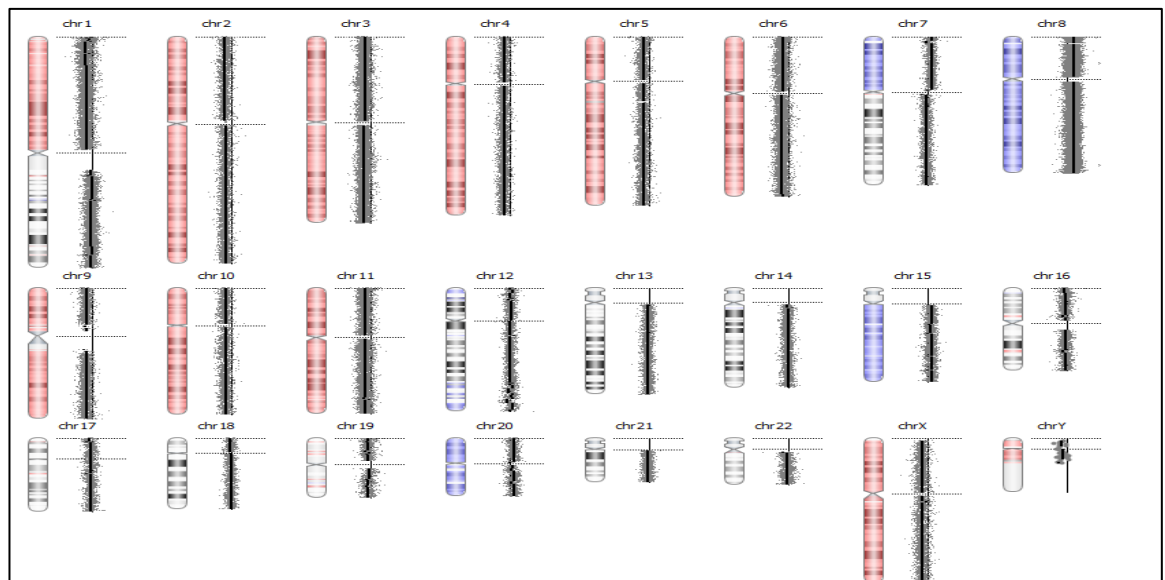

Figure 5.5: aCGH profile of a representative case as an example of category 4.

Genome View Ideograms illustrating the aberrant regions on the chromosome are shown as coloured shading (red represent deletion and blue represent amplification), while the black dots represent individual probes. Black vertical line represents magnitude of aberration log2 tumour/reference ratio for the corresponding region on the chromosome. Horizontal distance to the right of the Log ratio represents (Amplification) and the left (Deletion). The current case illustrate the range of CNAs represented by whole chromosome or segmental aneuploidy, where the significant aberration were found (whole arm loss of 1p, M3, loss of chromosome 6 and gain of 8), in addition to several region of amplification and deletions. Most of the CNAs in this tumour are suggestive of high level of aberration gain/loss.

Images output from Biodiscovery's Nexus v7.5, and FASST2 algorithm was used to detect all the CNAs.
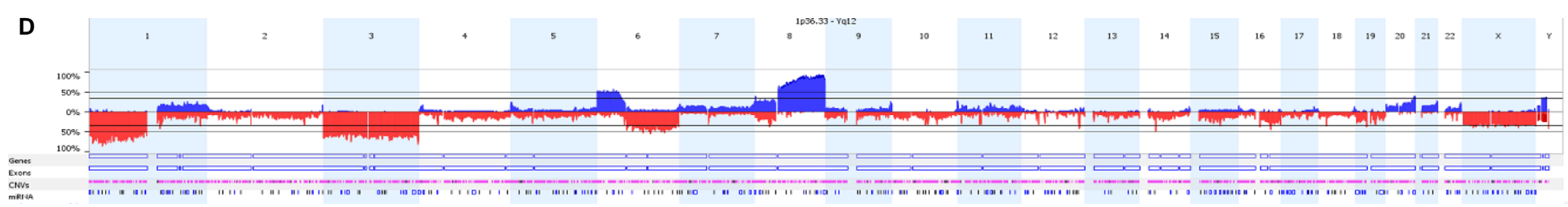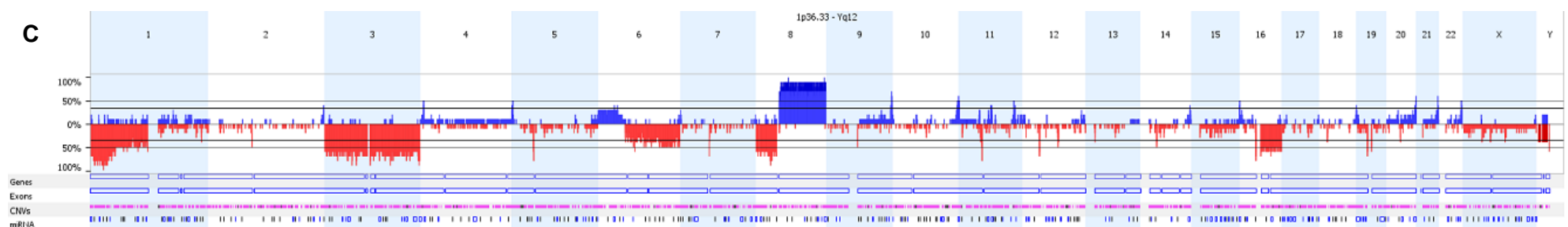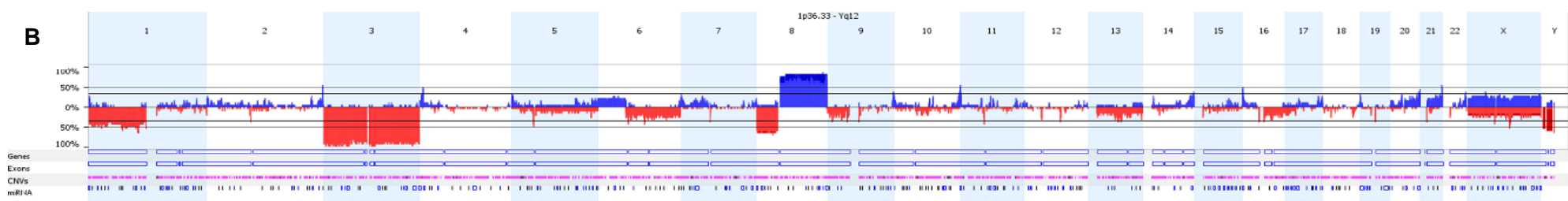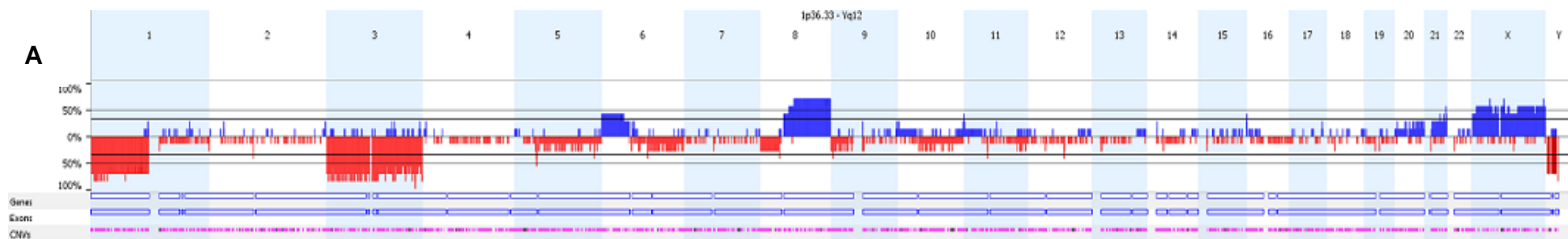
Figure 5.6: Frequency plots showing the genetic changes associated with 1p deletion

Genomic view displays the information on all of the chromosomes for different samples at once. The y-axis designates the percentage of the alteration in the selected samples at specific point along the genome and presents the $\log_2$ tumour/reference ratio, and the genome coordinates of the ~180,000 probes on the UM custom array positioned by chromosome location on the x-axis. Horizontally along the top blue lines plotted above the 0% indicates copy number gain, and red indicate copy number loss events and plotted below 0% baseline. These four ideograms illustrate the range of CNAs represented by whole and segmental chromosomal aneuploidy across the UM patients genome, and delineates the frequency of losses in 1p with M3, 6q, 8p, and gains in 6p, 8q. **A**. Category 1 demonstrating patients presenting first with the non-hepatic metastases, where 1p loss was the most common in all 7 cases. **B**. Category 2, demonstrates the multi hepatic tumours where 1p partial or whole arm deletion represents approximately 75% of the cases. **C**. Category 3, represents UM having 1p changes confirmed by cytogenetic and aCGH **D**. Category 4 UM for which aCGH identified 1p deletion (focal or entire arm loss) from 46 primary tumours.

Images output from Biodiscovery's Nexus v7.5, and FASST2 algorithm was used to detect all the CNAs

5.2.2 Overall survival

The clinical supportive data was variable for the series as a whole, as many patients had been referred from a long distance and subsequently lost to follow up. Although time interval from diagnosis of liver metastasis to death for the majority of the patients in this series was difficult to collect, survival data was analysed from the point of presentation (or treatment) to the point of death or known survival, and was compared for the 4 categories and is presented in table 5.1. Overall the categories 57% of the patients developed liver metastasis followed in frequency by lung in 19% and bone in 16%.

The current results illustrate that survival of the patients harbouring focal, partial or whole arm deletion of 1p are varied according to the pattern of metastases, for all patients from different categories. Whereas the involvement of the liver even it is associated with multi-organs metastasis is still a poor prognostic indicator as shown in Figure 5.7. However, metastases that originate first from non-liver site as lung or bone have a tendency for longer survival, patients with no liver metastasis presented with longer disease free survival. Although, the first 3 categories were having either hepatic or non-hepatic metastasis, category 4 however, had some patients was presented with no metastases and had a median survival of 69.66 months, and more than 5 year

disease free survival rate (Figure 5.7), whoever, patients with metastases had total median survival of 26.5 months in the same group.

Overall, time interval from liver metastasis to death was available in this study for (7 patients only out of 74), with 8.88 months average survival range. The most notable genetic changes were equal alterations of 1p deletions, M3 and 8q gain with 71% (5/7) each and 6q with 42% (3/7) and (2/7) 28% of 6p involvement, detailed cases with clinical and genetic findings attached in Appendices 3. Therefore, the current data suggested that the coexistence of 1p deletion and M3/8q+ with liver metastasis is an independent predictor of decrease disease free survival in UM patients.
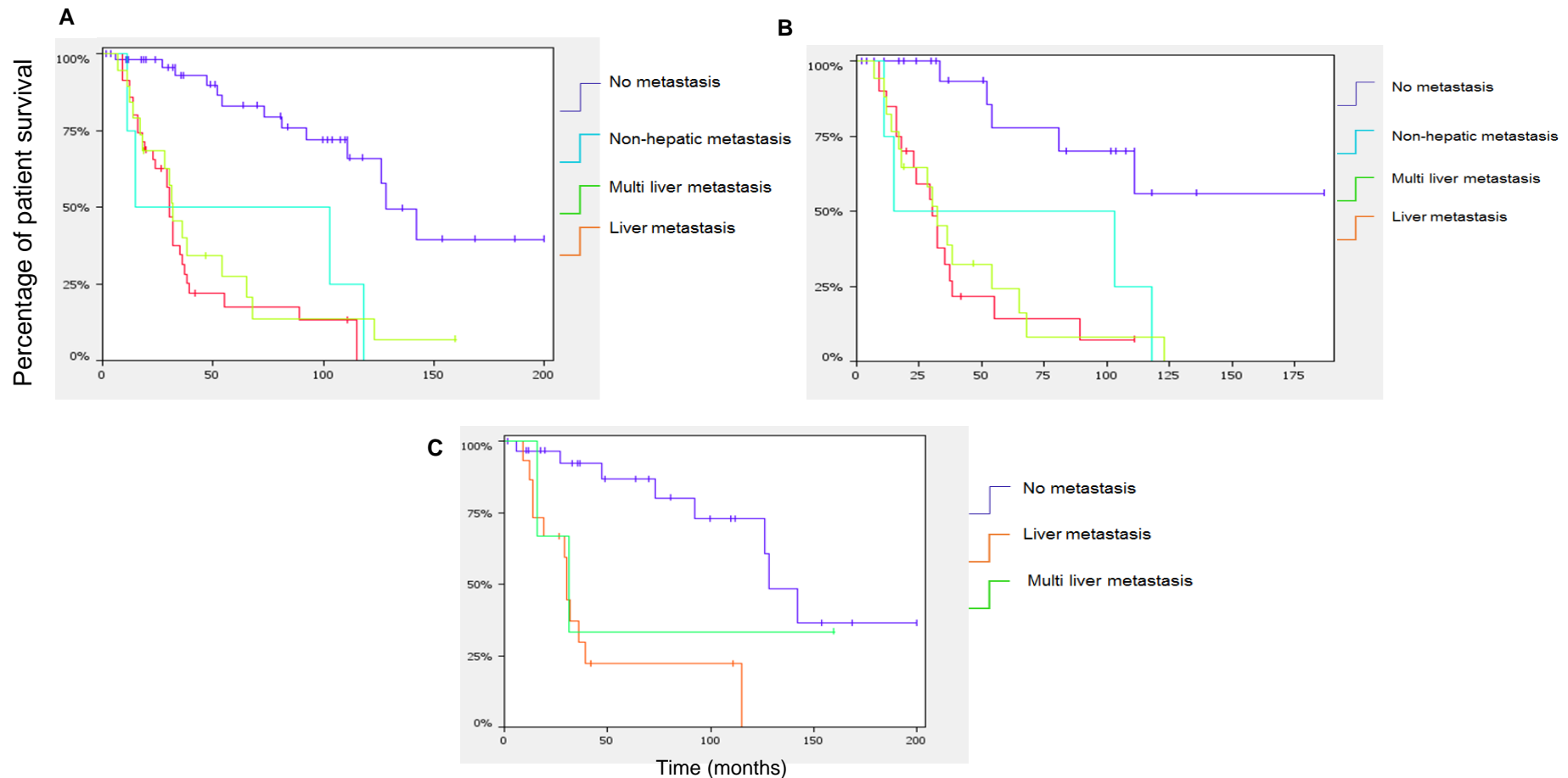
Figure 5.7: Kaplan-Meier survival curve for metastasis-related death according to genomic results with origin of metastases

The Y-axis represents the percentage of patients; X-axis is representing survival time by months. **A**. The diagram illustrate all 137 UM patients with non hepatic metastases/ with or without liver, the involvement of the liver shows the worst survival. **B**. The diagram shows 71 UM patients with 1p deletion only, in relation to liver, multi-hepatic and non-hepatic liver metastases, demonstrate the same pattern of survival as the whole series compared to **C**. which showing the metastatic UM in the absence of 1p deletion. Overall, no metastases development show an increase with disease free survival with more than 10 years, while Patients that harbouring liver/ multi liver metastasis and associated with 1p alterations show decrease in the disease free survival.

As an overview, for the series as a whole (137 cases), 54 patients were known to have developed metastases and out of 137 UM 71 had deletions of 1p. The relationship between 1p deletion and metastatic presentation was therefore as presented in Tables 5.2, 5.3

Table 5.2: Analysis of 1p deletion and metastatic presentation in patient with UM (Whole series n=137 cases)

	No Metastases	Liver metastases only	Non hepatic metastases/ with or without liver
UM with 1p deletions (n=71)	31 (22%)	20 (15%)	20 (15%)
UM without 1p deletions (n=66)	52 (38%)	12 (9%)	2 (1.4%)

Table 5.3: Analysis of cases with known metastases (n=54) and their relationship to 1p deletion

	Liver metastases only	Non hepatic metastases / with liver
UM with 1p deletions (n=40)	20 (37%)	20 (37%)
UM without 1p deletions (n=14)	12 (22%)	2 (3.7%)

5.2.3 Assessment of short list candidate genes

For most UM cases where deletions of 1p were found the whole arm was affected. However, in this current series 9 cases out of those with del 1p had focal deletions as shown in figure 5.8. Although previous studies of UM have observed that 1p36 was the most frequently deleted region on 1p, this current study highlighted a number of different regions of interest, with the most significant number of deleted genes were located at 1p35.3. Totally the genes were deleted in 41 cases having a large SCNA (partial or whole-arm deletion) covered the genomic area of interest included 1p35.3. Therefore, a short list of candidate genes was identified as explained in section (4.2.4), with GISTIC and STAC statistical approaches generating a validated shortlist of candidate genes that could act as possible genes of interest for UM patients who develop multiple metastases to sites in addition to the liver. The assessments of the chosen genes were based on the biological and molecular function of *MED18* (mediator complex subunit 18), *PHACTR4* (phosphatase and actin regulator 4), and *RCC1* (regulator of chromosome condensation 1). The final shortlist of candidate genes is shown in table 5.4
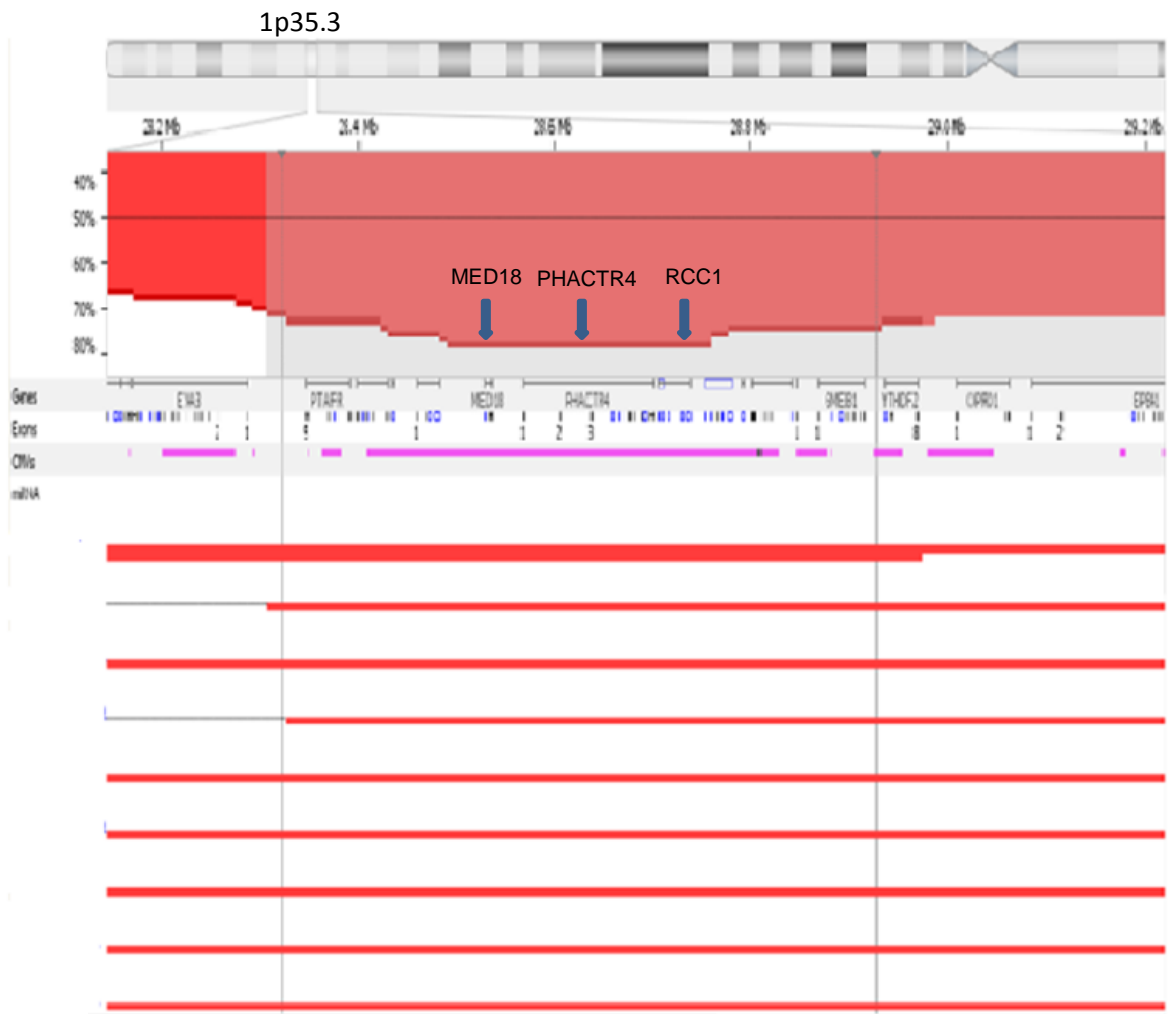
Figure 5.8: Focal deletions of chromosome 1p in 9 UM. Stacked SCNA from individuals UM cases with 1p deletion showing the most significant candidate genes in this genomic region.

The upper panel showing chromosomal region (1p35.3) and its approximate size, and the middle panel shows the frequency plot of alteration among the y-axis of the corresponding UM cases. The left horizontal line represents individual UM samples. The common aberrant regions are bolted along x-axis against their chromosomal positions, and the q value are blotted on the y-axis on a negative log10 scale where the most significant commonly deleted genomic regions are presented by the highest red bars. Statistically significant genomic regions with maximal G-score and minimal q-value (10 and 0.05 respectively) highlighted grey and contained the most important genes in this region where blue arrows represent MED18, PHACTR4, RCC1 genes respectively.

All aberration in each sample were called using FASST2 Algorithm

Gene Symbol and Name	Start	End	Length Kb	Biological Process	Molecular Function
MED18 mediator complex subunit 18	28528099	28535065	6967	regulation of transcription from RNA polymerase II promoter, transcription from RNA polymerase II promoter	RNA polymerase II transcription cofactor activity, protein binding
PHACTR4 phosphatase and actin regulator 4	28568679	28699468	130790	Rho protein signal transduction, actin cytoskeleton organization, closure of optic fissure, enteric nervous system development, negative regulation of integrin-mediated signaling pathway, neural crest cell migration, neural tube closure, positive regulation of catalytic activity, regulation of cell cycle	actin binding, protein phosphatase 1 binding, protein phosphatase type 1 activator activity
RCC1 regulator of chromosome condensation 1	28705041	28738295	33255	G1/S transition of mitotic cell cycle, cell division, chromosome segregation, mitotic nuclear division, mitotic spindle organization, regulation of mitotic nuclear division, spindle assembly, viral process	Ran guanyl-nucleotide exchange factor activity, chromatin binding, histone binding, nucleosomal DNA binding, protein binding
TRNAU1AP tRNA selenocysteine 1 associated protein 1	28752115	28777644	25530	selenocysteine incorporation	
SNHG3 small nucleolar RNA host gene 3 (non-protein coding)	28705041	28709991	4951		
SNORA73B small nucleolar RNA, H/ACA box 73B	28707656	28707814	159		

Table 5.4 Short list candidate genes located at 1p35.3

5.2.4 Mutational analysis for *GNAQ, GNA11* and *BRAF V600E*

Mutational screening for *GNAQ*, *GNA11* and *BRAF* was performed for the 74 primary UMs that either had presentation of multiple metastases, or deletions of 1p (categories 1-4) table 5.5. Sequencing was undertaken to confirm that all the cases were UM and not metastatic cutaneous melanoma. Due to the time frame it was not possible to sequence all 137 UM for which aCGH data was available, and efforts were concentrated on those cases of most pertinence to the current investigation. The majority of the UM were able to be sequenced for the most common mutations or *GNAQ* and *GNA11*, and most were positive for either *GNAQ* or *GNA11* and /or were wildtype for *BRAF,* confirming them as UM. Although 11 samples failed to sequence for *BRAF* or *GNA11* and one tumour failed to sequence *GNAQ* due to a problem with storage of the DNA. Overall, 60 tumours (81%) had mutually exclusive mutations affecting exon 5 codon 209 of the *G protein alpha-subunit Q* (*GNAQ*) gene (figure 5.10) and the *G protein alpha-subunit 11 (GNA11)* gene (figure 5.11) details are shown in table 4.1. None of the 74 UM had mutations of *BRAF* V600E (figure 5.9).
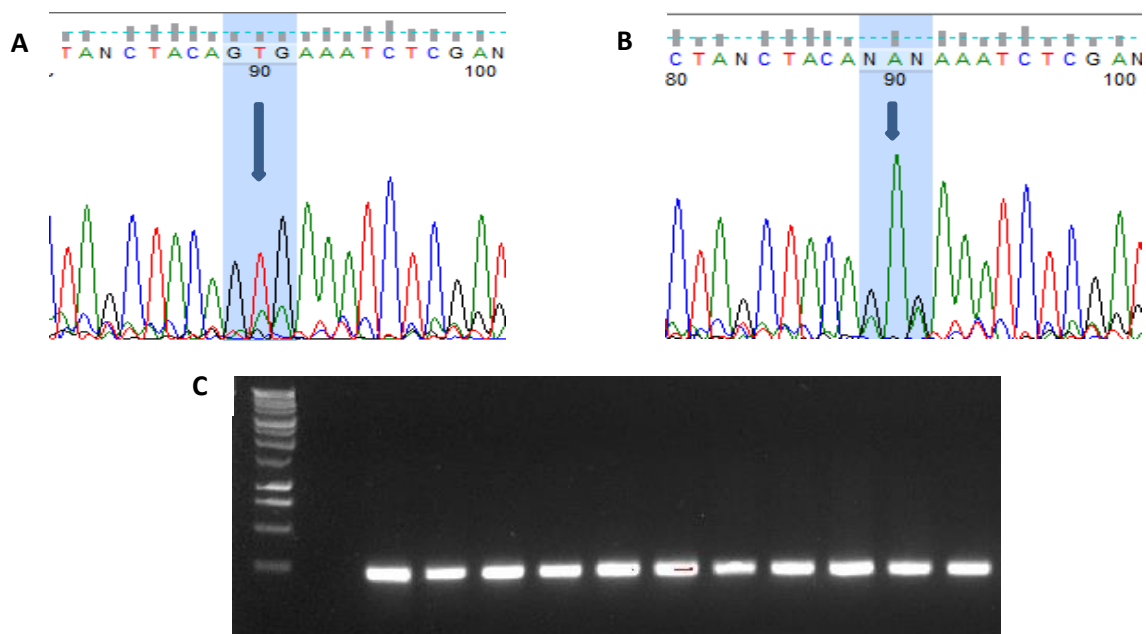
Figure 5.9: Chromatogram sequencing traces of wildtype and mutated BRAF gene

A. Is a wild type example of sequencing Chromatogram with *BRAF* codon 600 heterozygous (Highlighted by blue arrow with normal sequence GTG). **B**. a mutated example of BRAF at codon 600 at GTG>GAG (Highlighted by blue arrow GAG) resulting of substitutions of glutamic acid for valine (BRAFV600E: nucleotide 1799

T>A). **C**. gel electrophoresis with 1kb marker demonstrates BRAF amplified PCR product with 224bp template size.
Image output represents Forward sequence using Finch TV software (Geospiza)

5.2.4.1 *GNAQ* and *GNA11* (exon 5) screening

Purified PCR products were sequenced for *GNAQ* exon 5, mutations were detected at codon 209 within exon 5, over 74 tumour secerned for *GNAQ and GNA11* the overall mutation frequency for both was 49% (36/74) and 33% (24/74) subsequently. Mutations affecting codon 209 in GNAQ c.626A>T (Q209L) were 27% resulting in a glutamine to leucine substitution, and 22% of the tumours were found to have a mutation in codon 209 in GNAQ c.626A>C (Q209P) resulting in a glutamine to proline substitution as elucidated in figure (4.10). Mutations affecting codon 209 in GNA11 c.626A>T (Q209L) resulting in a glutamine to leucine substitution in all samples analysed, as elucidated in figure (4.11)
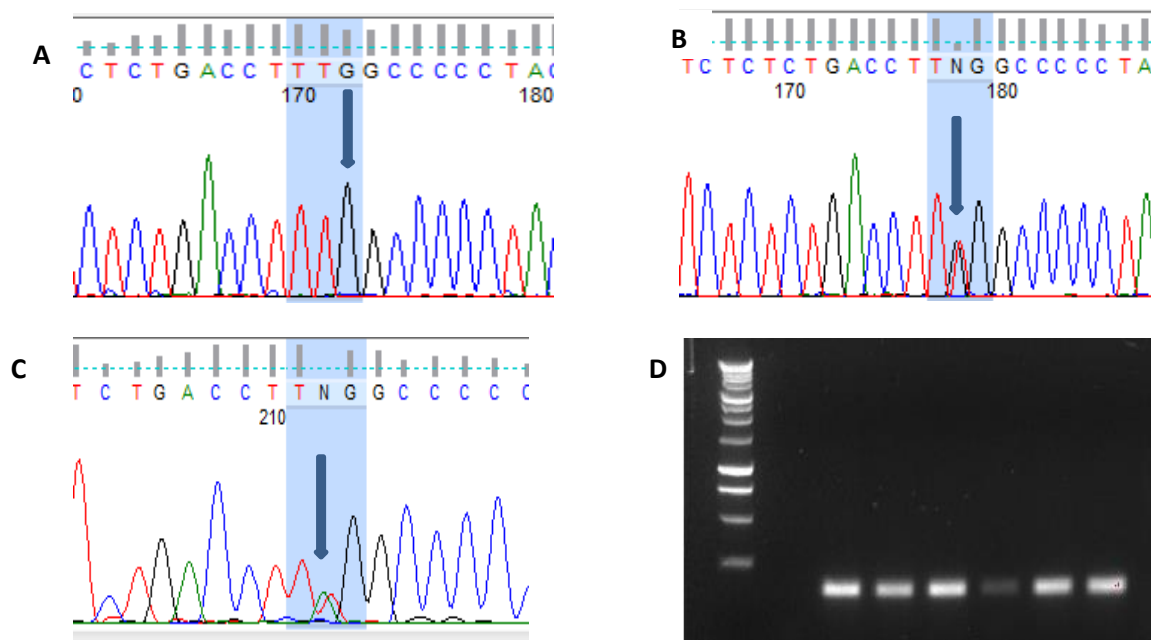
Figure 5.10: Chromatogram sequencing trace of wildtype and mutated GNAQ gene.

A. elucidates a wild type example of sequencing chromatogram with codon 209 (highlighted by blow arrow indicting the normal sequence of *GNAQ* TTG). **B**. elucidate a point mutation at Q209 **T to G** within the Uveal melanoma the nucleotide alteration highlighted by a blue arrow (TTG>TGG) **C**. is showing a point mutation at Q209 **T to A** within the Uveal melanoma (TTG>TAG). **D**. gel electrophoresis with 1kb marker demonstrates *GNAQ* amplified PCR products with 317bp template size.

Figure 5.11: Chromatogram sequencing trace of wildtype and mutated GNA11 gene.

A. elucidates a wild type example of sequencing chromatogram with codon 209 (highlighted by blow arrow indicting the normal sequence of GNA11 CTG). **B**. elucidate a point mutation at Q209 **T to A** within the UM the nucleotide alteration highlighted by a blue arrow (CTG>CAG) **C.** gel electrophoresis with 1kb marker demonstrates GNA11 amplified PCR product with 147bp template size.
Image output represents Reverse sequence using Finch TV software (Geospiza)

Table 5.5 Summary of all the samples sequenced with *GNAQ*/*GNA11Q209* and *BRAF* at the point of data analysis based on categories 1-4

Case Number	BRAF	GNAQ	GNA11
07	WT	WT	Q209L
38	WT	Q209L	WT
58	WT	Q209L	WT
63	WT	WT	WT
70	WT	Q209L	WT
73	WT	WT	WT
78	WT	Q209P	WT
18	WT	Q209P	WT
20	WT	Q209P	WT
21	WT	WT	Q209L
24	WT	Q209L	WT
31	WT	WT	WT
40	Failed	Q209L	Failed
64	WT	WT	Q209L
67	WT	WT	WT
68	WT	Q209P	WT
71	WT	WT	Q209L
02	WT	Q209P	WT
03	WT	Q209P	WT
15	WT	WT	Q209L
23	Failed	Q209P	Failed
52	WT	WT	Q209L
54	WT	Q209L	WT
57	WT	Q209P	WT
05	WT	WT	Q209L
12	WT	Q209L	WT
13	WT	WT	Q206L
16	WT	WT	Q209L
19	WT	Q209L	WT
28	WT	Q209L	WT
36	Failed	WT	Failed
62	WT	WT	Q209L
77	WT	WT	Q209L
79	WT	WT	Q209L
109	WT	WT	Q209L
120	WT	Q209P	WT
131	WT	Q209L	WT
136	WT	WT	WT

08	WT	Q209L	WT
22	WT	Q209L	WT
43	Failed	WT	Q209L
10	WT	WT	Q209L
11	WT	WT	Q209L
35	Failed	Q209P	Failed
37	Failed	Q209L	WT
42	Failed	WT	Failed
49	WT	WT	WT
48	WT	Failed	Failed
64	WT	Q209L	WT
75	WT	Q209L	WT
76	WT	Q209P	WT
81	WT	WT	Q209L
82	WT	WT	WT
83	Failed	WT	Failed
92	WT	Q209P	WT
93	WT	Q209P	WT
95	WT	WT	Failed
97	WT	Q209P	WT
98	WT	WT	Q209L
103	WT	WT	Q209L
104	WT	WT	Q209P
105	WT	Q209L	WT
106	WT	Q209L	WT
108	WT	Q209L	WT
111	WT	WT	Q209L
114	WT	WT	WT
122	WT	Q209P	WT
126	WT	WT	Q209L
129	WT	WT	WT
132	WT	Q209P	WT
133	WT	Q209L	WT
135	WT	WT	Q209L

5.2.4.2 *GNAQ* and *GNA11* (exon 4) screening

Around 12% (9/74) of the tumours show no mutations in either *GNAQ* or *GNA11*, where 2 of them was in category 1 (NHM), 2 from category 2 (MHM) and 5 tumours with GNAQ, GNA11 wild types were from category 4. Therefore, to investigate the mutations in these cases, (Dr. Rachel E Doherty) sequenced hot spot regions of GNAQ and GNA11 exon 4. No mutations were found in *GNAQ* exon 4, and only one tumour harboured point mutation affecting codon 183 within exon 4 in *GNA11* c.547C>T (R183C) resulting in arginine (R) to cysteine substations. The details are presented below in table 5.6.

Table 5.6 Summary of all the wt *GNAQ*/*GNA11Q209* samples sequenced with *GNAQ/GNA11 R183*

Sample	*GNAQ Q209*	*GNA11 Q209*	*GNAQ R183*	*GNA11 R183*
13	wt	wt	wt	wt
31	wt	wt	wt	wt
63	wt	wt	wt	wt
67	wt	wt	wt	wt
73	wt	wt	wt	wt
82	wt	wt	wt	wt
112	wt	wt	wt	C>T
129	wt	wt	wt	wt
136	wt	wt	wt	wt

WT= Wild type

Case Number	Genetic changes regarding 1p	Metastatic history
07	1p del	Lung, bone, spinal and liver (D 54 M) *
38	1p del	Lung, adrenal, and cerebral (D 118 M) *
58	del1p31.1	Ovarian, lung and liver (D 103 M) *
63	1p del	Brain first then multi hepatic (D 123 M) *
70	multi focal del	Bone and liver (D 38 M) *
73	1p del	Bone (D 28 M) *
78	1p del	Lung, skin, and liver (alive 47 M) *
18	No 1p del	Liver and bone (D 12 M) **
20	Focal del 1p21.1/1p31.1	Bone (Death not known) **
21	Focal del 1p21.1/p31.1	Subcutaneous and liver (D 32 M) **
24	1p del	Liver and spin (D 55 M) **
31	Focal del p21.1/p31.1	Liver and skin (D 36 M) **
40	1p del	Liver and bone (D 7 M) **
64	1p del	Carcinomatosis (D 15 M) **
67	Focal del p31.1	Lung, liver, pancreatic (D 18 M) **
68	Focal del 1p31.1-p21.3	Liver, lung, bone (D 14 M) **
71	Focal del 1p34.2-1pter/1p21.1	Carcinomatosis (D 11 M) **
02	1p del	Liver , brain, subcutaneous (D 86 M)
03	focal del1p34.3-1pter	LM (D 9 M)
15	del1p35.3	Liver and bone (D 30 M)
23	1p del	LM (D 35 M)
52	1p del	LM (D 32 M)
54	1p del	LM (D 18 M)
57	focal del1p33-1pter	LM (D 16 M)
05	Focal (p32.3/p22.1)	LM (D 30 M)
12	1p-	LM (D 17 M)
13	1p-	LM (D 16 M)
16	1p-	LM (D 23 M)
19	1p-	LM (D 38 M)
28	1p-	LM (D 32 M)
36	1p-	LM (D 24 M)
62	1p-	LM (D 89 M)
77	1p-	LM (D 37 M)
79	1p-	LM (29 M)
109	1p-	LM (alive 37 M)
120	1p-	LM (D 9 M)
131	1p-	Liver and spinal (alive 19 M)
136	1p-	LM (alive 20 M)
08	1p-	LM (D 12 M)
22	1p del	Lost follow up

43	focal del1p32.3-1pter	Cause Not confirmed (D 111 M)
10	Multi focal del	Alive (136 M)
11	1p-	Died Motor neurone disease (81 M)
35	Multi focal del	Alive (118 M)
37	1p-	Died CVA (54 M)
42	1p34.3-pter	Alive (111 M)
49	1p-	Alive (84 M)
48	Multi focal del	Alive (104 M)
64	1p-	Alive (108 M)
75	1p-	Alive (70 M)
76	1p-	Died cause not confirmed (80 M)
81	1p-	Alive (4 M)
82	1p-	Alive (31 M)
83	1p-	Alive (36 M)
92	1p-	Died cause of death unknown (14 M)
93	1p-	Alive (30 M)
95	1p-	Alive (15 M)
97	1p-	Died cause not confirm (52 M)
98	1p-	Alive (51 M)
103	1p-	Died date need to be confirmed
104	1p-	Alive (19 M)
105	Multi focal del	Died cause not confirm (33 M)
106	1p-	Alive (11 M)
108	1p33-pter	Alive (2 M)
111	1p-	Alive (7 month)
114	Multi focal del	Alive (37 M)
122	1p-	Alive (32 M)
126	Multi focal del	Alive (13 M)
129	1p-	Alive (24 M)
132	1p-	No data
133	1p36.11-21	Alive (17 M)
135	1p-	No data

Table 5.1 A: Clinical data with metastatic history for all patients with 1p deletion.

Case Number	Genetic changes regarding 1p	Metastatic history
27	No 1p del	Liver, lung, skin (D 65 M) **
39	No 1p del	Liver, lung, bone (D 11 M) **
137	No 1p del	MHM (D 16 M)
51	No 1p del	LM (D 9M)
32	No 1p del	LM (D 30 M)
1	No 1p del	LM (D 115 M)
9	No 1p del	LM (D 14 M)
80	No 1p del	LM (D 14 M)
100	No 1p del	LM (D 29 M)
55	No 1p del	LM (D 32 M)
59	No 1p del	LM (D 36 M)
60	No 1p del	LM (D 12 M)
85	No 1p del	LM (D 19 M)
86	No 1p del	LM (D 30 M)
87	No 1p del	LM (D 39 M)

Table 5.1 B: Clinical data based on the site of metastases in the absence of 1p deletion.

Out of 137 patients 54 have confirmed metastases at the point of data analysis.

 (*) Patients originally identified as non-hepatic metastases (NHM)

(**)Patients originally identified as Multi-hepatic Metastases (MHM)

LM: liver metastasis

D = Died

M= Month

5.3 Discussion

Survival for UM has not changed in over 30 years (Singh and Topham, 2003, Papastefanou and Cohen, 2011, Kujala et al., 2003), mainly reflecting the very poor outcome once hepatic metastases are detected. Although the liver is the most common site for metastasis (90%) other organs are also affected, but usually hepatic metastases are invariably the lesions that are detected first (Kath et al., 1993, Kujala et al., 2003, Bedikian, 2006). It is highly unusual for UM patients to first present with metastases in sites other than the liver, and in this study 7 such UM patients were identified as presenting initially with no liver involvement. The majority however did subsequently develop liver metastases. Although patients of interest were identified as part of subgroups, the series was examined as a whole.

Few studies have looked at prognosis for UM depending on site of metastasis, although Rietschel *et al*, found that UM patients who developed metastasis to the lung as the first site had prolonged survival (Rietschel et al., 2005), and Kath et al, found patients presenting with non-hepatic metastases also had longer survival (Kath et al., 1993).   Comparing our study with those previous ones, the subset of patients harbouring metastasis to lungs/bone and other organs had 77.8 months disease free survival, which is relatively a high proportion of long survival. In the other hand, survival was reduced while the initial metastasis was the liver compared to lung or bone with shorter interval from diagnosis to metastatic spread with 39.8 months, and that clearly indicates that tumours metastasize to liver tend to have worst prognosis. Although less studies, correlates the prognosis of metastasising tumours to the genetic changes of the disease, therefore, this study look in more depth genetically trying to identified more accurate prognostications, though Improving the identifications of high-risk tumours help targeted proper screening of the metastatic disease, and give better chance for clinical trials for different treatments.   Although, In this study (other than hepatic lesions), the lung and then bone were the organs that were mostly to present with first metastases, the number of cases however, was too small to further subdivide to see if these sites conferred a different survival.

Deletion of 1p is not exclusive to UM, it is also found in many solid tumours; such as neural crest derived neuroblastoma, and cutaneous melanoma, where is known to be predictor of unfavourable prognosis (Caron et al., 1996, Knuutila et al., 1999). In UM, deletion of 1p has been detected predominantly in metastasizing tumours with M3 (Naus et al., 2001) and although associated with a poorer outcome and though to

relate to tumour progression its prognostic significance is not as clear cut as M3 (Aalto et al., 2001, Hausler et al., 2005, Kilic et al., 2005).   Furthermore, the concurrent loss of 1p, M3 and gain of long arm of chromosome 8 are suggested in this study to be associated with metastasis related to death in UM patients. Where Sisley et al, demonstrate the association between 1p deletion and the large ciliary body melanoma, occurring after M3 and 8q gain (Sisley et al., 2000, Kilic et al., 2005, Kilic et al., 2006). Although this study demonstrates that loss of 1p was found to be the only alteration common to the majority of the primary tumours with non/multi-hepatic metastasis, hence, the non-random chromosome alterations are valuable in predicting the disease outcome, the exact relationship to the development of metastatic disease is poorly understood.

Loss of 1p36 region was frequently observed in many tumours types that originate from neural crest derived cells, including neuroblastoma and malignant melanoma, thus, loss of this chromosomal region was known to be predictor of unfavourable clinical outcome (Caron et al., 1996, Casciano et al., 2002, Poetsch et al., 2003). In UM the focused breakpoints in 1p deletion extents from 1p32-36, and the literature reported 36% of 1p36 deletion, and the majority of metastasising tumour with 1p36 loss has concurrent M3. (Sisley et al., 2000, Aalto et al., 2001, Naus et al., 2002, Kilic et al., 2005, Kilic et al., 2006, Hughes et al., 2005)

The present findings suggest that although the focal deletions affecting chromosome 1 target a large and gene dense region, several tumour suppressor genes are statistically relevant.   These candidates (*MED18*, *PHACTR4*, *and RCC1*) are found to be concurrently lost in UM with focal deletions at 1p35.1. Although *MED18* has not been detected as a mutational cancer driver in any cancer type, *PHACTR4* was identified as suppressors of tumorigenesis and/or proliferation (STOP) genes that have the ability to restrain normal cells proliferation, in may cancer types, and was demonstrated as a tumour suppressor that is deleted and mutant in several cancers (Solimini et al., 2013). *RCC1* has been identified as a critical cell cycle regulator (Ohtsubo et al., 1987), and loss of this gene expression correlates with tumor proliferation and invasion in gastric carcinoma, therefore, it was suggested that loss of *RCC1* play a tumor suppressor role in gastric carcinoma (Lin et al., 2015), and In colorectal carcinoma, the expression of endogenous RCC1 levels inhibited DNA damage (Cekan et al., 2016). The concurrent loss of these genes may affect survival by promoting tumourigenesis suggesting an interaction of the protein encoded by these genes. Therefore, more investigations are

needed to elucidate the function of these genes in UM which could promote the tumorigenesis and may assist in qualifying prognosis of patients.

Moreover, a very small focal deletion between p31.1-p31.3 observed in two tumours from categories 1 and 2, was arrayed with a commercial Male DNA as a control, due to the unavailability of the patient own blood. Thereby, the current evidence suggests that the copy number variations (CNVs) would be responsible for this observation, due to the accumulations of CNVs in the deleted region, this allelic loss on the short arm of chromosome 1 is in contrary with previous finding was documented this deletion in UM patients (Aalto et al., 2001).

Up until now the only genetic mutation proposed to clearly relate to metastasis is *BAP1* (Harbour et al., 2010, van Essen et al., 2014, Gupta et al., 2015). Mutations of *GNAQ* and *GNA11* are known to be the most common activating mutations in UM, occurring with a mutually exclusive pattern (Van Raamsdonk et al., 2009, Van Raamsdonk et al., 2010, Sisley et al., 2011). They are considered to be early events in UM progression and as mutations of these genes, including the rare mutations, are found in over 90% of UM, they are not predictive of a poor outcome in the same manner than M3 and 8q+ are (Onken et al., 2008, Bauer et al., 2009). In this study the majority of the 74 UM sequenced were positive for either *GNAQ* or *GNA11* (Table 5.1), with one UM having a rare variant of *GNA11* (Table 5.3). All 74 UM were wildtype for *BRAF*, reported in approximately 50% of cutaneous melanoma (Sekulic et al., 2008), and combined with the mutational analysis of *GNAQ* and *GNA11,* excludes the possibility that the ocular lesions were metastatic cutaneous melanoma in the majority of cases. There were however 12% of the UM (9/74) where no mutations in *BRAF*, or *GNAQ* and *GNA11* were detected (table 4.2). In all instances the cases has M3 and 8q+ so in other ways were genetically clearly classified as UM (cases attached in appendices 2). Although, 2 cases (Mel 31, 36) presented with different genetic discrepancies, where 9p deletion was the common alteration in both of them in addition to 1p deletion, M3 and i6p, i8q. However, clinically the first patient developed a multi liver metastasis where metastasis was detected first at the brain, and the other showed metastasis to liver and skin, though the first site of metastasis was not reported in both cases. Despite the fact that loss of 9p have been reported in both UM, and CM (Hoglund et al., 2004), however, in CM one of the characterising tumour suppressor gene *CDKN2*A located in 9p21 (Sharpless and Chin, 2003), and deletion of 9p was confirmed in these UM tumours. The present data however, cannot exclude CM as initiation of metastasis for these 2 tumours.

The findings of UM that are negative for all *GNAQ* and *GNA11* mutations has not been previously reported. Moreover, this small subset of tumours with wild type *GNAQ, and GNA11* in non or multi-hepatic tumours shows an average survival of 51.2 months, compared to tumours from category 4 which shows a good prognosis, where all the patients still alive with no metastases. It is therefore possible that some UM with a multi metastatic presentation are initiated under different circumstances to the majority of most UM that have the initiating mutations of *GNAQ* or *GNA11*, further more extensive sequencing of mutations will be required to verify this point.

It was believed that metastasising UM originate exclusively from tumours harbouring M3 early in tumorigenesis (Prescher et al., 1994, Prescher et al., 1996). However, the current data shows that among the metastasizing tumours whether hepatic/multi or non-hepatic, deletion in chromosome 1p was the only common aberration associated with M3 and 8q gain in a small subset of poor prognosis patients (7/74) with liver metastasis, were having proper follow up from metastasis to death with 8.88 months average survival range (appendices 3 table1). Additionally, the current observation confirmed that although metastatic UM has a poor clinical outcome, and the liver is the most common site of metastasis, a subset of patients showed longer survival with organs other than the liver. These suggest that with the 1p deletion, despite the genetic involvement of chromosomes 3 and 8 survival post metastasis is better than without 1p.

Furthermore, detection of novel tumour suppressors genes (*PHACTR4, and RCC1)* in UM and correlates them with 1p deletion and multiple metastases, could play a role in UM pathogenesis of UM, however, the expression of these genes in metastasising tumours need further investigations to find how their altered expression affects the behaviour of UM.

In summary associated changes of 1p, M3 and 8q+ closely correlate with metastatic presentation. The findings however suggest that deletion of 1p may identify a subset of UM that can spread to sites other than the liver and may assist in qualifying prognosis of patients.

6 Chapter Six

General discussion and future prospects

Chromosome 1

Chromosome 6

P arm

q arm
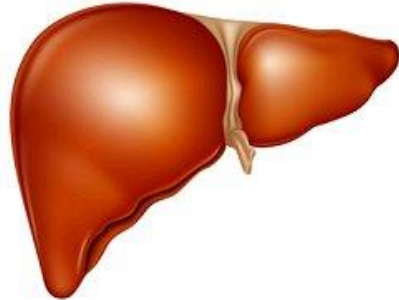
Chapter 5
Metastatic UM

Previous studies have associated 1p deletion with metastatic UM and reduced disease free survival rate. In this study, for the first time potential genetic biomarkers were examined in relation to the presentation of metastases rather than their development. In confirmation of other studies presentation at a site other than the liver associates with longer survival post metastases. Deletion of 1p appears to be intimately associated with metastases, and probably extra hepatic spread, but further studies with more comprehensive clinical information are required to support these initial findings.

Chapter 3
6p and prognosis

The association of 6p with a better prognosis was confirmed; however, it is clear that 6p+ is not mutually exclusive to M3 and 8q+. In particular, Group 2 are almost always associated with the presence of 8q+.

Chapter 4
Identified genes in 6p gain (*FOXQ1*, *FARS2*) and *AMD1* on 6q loss, as prognostic indicators for UM

FOXQ1

FARS2

AMD1

Figure 6.1: Summary of the approach taken in this study and the major findings in each section, resulting in the identification of potential driver genes associated with subgroups of uveal melanoma

6.1 General discussion

6.1.1 Objective of this work

In UM a number of clinical, histological, and genetic prognostic factors are well characterised (Mooy and De Jong, 1996, Singh et al., 2001, Kilic et al., 2005). Although a clear association was made from early investigations, between certain chromosomal abnormalities in UM and the patient outcome (Sisley et al., 1990, Sisley et al., 1997), these factors however, despite being highly discriminative in predicting prognosis, have not ultimately helped gain a better understanding of the metastatic process and what drives it in UM. The essential problem arises in part because the most effective genetic biomarkers still rely heavily on large regional genetic imbalances and not specific mutations or rearrangements of individual genes. The mutation of *BAP1* is of interest but there is conflicting data relating to its potential impact (Koopmans et al., 2014, Van Beek et al., 2015) and in the end assessment of it expression by IHC may be the most fruitful approach.

The aim of this thesis was to address both central issues. Firstly to better understand how genetic biomarkers identify UM that will metastasize, and whether they can be used to further subtype UM. Secondly to see if potential driver genes could be identified that may lead both to an improved understanding of UM metastasis and how to treat it. The approach taken was to use a customised high-resolution aCGH. Which, because it was specifically designed for UM, was hoped to identify recurrent focal SCNA that could have been missed by previous studies using lower resolution and unfocussed approaches, such as chromosomal CGH, classical karyotyping, or even BAC arrays. Altogether 137 primary UM were analysed, and as part of a small pilot study possible drivers were further investigated using IHC.

6.1.2 Prognosis of UM using genetic biomarkers assessed by aCGH profiling data

As mentioned earlier, this study indicates that all commonly reported changes in UM are also detectable in this series including those of 1, 3, 6 and 8 at frequencies previously recorded, and the clinical-pathological data is comparable to other series of UM (section 3.2.2); it is therefore reasonable to assume that the findings of this study are not biased through patient selection. Past studies have not really intensively

investigated chromosome 6 changes, which are the focus of chapters 3 and 4, with the findings clearly indicating that abnormalities of chromosome 6 are under-represented in past lower resolution investigations (Figure 3.14). Furthermore this study has provided clear contrary evidence to previous studies linking 6p gain to a more favourable prognosis and the proposed mutually exclusivity between M3 and 6p in UM with suggested bifurcated pathway in tumour progression (Kath et al., 1993, Prescher et al., 1995, White et al., 1998, Parrella et al., 1999, Landreville et al., 2008). Here abnormalities of chromosome 6 were found for the first time to be effective at stratifying UM in a manner independent of M3 and 8q+. Indeed, a potential new subtype was identified whereby random changes of chromosome 6 appeared to associate with unusually highly unstable UM (Figure 3.15 and group 3). The data classification also determined that there was a roughly equally split for abnormalities affecting just the p or q arm or both arms. In terms of prognosis the outcome for patients with 6p gain was similar whether in the form of an i(6)p or just 6p (Figure 3.13). Although the association of 6p with a better prognosis was confirmed in this study, it is clear however that 6p+ is not mutually exclusive to M3 and 8q+, and in particular Group 2 are almost always associated with the presence of 8q+. Bearing in mind that the most frequent findings is that of 8q+ in metastases (Aalto et al., 2001, Singh et al., 2009, Ewens et al., 2013), suggests at the very least, that 6p+ must be interpreted in the context of other genetic biomarkers, and that of itself group 2 represent a subtype of UM with lower, but nevertheless metastatic potential. Furthermore, interrogation of the data for the series as a whole (regardless of original groupings) provided clear evidence for a subgroup of UM associated with 6p gain M3 and 8q gain, which may improve understanding of tumour progression. As this association between the 3 chromosome abnormalities was found for UM in both groups 1 and 2 it may explain similarities in outcome between these groups (Figures 3.10, 3.14). Indeed, recent results from the research team have directly impacted and supported findings of this current study. One UM from this series in group 4 (case 87) was established in culture and subsequently its aCGH profile was monitored over a period of 5 years growth and progression, resulting in the successive acquisition of genetic changes in the order of (M3) to (M3, +8) to (M3, +i(8q)) to finally (M3, +i(8q), +pseudo i(6p). In this unpublished data (submitted for publication) the acquisition of 6p gain is a much later event and clearly supports the lack of mutual exclusivity between M3 and 6p and the findings of this study where a subset of UM had associated changes of M3, 8q+ and 6p+ (Figure 3.10, 3.14). This current study unfortunately was restricted in drawing many conclusions because of the limited nature of the follow up available for many UM at the point of conclusion. However, individual comparison of those cancers where there were associated changes of 3, 6 and 8 found

that their average survival was 36.77 months compared to the series as a whole where survival was 52.77 months.

Nevertheless, this study also established potential differences in the regions of 6p gained in subgroups of UM, and suggested that a part of the short and long arm of chromosome 6 contains one or more oncogenes which maybe directly involved in UM progression. Using powerful software like Nexus 7.5 helped to demonstrate the associations and linked the gene behaviours that clustered in 6p and 6q to other chromosomal changes including 3 and 8. The identified genes in this study on chromosome 6 were further investigated using IHC and the expression of *FARS2*, *FOXQ1* and *AMD1* (Figures 4.12, 4.13, 4.14) showed clear differences between tumours with and without M3, as well as an ability to indicate prognosis on the basis of their amplification (Figure 4.13). It is too early to draw conclusions on the role of these genes and further studies are required to explore their impact in UM.

6.1.3 Dose site of tumour metastasis affect the disease free survival in UM patients?

UM have a higher tendency to metastasize to the liver exclusively and or with other organs involved (Kath et al., 1993, Kujala et al., 2003, Collaborative Ocular Melanoma Study, 2001, Bedikian, 2006, Diener-West et al., 2005); metastasis to other organs as the first site is rarely documented (Rietschel et al., 2005). Unfortunately, the difficulties in obtaining extensive clinical follow up for all cases severely impacted on this aspect of the study, specifically as a detailed interrogation of the patients notes was required to confirm not only the sites affected but the timing of presentation. This study did however confirm previous reports for prolonged survival amongst UM patients were organs other the liver presented first (Figure 5.7)

Interrogation of the whole series data (137) by nexus was able to confirm previous studies whereby partial or whole arm deletion of chromosome 1, accompanied with M3 and 8q gain associated to the worst prognosis ((Prescher et al., 1996, Sisley et al., 1997, White et al., 1998, Sisley et al., 2000, Aalto et al., 2001, Damato et al., 2010). Most of these studies suggested that 1p36 region could encode for a protein that could promoted tumor progression and metastasis (Sisley et al., 2000, Aalto et al., 2001, Naus et al., 2002, Kilic et al., 2005, Kilic et al., 2006, Hughes et al., 2005). However, this study highlighted a significant region 1p35.3 (Figure 5.8) in this subgroup of

patients, that included the potential UM tumor suppressor genes (*MED18*, *PHACTR4*, and *RCC1*), the importance of these genes will need to be assessed in future studies.

6.2 Limitations of this study

Although this study included a large number of UM patients (137), the most common limitation was obtaining the relevant clinical outcome for all the patients in this series. In Chapter 4, preliminary results for the protein expression of *FOXQ1*, *FARS2*, and *AMD1* were documented, which were naturally limited because of the sample size and time available at the end of this PhD. Furthermore, in chapter 5, 3 candidate genes on chromosome 1 were identified (*MED18*, *PHACTR4*, *and RCC1*), but the lack of access to nexus due to circumstances prevented serious exploration of the findings.

6.3 Future work

In this study several potentially interesting candidate genes have been identified. Additional UM need to be studied for the expression of (*FOXQ1*, *FARS2*, and *AMD1*) proteins in UM tissue. Equally a more complete investigation of the identified genes on 6p, 6q and 1p needs to be undertaken, but more comprehensive clinical information, which is currently being sought, will dramatically enhance this aspect. Later steps to target these genes could use additional technologies such as next-generation exome or whole genome sequencing, to establish it mutations also exist of these genes in UM. If these investigations prove of value then the functional aspects of these genes could be explored in UM cell lines, (CRISPR) investigating how their altered expression affects the behaviour of UM.

6.4 Summary of study findings

- This study looked more specifically at chromosome 6 and indicates that abnormalities are more frequent than reported in early studies, and pinpoints novel candidate genes that could act as a possible driver for UM tumorigenesis.

- The association of 6p with a better prognosis was confirmed, however it is clear that 6p+ is not mutually exclusive to M3 and 8q+. In particular, Group 2 are almost always associated with the presence of 8q+.

- This study Identified distinctive genetic patterns of UM that could be used to further stratify. Specifically, M3, 8q+ and 6p+ identify a subset with very poor prognosis and other changes of chromosome 6 appear to correlate with more unstable UM.

- 1p deletion was examined as a genetic biomarker that could be predictive of tumour site of metastasis.

References

1990. Accuracy of diagnosis of choroidal melanomas in the Collaborative Ocular Melanoma Study. COMS report no. 1. *Arch Ophthalmol,* 108**,** 1268-73.

1994. Schistosomes, liver flukes and Helicobacter pylori. IARC Working Group on the Evaluation of Carcinogenic Risks to Humans. Lyon, 7-14 June 1994. *IARC Monogr Eval Carcinog Risks Hum,* 61**,** 1-241.

AALTO, Y., ERIKSSON, L., SEREGARD, S., LARSSON, O. & KNUUTILA, S. 2001. Concomitant loss of chromosome 3 and whole arm losses and gains of chromosome 1, 6, or 8 in metastasizing primary uveal melanoma. *Invest Ophthalmol Vis Sci,* 42**,** 313-7.

ABDEL-RAHMAN, M. H., PILARSKI, R., CEBULLA, C. M., MASSENGILL, J. B., CHRISTOPHER, B. N., BORU, G., HOVLAND, P. & DAVIDORF, F. H. 2011. Germline BAP1 mutation predisposes to uveal melanoma, lung adenocarcinoma, meningioma, and other cancers. *J Med Genet,* 48**,** 856-9.

ABDEL-RAHMAN, M. H., YANG, Y., ZHOU, X. P., CRAIG, E. L., DAVIDORF, F. H. & ENG, C. 2006. High frequency of submicroscopic hemizygous deletion is a major mechanism of loss of expression of PTEN in uveal melanoma. *J Clin Oncol,* 24**,** 288-95.

ADAMI, H. O., KUPER, H., ANDERSSON, S. O., BERGSTROM, R. & DILLNER, J. 2003. Prostate cancer risk and serologic evidence of human papilloma virus infection: a population-based case-control study. *Cancer Epidemiol Biomarkers Prev,* 12**,** 872-5.

ADAMS, E. J., GREEN, J. A., CLARK, A. H. & YOUNGSON, J. H. 1999. Comparison of different scoring systems for immunohistochemical staining. *J Clin Pathol,* 52**,** 75-7.

AKSLEN, L. A., ANGELINI, S., STRAUME, O., BACHMANN, I. M., MOLVEN, A., HEMMINKI, K. & KUMAR, R. 2005. BRAF and NRAS mutations are frequent in nodular melanoma but are not associated with tumor cell proliferation or patient survival. *J Invest Dermatol,* 125**,** 312-7.

ALBERTSON, D. G. & PINKEL, D. 2003. Genomic microarrays in human genetic disease and cancer. *Hum Mol Genet,* 12 Spec No 2**,** R145-52.

ALEXANDER, H. R., LIBUTTI, S. K., BARTLETT, D. L., PUHLMANN, M., FRAKER, D. L. & BACHENHEIMER, L. C. 2000. A phase I-II study of isolated hepatic perfusion using melphalan with or without tumor necrosis factor for patients with ocular melanoma metastatic to liver. *Clin Cancer Res,* 6**,** 3062-70.

ALMALKI, A., ALSTON, C. L., PARKER, A., SIMONIC, I., MEHTA, S. G., HE, L., REZA, M., OLIVEIRA, J. M., LIGHTOWLERS, R. N., MCFARLAND, R., TAYLOR, R. W. & CHRZANOWSKA-LIGHTOWLERS, Z. M. 2014. Mutation of the human mitochondrial phenylalanine-tRNA synthetase causes infantile-onset epilepsy and cytochrome c oxidase deficiency. *Biochim Biophys Acta,* 1842**,** 56-64.

ARAUJO, I., BITTENCOURT, A. L., BARBOSA, H. S., NETTO, E. M., MENDONCA, N., FOSS, H. D., HUMMEL, M. & STEIN, H. 2006. The high frequency of EBV infection in pediatric Hodgkin lymphoma is related to the classical type in Bahia, Brazil. *Virchows Arch,* 449**,** 315-9.

ARONOW, M., SUN, Y., SAUNTHARARAJAH, Y., BISCOTTI, C., TUBBS, R., TRIOZZI, P. & SINGH, A. D. 2012. Monosomy 3 by FISH in uveal melanoma: variability in techniques and results. *Survey of Ophthalmology,* 57**,** 463-73.

AUGSBURGER, J. J., CORREA, Z. M. & SHAIKH, A. H. 2009. Effectiveness of treatments for metastatic uveal melanoma. *Am J Ophthalmol,* 148**,** 119-27.

BAGGETTO, L. G., GAMBRELLE, J., DAYAN, G., LABIALLE, S., BARAKAT, S., MICHAUD, M., GRANGE, J. D. & GAYET, L. 2005. Major cytogenetic aberrations and typical multidrug resistance phenotype of uveal melanoma: current views and new therapeutic prospects. *Cancer Treat Rev,* 31**,** 361-79.

BAIK, S. C., YOUN, H. S., CHUNG, M. H., LEE, W. K., CHO, M. J., KO, G. H., PARK, C. K., KASAI, H. & RHEE, K. H. 1996. Increased oxidative DNA damage in Helicobacter pylori-infected human gastric mucosa. *Cancer Res,* 56**,** 1279-82.

BALCH, C. M., GERSHENWALD, J. E., SOONG, S. J., THOMPSON, J. F., ATKINS, M. B., BYRD, D. R., BUZAID, A. C., COCHRAN, A. J., COIT, D. G., DING, S., EGGERMONT, A. M., FLAHERTY, K. T., GIMOTTY, P. A., KIRKWOOD, J. M., MCMASTERS, K. M., MIHM, M. C., JR., MORTON, D. L., ROSS, M. I., SOBER, A. J. & SONDAK, V. K. 2009. Final version of 2009 AJCC melanoma staging and classification. *J Clin Oncol,* 27**,** 6199-206.

BALCH, C. M., GERSHENWALD, J. E., SOONG, S. J., THOMPSON, J. F., DING, S., BYRD, D. R., CASCINELLI, N., COCHRAN, A. J., COIT, D. G., EGGERMONT, A. M., JOHNSON, T., KIRKWOOD, J. M., LEONG, S. P., MCMASTERS, K. M., MIHM, M. C., JR., MORTON, D. L., ROSS, M. I. & SONDAK, V. K. 2010. Multivariate analysis of prognostic factors among 2,313 patients with stage III melanoma: comparison of nodal micrometastases versus macrometastases. *J Clin Oncol,* 28**,** 2452-9.

BARRETT, M. T., SCHEFFER, A., BEN-DOR, A., SAMPAS, N., LIPSON, D., KINCAID, R., TSANG, P., CURRY, B., BAIRD, K., MELTZER, P. S., YAKHINI, Z., BRUHN, L. & LADERMAN, S. 2004. Comparative genomic hybridization using oligonucleotide microarrays and total genomic DNA. *Proc Natl Acad Sci U S A,* 101**,** 17765-70.

BASTIAN, B. C. 2014. The molecular pathology of melanoma: an integrated taxonomy of melanocytic neoplasia. *Annu Rev Pathol,* 9**,** 239-71.

BASTIAN, B. C., OLSHEN, A. B., LEBOIT, P. E. & PINKEL, D. 2003. Classifying melanocytic tumors based on DNA copy number changes. *Am J Pathol,* 163**,** 1765-70.

BAUER, J., KILIC, E., VAARWATER, J., BASTIAN, B. C., GARBE, C. & DE KLEIN, A. 2009. Oncogenic GNAQ mutations are not correlated with disease-free survival in uveal melanoma. *Br J Cancer,* 101**,** 813-5.

BEAVON, I. R. 2000. The E-cadherin-catenin complex in tumour metastasis: structure, function and regulation. *Eur J Cancer,* 36**,** 1607-20.

BECSEI-KILBORN, E. 2010. Scientific discovery and scientific reputation: the reception of Peyton Rous' discovery of the chicken sarcoma virus. *J Hist Biol,* 43**,** 111-57.

BEDIKIAN, A. Y. 2006. Metastatic uveal melanoma therapy: current options. *Int Ophthalmol Clin,* 46**,** 151-66.

BERGMAN, L., SEREGARD, S., NILSSON, B., LUNDELL, G., RINGBORG, U. & RAGNARSSON-OLDING, B. 2003. Uveal melanoma survival in Sweden from 1960 to 1998. *Invest Ophthalmol Vis Sci,* 44**,** 3282-7.

BERNSTEIN, H., BERNSTEIN, C., PAYNE, C. M. & DVORAK, K. 2009. Bile acids as endogenous etiologic agents in gastrointestinal cancer. *World Journal of Gastroenterology : WJG,* 15**,** 3329-3340.

BEROUKHIM, R., GETZ, G., NGHIEMPHU, L., BARRETINA, J., HSUEH, T., LINHART, D., VIVANCO, I., LEE, J. C., HUANG, J. H., ALEXANDER, S., DU, J., KAU, T., THOMAS, R. K., SHAH, K., SOTO, H., PERNER, S., PRENSNER, J., DEBIASI, R. M., DEMICHELIS, F., HATTON, C., RUBIN, M. A., GARRAWAY, L. A., NELSON, S. F., LIAU, L., MISCHEL, P. S., CLOUGHESY, T. F., MEYERSON, M., GOLUB, T. A., LANDER, E. S., MELLINGHOFF, I. K. & SELLERS, W. R. 2007. Assessing the significance of chromosomal aberrations in cancer: methodology and application to glioma. *Proc Natl Acad Sci U S A,* 104**,** 20007-12.

BEROUKHIM, R., MERMEL, C. H., PORTER, D., WEI, G., RAYCHAUDHURI, S., DONOVAN, J., BARRETINA, J., BOEHM, J. S., DOBSON, J., URASHIMA, M., MC HENRY, K. T., PINCHBACK, R. M., LIGON, A. H., CHO, Y. J., HAERY, L., GREULICH, H., REICH, M.,

WINCKLER, W., LAWRENCE, M. S., WEIR, B. A., TANAKA, K. E., CHIANG, D. Y., BASS, A. J., LOO, A., HOFFMAN, C., PRENSNER, J., LIEFELD, T., GAO, Q., YECIES, D., SIGNORETTI, S., MAHER, E., KAYE, F. J., SASAKI, H., TEPPER, J. E., FLETCHER, J. A., TABERNERO, J., BASELGA, J., TSAO, M. S., DEMICHELIS, F., RUBIN, M. A., JANNE, P. A., DALY, M. J., NUCERA, C., LEVINE, R. L., EBERT, B. L., GABRIEL, S., RUSTGI, A. K., ANTONESCU, C. R., LADANYI, M., LETAI, A., GARRAWAY, L. A., LODA, M., BEER, D. G., TRUE, L. D., OKAMOTO, A., POMEROY, S. L., SINGER, S., GOLUB, T. R., LANDER, E. S., GETZ, G., SELLERS, W. R. & MEYERSON, M. 2010. The landscape of somatic copy-number alteration across human cancers. *Nature,* 463**,** 899-905.

BERTRAM, J. S. 2000. The molecular biology of cancer. *Mol Aspects Med,* 21**,** 167-223.

BESARATINIA, A. & PFEIFER, G. P. 2011. Uveal melanoma and GNA11 mutations: a new piece added to the puzzle. *Pigment Cell Melanoma Res,* 24**,** 18-20.

BIELLER, A., PASCHE, B., FRANK, S., GLASER, B., KUNZ, J., WITT, K. & ZOLL, B. 2001. Isolation and characterization of the human forkhead gene FOXQ1. *DNA Cell Biol,* 20**,** 555-61.

BONIOL, M., AUTIER, P., BOYLE, P. & GANDINI, S. 2012. Cutaneous melanoma attributable to sunbed use: systematic review and meta-analysis. *BMJ,* 345**,** e4757.

BORTHWICK, N. J., THOMBS, J., POLAK, M., GABRIEL, F. G., HUNGERFORD, J. L., DAMATO, B., RENNIE, I. G., JAGER, M. J. & CREE, I. A. 2011. The biology of micrometastases from uveal melanoma. *J Clin Pathol,* 64**,** 666-71.

BRONKHORST, I. H., MAAT, W., JORDANOVA, E. S., KROES, W. G., SCHALIJ-DELFOS, N. E., LUYTEN, G. P. & JAGER, M. J. 2011. Effect of heterogeneous distribution of monosomy 3 on prognosis in uveal melanoma. *Arch Pathol Lab Med,* 135**,** 1042-7.

BULLARD, J. M., CAI, Y. C., DEMELER, B. & SPREMULLI, L. L. 1999. Expression and characterization of a human mitochondrial phenylalanyl-tRNA synthetase. *J Mol Biol,* 288**,** 567-77.

CAHILL, D. P., KINZLER, K. W., VOGELSTEIN, B. & LENGAUER, C. 1999. Genetic instability and darwinian selection in tumours. *Trends Cell Biol,* 9**,** M57-60.

CANDELARIO, J., CHEN, L. Y., MARJORAM, P., REDDY, S. & COMAI, L. 2012. A filtering strategy identifies FOXQ1 as a potential effector of lamin A dysfunction. *Aging (Albany NY),* 4**,** 567-77.

CANNING, C. R. & HUNGERFORD, J. 1988. Familial uveal melanoma. *Br J Ophthalmol,* 72**,** 241-3.

CARON, H., VAN SLUIS, P., DE KRAKER, J., BOKKERINK, J., EGELER, M., LAUREYS, G., SLATER, R., WESTERVELD, A., VOUTE, P. A. & VERSTEEG, R. 1996. Allelic loss of chromosome 1p as a predictor of unfavorable outcome in patients with neuroblastoma. *N Engl J Med,* 334**,** 225-30.

CARTER, S. L., EKLUND, A. C., KOHANE, I. S., HARRIS, L. N. & SZALLASI, Z. 2006. A signature of chromosomal instability inferred from gene expression profiles predicts clinical outcome in multiple human cancers. *Nat Genet,* 38**,** 1043-8.

CARVAJAL, R. D., SOSMAN, J. A., QUEVEDO, J. F., MILHEM, M. M., JOSHUA, A. M., KUDCHADKAR, R. R., LINETTE, G. P., GAJEWSKI, T. F., LUTZKY, J., LAWSON, D. H., LAO, C. D., FLYNN, P. J., ALBERTINI, M. R., SATO, T., LEWIS, K., DOYLE, A., ANCELL, K., PANAGEAS, K. S., BLUTH, M., HEDVAT, C., ERINJERI, J., AMBROSINI, G., MARR, B., ABRAMSON, D. H., DICKSON, M. A., WOLCHOK, J. D., CHAPMAN, P. B. & SCHWARTZ, G. K. 2014. Effect of selumetinib vs chemotherapy on progression-free survival in uveal melanoma: a randomized clinical trial. *JAMA,* 311**,** 2397-405.

CASCIANO, I., MAZZOCCO, K., BONI, L., PAGNAN, G., BANELLI, B., ALLEMANNI, G., PONZONI, M., TONINI, G. P. & ROMANI, M. 2002. Expression of DeltaNp73 is a molecular marker for adverse outcome in neuroblastoma patients. *Cell Death Differ,* 9**,** 246-51.

CASSOUX, N., RODRIGUES, M. J., PLANCHER, C., ASSELAIN, B., LEVY-GABRIEL, C., LUMBROSO-LE ROUIC, L., PIPERNO-NEUMANN, S., DENDALE, R., SASTRE, X., DESJARDINS, L. & COUTURIER, J. 2014. Genome-wide profiling is a clinically relevant and affordable

prognostic test in posterior uveal melanoma. *British Journal of Ophthalmology,* 98**,** 769-774.

CHANA, J. S., WILSON, G. D., CREE, I. A., ALEXANDER, R. A., MYATT, N., NEALE, M., FOSS, A. J. & HUNGERFORD, J. L. 1999. c-myc, p53, and Bcl-2 expression and clinical outcome in uveal melanoma. *Br J Ophthalmol,* 83**,** 110-4.

CHEN, Z., ISSA, B., BROTHMAN, L. J., HENDRICKSEN, M., BUTTON, D. & BROTHMAN, A. R. 2000. Nonrandom rearrangements of 6p in malignant hematological disorders. *Cancer Genet Cytogenet,* 121**,** 22-5.

CHRISTENSEN, J., BENTZ, S., SENGSTAG, T., SHASTRI, V. P. & ANDERLE, P. 2013. FOXQ1, a novel target of the Wnt pathway and a new marker for activation of Wnt signaling in solid tumors. *PLoS One,* 8**,** e60051.

CHUNG, H. Y., LEE, E. K., CHOI, Y. J., KIM, J. M., KIM, D. H., ZOU, Y., KIM, C. H., LEE, J., KIM, H. S., KIM, N. D., JUNG, J. H. & YU, B. P. 2011. Molecular inflammation as an underlying mechanism of the aging process and age-related diseases. *J Dent Res,* 90**,** 830-40.

COHEN, Y., GOLDENBERG-COHEN, N., PARRELLA, P., CHOWERS, I., MERBS, S. L., PE'ER, J. & SIDRANSKY, D. 2003. Lack of BRAF mutation in primary uveal melanoma. *Invest Ophthalmol Vis Sci,* 44**,** 2876-8.

COLLABORATIVE OCULAR MELANOMA STUDY, G. 2001. Assessment of metastatic disease status at death in 435 patients with large choroidal melanoma in the Collaborative Ocular Melanoma Study (COMS): COMS report no. 15. *Arch Ophthalmol,* 119**,** 670-6.

CONRAD, D. F., PINTO, D., REDON, R., FEUK, L., GOKCUMEN, O., ZHANG, Y., AERTS, J., ANDREWS, T. D., BARNES, C., CAMPBELL, P., FITZGERALD, T., HU, M., IHM, C. H., KRISTIANSSON, K., MACARTHUR, D. G., MACDONALD, J. R., ONYIAH, I., PANG, A. W., ROBSON, S., STIRRUPS, K., VALSESIA, A., WALTER, K., WEI, J., WELLCOME TRUST CASE CONTROL, C., TYLER-SMITH, C., CARTER, N. P., LEE, C., SCHERER, S. W. & HURLES, M. E. 2010. Origins and functional impact of copy number variation in the human genome. *Nature,* 464**,** 704-12.

CRASTA, K., GANEM, N. J., DAGHER, R., LANTERMANN, A. B., IVANOVA, E. V., PAN, Y., NEZI, L., PROTOPOPOV, A., CHOWDHURY, D. & PELLMAN, D. 2012. DNA breaks and chromosome pulverization from errors in mitosis. *Nature,* 482**,** 53-8.

CROSS, N. A., GANESH, A., PARPIA, M., MURRAY, A. K., RENNIE, I. G. & SISLEY, K. 2006. Multiple locations on chromosome 3 are the targets of specific deletions in uveal melanoma. *Eye (Lond),* 20**,** 476-81.

CROSS, N. A., MURRAY, A. K., RENNIE, I. G., GANESH, A. & SISLEY, K. 2003. Instability of microsatellites is an infrequent event in uveal melanoma. *Melanoma Res,* 13**,** 435-40.

CROSS, N. A., RENNIE, I. G., MURRAY, A. K. & SISLEY, K. 2005. The identification of chromosome abnormalities associated with the invasive phenotype of uveal melanoma in vitro. *Clin Exp Metastasis,* 22**,** 107-13.

CRUZ, F., 3RD, RUBIN, B. P., WILSON, D., TOWN, A., SCHROEDER, A., HALEY, A., BAINBRIDGE, T., HEINRICH, M. C. & CORLESS, C. L. 2003. Absence of BRAF and NRAS mutations in uveal melanoma. *Cancer Res,* 63**,** 5761-6.

CURTIN, J. A., FRIDLYAND, J., KAGESHITA, T., PATEL, H. N., BUSAM, K. J., KUTZNER, H., CHO, K. H., AIBA, S., BROCKER, E. B., LEBOIT, P. E., PINKEL, D. & BASTIAN, B. C. 2005. Distinct sets of genetic alterations in melanoma. *N Engl J Med,* 353**,** 2135-47.

DAHLENFORS, R., TORNQVIST, G., WETTRELL, K. & MARK, J. 1993. Cytogenetical observations in nine ocular malignant melanomas. *Anticancer Res,* 13**,** 1415-20.

DAMATO, B. 2006. Treatment of primary intraocular melanoma. *Expert Rev Anticancer Ther,* 6**,** 493-506.

DAMATO, B., DOPIERALA, J., KLAASEN, A., VAN DIJK, M., SIBBRING, J. & COUPLAND, S. E. 2009. Multiplex ligation-dependent probe amplification of uveal melanoma: correlation with metastatic death. *Invest Ophthalmol Vis Sci,* 50**,** 3048-55.

DAMATO, B., DOPIERALA, J. A. & COUPLAND, S. E. 2010. Genotypic profiling of 452 choroidal melanomas with multiplex ligation-dependent probe amplification. *Clin Cancer Res,* 16**,** 6083-92.

DAMATO, B., DUKE, C., COUPLAND, S. E., HISCOTT, P., SMITH, P. A., CAMPBELL, I., DOUGLAS, A. & HOWARD, P. 2007. Cytogenetics of uveal melanoma: a 7-year clinical experience. *Ophthalmology,* 114**,** 1925-31.

DANAEI, G., VANDER HOORN, S., LOPEZ, A. D., MURRAY, C. J., EZZATI, M. & COMPARATIVE RISK ASSESSMENT COLLABORATING, G. 2005. Causes of cancer in the world: comparative risk assessment of nine behavioural and environmental risk factors. *Lancet,* 366**,** 1784-93.

DAVIES, H., BIGNELL, G. R., COX, C., STEPHENS, P., EDKINS, S., CLEGG, S., TEAGUE, J., WOFFENDIN, H., GARNETT, M. J., BOTTOMLEY, W., DAVIS, N., DICKS, E., EWING, R., FLOYD, Y., GRAY, K., HALL, S., HAWES, R., HUGHES, J., KOSMIDOU, V., MENZIES, A., MOULD, C., PARKER, A., STEVENS, C., WATT, S., HOOPER, S., WILSON, R., JAYATILAKE, H., GUSTERSON, B. A., COOPER, C., SHIPLEY, J., HARGRAVE, D., PRITCHARD-JONES, K., MAITLAND, N., CHENEVIX-TRENCH, G., RIGGINS, G. J., BIGNER, D. D., PALMIERI, G., COSSU, A., FLANAGAN, A., NICHOLSON, A., HO, J. W., LEUNG, S. Y., YUEN, S. T., WEBER, B. L., SEIGLER, H. F., DARROW, T. L., PATERSON, H., MARAIS, R., MARSHALL, C. J., WOOSTER, R., STRATTON, M. R. & FUTREAL, P. A. 2002. Mutations of the BRAF gene in human cancer. *Nature,* 417**,** 949-54.

DE LA CRUZ, P. O., JR., SPECHT, C. S. & MCLEAN, I. W. 1990. Lymphocytic infiltration in uveal malignant melanoma. *Cancer,* 65**,** 112-5.

DECATUR, C. L., ONG, E., GARG, N., ANBUNATHAN, H., BOWCOCK, A. M., FIELD, M. G. & HARBOUR, J. W. 2016. Driver Mutations in Uveal Melanoma: Associations With Gene Expression Profile and Patient Outcomes. *JAMA Ophthalmol,* 134**,** 728-33.

DIENER-WEST, M., REYNOLDS, S. M., AGUGLIARO, D. J., CALDWELL, R., CUMMING, K., EARLE, J. D., HAWKINS, B. S., HAYMAN, J. A., JAIYESIMI, I., JAMPOL, L. M., KIRKWOOD, J. M., KOH, W. J., ROBERTSON, D. M., SHAW, J. M., STRAATSMA, B. R., THOMA, J. & COLLABORATIVE OCULAR MELANOMA STUDY, G. 2005. Development of metastatic disease after enrollment in the COMS trials for treatment of choroidal melanoma: Collaborative Ocular Melanoma Study Group Report No. 26. *Arch Ophthalmol,* 123**,** 1639-43.

DING, S. Z., MINOHARA, Y., FAN, X. J., WANG, J., REYES, V. E., PATEL, J., DIRDEN-KRAMER, B., BOLDOGH, I., ERNST, P. B. & CROWE, S. E. 2007. Helicobacter pylori infection induces oxidative stress and programmed cell death in human gastric epithelial cells. *Infect Immun,* 75**,** 4030-9.

DISKIN, S. J., ECK, T., GRESHOCK, J., MOSSE, Y. P., NAYLOR, T., STOECKERT, C. J., JR., WEBER, B. L., MARIS, J. M. & GRANT, G. R. 2006. STAC: A method for testing the significance of DNA copy number aberrations across multiple array-CGH experiments. *Genome Res,* 16**,** 1149-58.

DMOCHOWSKI, L., OHTSUKI, Y., SEMAN, G., MARUYAMA, K., KNESEK, J. E., EAST, J. L., BOWEN, J. M., YOSHIDA, H. & JOHNSON, D. E. 1977. Search for oncogenic viruses in human prostate cancer. *Cancer Treat Rep,* 61**,** 119-27.

DOLL, R. & PETO, R. 1981. The causes of cancer: quantitative estimates of avoidable risks of cancer in the United States today. *J Natl Cancer Inst,* 66**,** 1191-308.

DUMAZ, N. 2011. Mechanism of RAF isoform switching induced by oncogenic RAS in melanoma. *Small GTPases,* 2**,** 289-292.

DUNN, K. L., ESPINO, P. S., DROBIC, B., HE, S. & DAVIE, J. R. 2005. The Ras-MAPK signal transduction pathway, cancer and chromatin remodeling. *Biochem Cell Biol,* 83**,** 1-14.

EDMUNDS, S. C., CREE, I. A., DI NICOLANTONIO, F., HUNGERFORD, J. L., HURREN, J. S. & KELSELL, D. P. 2003. Absence of BRAF gene mutations in uveal melanomas in contrast to cutaneous melanomas. *Br J Cancer,* 88**,** 1403-5.

EGAN, K. M., SEDDON, J. M., GLYNN, R. J., GRAGOUDAS, E. S. & ALBERT, D. M. 1988. Epidemiologic aspects of uveal melanoma. *Survey of Ophthalmology,* 32**,** 239-51.

EHLERS, J. P. & HARBOUR, J. W. 2005. NBS1 expression as a prognostic marker in uveal melanoma. *Clin Cancer Res,* 11**,** 1849-53.

EHLERS, J. P., WORLEY, L., ONKEN, M. D. & HARBOUR, J. W. 2005. DDEF1 is located in an amplified region of chromosome 8q and is overexpressed in uveal melanoma. *Clin Cancer Res,* 11**,** 3609-13.

EHLERS, J. P., WORLEY, L., ONKEN, M. D. & HARBOUR, J. W. 2008. Integrative genomic analysis of aneuploidy in uveal melanoma. *Clin Cancer Res,* 14**,** 115-22.

ELO, J. M., YADAVALLI, S. S., EURO, L., ISOHANNI, P., GOTZ, A., CARROLL, C. J., VALANNE, L., ALKURAYA, F. S., UUSIMAA, J., PAETAU, A., CARUSO, E. M., PIHKO, H., IBBA, M., TYYNISMAA, H. & SUOMALAINEN, A. 2012. Mitochondrial phenylalanyl-tRNA synthetase mutations underlie fatal infantile Alpers encephalopathy. *Hum Mol Genet,* 21**,** 4521-9.

ESKELIN, S., PYRHONEN, S., SUMMANEN, P., HAHKA-KEMPPINEN, M. & KIVELA, T. 2000. Tumor doubling times in metastatic malignant melanoma of the uvea: tumor progression before and after treatment. *Ophthalmology,* 107**,** 1443-9.

EWENS, K. G., KANETSKY, P. A., RICHARDS-YUTZ, J., AL-DAHMASH, S., DE LUCA, M. C., BIANCIOTTO, C. G., SHIELDS, C. L. & GANGULY, A. 2013. Genomic profile of 320 uveal melanoma cases: chromosome 8p-loss and metastatic outcome. *Invest Ophthalmol Vis Sci,* 54**,** 5721-9.

FARINATI, F., CARDIN, R., DEGAN, P., RUGGE, M., MARIO, F. D., BONVICINI, P. & NACCARATO, R. 1998. Oxidative DNA damage accumulation in gastric carcinogenesis. *Gut,* 42**,** 351-6.

FENG, J., ZHANG, X., ZHU, H., WANG, X., NI, S. & HUANG, J. 2012. FoxQ1 overexpression influences poor prognosis in non-small cell lung cancer, associates with the phenomenon of EMT. *PLoS One,* 7**,** e39937.

FEUERBORN, A., SRIVASTAVA, P. K., KUFFER, S., GRANDY, W. A., SIJMONSMA, T. P., GRETZ, N., BRORS, B. & GRONE, H. J. 2011. The Forkhead factor FoxQ1 influences epithelial differentiation. *J Cell Physiol,* 226**,** 710-9.

FIALA, E. S., SOHN, O. S., WANG, C. X., SEIBERT, E., TSURUTANI, J., DENNIS, P. A., EL-BAYOUMY, K., SODUM, R. S., DESAI, D., REINHARDT, J. & ALIAGA, C. 2005. Induction of preneoplastic lung lesions in guinea pigs by cigarette smoke inhalation and their exacerbation by high dietary levels of vitamins C and E. *Carcinogenesis,* 26**,** 605-12.

FINGER, P. T. 1997. Radiation therapy for choroidal melanoma. *Survey of Ophthalmology,* 42**,** 215-32.

FINGER, P. T. & TH EDITION, A.-U. O. O. T. F. 2009. The 7th edition AJCC staging system for eye cancer: an international language for ophthalmic oncology. *Arch Pathol Lab Med,* 133**,** 1197-8.

FISHER, C. J., GILLETT, C. E., VOJTESEK, B., BARNES, D. M. & MILLIS, R. R. 1994. Problems with p53 immunohistochemical staining: the effect of fixation and variation in the methods of evaluation. *Br J Cancer,* 69**,** 26-31.

FOLBERG, R., RUMMELT, V., PARYS-VAN GINDERDEUREN, R., HWANG, T., WOOLSON, R. F., PE'ER, J. & GRUMAN, L. M. 1993. The prognostic value of tumor blood vessel morphology in primary uveal melanoma. *Ophthalmology,* 100**,** 1389-98.

FOSBRINK, M., NICULESCU, F., RUS, V., SHIN, M. L. & RUS, H. 2006. C5b-9-induced endothelial cell proliferation and migration are dependent on Akt inactivation of forkhead transcription factor FOXO1. *J Biol Chem,* 281**,** 19009-18.

GALLAGHER, R. P., ELWOOD, J. M., ROOTMAN, J., SPINELLI, J. J., HILL, G. B., THRELFALL, W. J. & BIRDSELL, J. M. 1985. Risk factors for ocular melanoma: Western Canada Melanoma Study. *J Natl Cancer Inst,* 74**,** 775-8.

GASS, J. D. 1985. Comparison of uveal melanoma growth rates with mitotic index and mortality. *Arch Ophthalmol,* 103**,** 924-31.

GERNER, E. W., IGNATENKO, N. A., LANCE, P. & HURLEY, L. H. 2005. A comprehensive strategy to combat colon cancer targeting the adenomatous polyposis coli tumor suppressor gene. *Ann N Y Acad Sci,* 1059**,** 97-105.

GILL, H. S. & CHAR, D. H. 2012. Uveal melanoma prognostication: from lesion size and cell type to molecular class. *Can J Ophthalmol,* 47**,** 246-53.

GIORDANO, T. P., HENDERSON, L., LANDGREN, O., CHIAO, E. Y., KRAMER, J. R., EL-SERAG, H. & ENGELS, E. A. 2007. Risk of non-Hodgkin lymphoma and lymphoproliferative precursor diseases in US veterans with hepatitis C virus. *JAMA,* 297**,** 2010-7.

GLATZ-KRIEGER, K., PACHE, M., TAPIA, C., FUCHS, A., SAVIC, S., GLATZ, D., MIHATSCH, M. & MEYER, P. 2006. Anatomic site-specific patterns of gene copy number gains in skin, mucosal, and uveal melanomas detected by fluorescence in situ hybridization. *Virchows Arch,* 449**,** 328-33.

GOLDSTEIN, A. M. 2011. Germline BAP1 mutations and tumor susceptibility. *Nat Genet,* 43**,** 925-6.

GORDON, K. B., THOMPSON, C. T., CHAR, D. H., O'BRIEN, J. M., KROLL, S., GHAZVINI, S. & GRAY, J. W. 1994. Comparative genomic hybridization in the detection of DNA copy number abnormalities in uveal melanoma. *Cancer Res,* 54**,** 4764-8.

GRAGOUDAS, E., LI, W., GOITEIN, M., LANE, A. M., MUNZENRIDER, J. E. & EGAN, K. M. 2002. Evidence-based estimates of outcome in patients irradiated for intraocular melanoma. *Arch Ophthalmol,* 120**,** 1665-71.

GRAGOUDAS, E. S., EGAN, K. M., SEDDON, J. M., GLYNN, R. J., WALSH, S. M., FINN, S. M., MUNZENRIDER, J. E. & SPAR, M. D. 1991. Survival of patients with metastases from uveal melanoma. *Ophthalmology,* 98**,** 383-9; discussion 390.

GREENBLATT, M. S., BENNETT, W. P., HOLLSTEIN, M. & HARRIS, C. C. 1994. Mutations in the p53 tumor suppressor gene: clues to cancer etiology and molecular pathogenesis. *Cancer Res,* 54**,** 4855-78.

GREENE, V. R., JOHNSON, M. M., GRIMM, E. A. & ELLERHORST, J. A. 2009. Frequencies of NRAS and BRAF mutations increase from the radial to the vertical growth phase in cutaneous melanoma. *J Invest Dermatol,* 129**,** 1483-8.

GRIFFIN, C. A., LONG, P. P. & SCHACHAT, A. P. 1988. Trisomy 6p in an ocular melanoma. *Cancer Genet Cytogenet,* 32**,** 129-32.

GROSSNIKLAUS, H. E., BARRON, B. C. & WILSON, M. W. 1995. Murine model of anterior and posterior ocular melanoma. *Curr Eye Res,* 14**,** 399-404.

HABER, M. & STEWART, B. W. 1985. Oncogenes. A possible role for cancer genes in human malignant disease. *Med J Aust,* 142**,** 402-6.

HALL, J. & ANGELE, S. 1999. Radiation, DNA damage and cancer. *Mol Med Today,* 5**,** 157-64.

HAMMOND, D. W., AL-SHAMMARI, N. S., DANSON, S., JACQUES, R., RENNIE, I. G. & SISLEY, K. 2015. High-Resolution Array CGH Analysis Identifies Regional Deletions and Amplifications of Chromosome 8 in Uveal Melanoma. *Invest Ophthalmol Vis Sci,* 56**,** 3460-6.

HANAHAN, D. & WEINBERG, R. A. 2011. Hallmarks of cancer: the next generation. *Cell,* 144**,** 646-74.

HARBOUR, J. W. 2009. Molecular prognostic testing and individualized patient care in uveal melanoma. *Am J Ophthalmol,* 148**,** 823-9 e1.

HARBOUR, J. W. 2012. The genetics of uveal melanoma: an emerging framework for targeted therapy. *Pigment Cell Melanoma Res,* 25**,** 171-81.

HARBOUR, J. W., ONKEN, M. D., ROBERSON, E. D., DUAN, S., CAO, L., WORLEY, L. A., COUNCIL, M. L., MATATALL, K. A., HELMS, C. & BOWCOCK, A. M. 2010. Frequent mutation of BAP1 in metastasizing uveal melanomas. *Science,* 330**,** 1410-3.

HARBOUR, J. W., ROBERSON, E. D. O., ANBUNATHAN, H., ONKEN, M. D., WORLEY, L. A. & BOWCOCK, A. M. 2013. Recurrent mutations at codon 625 of the splicing factor SF3B1 in uveal melanoma. *Nat Genet,* 45**,** 133-135.

HARRIS, H. 2008. Concerning the origin of malignant tumours by Theodor Boveri. Translated and annotated by Henry Harris. Preface. *J Cell Sci,* 121 Suppl 1**,** v-vi.

HAYASHI, S., IMOTO, I., AIZU, Y., OKAMOTO, N., MIZUNO, S., KUROSAWA, K., OKAMOTO, N., HONDA, S., ARAKI, S., MIZUTANI, S., NUMABE, H., SAITOH, S., KOSHO, T., FUKUSHIMA, Y., MITSUBUCHI, H., ENDO, F., CHINEN, Y., KOSAKI, R., OKUYAMA, T., OHKI, H., YOSHIHASHI, H., ONO, M., TAKADA, F., ONO, H., YAGI, M., MATSUMOTO, H., MAKITA, Y., HATA, A. & INAZAWA, J. 2011. Clinical application of array-based comparative genomic hybridization by two-stage screening for 536 patients with mental retardation and multiple congenital anomalies. *J Hum Genet,* 56**,** 110-24.

HEALY, E., BELGAID, C., TAKATA, M., HARRISON, D., ZHU, N. W., BURD, D. A., RIGBY, H. S., MATTHEWS, J. N. & REES, J. L. 1998. Prognostic significance of allelic losses in primary melanoma. *Oncogene,* 16**,** 2213-8.

HENRIQUEZ, F., JANSSEN, C., KEMP, E. G. & ROBERTS, F. 2007. The T1799A BRAF mutation is present in iris melanoma. *Invest Ophthalmol Vis Sci,* 48**,** 4897-900.

HIRSCH, D., KEMMERLING, R., DAVIS, S., CAMPS, J., MELTZER, P. S., RIED, T. & GAISER, T. 2013. Chromothripsis and focal copy number alterations determine poor outcome in malignant melanoma. *Cancer Res,* 73**,** 1454-60.

HOGLUND, M., GISSELSSON, D., HANSEN, G. B., WHITE, V. A., SALL, T., MITELMAN, F. & HORSMAN, D. 2004. Dissecting karyotypic patterns in malignant melanomas: temporal clustering of losses and gains in melanoma karyotypic evolution. *Int J Cancer,* 108**,** 57-65.

HOLLY, E. A., ASTON, D. A., CHAR, D. H., KRISTIANSEN, J. J. & AHN, D. K. 1990. Uveal melanoma in relation to ultraviolet light exposure and host factors. *Cancer Res,* 50**,** 5773-7.

HORSMAN, D. E., SROKA, H., ROOTMAN, J. & WHITE, V. A. 1990. Monosomy 3 and isochromosome 8q in a uveal melanoma. *Cancer Genet Cytogenet,* 45**,** 249-53.

HORSMAN, D. E. & WHITE, V. A. 1993. Cytogenetic analysis of uveal melanoma. Consistent occurrence of monosomy 3 and trisomy 8q. *Cancer,* 71**,** 811-9.

HSU, S. M., RAINE, L. & FANGER, H. 1981. Use of avidin-biotin-peroxidase complex (ABC) in immunoperoxidase techniques: a comparison between ABC and unlabeled antibody (PAP) procedures. *J Histochem Cytochem,* 29**,** 577-80.

HU, D. N. 2005. Photobiology of ocular melanocytes and melanoma. *Photochem Photobiol,* 81**,** 506-9.

HUGHES, S., DAMATO, B. E., GIDDINGS, I., HISCOTT, P. S., HUMPHREYS, J. & HOULSTON, R. S. 2005. Microarray comparative genomic hybridisation analysis of intraocular uveal melanomas identifies distinctive imbalances associated with loss of chromosome 3. *Br J Cancer,* 93**,** 1191-6.

HURET, J. L., AHMAD, M., ARSABAN, M., BERNHEIM, A., CIGNA, J., DESANGLES, F., GUIGNARD, J. C., JACQUEMOT-PERBAL, M. C., LABARUSSIAS, M., LEBERRE, V., MALO, A., MOREL-PAIR, C., MOSSAFA, H., POTIER, J. C., TEXIER, G., VIGUIE, F., YAU CHUN WAN-SENON, S., ZASADZINSKI, A. & DESSEN, P. 2013. Atlas of genetics and cytogenetics in oncology and haematology in 2013. *Nucleic Acids Res,* 41**,** D920-4.

HURST, E. A., HARBOUR, J. W. & CORNELIUS, L. A. 2003. Ocular melanoma: a review and the relationship to cutaneous melanoma. *Arch Dermatol,* 139**,** 1067-73.

HUSSAIN, S. P., SCHWANK, J., STAIB, F., WANG, X. W. & HARRIS, C. C. 2007. TP53 mutations and hepatocellular carcinoma: insights into the etiology and pathogenesis of liver cancer. *Oncogene,* 26**,** 2166-76.

IAFRATE, A. J., FEUK, L., RIVERA, M. N., LISTEWNIK, M. L., DONAHOE, P. K., QI, Y., SCHERER, S. W. & LEE, C. 2004. Detection of large-scale variation in the human genome. *Nat Genet,* 36**,** 949-51.

IANNACONE, M. R., YOULDEN, D. R., BAADE, P. D., AITKEN, J. F. & GREEN, A. C. 2015. Melanoma incidence trends and survival in adolescents and young adults in Queensland, Australia. *Int J Cancer,* 136**,** 603-609.

JACKSON, A. L. & LOEB, L. A. 1998. On the origin of multiple mutations in human cancers. *Semin Cancer Biol,* 8**,** 421-9.

JEMAL, A., SIEGEL, R., WARD, E., HAO, Y., XU, J. & THUN, M. J. 2009. Cancer statistics, 2009. *CA Cancer J Clin,* 59**,** 225-49.

JEMAL, A., SIEGEL, R., XU, J. & WARD, E. 2010. Cancer statistics, 2010. *CA Cancer J Clin,* 60**,** 277-300.

JONSSON, H. & PENG, S. L. 2005. Forkhead transcription factors in immunology. *Cell Mol Life Sci,* 62**,** 397-409.

KALIALIS, L. V., DRZEWIECKI, K. T. & KLYVER, H. 2009. Spontaneous regression of metastases from melanoma: review of the literature. *Melanoma Res,* 19**,** 275-82.

KALINEC, G., NAZARALI, A. J., HERMOUET, S., XU, N. & GUTKIND, J. S. 1992. Mutated alpha subunit of the Gq protein induces malignant transformation in NIH 3T3 cells. *Mol Cell Biol,* 12**,** 4687-93.

KANEDA, H., ARAO, T., TANAKA, K., TAMURA, D., AOMATSU, K., KUDO, K., SAKAI, K., DE VELASCO, M. A., MATSUMOTO, K., FUJITA, Y., YAMADA, Y., TSURUTANI, J., OKAMOTO, I., NAKAGAWA, K. & NISHIO, K. 2010. FOXQ1 is overexpressed in colorectal cancer and enhances tumorigenicity and tumor growth. *Cancer Res,* 70**,** 2053-63.

KATH, R., HAYUNGS, J., BORNFELD, N., SAUERWEIN, W., HOFFKEN, K. & SEEBER, S. 1993. Prognosis and treatment of disseminated uveal melanoma. *Cancer,* 72**,** 2219-23.

KAUL, D., WU, C. L., ADKINS, C. B., JORDAN, K. W., DEFEO, E. M., HABBEL, P., PETERSON, R. T., MCDOUGAL, W. S., POHL, U. & CHENG, L. L. 2010. Assessing prostate cancer growth with mRNA of spermine metabolic enzymes. *Cancer Biol Ther,* 9**,** 736-42.

KAUR, C., THOMAS, R. J., DESAI, N., GREEN, M. A., LOVELL, D., POWELL, B. W. & COOK, M. G. 2008. The correlation of regression in primary melanoma with sentinel lymph node status. *J Clin Pathol,* 61**,** 297-300.

KILIC, E., NAUS, N. C., VAN GILS, W., KLAVER, C. C., VAN TIL, M. E., VERBIEST, M. M., STIJNEN, T., MOOY, C. M., PARIDAENS, D., BEVERLOO, H. B., LUYTEN, G. P. & DE KLEIN, A. 2005. Concurrent loss of chromosome arm 1p and chromosome 3 predicts a decreased disease-free survival in uveal melanoma patients. *Invest Ophthalmol Vis Sci,* 46**,** 2253-7.

KILIC, E., VAN GILS, W., LODDER, E., BEVERLOO, H. B., VAN TIL, M. E., MOOY, C. M., PARIDAENS, D., DE KLEIN, A. & LUYTEN, G. P. 2006. Clinical and cytogenetic analyses in uveal melanoma. *Invest Ophthalmol Vis Sci,* 47**,** 3703-7.

KNUDSON, A. G. 2001. Two genetic hits (more or less) to cancer. *Nat Rev Cancer,* 1**,** 157-62.

KNUUTILA, S., AALTO, Y., AUTIO, K., BJORKQVIST, A. M., EL-RIFAI, W., HEMMER, S., HUHTA, T., KETTUNEN, E., KIURU-KUHLEFELT, S., LARRAMENDY, M. L., LUSHNIKOVA, T., MONNI, O., PERE, H., TAPPER, J., TARKKANEN, M., VARIS, A., WASENIUS, V. M., WOLF, M. & ZHU, Y. 1999. DNA copy number losses in human neoplasms. *Am J Pathol,* 155**,** 683-94.

KODJIKIAN, L., NGUYEN, K., LUMBROSO, L., GAUTHIER-VILLARS, M., CHAUVEL, P., PLAUCHU, H., STERKERS, M., DEVOUASSOUX, M. & GRANGE, J. D. 2003. Familial uveal melanoma: a report on two families and a review of the literature. *Acta Ophthalmol Scand,* 81**,** 389-95.

KONOVALOVA, S. & TYYNISMAA, H. 2013. Mitochondrial aminoacyl-tRNA synthetases in human disease. *Mol Genet Metab,* 108**,** 206-11.

KOOPMANS, A. E., VERDIJK, R. M., BROUWER, R. W., VAN DEN BOSCH, T. P., VAN DEN BERG, M. M., VAARWATER, J., KOCKX, C. E., PARIDAENS, D., NAUS, N. C., NELLIST, M., VAN, I. W. F., KILIC, E. & DE KLEIN, A. 2014. Clinical significance of immunohistochemistry for detection of BAP1 mutations in uveal melanoma. *Mod Pathol,* 27**,** 1321-30.

KUJALA, E., MAKITIE, T. & KIVELA, T. 2003. Very long-term prognosis of patients with malignant uveal melanoma. *Invest Ophthalmol Vis Sci,* 44**,** 4651-4659.

LAI, K., CONWAY, R. M., CROUCH, R., JAGER, M. J. & MADIGAN, M. C. 2008. Expression and distribution of MMPs and TIMPs in human uveal melanoma. *Exp Eye Res,* 86**,** 936-41.

LAMBA, S., FELICIONI, L., BUTTITTA, F., BLEEKER, F. E., MALATESTA, S., CORBO, V., SCARPA, A., RODOLFO, M., KNOWLES, M., FRATTINI, M., MARCHETTI, A. & BARDELLI, A. 2009. Mutational profile of GNAQQ209 in human tumors. *PLoS One,* 4**,** e6833.

LANDER, E. S., LINTON, L. M., BIRREN, B., NUSBAUM, C., ZODY, M. C., BALDWIN, J., DEVON, K., DEWAR, K., DOYLE, M., FITZHUGH, W., FUNKE, R., GAGE, D., HARRIS, K., HEAFORD, A., HOWLAND, J., KANN, L., LEHOCZKY, J., LEVINE, R., MCEWAN, P., MCKERNAN, K., MELDRIM, J., MESIROV, J. P., MIRANDA, C., MORRIS, W., NAYLOR, J., RAYMOND, C., ROSETTI, M., SANTOS, R., SHERIDAN, A., SOUGNEZ, C., STANGE-THOMANN, N., STOJANOVIC, N., SUBRAMANIAN, A., WYMAN, D., ROGERS, J., SULSTON, J., AINSCOUGH, R., BECK, S., BENTLEY, D., BURTON, J., CLEE, C., CARTER, N., COULSON, A., DEADMAN, R., DELOUKAS, P., DUNHAM, A., DUNHAM, I., DURBIN, R., FRENCH, L., GRAFHAM, D., GREGORY, S., HUBBARD, T., HUMPHRAY, S., HUNT, A., JONES, M., LLOYD, C., MCMURRAY, A., MATTHEWS, L., MERCER, S., MILNE, S., MULLIKIN, J. C., MUNGALL, A., PLUMB, R., ROSS, M., SHOWNKEEN, R., SIMS, S., WATERSTON, R. H., WILSON, R. K., HILLIER, L. W., MCPHERSON, J. D., MARRA, M. A., MARDIS, E. R., FULTON, L. A., CHINWALLA, A. T., PEPIN, K. H., GISH, W. R., CHISSOE, S. L., WENDL, M. C., DELEHAUNTY, K. D., MINER, T. L., DELEHAUNTY, A., KRAMER, J. B., COOK, L. L., FULTON, R. S., JOHNSON, D. L., MINX, P. J., CLIFTON, S. W., HAWKINS, T., BRANSCOMB, E., PREDKI, P., RICHARDSON, P., WENNING, S., SLEZAK, T., DOGGETT, N., CHENG, J. F., OLSEN, A., LUCAS, S., ELKIN, C., UBERBACHER, E., FRAZIER, M., et al. 2001. Initial sequencing and analysis of the human genome. *Nature,* 409**,** 860-921.

LANDIS, C. A., MASTERS, S. B., SPADA, A., PACE, A. M., BOURNE, H. R. & VALLAR, L. 1989. GTPase inhibiting mutations activate the alpha chain of Gs and stimulate adenylyl cyclase in human pituitary tumours. *Nature,* 340**,** 692-6.

LANDREVILLE, S., AGAPOVA, O. A. & HARBOUR, J. W. 2008. Emerging insights into the molecular pathogenesis of uveal melanoma. *Future Oncol,* 4**,** 629-36.

LAU, C. C., HARRIS, C. P., LU, X. Y., PERLAKY, L., GOGINENI, S., CHINTAGUMPALA, M., HICKS, J., JOHNSON, M. E., DAVINO, N. A., HUVOS, A. G., MEYERS, P. A., HEALY, J. H., GORLICK, R. & RAO, P. H. 2004. Frequent amplification and rearrangement of chromosomal bands 6p12-p21 and 17p11.2 in osteosarcoma. *Genes Chromosomes Cancer,* 39**,** 11-21.

LAWSON, J. S., GLENN, W. K., HENG, B., YE, Y., TRAN, B., LUTZE-MANN, L. & WHITAKER, N. J. 2009. Koilocytes indicate a role for human papilloma virus in breast cancer. *Br J Cancer,* 101**,** 1351-6.

LEBLANC, M., KULLE, B., SUNDET, K., AGARTZ, I., MELLE, I., DJUROVIC, S., FRIGESSI, A. & ANDREASSEN, O. A. 2012. Genome-wide study identifies PTPRO and WDR72 and FOXQ1-SUMO1P1 interaction associated with neurocognitive function. *J Psychiatr Res,* 46**,** 271-8.

LEE, A. J., ENDESFELDER, D., ROWAN, A. J., WALTHER, A., BIRKBAK, N. J., FUTREAL, P. A., DOWNWARD, J., SZALLASI, Z., TOMLINSON, I. P., HOWELL, M., KSCHISCHO, M. & SWANTON, C. 2011. Chromosomal instability confers intrinsic multidrug resistance. *Cancer Res,* 71**,** 1858-70.

LENGAUER, C., KINZLER, K. W. & VOGELSTEIN, B. 1997. Genetic instability in colorectal cancers. *Nature,* 386**,** 623-7.

LIANG, S. H., YAN, X. Z., WANG, B. L., JIN, H. F., YAO, L. P., LI, Y. N., CHEN, M., NIE, Y. Z., WANG, X., GUO, X. G., WU, K. C., DING, J. & FAN, D. M. 2013. Increased expression of FOXQ1 is a prognostic marker for patients with gastric cancer. *Tumour Biol,* 34**,** 2605-9.

LISZKAY, G., OROSZ, Z., PELEY, G., CSUKA, O., PLOTAR, V., SINKOVICS, I., BANFALVI, T., FEJOS, Z., GILDE, K. & KASLER, M. 2005. Relationship between sentinel lymph node status and regression of primary malignant melanoma. *Melanoma Res,* 15**,** 509-13.

LOERCHER, A. E. & HARBOUR, J. W. 2003. Molecular genetics of uveal melanoma. *Curr Eye Res,* 27**,** 69-74.

LUKE, J. J. & HODI, F. S. 2012. Vemurafenib and BRAF inhibition: a new class of treatment for metastatic melanoma. *Clin Cancer Res,* 18**,** 9-14.

MALAPONTE, G., LIBRA, M., GANGEMI, P., BEVELACQUA, V., MANGANO, K., D'AMICO, F., MAZZARINO, M. C., STIVALA, F., MCCUBREY, J. A. & TRAVALI, S. 2006. Detection of BRAF gene mutation in primary choroidal melanoma tissue. *Cancer Biol Ther,* 5**,** 225-7.

MANCINI, M., VEGNA, M. L., CASTOLDI, G. L., MECUCCI, C., SPIRITO, F., ELIA, L., TAFURI, A., ANNINO, L., PANE, F., REGE-CAMBRIN, G., GOTTARDI, M., LEONI, P., GALLO, E., CAMERA, A., LUCIANO, L., SPECCHIA, G., TORELLI, G., SBORGIA, M., GABBAS, A., TEDESCHI, A., DELLA STARZA, I., CASCAVILLA, N., DI RAIMONDO, F., MANDELLI, F. & FOA, R. 2002. Partial deletions of long arm of chromosome 6: biologic and clinical implications in adult acute lymphoblastic leukemia. *Leukemia,* 16**,** 2055-61.

MANSCHOT, W. A. & VAN STRIK, R. 1987. Is irradiation a justifiable treatment of choroidal melanoma? Analysis of published results. *Br J Ophthalmol,* 71**,** 348-52.

MARGO, C. E. 2004. The Collaborative Ocular Melanoma Study: an overview. *Cancer Control,* 11**,** 304-9.

MARIC, S. C., CROZAT, A., LOUHIMO, J., KNUUTILA, S. & JANNE, O. A. 1995. The human S-adenosylmethionine decarboxylase gene: nucleotide sequence of a pseudogene and chromosomal localization of the active gene (AMD1) and the pseudogene (AMD2). *Cytogenet Cell Genet,* 70**,** 195-9.

MARTIN, M., MASSHOFER, L., TEMMING, P., RAHMANN, S., METZ, C., BORNFELD, N., VAN DE NES, J., KLEIN-HITPASS, L., HINNEBUSCH, A. G., HORSTHEMKE, B., LOHMANN, D. R. & ZESCHNIGK, M. 2013. Exome sequencing identifies recurrent somatic mutations in EIF1AX and SF3B1 in uveal melanoma with disomy 3. *Nat Genet,* 45**,** 933-6.

MCCARROLL, S. A. & ALTSHULER, D. M. 2007. Copy-number variation and association studies of human disease. *Nat Genet*.

MCGRANAHAN, N., BURRELL, R. A., ENDESFELDER, D., NOVELLI, M. R. & SWANTON, C. 2012. Cancer chromosomal instability: therapeutic and diagnostic challenges. *EMBO Rep,* 13**,** 528-38.

MCKUSICK, V. A. 1985. Marcella O'Grady Boveri (1865-1950) and the chromosome theory of cancer. *J Med Genet,* 22**,** 431-40.

MCLEAN, M. J., FOSTER, W. D. & ZIMMERMAN, L. E. 1977. Prognostic factors in small malignant melanomas of choroid and ciliary body. *Arch Ophthalmol,* 95**,** 48-58.

MENG, X. R. & LU, P. 2012. [Relationship between heat shock protein 70 expression and radiotherapeutic effect in esophageal squamous cell carcinoma]. *Zhonghua Yi Xue Za Zhi,* 92**,** 3367-70.

MERBS, S. L. & SIDRANSKY, D. 1999. Analysis of p16 (CDKN2/MTS-1/INK4A) alterations in primary sporadic uveal melanoma. *Invest Ophthalmol Vis Sci,* 40**,** 779-83.

MEYERSON, M., GABRIEL, S. & GETZ, G. 2010. Advances in understanding cancer genomes through second-generation sequencing. *Nat Rev Genet,* 11**,** 685-96.

MOOY, C. M. & DE JONG, P. T. 1996. Prognostic parameters in uveal melanoma: a review. *Survey of Ophthalmology,* 41**,** 215-28.

MOOY, C. M., LUYTEN, G. P., DE JONG, P. T., LUIDER, T. M., STIJNEN, T., VAN DE HAM, F., VAN VROONHOVEN, C. C. & BOSMAN, F. T. 1995. Immunohistochemical and prognostic analysis of apoptosis and proliferation in uveal melanoma. *Am J Pathol,* 147**,** 1097-104.

MORT, R. L., JACKSON, I. J. & PATTON, E. E. 2015. The melanocyte lineage in development and disease. *Development,* 142**,** 620-32.

MULTANI, A. S., OZEN, M., NARAYAN, S., KUMAR, V., CHANDRA, J., MCCONKEY, D. J., NEWMAN, R. A. & PATHAK, S. 2000. Caspase-dependent apoptosis induced by telomere cleavage and TRF2 loss. *Neoplasia,* 2**,** 339-45.

NAMIKI, T., YANAGAWA, S., IZUMO, T., ISHIKAWA, M., TACHIBANA, M., KAWAKAMI, Y., YOKOZEKI, H., NISHIOKA, K. & KANEKO, Y. 2005. Genomic alterations in primary cutaneous melanomas detected by metaphase comparative genomic hybridization with laser capture or manual microdissection: 6p gains may predict poor outcome. *Cancer Genet Cytogenet,* 157**,** 1-11.

NAUS, N. C., VAN DRUNEN, E., DE KLEIN, A., LUYTEN, G. P., PARIDAENS, D. A., ALERS, J. C., KSANDER, B. R., BEVERLOO, H. B. & SLATER, R. M. 2001. Characterization of complex chromosomal abnormalities in uveal melanoma by fluorescence in situ hybridization, spectral karyotyping, and comparative genomic hybridization. *Genes Chromosomes Cancer,* 30**,** 267-73.

NAUS, N. C., VERHOEVEN, A. C., VAN DRUNEN, E., SLATER, R., MOOY, C. M., PARIDAENS, D. A., LUYTEN, G. P. & DE KLEIN, A. 2002. Detection of genetic prognostic markers in uveal melanoma biopsies using fluorescence in situ hybridization. *Clin Cancer Res,* 8**,** 534-9.

NEVES, S. R., RAM, P. T. & IYENGAR, R. 2002. G protein pathways. *Science,* 296**,** 1636-9.

NORDLING, C. O. 1953. A new theory on cancer-inducing mechanism. *Br J Cancer,* 7**,** 68-72.

NOWELL, P. C. 1976. The clonal evolution of tumor cell populations. *Science,* 194**,** 23-8.

NOWELL, P. C. 2007. Discovery of the Philadelphia chromosome: a personal perspective. *Journal of Clinical Investigation,* 117**,** 2033-2035.

OGAKI, S., HARADA, S., SHIRAKI, N., KUME, K. & KUME, S. 2011. An expression profile analysis of ES cell-derived definitive endodermal cells and Pdx1-expressing cells. *BMC Dev Biol,* 11**,** 13.

OHTA, M., BERD, D., SHIMIZU, M., NAGAI, H., COTTICELLI, M. G., MASTRANGELO, M., SHIELDS, J. A., SHIELDS, C. L., CROCE, C. M. & HUEBNER, K. 1996. Deletion mapping of chromosome region 9p21-p22 surrounding the CDKN2 locus in melanoma. *Int J Cancer,* 65**,** 762-7.

OLOPADE, O. I. & PICHERT, G. 2001. Cancer genetics in oncology practice. *Ann Oncol,* 12**,** 895-908.

ONKEN, M. D., WORLEY, L. A., EHLERS, J. P. & HARBOUR, J. W. 2004. Gene expression profiling in uveal melanoma reveals two molecular classes and predicts metastatic death. *Cancer Res,* 64**,** 7205-9.

ONKEN, M. D., WORLEY, L. A., LONG, M. D., DUAN, S., COUNCIL, M. L., BOWCOCK, A. M. & HARBOUR, J. W. 2008. Oncogenic mutations in GNAQ occur early in uveal melanoma. *Invest Ophthalmol Vis Sci,* 49**,** 5230-4.

ONKEN, M. D., WORLEY, L. A., PERSON, E., CHAR, D. H., BOWCOCK, A. M. & HARBOUR, J. W. 2007. Loss of heterozygosity of chromosome 3 detected with single nucleotide polymorphisms is superior to monosomy 3 for predicting metastasis in uveal melanoma. *Clin Cancer Res,* 13**,** 2923-7.

ONKEN, M. D., WORLEY, L. A., TUSCAN, M. D. & HARBOUR, J. W. 2010. An accurate, clinically feasible multi-gene expression assay for predicting metastasis in uveal melanoma. *J Mol Diagn,* 12**,** 461-8.

OZAKI, T., SCHAEFER, K. L., WAI, D., BUERGER, H., FLEGE, S., LINDNER, N., KEVRIC, M., DIALLO, R., BANKFALVI, A., BRINKSCHMIDT, C., JUERGENS, H., WINKELMANN, W., DOCKHORN-

DWORNICZAK, B., BIELACK, S. S. & POREMBA, C. 2002. Genetic imbalances revealed by comparative genomic hybridization in osteosarcomas. *Int J Cancer,* 102**,** 355-65.

PANDA-JONAS, S., JONAS, J. B. & JAKOBCZYK-ZMIJA, M. 1996. Retinal pigment epithelial cell count, distribution, and correlations in normal human eyes. *Am J Ophthalmol,* 121**,** 181-9.

PANE, A. R. & HIRST, L. W. 2000. Ultraviolet light exposure as a risk factor for ocular melanoma in Queensland, Australia. *Ophthalmic Epidemiol,* 7**,** 159-67.

PAPADOPOULOS, S., BENTER, T., ANASTASSIOU, G., PAPE, M., GERHARD, S., BORNFELD, N., LUDWIG, W.-D. & DÖRKEN, B. 2002. Assessment of genomic instability in breast cancer and uveal melanoma by random amplified polymorphic DNA analysis. *International Journal of Cancer,* 99**,** 193-200.

PARKIN, D. M., PISANI, P., LOPEZ, A. D. & MASUYER, E. 1994. At least one in seven cases of cancer is caused by smoking. Global estimates for 1985. *Int J Cancer,* 59**,** 494-504.

PARRELLA, P., CABALLERO, O. L., SIDRANSKY, D. & MERBS, S. L. 2001. Detection of c-myc amplification in uveal melanoma by fluorescent in situ hybridization. *Invest Ophthalmol Vis Sci,* 42**,** 1679-84.

PARRELLA, P., SIDRANSKY, D. & MERBS, S. L. 1999. Allelotype of posterior uveal melanoma: implications for a bifurcated tumor progression pathway. *Cancer Res,* 59**,** 3032-7.

PATEL, K. A., EDMONDSON, N. D., TALBOT, F., PARSONS, M. A., RENNIE, I. G. & SISLEY, K. 2001. Prediction of prognosis in patients with uveal melanoma using fluorescence in situ hybridisation. *Br J Ophthalmol,* 85**,** 1440-4.

POETSCH, M., DITTBERNER, T. & WOENCKHAUS, C. 2003. Microsatellite analysis at 1p36.3 in malignant melanoma of the skin: fine mapping in search of a possible tumour suppressor gene region. *Melanoma Res,* 13**,** 29-33.

POLLACK, J. R., PEROU, C. M., ALIZADEH, A. A., EISEN, M. B., PERGAMENSCHIKOV, A., WILLIAMS, C. F., JEFFREY, S. S., BOTSTEIN, D. & BROWN, P. O. 1999. Genome-wide analysis of DNA copy-number changes using cDNA microarrays. *Nat Genet,* 23**,** 41-6.

POLYAK, K. & WEINBERG, R. A. 2009. Transitions between epithelial and mesenchymal states: acquisition of malignant and stem cell traits. *Nat Rev Cancer,* 9**,** 265-73.

POPULO, H., VINAGRE, J., LOPES, J. M. & SOARES, P. 2011. Analysis of GNAQ mutations, proliferation and MAPK pathway activation in uveal melanomas. *Br J Ophthalmol,* 95**,** 715-9.

PRESCHER, G., BORNFELD, N. & BECHER, R. 1990. Nonrandom chromosomal abnormalities in primary uveal melanoma. *J Natl Cancer Inst,* 82**,** 1765-9.

PRESCHER, G., BORNFELD, N. & BECHER, R. 1994. Two subclones in a case of uveal melanoma. Relevance of monosomy 3 and multiplication of chromosome 8q. *Cancer Genet Cytogenet,* 77**,** 144-6.

PRESCHER, G., BORNFELD, N., FRIEDRICHS, W., SEEBER, S. & BECHER, R. 1995. Cytogenetics of twelve cases of uveal melanoma and patterns of nonrandom anomalies and isochromosome formation. *Cancer Genet Cytogenet,* 80**,** 40-6.

PRESCHER, G., BORNFELD, N., HIRCHE, H., HORSTHEMKE, B., JOCKEL, K. H. & BECHER, R. 1996. Prognostic implications of monosomy 3 in uveal melanoma. *Lancet,* 347**,** 1222-5.

QIAO, Y., JIANG, X., LEE, S. T., KARUTURI, R. K., HOOI, S. C. & YU, Q. 2011. FOXQ1 regulates epithelial-mesenchymal transition in human cancers. *Cancer Res,* 71**,** 3076-86.

RAMAIYA, K. J. & HARBOUR, J. W. 2007. Current management of uveal melanoma. *Expert Review of Ophthalmology,* 2**,** 939-946.

RAMOS, J., VILLA, J., RUIZ, A., ARMSTRONG, R. & MATTA, J. 2004. UV dose determines key characteristics of nonmelanoma skin cancer. *Cancer Epidemiol Biomarkers Prev,* 13**,** 2006-11.

RAUSCH, T., JONES, D. T., ZAPATKA, M., STUTZ, A. M., ZICHNER, T., WEISCHENFELDT, J., JAGER, N., REMKE, M., SHIH, D., NORTHCOTT, P. A., PFAFF, E., TICA, J., WANG, Q., MASSIMI, L.,

WITT, H., BENDER, S., PLEIER, S., CIN, H., HAWKINS, C., BECK, C., VON DEIMLING, A., HANS, V., BRORS, B., EILS, R., SCHEURLEN, W., BLAKE, J., BENES, V., KULOZIK, A. E., WITT, O., MARTIN, D., ZHANG, C., PORAT, R., MERINO, D. M., WASSERMAN, J., JABADO, N., FONTEBASSO, A., BULLINGER, L., RUCKER, F. G., DOHNER, K., DOHNER, H., KOSTER, J., MOLENAAR, J. J., VERSTEEG, R., KOOL, M., TABORI, U., MALKIN, D., KORSHUNOV, A., TAYLOR, M. D., LICHTER, P., PFISTER, S. M. & KORBEL, J. O. 2012. Genome sequencing of pediatric medulloblastoma links catastrophic DNA rearrangements with TP53 mutations. *Cell,* 148**,** 59-71.

REY, J. A., BELLO, M. J., DE CAMPOS, J. M., RAMOS, M. C. & BENITEZ, J. 1985. Cytogenetic findings in a human malignant melanoma metastatic to the brain. *Cancer Genet Cytogenet,* 16**,** 179-83.

RIED, T., HESELMEYER-HADDAD, K., BLEGEN, H., SCHROCK, E. & AUER, G. 1999. Genomic changes defining the genesis, progression, and malignancy potential in solid human tumors: a phenotype/genotype correlation. *Genes Chromosomes Cancer,* 25**,** 195-204.

RIETSCHEL, P., PANAGEAS, K. S., HANLON, C., PATEL, A., ABRAMSON, D. H. & CHAPMAN, P. B. 2005. Variates of survival in metastatic uveal melanoma. *J Clin Oncol,* 23**,** 8076-80.

ROH, C. & LYLE, S. 2006. Cutaneous stem cells and wound healing. *Pediatr Res,* 59**,** 100R-3R.

ROYDS, J. A., SHARRARD, R. M., PARSONS, M. A., LAWRY, J., REES, R., COTTAM, D., WAGNER, B. & RENNIE, I. G. 1992. C-myc oncogene expression in ocular melanomas. *Graefes Arch Clin Exp Ophthalmol,* 230**,** 366-71.

RUEDA, O. M., DIAZ-URIARTE, R. & CALDAS, C. 2013. Finding common regions of alteration in copy number data. *Methods Mol Biol,* 973**,** 339-53.

SCHILLER, J. T. & LOWY, D. R. 2001. Papillomavirus-like particle vaccines. *J Natl Cancer Inst Monogr,* 50-4.

SCHMIDT-POKRZYWNIAK, A., JOCKEL, K. H., BORNFELD, N., SAUERWEIN, W. & STANG, A. 2009. Positive interaction between light iris color and ultraviolet radiation in relation to the risk of uveal melanoma: a case-control study. *Ophthalmology,* 116**,** 340-8.

SCOLYER, R. A., THOMPSON, J. F., SHAW, H. M. & MCCARTHY, S. W. 2006. The importance of mitotic rate as a prognostic factor for localized primary cutaneous melanoma. *J Cutan Pathol,* 33**,** 395-6; author reply 397-9.

SCOTTO, J., FRAUMENI, J. F., JR. & LEE, J. A. 1976. Melanomas of the eye and other noncutaneous sites: epidemiologic aspects. *J Natl Cancer Inst,* 56**,** 489-91.

SCUOPPO, C., MIETHING, C., LINDQVIST, L., REYES, J., RUSE, C., APPELMANN, I., YOON, S., KRASNITZ, A., TERUYA-FELDSTEIN, J., PAPPIN, D., PELLETIER, J. & LOWE, S. W. 2012. A tumour suppressor network relying on the polyamine-hypusine axis. *Nature,* 487**,** 244-8.

SEDDON, J. M., ALBERT, D. M., LAVIN, P. T. & ROBINSON, N. 1983. A prognostic factor study of disease-free interval and survival following enucleation for uveal melanoma. *Arch Ophthalmol,* 101**,** 1894-9.

SEDDON, J. M., GRAGOUDAS, E. S., GLYNN, R. J., EGAN, K. M., ALBERT, D. M. & BLITZER, P. H. 1990. Host factors, UV radiation, and risk of uveal melanoma. A case-control study. *Arch Ophthalmol,* 108**,** 1274-80.

SHAFFER, L. G., BEJJANI, B. A., TORCHIA, B., KIRKPATRICK, S., COPPINGER, J. & BALLIF, B. C. 2007. The identification of microdeletion syndromes and other chromosome abnormalities: cytogenetic methods of the past, new technologies for the future. *Am J Med Genet C Semin Med Genet,* 145C**,** 335-45.

SHAH, C. P., WEIS, E., LAJOUS, M., SHIELDS, J. A. & SHIELDS, C. L. 2005. Intermittent and chronic ultraviolet light exposure and uveal melanoma: a meta-analysis. *Ophthalmology,* 112**,** 1599-607.

SHAMSELDIN, H. E., ALSHAMMARI, M., AL-SHEDDI, T., SALIH, M. A., ALKHALIDI, H., KENTAB, A., REPETTO, G. M., HASHEM, M. & ALKURAYA, F. S. 2012. Genomic analysis of

mitochondrial diseases in a consanguineous population reveals novel candidate disease genes. *J Med Genet,* 49**,** 234-41.

SHARPLESS, E. & CHIN, L. 2003. The INK4a/ARF locus and melanoma. *Oncogene,* 22**,** 3092-8.

SHIELDS, C. L., FURUTA, M., THANGAPPAN, A., NAGORI, S., MASHAYEKHI, A., LALLY, D. R., KELLY, C. C., RUDICH, D. S., NAGORI, A. V., WAKADE, O. A., MEHTA, S., FORTE, L., LONG, A., DELLACAVA, E. F., KAPLAN, B. & SHIELDS, J. A. 2009. Metastasis of uveal melanoma millimeter-by-millimeter in 8033 consecutive eyes. *Arch Ophthalmol,* 127**,** 989-98.

SHIELDS, C. L., GANGULY, A., BIANCIOTTO, C. G., TURAKA, K., TAVALLALI, A. & SHIELDS, J. A. 2011. Prognosis of uveal melanoma in 500 cases using genetic testing of fine-needle aspiration biopsy specimens. *Ophthalmology,* 118**,** 396-401.

SHIELDS, C. L., GANGULY, A., MATERIN, M. A., TEIXEIRA, L., MASHAYEKHI, A., SWANSON, L. A., MARR, B. P. & SHIELDS, J. A. 2007. Chromosome 3 analysis of uveal melanoma using fine-needle aspiration biopsy at the time of plaque radiotherapy in 140 consecutive cases. *Trans Am Ophthalmol Soc,* 105**,** 43-52; discussion 52-3.

SINGH, A. D., BERGMAN, L. & SEREGARD, S. 2005. Uveal melanoma: epidemiologic aspects. *Ophthalmol Clin North Am,* 18**,** 75-84, viii.

SINGH, A. D., BOGHOSIAN-SELL, L., WARY, K. K., SHIELDS, C. L., DE POTTER, P., DONOSO, L. A., SHIELDS, J. A. & CANNIZZARO, L. A. 1994. Cytogenetic findings in primary uveal melanoma. *Cancer Genet Cytogenet,* 72**,** 109-15.

SINGH, A. D., RENNIE, I. G., SEREGARD, S., GIBLIN, M. & MCKENZIE, J. 2004. Sunlight exposure and pathogenesis of uveal melanoma. *Survey of Ophthalmology,* 49**,** 419-28.

SINGH, A. D., SHIELDS, C. L. & SHIELDS, J. A. 2001. Prognostic factors in uveal melanoma. *Melanoma Res,* 11**,** 255-63.

SINGH, A. D., SHIELDS, C. L., SHIELDS, J. A. & DE POTTER, P. 1996. Bilateral primary uveal melanoma. Bad luck or bad genes? *Ophthalmology,* 103**,** 256-62.

SINGH, A. D., SISLEY, K., XU, Y., LI, J., FABER, P., PLUMMER, S. J., MUDHAR, H. S., RENNIE, I. G., KESSLER, P. M., CASEY, G. & WILLIAMS, B. G. 2007. Reduced expression of autotaxin predicts survival in uveal melanoma. *Br J Ophthalmol,* 91**,** 1385-92.

SINGH, A. D. & TOPHAM, A. 2003. Incidence of uveal melanoma in the United States: 1973-1997. *Ophthalmology,* 110**,** 956-61.

SINGH, A. D., TUBBS, R., BISCOTTI, C., SCHOENFIELD, L. & TRIZZOI, P. 2009. Chromosomal 3 and 8 status within hepatic metastasis of uveal melanoma. *Arch Pathol Lab Med,* 133**,** 1223-7.

SINGH, A. D., TURELL, M. E. & TOPHAM, A. K. 2011. Uveal melanoma: trends in incidence, treatment, and survival. *Ophthalmology,* 118**,** 1881-5.

SINGH, M., KAUR, B. & ANNUAR, N. M. 1988. Malignant melanoma of the choroid in a naevus of Ota. *Br J Ophthalmol,* 72**,** 131-3.

SISLEY, K. 2015. Tumors of the eye. *In:* SVERRE HEIM, F. M. (ed.) *Cancer Cytogenetics.* 554 ed.: John Wiley& Sons, Ltd.

SISLEY, K., PARSONS, M. A., GARNHAM, J., POTTER, A. M., CURTIS, D., REES, R. C. & RENNIE, I. G. 2000. Association of specific chromosome alterations with tumour phenotype in posterior uveal melanoma. *Br J Cancer,* 82**,** 330-8.

SISLEY, K., RENNIE, I. G., COTTAM, D. W., POTTER, A. M., POTTER, C. W. & REES, R. C. 1990. Cytogenetic findings in six posterior uveal melanomas: involvement of chromosomes 3, 6, and 8. *Genes Chromosomes Cancer,* 2**,** 205-9.

SISLEY, K., RENNIE, I. G., PARSONS, M. A., JACQUES, R., HAMMOND, D. W., BELL, S. M., POTTER, A. M. & REES, R. C. 1997. Abnormalities of chromosomes 3 and 8 in posterior uveal melanoma correlate with prognosis. *Genes Chromosomes Cancer,* 19**,** 22-8.

SISLEY, K., TATTERSALL, N., DYSON, M., SMITH, K., MUDHAR, H. S. & RENNIE, I. G. 2006. Multiplex fluorescence in situ hybridization identifies novel rearrangements of chromosomes 6, 15, and 18 in primary uveal melanoma. *Exp Eye Res,* 83**,** 554-9.

SLOMINSKI, A., TOBIN, D. J., SHIBAHARA, S. & WORTSMAN, J. 2004. Melanin pigmentation in mammalian skin and its hormonal regulation. *Physiol Rev,* 84**,** 1155-228.

SOUFIR, N., QUEILLE, S., LIBOUTET, M., THIBAUDEAU, O., BACHELIER, F., DELESTAING, G., BALLOY, B. C., BREUER, J., JANIN, A., DUBERTRET, L., VILMER, C. & BASSET-SEGUIN, N. 2007. Inactivation of the CDKN2A and the p53 tumour suppressor genes in external genital carcinomas and their precursors. *British Journal of Dermatology,* 156, 448-453.

SPEICHER, M. R., PRESCHER, G., DU MANOIR, S., JAUCH, A., HORSTHEMKE, B., BORNFELD, N., BECHER, R. & CREMER, T. 1994. Chromosomal gains and losses in uveal melanomas detected by comparative genomic hybridization. *Cancer Res,* 54**,** 3817-23.

SPENDLOVE, H. E., DAMATO, B. E., HUMPHREYS, J., BARKER, K. T., HISCOTT, P. S. & HOULSTON, R. S. 2004. BRAF mutations are detectable in conjunctival but not uveal melanomas. *Melanoma Res,* 14**,** 449-52.

SQUIRE, J., PHILLIPS, R. A., BOYCE, S., GODBOUT, R., ROGERS, B. & GALLIE, B. L. 1984. Isochromosome 6p, a unique chromosomal abnormality in retinoblastoma: verification by standard staining techniques, new densitometric methods, and somatic cell hybridization. *Hum Genet,* 66**,** 46-53.

STEILING, K., RYAN, J., BRODY, J. S. & SPIRA, A. 2008. The field of tissue injury in the lung and airway. *Cancer Prev Res (Phila),* 1**,** 396-403.

STEPHENS, P. J., GREENMAN, C. D., FU, B., YANG, F., BIGNELL, G. R., MUDIE, L. J., PLEASANCE, E. D., LAU, K. W., BEARE, D., STEBBINGS, L. A., MCLAREN, S., LIN, M. L., MCBRIDE, D. J., VARELA, I., NIK-ZAINAL, S., LEROY, C., JIA, M., MENZIES, A., BUTLER, A. P., TEAGUE, J. W., QUAIL, M. A., BURTON, J., SWERDLOW, H., CARTER, N. P., MORSBERGER, L. A., IACOBUZIO-DONAHUE, C., FOLLOWS, G. A., GREEN, A. R., FLANAGAN, A. M., STRATTON, M. R., FUTREAL, P. A. & CAMPBELL, P. J. 2011. Massive genomic rearrangement acquired in a single catastrophic event during cancer development. *Cell,* 144**,** 27-40.

STRATTON, M. R., CAMPBELL, P. J. & FUTREAL, P. A. 2009. The cancer genome. *Nature,* 458**,** 719-24.

SUNTERS, A., FERNANDEZ DE MATTOS, S., STAHL, M., BROSENS, J. J., ZOUMPOULIDOU, G., SAUNDERS, C. A., COFFER, P. J., MEDEMA, R. H., COOMBES, R. C. & LAM, E. W. 2003. FoxO3a transcriptional regulation of Bim controls apoptosis in paclitaxel-treated breast cancer cell lines. *J Biol Chem,* 278**,** 49795-805.

TAN, D. S., LAMBROS, M. B., NATRAJAN, R. & REIS-FILHO, J. S. 2007. Getting it right: designing microarray (and not 'microawry') comparative genomic hybridization studies for cancer research. *Lab Invest,* 87**,** 737-54.

THOMAS, N. E. 2006. BRAF somatic mutations in malignant melanoma and melanocytic naevi. *Melanoma Res,* 16**,** 97-103.

THOMPSON, J. F., SOONG, S. J., BALCH, C. M., GERSHENWALD, J. E., DING, S., COIT, D. G., FLAHERTY, K. T., GIMOTTY, P. A., JOHNSON, T., JOHNSON, M. M., LEONG, S. P., ROSS, M. I., BYRD, D. R., CASCINELLI, N., COCHRAN, A. J., EGGERMONT, A. M., MCMASTERS, K. M., MIHM, M. C., JR., MORTON, D. L. & SONDAK, V. K. 2011. Prognostic significance of mitotic rate in localized primary cutaneous melanoma: an analysis of patients in the multi-institutional American Joint Committee on Cancer melanoma staging database. *J Clin Oncol,* 29**,** 2199-205.

TOTH-MOLNAR, E., HAMMER, H. & OLAH, J. 2000. Cutaneous dysplastic naevi in uveal melanoma patients: markers for prognosis? *Melanoma Res,* 10**,** 36-9.

TROLET, J., HUPE, P., HUON, I., LEBIGOT, I., DECRAENE, C., DELATTRE, O., SASTRE-GARAU, X., SAULE, S., THIERY, J. P., PLANCHER, C., ASSELAIN, B., DESJARDINS, L., MARIANI, P., PIPERNO-NEUMANN, S., BARILLOT, E. & COUTURIER, J. 2009. Genomic profiling and identification of high-risk uveal melanoma by array CGH analysis of primary tumors and liver metastases. *Invest Ophthalmol Vis Sci,* 50, 2572-80.

TSCHENTSCHER, F., PRESCHER, G., ZESCHNIGK, M., HORSTHEMKE, B. & LOHMANN, D. R. 2000. Identification of chromosomes 3, 6, and 8 aberrations in uveal melanoma by microsatellite analysis in comparison to comparative genomic hybridization. *Cancer Genet Cytogenet,* 122**,** 13-7.

TUCKER, M. A., SHIELDS, J. A., HARTGE, P., AUGSBURGER, J., HOOVER, R. N. & FRAUMENI, J. F., JR. 1985. Sunlight exposure as risk factor for intraocular malignant melanoma. *N Engl J Med,* 313**,** 789-92.

TYZZER, E. E. 1916. Tumor Immunity. *The Journal of Cancer Research,* 1**,** 125-156.

VAISANEN, A., KALLIOINEN, M., VON DICKHOFF, K., LAATIKAINEN, L., HOYHTYA, M. & TURPEENNIEMI-HUJANEN, T. 1999. Matrix metalloproteinase-2 (MMP-2) immunoreactive protein--a new prognostic marker in uveal melanoma? *J Pathol,* 188**,** 56-62.

VALSESIA, A., MACE, A., JACQUEMONT, S., BECKMANN, J. S. & KUTALIK, Z. 2013. The Growing Importance of CNVs: New Insights for Detection and Clinical Interpretation. *Front Genet,* 4**,** 92.

VAN BEEK, J. G., KOOPMANS, A. E., VAARWATER, J., VERDIJK, R. M., DE KLEIN, A., NAUS, N. C. & KILIC, E. 2015. Metastatic disease in uveal melanoma: importance of a genetic profile? *Melanoma Res,* 25**,** 447-9.

VAN DE NES, J. A., NELLES, J., KREIS, S., METZ, C. H., HAGER, T., LOHMANN, D. R. & ZESCHNIGK, M. 2016. Comparing the Prognostic Value of BAP1 Mutation Pattern, Chromosome 3 Status, and BAP1 Immunohistochemistry in Uveal Melanoma. *Am J Surg Pathol,* 40**,** 796-805.

VAN DEN BOSCH, T., KILIC, E., PARIDAENS, D. & DE KLEIN, A. 2010. Genetics of uveal melanoma and cutaneous melanoma: two of a kind? *Dermatol Res Pract,* 2010**,** 360136.

VAN DER VELDEN, P. A., METZELAAR-BLOK, J. A., BERGMAN, W., MONIQUE, H., HURKS, H., FRANTS, R. R., GRUIS, N. A. & JAGER, M. J. 2001. Promoter hypermethylation: a common cause of reduced p16(INK4a) expression in uveal melanoma. *Cancer Res,* 61**,** 5303-6.

VAN GILS, W., KILIC, E., BRUGGENWIRTH, H. T., VAARWATER, J., VERBIEST, M. M., BEVERLOO, B., VAN TIL-BERG, M. E., PARIDAENS, D., LUYTEN, G. P. & DE KLEIN, A. 2008. Regional deletion and amplification on chromosome 6 in a uveal melanoma case without abnormalities on chromosomes 1p, 3 and 8. *Melanoma Res,* 18**,** 10-5.

VAN HEES, C. L., DE BOER, A., JAGER, M. J., BLEEKER, J. C., KAKEBEEKE, H. M., CRIJNS, M. B., VANDENBROUCKE, J. P. & BERGMAN, W. 1994. Are atypical nevi a risk factor for uveal melanoma? A case-control study. *J Invest Dermatol,* 103**,** 202-5.

VAN RAAMSDONK, C. D., BEZROOKOVE, V., GREEN, G., BAUER, J., GAUGLER, L., O'BRIEN, J. M., SIMPSON, E. M., BARSH, G. S. & BASTIAN, B. C. 2009. Frequent somatic mutations of GNAQ in uveal melanoma and blue naevi. *Nature,* 457**,** 599-602.

VAN RAAMSDONK, C. D., FITCH, K. R., FUCHS, H., DE ANGELIS, M. H. & BARSH, G. S. 2004. Effects of G-protein mutations on skin color. *Nat Genet,* 36**,** 961-8.

VAN RAAMSDONK, C. D., GRIEWANK, K. G., CROSBY, M. B., GARRIDO, M. C., VEMULA, S., WIESNER, T., OBENAUF, A. C., WACKERNAGEL, W., GREEN, G., BOUVIER, N., SOZEN, M. M., BAIMUKANOVA, G., ROY, R., HEGUY, A., DOLGALEV, I., KHANIN, R., BUSAM, K., SPEICHER, M. R., O'BRIEN, J. & BASTIAN, B. C. 2010. Mutations in GNA11 in uveal melanoma. *N Engl J Med,* 363**,** 2191-9.

WANG, W., HE, S., JI, J., HUANG, J., ZHANG, S. & ZHANG, Y. 2013. The prognostic significance of FOXQ1 oncogene overexpression in human hepatocellular carcinoma. *Pathol Res Pract,* 209**,** 353-8.

WEAVER, B. A. & CLEVELAND, D. W. 2006. Does aneuploidy cause cancer? *Curr Opin Cell Biol,* 18**,** 658-67.

WEBER, A., HENGGE, U. R., URBANIK, D., MARKWART, A., MIRMOHAMMADSAEGH, A., REICHEL, M. B., WITTEKIND, C., WIEDEMANN, P. & TANNAPFEL, A. 2003. Absence of mutations of the BRAF gene and constitutive activation of extracellular-regulated kinase in malignant melanomas of the uvea. *Lab Invest,* 83**,** 1771-6.

WHITE, V. A., MCNEIL, B. K. & HORSMAN, D. E. 1998. Acquired homozygosity (isodisomy) of chromosome 3 in uveal melanoma. *Cancer Genet Cytogenet,* 102**,** 40-5.

WUNDERLICH, V. 2007. Early references to the mutational origin of cancer. *Int J Epidemiol,* 36**,** 246-7.

XIA, L., HUANG, W., TIAN, D., ZHANG, L., QI, X., CHEN, Z., SHANG, X., NIE, Y. & WU, K. 2014. Forkhead box Q1 promotes hepatocellular carcinoma metastasis by transactivating ZEB2 and VersicanV1 expression. *Hepatology,* 59**,** 958-73.

XUE, W., KITZING, T., ROESSLER, S., ZUBER, J., KRASNITZ, A., SCHULTZ, N., REVILL, K., WEISSMUELLER, S., RAPPAPORT, A. R., SIMON, J., ZHANG, J., LUO, W., HICKS, J., ZENDER, L., WANG, X. W., POWERS, S., WIGLER, M. & LOWE, S. W. 2012. A cluster of cooperating tumor-suppressor gene candidates in chromosomal deletions. *Proc Natl Acad Sci U S A,* 109**,** 8212-7.

YANG, Y., LIU, W., FANG, Z., SHI, J., CHE, F., HE, C., YAO, L., WANG, E. & WU, Y. 2016. A Newly Identified Missense Mutation in FARS2 Causes Autosomal-Recessive Spastic Paraplegia. *Hum Mutat,* 37**,** 165-9.

YUCEL, Y. H., JOHNSTON, M. G., LY, T., PATEL, M., DRAKE, B., GUMUS, E., FRAENKL, S. A., MOORE, S., TOBBIA, D., ARMSTRONG, D., HORVATH, E. & GUPTA, N. 2009. Identification of lymphatics in the ciliary body of the human eye: a novel "uveolymphatic" outflow pathway. *Exp Eye Res,* 89**,** 810-9.

ZESCHNIGK, M., TSCHENTSCHER, F., LICH, C., BRANDT, B., HORSTHEMKE, B. & LOHMANN, D. R. 2003. Methylation analysis of several tumour suppressor genes shows a low frequency of methylation of CDKN2A and RARB in uveal melanomas. *Comp Funct Genomics,* 4**,** 329-36.

ZHANG, B., LIU, X. X., ZHANG, Y., JIANG, C. Y., HU, H. Y., GONG, L., LIU, M. & TENG, Q. S. 2006. Polyamine depletion by ODC-AdoMetDC antisense adenovirus impairs human colorectal cancer growth and invasion in vitro and in vivo. *J Gene Med,* 8**,** 980-9.

ZHANG, H., MENG, F., LIU, G., ZHANG, B., ZHU, J., WU, F., ETHIER, S. P., MILLER, F. & WU, G. 2011. Forkhead transcription factor foxq1 promotes epithelial-mesenchymal transition and breast cancer metastasis. *Cancer Res,* 71**,** 1292-301.

ZHANG, J., LI, W., DAI, S., TAI, X., JIA, J. & GUO, X. 2015. FOXQ1 is overexpressed in laryngeal carcinoma and affects cell growth, cell cycle progression and cell invasion. *Oncol Lett,* 10**,** 2499-2504.

ZHANG, Y. & HE, J. 2013. The development of targeted therapy in small cell lung cancer. *Journal of Thoracic Disease,* 5**,** 538-548.

ZHOU, Y., MA, B. G. & ZHANG, H. Y. 2007. Human oncogene tissue-specific expression level significantly correlates with sequence compositional features. *FEBS Lett,* 581**,** 4361-5.

ZHU, Z., ZHU, Z., PANG, Z., XING, Y., WAN, F., LAN, D. & WANG, H. 2013. Short hairpin RNA targeting FOXQ1 inhibits invasion and metastasis via the reversal of epithelial-mesenchymal transition in bladder cancer. *Int J Oncol,* 42**,** 1271-8.

ZIELINSKI, B., GRATIAS, S., TOEDT, G., MENDRZYK, F., STANGE, D. E., RADLWIMMER, B., LOHMANN, D. R. & LICHTER, P. 2005. Detection of chromosomal imbalances in retinoblastoma by matrix-based comparative genomic hybridization. *Genes Chromosomes Cancer,* 43**,** 294-301.

ZIMMERMAN, L. E., MCLEAN, I. W. & FOSTER, W. D. 1978. Does enucleation of the eye containing a malignant melanoma prevent or accelerate the dissemination of tumour cells. *Br J Ophthalmol,* 62**,** 420-5.

ZUIDERVAART, W., VAN NIEUWPOORT, F., STARK, M., DIJKMAN, R., PACKER, L., BORGSTEIN, A. M., PAVEY, S., VAN DER VELDEN, P., OUT, C., JAGER, M. J., HAYWARD, N. K. & GRUIS, N. A. 2005. Activation of the MAPK pathway is a common event in uveal melanomas although it rarely occurs through mutation of BRAF or RAS. *Br J Cancer,* 92**,** 2032-8.

ZUR HAUSEN, H. 2001. Proliferation-inducing viruses in non-permissive systems as possible causes of human cancers. *Lancet,* 357**,** 381-4.

OIUF | Uveitis is the third leading cause of blindness in developed countries. 2013. *OIUF | Uveitis is the third leading cause of blindness in developed countries.* [ONLINE] Available at: http://www.uveitis.org/. [Accessed 15 November 2016

APPENDICES

APPENDIX 1

Table1: Summery of clinical information and genetic findings for 1p- cases were found with follow up interval from hepatic metastases to death associated with M3 and 8q+.

Case number	Metastatic history	category	Survival interval	Genetic changes
7	Presented (06.08.1999) with lung, spinal and LM, where the spinal detected first. Died at (26.11.1999) from LM	2	3.66 months	1p-, M3, and i(6p)
12	LM diagnosed at (14.02.1996) Died LM at (23.03.1997)	4	13.3 months	1p-, 6p+/q-, 8q+
18	Presented with Bone and liver metastasise (17.12.1998) Died LM at (16.02.1999)	2	10 months	M3
21	Sub-cutaneous and liver (20.09.1999) Died LM at (13.05.2001)	2	8.23 months	1p-, M3, 6q-, and 8q+
23	LM (16.03.2001) and subcutaneous metastases (31.11.2001) Died LM at (09.05.2002)	3	14 months	1p-, M3, and 8q+
24	LM and bone metastases (04.08.2002) Died LM at March 2003	2	7 months	1p-, M3, and 8q+
27	Liver, Lung Skin (13.06.2006) Died LM at (15.08.06)	2	6 months	M3, 8q+